Institute of Fundamental Technological
Research of the Polish Academy of Sciences

Adaptive stabilization algorithms for engineering systems subjected to change of structural parameters and excitations

Maciej Wasilewski

Supervisor
prof. dr hab. inż. Czesław Bajer
Auxiliary supervisor
dr inż. Dominik Pisarski

Warsaw, Poland

2019

Acknowledgements

The research presented in this thesis has received funding from the project: **Adaptive distributed vibration control of modular structures (Adaptacyjne rozproszone tłumienie drgań konstrukcji modułowych), funded by National Science Centre, Poland under grant agreement DEC-2017/26/D/ST8/00883.**

Streszczenie

Tematem niniejszej pracy jest projekt i numeryczna weryfikacja adaptacyjnych metod aktywnego i półaktywnego sterowania układów inżynieryjnych poddanych zmianom parametrów i zewnętrznym wymuszeniom. Przykładem takich układów jest budynek poddany trzęsieniu ziemi, most wzbudzony przez przejazd pojazdów, czy konstrukcja, która uległa częściowemu zniszczeniu. Celem zaproponowanych rozwiązań jest stabilizacja sterowanych konstrukcji wokół zadanego punktu pracy poprzez zadanego minimalizację funkcjonału celu. Sterowanie realizowane jest przez aktywne i półaktywne elementy wykonawcze.

W pracy sformułowano ogólny problem sterowania optymalnego dla układów poddanych zakłóceniom. Za pomocą rachunku wariacyjnego wyznaczono warunek konieczny optymalności. Podano również ogólniejszy warunek konieczny w postaci Zasady Maksimum oraz warunek wystarczający wynikający z równania Hamiltona-Jacobiego-Bellmana. Na podstawie uzyskanych wyników wykazano, że sterowanie optymalne jest niemożliwe do wyznaczenia w praktyce, kiedy przyszły przebieg zakłócenia jest nieznany. Jako rozwiązanie zaproponowano ogólną adaptacyjną metodę sterowania polegającą na sukcesywnej aproksymacji zakłócanego układu przez modele dynamiczne, które są niezmienne w czasie.

Pierwszym rozpatrywanym przypadkiem jest stabilizacja układów poddanych działaniu zewnętrznego wymuszenia. Zaproponowane podejście polega na sekwencyjnej aproksymacji wymuszenia przez liniowy autonomiczny model dynamiczny. W rezultacie otrzymywany jest powiększony model dynamiczny całego układu, który uwzględnia wpływ wymuszenia a także jego zmienność w czasie. W przypadku sterowania aktywnego, rozwiązaniem tak zmodyfikowanego problemu sterowania optymalnego jest regulator liniowo-kwadratowy. W pracy zaproponowano dwa warianty: optymalizacja na skończonym oraz, charakteryzująca się znacznie mniejszą złożonością obliczeniową, na nieskończonym horyzoncie czasu. W wypadku sformułowania z nieskończonym horyzontem, istnienie rozwiązania zadania sterowania zapewniono poprzez odpowiednią modyfikację funkcjonału celu. W wypadku sterowania półaktywnego, zaproponowano bliskie optymalnemu sterowanie przełączeniowe. Jego postać wyznaczana jest poprzez rozwiązanie odpowiedniego równania Lapunova. W pracy udowodniono istnienie rozwiązania tego równania, jak również stabilność i górne oszacowanie jakości sterowania przełączeniowego.

Drugim problemem będącym tematem pracy jest stabilizacja układów poddanych nagłym zmianom parametrów wewnętrznych, takich jak sztywności połączeń czy masy elementów konstrukcji. Zaproponowana metoda aktywnego sterowania wykrywa nagłą zmianę parametrów konstrukcji poprzez chwilowy pomiar stanu i wartości zadanego funkcjonału celu. Na tej podstawie generuje ona ciąg praw sterowania, które zbiega do sterowania optymalnego. Do prawidłowego działania metody nie jest wymagana wiedza na temat parametrów wewnętrznych układu.

Sformułowane metody sterowania zweryfikowano numerycznie poprzez symulacje praktycznych problemów stabilizacji. Działanie zaproponowanych metod porównano w każdym przypadku do klasycznych, nieadaptacyjnych i powszechnie stosowanych rozwiązań, takich jak regulacja H_∞ i liniowo-kwadratowa-Gaussa. Cztery metody sterowania przetestowano w ramach czterech różnych zagadnień symulacji: maszyna wiertnicza poddana zmiennemu tarciu, budynek poddany trzęsieniu ziemi, belka

wzbudzana przez ruchome obciążenie i układ oscylatorów sprzężonych z nagłym częściowym zniszczeniem sztywnego połączenia. W każdym z rozpatrywanych przypadków dana metoda przewyższała porównawcze algorytmy sterowania w ramach zadanych kryteriów jakości.

Abstract

The subject of the present work is the design and numerical verification of adaptive active and semi-active control methods for stabilization of engineering systems subjected to changes of parameters and external disturbances. Examples of such systems are: a building subjected to an earthquake, a bridge excited by passing vehicles, or a mechanical structure that has been subjected to sudden damage. The aim of the proposed solutions is to stabilize the controlled structures around the given set-point via minimization of the cost functional. The control is assumed to be carried out by active and semi-active devices.

The general optimal control problem for systems subjected to time-varying uncertainties is formulated. The necessary condition of optimality was determined using the calculus of variations. A more general necessary condition in the form of the Maximum Principle and the sufficient condition resulting from the Hamilton-Jacobi-Bellman equation are also given. Based on the obtained results, it is shown that optimal control is impossible to determine in practice when the future course of the uncertainty is not fully known. As a solution, this Thesis proposes a general adaptive control method that is based on the successive approximation of the disturbed system via dynamical time-invariant models.

The first considered case is the stabilization of systems subjected to an external disturbance. The proposed approach is based on the sequential approximation of the disturbance by a linear autonomous dynamic model. As a result, the augmented dynamic model of the whole system is obtained, which approximately reproduces not only the influence of the disturbance but also its variation over time. In the case of active control, the solution of such modified optimal control problem is the linear-quadratic regulator. In the present work, two variants are considered: optimization on a finite and, characterized by significantly lower computational complexity, on an infinite time horizon. In the case of infinite horizon setting, the existence of a solution to the optimal control problem is ensured by appropriate modification of the target function. In the case of a semi-active control, the proposed near-optimal control is of the form of switching control law. Its parameters are determined via the solution of the corresponding Lyapunov equation. The existence of a solution to this equation is proven in Thesis, as well as the stability of the proposed control law and the upper bound of its quality.

The second problem that is the subject of the present work is the stabilization of systems subjected to sudden changes in internal parameters, such as joint stiffness or the mass of structural elements. The proposed active control method detects a sudden change of parameters by measuring the instantaneous values of the state and the performance criterion. Based on these values, it generates a sequence of control laws that converges to the optimal control. For proper operation of the method, knowledge about the internal parameters of the system is not required.

The formulated control methods have been verified numerically by simulations of practical stabilization problems. The operation of the proposed methods was compared in each case to the classic, non-adaptive and commonly used approaches, such as H_∞ and linear-quadratic-Gauss regulators. Four control methods have been tested via four different simulation scenarios: a drilling machine subjected to varying friction, a building subjected to an earthquake, a beam excited by a moving load and a system of

conjugate oscillators with sudden partial failure of a rigid connection. In each of the considered cases, the method outperformed comparative control algorithms in terms of stability and value of the performance criteria.

Contents

Chapter 1

Introduction

Engineering structures have accompanied people since the beginning of history. They are used in almost every area of human activity: buildings serve as shelter and fulfil many social functions, while without machines, today's industry would not be able to exist. The exponential pace of the development of civilization poses new challenges to structural and mechanical engineering. Buildings need to be lighter, higher and cheaper to produce. To ensure the competitiveness of their production, industrial machines must work faster, more cheaply and more efficiently.

The rush for efficiency and low cost is associated with the optimization of the construction and the specialization to the desired process conditions. As a result, an undesirable effect occurs: an increase in efficiency often leads to increased sensitivity to any changes in the working conditions. The protection of buildings against damage is a particularly important field of engineering, as it affects directly the safety of the people using them. Meanwhile, slender and flexible structures, however cheap and quick to build, are easily damaged by wind, earthquake and other dynamic loads. History records many cases of structural damage due to such loads.

One of the most well-known examples is the failure of the Tacoma Narrows Bridge. Although the bridge had unprecedented slenderness, low mass and stiffness, a later report [1] showed that the bridge design was made correctly in accordance with the established norms. The reason for the destruction was the vertical vibrations caused by the dynamically operating wind.

Although the next example happened 60 years later, the by then mature technology still couldn't prevent a malfunction caused by the same combination of causes: an extremely flexible structure subjected to dynamic loads. The Millennium Bridge, opened in 2000, had to be closed merely two days after its official opening due to significant vibrations of the structure [2]. In this case, the cause of the failure was the vibration resonance induced by synchronized pedestrian steps.

Although the failure of machines, unlike buildings, is not usually associated with the loss of human life, ensuring the proper operation of industrial equipment is also a key issue of modern engineering. Machines that operate at higher speeds and under greater loads are more prone to dangerous vibrations due to imbalances and external disturbances. Large

and flexible machines, such as drill strings and flexible robot links, are especially vulnerable. The development of effective methods of attenuation of such vibrations is then crucial to ensure their safe and effective operation.

As shown in the examples above, the design of mechanical systems based only on the influence of static loads is often insufficient. Dynamic disturbances in the system, such as a sudden change in parameters or an external, unpredictable disturbance may lead to destruction even if the magnitude of these changes does not exceed the permissible static loads.

The development of control theory is the solution to the growing importance of mechanical and structural stabilization problems. Control theory provides methods for designing efficient methods that implement various goals and paradigms such as optimization of the control goal, robustness against the variety of disturbances, fault tolerance or adaptation to the changing conditions. In addition, the development of computational technology allows creating more and more sophisticated methods that implement a control for increasingly complex dynamic systems.

In addition to new control techniques, extensive research is also being devoted to the development of new control devices. A typical, and historically the first, approach is the employment of active elements, such as hydraulic actuators or electric motors. These devices directly generate force or torque that is applied to the controlled object. However, the last few decades have marked the development of a new type of control device, namely semi-active elements. These are devices that instead of force generate a change in mechanical parameters, such as the damping factor, stiffness, or friction coefficient. Examples of such devices are magnetorheological and electrorheological dampers. Although semi-active devices cannot implement a control that is as aggressive as one implemented by active elements, they are characterized by a significantly lower energy demand and increased operational stability in the case of failure of the control method. These two features make semi-active devices extremely attractive for structural stabilization tasks.

The commonly used approaches for stabilization of mechanical systems are non-adaptive. An external disturbance is typically treated as a stationary stochastic signal with specific predefined parameters. Based on these assumptions, a fixed stabilization method is designed. The influence of the uncertainties of the system is mitigated by the means of robust techniques that guarantee an upper bound on the system's performance for a predefined range of failure. It is a common phenomenon, however, that changes occurring in a stabilized system are sudden, varying over time, and difficult to predict at the controller design stage. Excitations such as earthquake or wind are non-stationary processes, and their parameters are difficult to predict before their emergence. A sudden change of parameters, such as partial destruction or a new type of load, causes a shift of the natural frequencies of the system - the quality of stabilization performed by non-adaptive controllers in this situation deteriorates significantly.

The above-mentioned, classic solutions guarantee the stabilization of a mechanical system, but due to their lack of adaptability the stabilization process cannot be optimal.

In contrast to fixed stabilization methods, this work focuses on the **adaptive** control of structures subjected to parameter changes or disturbances. Because the adaptive control is conducted by frequent adjustment of the control law, it is characterized by a greater demand for computing power. In exchange, it has a significant advantage over the classic approach: it detects the change in the system and adjusts the control accordingly. As a consequence, adaptive controllers operate satisfactorily for a larger class of disturbance signals and very often guarantee not only the stability but also a control behaviour that is close to the optimal one. The stabilization of buildings and machines can be carried out with the use of both types of actuators: active and semi-active. Both approaches are widespread in practical applications. In order to present a full and coherent picture of the adaptive stabilization of engineering structures, both **active** and **semi-active** paradigms are considered in this work in parallel.

The research of the thesis has been conducted in the context of the project *Adaptacyjne rozproszone tłumienie drgań konstrukcji modułowych* (Adaptive distributed vibration control of modular structures) funded by the National Science Centre, Poland. The aim of the project is to develop novel distributed control methods for the control of modular structures subjected to vibrations. The focus of the research is motivated by the growing popularity of the employment of modular, autonomous automation devices equipped with sensors, actuators and controllers. Such independent systems benefit from low manufacturing costs and the capability of fast and easy reconfiguration, allowing for rapid prototyping of different control designs with the use of the same control elements. They are especially attractive for large-scale and robotics control problems, where centralized design would be costly and infeasible. As part of the project, this thesis focuses on the formulation and analysis of centralized adaptive controllers for the stabilization of mechanical structures, which in the future will form the basis for the formulation of novel, decentralized approaches.

1.1 Aims and scope of the thesis

The main goal of the thesis is to design effective methods of stabilizing mechanical systems subjected to changes of parameters or external disturbances. The purpose of the proposed control methods is to damp the induced vibrations of the mechanical system. The measure of the degree to which this goal is achieved is formulated as the minimization of a positive definite quadratic functional defined over a certain time horizon. This functional depends on the state of the structure and/or the current control value and can often be treated as a measure of the internal energy of the system. The optimization of this criterion corresponds then to the minimization of the vibration amplitudes of the mechanical structure.

The thesis considers two different actuation methods:

- active control,
- semi-active control.

These approaches differ significantly in terms of the used actuators and the overall effectiveness of the stabilization. From the perspective of this work, which is focused on the theoretical aspects of control, the main difference is the distinct mathematical models of these control systems, and the consequent distinct formulations of the stabilization problem. For this reason, the design of control methods for these approaches requires the use of radically different mathematical tools.

The proposed adaptive methods differ also due to the changes considered as taking place in the control system. The work focuses on two sources of destabilization:

- a jump change of the system's parameters,
- an excitation due to an external and changing disturbance.

The first scenario corresponds to a situation where the stabilized structure suffers from a sudden, partial destruction, for example, the breaking of a tendon of a bridge or the malfunction of supporting structure elements of a building. Another example of such a scenario is the operation of an industrial robot with loads of changing inertia. The second scenario is assumed to reflect three different types of excitation distinguished by the degree of stochasticity:

- a disturbance obeying a known dynamical model but with continuously varying parameters, such as the passage of vehicles with changing velocities,
- a disturbance with stochastically and discontinuously varying parameters, such as a sudden change in the friction coefficient,
- a purely stochastic disturbance, such as wind or earthquake.

In summary, the aim of this work is to examine three issues in parallel:

- active stabilization of a structure subjected to a sudden change of internal parameters,
- active stabilization of a structure subjected to a varying disturbance,
- semi-active stabilization of a structure subjected to a varying disturbance.

Consideration of different actuation methods and different types of change allows for a holistic analysis of adaptive control for mechanical stabilization.

An important goal of this work is also to ensure the high computational efficiency of the proposed methods. To keep up with the changes taking place in the considered system, the adaptive control methods have to recompute the control laws with a high frequency. For this reason, the key issue in the design of the controllers is to guarantee real-time operation, i.e. to ensure that the control law update occurs within a given time regime. Because the complexity of the adaptation algorithms depends polynomially on the number of degrees of freedom of the stabilized system, ensuring a sufficiently fast computation for large and complex structures is a difficult task. The adaptation methods proposed in this work are

designed to meet the criterion of timely execution. Each of the methods is accompanied by a computational complexity analysis.

The ultimate goal of the thesis is to validate numerically the proposed methods. The operation of each of the adaptive methods is tested via numerical simulations that closely mimic real-life stabilization scenarios. The results are compared to the simulations of classic, non-adaptive and established approaches, such as linear-quadratic (LQR), linear-quadratic Gaussian (LQG) and H_∞ regulators.

The scope of the thesis is as follows:

1. A literature review and the placement of the thesis' contributions within existing solutions.
2. The definition of the general control problem of adaptive stabilization of a dynamic system with the associated performance functional.
3. The determination of necessary and sufficient conditions for the optimality and feasibility analysis of the obtained results.
4. The formulation of three adaptive methods to stabilize mechanical structures, as well as the analysis of their stability, optimality and computational complexity.
5. The definition of models of the mechanical systems, simulation scenarios and comparative controllers used for the numerical validation of the proposed methods.
6. An analysis of the results of the numerical simulations and a comparison to non-adaptive controllers.
7. A summary of the results and proposals for further work.

1.2 Stabilisation of mechanical systems: State of the art

Structural control began to be considered by the scientific community in the 1970s [3] as a field of science exploring the theoretical possibilities of using control theory techniques for the stabilization of mechanical systems. The first recorded practical application of the use of active control dates back to 1989 [4] when the Active Mass Driver system was proposed to stabilize a structure excited by stochastic disturbances. Since then, the discipline has developed significantly, with the implementation of novel theoretical and practical solutions. Below is a review of the literature on the methods of stabilization of mechanical systems, classifying the results relative to the employed control devices. Because this thesis is focused on adaptive methods of stabilization, a review of adaptive control methods is presented in a separate section.

Active control of mechanical systems

The modern approach to the control of mechanical systems assumes the use of feedback and feedforward control methods. The functions that define how the control depends on

the measured signals can be heuristic or based on one of many mathematically formulated control objectives. One of the fundamental approaches is the use of the optimal control theory.

Optimal control focuses on a control that minimizes a given performance criterion. One of the fundamental methods of optimal control, which is also successfully employed in the control of mechanical systems, is the linear-quadratic regulator (LQR) [5] theory. Assuming that the stabilized system is represented by a linear dynamical model and the criterion for minimization is a quadratic functional, the problem of optimal control is solved by the LQR controller whose control law is affine with respect to the currently measured system state. The gain of an LQR regulator is determined in two ways. In the case of a performance criterion formulated for a finite time horizon or in the case of variable dynamic parameters of the system, the solution is obtained by solving Riccati's dynamic equation. The algebraic Riccati equation is used when the control criterion is formulated on an infinite time horizon. Both formulations are popular approaches to stabilization problems due to the simple form of the control law and their low computational complexity. The variant with an infinite horizon is particularly attractive, since the control law does not vary in time, and the algorithms used to solve the algebraic Riccati equation have a low computational complexity, proportional to the cube of the size of the system [6]. K. Seto et al. [7] employ an LQR regulator to stabilize two tall buildings by an actuator placed between them. Another interesting approach is to modify LQR to incorporate the influence of the disturbance on the system. In [8], a forecast of the future values of an earthquake is proposed by the employment of a fixed dynamic and linear model of the disturbance. This model is then included in the formulation of the LQR problem. As a consequence, the resulting controller computes the control value as a function of not only the system's state but also the value of an earthquake. A similar approach is proposed in [9], but rather than being fixed, the model of the disturbance is continuously identified online and a change in this model triggers the recomputation of the control law. The incorporation of the effect of the disturbance in the formulation of the control law allows these methods to stabilize structures more effectively.

The LQG regulator is an extension of the LQR control theory that is used to stabilize systems with incomplete state measurement and subject to white measurement and process noise. [10] uses the LQG theory to stabilize a wind-excited transmission tower. The results show that by the proper identification of the spectral density of the wind excitation, the resulting LQG regulator significantly outperforms the case without control. In [11], there is proposed a modified LQG controller. This modification employs the *alpha shift* [12] approach in a way that guarantees a prescribed level of stability of the whole control system.

Another approach to active optimal control is the Model Predictive Control (MPC). MPC shares similarities with the finite-horizon LQR. The problem of optimal control for MPC is also formulated over a finite time horizon. MPC uses an internal model of the mechanical system to predict the future trajectory of the state. The difference between MPC and LQR is that in the former, the solution to the control problem is obtained rather

by direct discrete optimization methods, such as quadratic and nonlinear programming, and not indirect optimization, as in the case of LQR. This allows a more general control problem formulation: the control and state can have defined constraints, the considered model of the system is allowed to be nonlinear, and the performance functional is not restricted to being quadratic. The optimal control problem is recalculated with high frequency, as a new state is measured. The disadvantage of this approach is the significant computational cost associated with direct optimization methods. In addition, a time horizon that is not long enough can result in a destabilizing control. The comprehensive numerical analysis of the MPC employed for structural control is a topic of [13]. In [14], MPC is employed on a wind-excited benchmark building with varying stiffness. Their results confirm that the MPC approach shows great robustness against the system's uncertainty.

The goal of robust control is to determine a controller that guarantees the minimization of a given performance criterion for a certain range of uncertainties in the system and disturbance. The robust control method tries to minimize the worst possible value of the performance index and, as a consequence, gives an estimate of its worst behaviour. The most popular example of robust control is the H_∞ theory. By solving the corresponding matrix inequalities, a control system is obtained that ensures that the gain of the system's response to the disturbance will not exceed a prescribed bound of H_∞ norm. As an approach to the stabilization of mechanical structures, the H_∞ techniques were presented for the first time in [15]. The control of structures in the event of the saturation of the actuators was formulated in [16]. To incorporate the nonlinearity associated with the saturation, they proposed a reformulation of the original dynamical model as a Lur'e system.

The H_∞ control optimizes the behaviour of the control system over the entire frequency spectrum of a disturbance. Therefore, an interesting modification of this idea is included in [17], where the system response is optimized only for a certain range of excitation frequencies. This range has been chosen to correspond to the typical frequencies of earthquakes. The resulting controller surpasses the traditional H_∞ in seismic control scenarios. The theory of H_∞ is also employed for non-linear mechanical systems. In [18], there is proposed a robust-adaptive-control to stabilize a car's suspension system using highly nonlinear hydraulic actuators. The proposed idea is to compute the ideal robust feedback control that guarantees a bound of the system's response and to synthesize the actual adaptive control law that tracks this desired reference control.

A separate branch of active control is the employment of artificial intelligence methods, such as regulators based on fuzzy logic or neural networks. These approaches allow formulating a large variety of controllers. Neural networks are especially attractive as a tool for control computation because they can successfully approximate an arbitrary nonlinear mapping. On the other hand, fuzzy logic allows easily reproducing control laws of heuristic origins. In [19], there is proposed a combination of sliding mode control and neural network techniques to stabilize a building subjected to an earthquake. Fuzzy control for an electric drive is analysed in [20]. A control method that employs a fuzzy disturbance observer is considered in [21].

Semi-active control of mechanical systems

In comparison to the active approach, semi-active control theory does not exhibit analytical solutions as do LQR and LQG. The smaller number of its theoretical results is caused by the fundamental difference between semi-active and active systems: a semi-active control system is nonlinear. There are, however, many approximate and heuristic solutions that guarantee, among other things, stability and near-optimal operation. As an example, a fundamental and commonly used semi-active stabilization method is Skyhook [22]. It is used in particular to stabilize the suspension of vehicles moving on uneven ground.

One of the most popular methods for the formulation of a semi-active control is the Lyapunov method. The Lyapunov theory of stability states that if the derivative of a positive definite function of the system's state V is strictly negative along the state trajectories, then the control system is asymptotically stable. Lyapunov-based control depends then on choosing a control value that minimizes this derivative, i.e. $u = \arg\min \dot{V}$. The first theoretical considerations on the application of semi-active Lyapunov-based control were presented in [23], where two different Lyapunov functions were proposed: the first represents the mechanical energy of the system, the second corresponds to the solution of the algebraic Lyapunov equation. When choosing the first function, the resulting control law minimizes the instantaneous energy of the system. The second approach, in contrast to instantaneous energy minimization, guarantees the global asymptotic stability of the control system.

The energy-based control method was employed to stabilize the structure by means of an electrorheological damper in [24]. The simulation results confirmed the attractiveness of this approach to structural stabilization tasks. The second variant, based on the algebraic Lyapunov equation, was experimentally tested using magnetorheological dampers for the first time in [25]. In [26] the energy-based Lyapunov control was employed to stabilize coupled beams by changes in the stiffness. As the numerical simulations showed, the Lyapunov control outperforms the passive one by over 50%. An interesting approach is presented also in [27], where the Lyapunov method has been used to formulate a decentralized control method. This approach was tested in the coupled beams stabilization problem in variants with different degrees of decentralization. The results show that decentralized solutions stabilize the system with an efficiency similar to that of the centralized approach.

As discussed at the beginning of the section, semi-active control theory lacks analytical solutions of optimal control problems, equivalent to LQR or LQG. Nevertheless, there are many attractive approaches that are based on approximate optimal control. One example is the clipped-optimal control, proposed in [28]. The idea behind this solution consists of two design steps. In the first one, a linear optimal control regulator is synthesized. This regulator provides information about the desired force that should be generated to guarantee optimal behaviour. The semi-active element is then controlled in such a way that the force generated by it is as close as possible to the force determined by the optimal regulator. A special case of this approach is clipped-LQR [29], a semi-active controller that realizes an approximate LQR control. Another approach to the optimal control of semi-active systems is to directly employ necessary conditions for the existence of an optimal control, given by

the Maximum Principle. In [30], a control in the form of an open loop for the stabilization of a beam system subjected to a moving load is proposed. An innovative approach to determining the optimal control consists of the explicit assumption of a bang-bang shape of the control and the optimization of only the switching times. This was extended in [31], where the structure to be stabilized is excited by a moving load with varying speed.

As in the active control case, artificial intelligence methods have also been proposed as tools for semi-active control. In [32], a method that uses fuzzy logic for the semi-active stabilization of a bridge is proposed. The use of a fuzzy controller for the stabilization of a three-story building is the subject of [33]. A nonlinear vehicle suspension control method based on a neural network is presented in [34].

Adaptive control of mechanical systems

Among the many active and semi-active paradigms for mechanical stabilization, adaptive control is the most adequate approach to tackling the control problem for systems subjected to a change. As mentioned at the beginning of this chapter, the most important property of adaptive control is the adjustability of the controller's gains in response to measured changes in the control system.

Adaptation is typically carried out in two distinct ways. First, the direct adaptive controller recomputes the control law with the direct employment of the measured parameters. Second, an indirect adaptive controller rather conducts online identification of the system and then changes the control law depending on the adjusted model.

One example of direct adaptive control employed for nonlinear stabilization is gain scheduling. The idea of gain scheduling is to compute many distinct controller gains, each of them adapted to a different operating point of the control system. Based on the measurements of the operating point, the control is then generated using the most appropriate gain. In the stabilization of mechanical systems, gain scheduling is used, among other things, for the stabilization of a non-linear building subjected to an earthquake in [35]. In that work, several robust regulators are synthesized based on the H_∞ theory for various states of the structure and earthquakes of different magnitudes. Based on the measured inter-story ductility and amplitude of the earthquake, the appropriate gain of the H_∞ regulator is then selected. The proposed gain schedule method gives similar stabilization results to a constant-gain controller but uses significantly smaller control forces.

Another example of the direct method is the Simple Adaptive Control Method (SACM). The idea of SACM is to adjust the control value in such a way that the trajectory of the stabilized system coincides with the trajectory of the reference model. This adjustment is determined as a combination of proportional and integral actions depending on the system's error. An interesting application of SACM is presented in [36], where the method is employed for the seismic stabilization of a structure subjected to structural damage and failures of the sensors.

An interesting example of an adaptive method for stabilizing structures subjected to moving loads and with the use of semi-active dampers is presented in [37], which uses a

sensitivity analysis and precomputed reference optimal control signals for adaptation to the measured state of the structure and velocity of the load. An adaptive policy-iteration method is introduced in [38] as a solution to the stabilization problem of an uncertain linear system.

Another solution is to employ the adaptive variant of MPC. Adaptivity is typically introduced to the MPC framework by the online parametric identification of the controlled object and the computation of the MPC control law according to the identified model. In [39], the adaptive MPC is employed for the stabilization of a nonlinear system subjected to both parametric uncertainties and auxiliary disturbances. A similar approach is presented in [40], where the uncertain model of the system is estimated with the use of the gradient optimization method. The proposed adaptive MPC method guarantees bounds on the estimation and asymptotic stability of the estimated state error.

Recent developments of adaptive control theory have been focused on the employment of artificial intelligence methods. In [41], a manipulator with uncertain parameters is controlled by a method based on a neural network combined with a recursive back-stepping method. The consequent virtual control laws are defined by nonlinear mappings provided by neural networks. The weights of these networks are updated continuously in time in accordance with the measured tracking errors. Many similar approaches have been also proposed for specific control problems, such as the stabilization of a robot with uncertain dynamics [42], systems with unknown hysteresis [43] or manipulators with an unknown deadzone [44]. The fuzzy logic approach for the stabilization of an uncertain dynamical system is proposed in [45]. The proposed sliding control law depends on the local approximation of the system's dynamical parameters. This approximation takes the form of fuzzy logic. The proposed choice of the online adaptation law of this fuzzy approximation guarantees the stability of the controller.

Novel approach proposed in Thesis

The stabilization of mechanical structures, as can be seen from the above review, is usually carried out by using classical, fixed control methods. In case of mechanical stabilization problems subjected to external disturbance, the excitations are usually treated as white noise and an LQG-like regulator is employed or a robust H_∞ controller is proposed, which guarantees bounds on the performance for a wide range of excitation frequencies. However, the classic solutions do not guarantee optimal or near-optimal performance in the case of sudden and varying changes.

The solution is to use a control method that adjusts to new operating conditions. The adaptive approaches found in the literature guarantee the stabilization of dynamic systems for a wide range of changes. But in this thesis, the present author would like to focus on two assumptions that are rarely seen together as design goals in the adaptive methods found in the literature:

1. near-optimal performance,

2. fast re-evaluation of the control law.

Adaptive MPC methods can guarantee near-optimal control. However, the optimization procedure is based on the use of direct optimization methods, which are computationally complex. In the case of large, complex systems subjected to significantly varying changes (e.g. buildings subjected to an earthquake), this approach may not guarantee the required speed of adaptation. The latest methods based on the use of artificial intelligence techniques rely on the approximation of nonlinear functions with complex neural networks or fuzzy logic models. The adaptation of such models is conducted by the gradient optimization of a significant number of parameters, which seems infeasible for control problems with sudden changes.

Only a small number of studies, such as [9, 8, 37], directly refer to the problem of adaptation to sudden and varying uncertainties. In this thesis, the author pursue the further development of this approach. The novel methods presented in this thesis detect changes in a system to be stabilized, and on this basis perform an online computation of a new control law. This approach ensures not only stabilization for a wide range of changes and disturbances, but, unlike the robust approach, the adjustment of the control provides near-optimal performance. In addition, the proposed solutions are designed with a focus on having low computational complexity.

As a consequence, the theses of this work are as follows:

For the problem of the stabilization of mechanical systems subjected to a sudden change of parameters or excited by a time-varying disturbance, non-adaptive and time-fixed control methods do not provide optimal or near-optimal performance. There exist more efficient control approaches that provide better stability and performance. The adaptive stabilization methods proposed in this thesis adjust their parameters to the current status of the controlled system and outperform non-adaptive control methods in terms of the associated performance index. The improvement of the performance of the proposed method is observed for both active and semi-active types of actuation. In addition, the formulated adaptive control methods have low computational complexity and are feasible for real-time operation.

1.3 Contributions

The contributions of this thesis are as follows.

1. The formulation and theoretical analysis of a novel adaptive active control method based on the autoregressive identification proposed in [9] with an infinite time horizon and an alpha-shift for stabilizing mechanical systems affected by an external and varying disturbance.

2. The formulation and theoretical analysis of a semi-active adaptive controller, based on the Lyapunov control theory and an autoregressive identification, for stabilizing mechanical systems affected by an external and varying disturbance.

3. The formulation and theoretical analysis of an active adaptive controller based on a policy iteration scheme for stabilizing mechanical systems affected by a sudden change of parameters.

4. The numerical examination of a finite time horizon variant of the active control method based on an autoregressive identification procedure.

5. The numerical analysis of an active adaptive controller for systems affected by an external disturbance, in two separate simulation cases: stabilizing a machine affected by a nonlinear and changing friction, and stabilizing a building exposed to earthquakes.

6. The numerical analysis of the semi-active controller for problems with external disturbances via simulation of a mechanical structure subjected to a moving load.

7. The numerical analysis of an active controller for problems with a sudden change of parameters via simulation of a mechanical structure subjected to partial failure.

These contributions have been published in the following journal papers: [46], [47] (in print) and in the conference proceedings: [48], [49]. The contributions to be published are: [50], [51].

1.4 Thesis structure

The structure of the Thesis is as follows:

Chapter 2 In this chapter, the general control problem considered in this Thesis is formulated. The control problem is defined by the system of ordinary differential equations that describe the dynamical behaviour of the control system, the functional criterion that gives the quantitative measure of the performance of a controller and the set of constraints imposed on the system. For this general formulation, the necessary conditions of optimality are stated using the calculus of variation. A more general necessary and sufficient conditions of optimality are also formulated via the Maximum Principle and Hamilton-Jacobi-Bellman equation that is associated with Bellman's

optimality principle. Next, the infeasibility of the optimal control in the presence of uncertainties and disturbances is discussed and the proposed solution in the form of near-optimal adaptive controller is presented. Finally, the particular control problems that are the focus of the present work are formulated. These control problems differ by the method of control (active and semi-active) and the source of the uncertainty in the control system (unknown external disturbance and unpredictable change of the internal parameters of the system).

Chapter 3 In this part of the Thesis, the control problem of the dynamical system subjected to an external disturbance is addressed. The general formulation of the considered problem is presented in the optimal control framework. The adaptive approach that is based on the identification of the disturbance is presented in the most general form. Next, two different methods of identification: autoregressive and parametric that are used by the proposed control method are described. The main focus of this chapter is the formulation of three distinct control schemes that provide near-optimal control for the mechanical systems affected by a disturbance. The first two control methods are suitable for systems with active control. The third method is designed to use with the semi-active control devices. For each considered control method, stability and near-optimality are discussed and analysed. Each control method is summarized in the algorithmic fashion. The computational complexity of the method is also studied.

Chapter 4 The focus of this chapter is on the stabilization of the system affected by the sudden change of its internal parameters. The near-optimal control scheme based on the Policy Iteration is then formulated. It is also proven that the associated series of control laws is stabilizing and converges to the optimal control. Similarly to Chapter 3, the control method is described as an algorithm and its computational complexity is also analysed.

Chapter 5 In this part of the Thesis, the numerical verification of the methods proposed in Chapters 3 and 4 is presented. Each control method is tested in the separate stabilization problem and their performance is compared to the number of classical controllers such as LQR and H_∞ regulators. The considered simulation scenarios are designed to correspond to the real-life engineering problems and are as follows: stabilization of a drilling machine subjected to the varying friction, vibration attenuation of the building affected by an earthquake, control of the beam subjected to the moving load and stabilization of the system of conjugate oscillators exposed to the sudden damage.

Chapter 2

General control problem

2.1 Optimal control of disturbed mechanical systems

The focus of this thesis is on a finite time horizon optimal control problem for a dynamical system defined by the generic dynamical equation:

$$\dot{\mathbf{x}}(t) = \mathbf{f}(\mathbf{x}(t), \mathbf{u}(t), \boldsymbol{\gamma}(t)), \quad \mathbf{x}(0) = \mathbf{x_0}, \quad t \in \mathbb{T}, \tag{2.1}$$

where $\mathbf{x} : [0, T_f] \mapsto \mathbb{R}^n$ represents an absolutely continuous state vector trajectory, $\mathbf{u} : \mathbb{T} \mapsto \mathcal{U} \subset \mathbb{R}^m$ is a measurable control signal applied to a system that has values in a compact set $\mathcal{U}$ and $\boldsymbol{\gamma} : \mathbb{T} \mapsto \mathbb{R}^p$ represents a piecewise continuous disturbance affecting the system, $\boldsymbol{\gamma} \in L_\infty(\mathbb{T})$. This disturbance can correspond to both a variation of the system's internal parameters and an auxiliary excitation. The function $\mathbf{f}$ is assumed continuous with respect to the state $\mathbf{x}$, the control input $\mathbf{u}$ and the vector of the disturbance $\boldsymbol{\gamma}$. Observe that, because the disturbance $\boldsymbol{\gamma}(t)$ is allowed to change sharply, the function $\mathbf{f}(\mathbf{x}(t), \mathbf{u}(t), \boldsymbol{\gamma}(t))$ is only almost everywhere continuous with respect to t. In addition, the next condition is assumed:

Assumption 2.1. *For every pair $(t, \mathbf{x})$, the set $\{\mathbf{f}(\mathbf{x}, \mathbf{u}, \boldsymbol{\gamma}(t)) : \mathbf{u} \in \mathcal{U}\}$ is compact and convex.*

The existence of the solution of the Cauchy problem (2.1) is guaranteed by the Carathéodory's existence theorem.

The goal of the control is to stabilize the system around a set-point (such as an equilibrium point of a mechanical structure or an operating point of a machine) with a focus on optimization of an integral performance criterion:

$$J(\mathbf{u}) = \int_0^{T_f} L(\mathbf{x}(t), \mathbf{u}(t))\, \mathrm{d}t. \tag{2.2}$$

where $L : \mathbb{R}^n \times \mathcal{U} \mapsto \mathbb{R}$ is a positive semidefinite function with respect to both $\mathbf{x}$ and $\mathbf{u}$. In addition, the next condition holds:

Assumption 2.2. *The function L is differentiable with respect to $\mathbf{x}$ and $\mathbf{u}$.*

The optimal control problem can be stated as follows:

$$\begin{aligned} &\textbf{Find } \mathbf{u}^* : \mathbb{T} \mapsto \mathcal{U} \subset \mathbb{R}^m, \quad \mathbb{T} = [0, T_f], \\ &\textbf{such that: } \mathbf{u}^* = \underset{\mathbf{u}(t)\in\mathcal{U},\ \forall t\in\mathbb{T}}{\arg\min}\ J(\mathbf{u}) = \int_0^{T_f} L(\mathbf{x}(t), \mathbf{u}(t))\,\mathrm{d}t, , \\ &\textbf{subject to: } \dot{\mathbf{x}}(t) = \mathbf{f}(\mathbf{x}(t), \mathbf{u}(t), \boldsymbol{\gamma}(t)), \\ &\qquad\qquad \mathbf{x}(0) = \mathbf{x_0}. \end{aligned} \tag{2.3}$$

With the Assumptions 2.1 and 2.2, the existence of the solution to the problem (2.3) can be established via the Filippov Theorem and the Weierstrass Theorem (see [52, Ch. 4.5] for the discussion).

Necessary and sufficient conditions of optimality

In this section, the necessary and sufficient conditions of optimality for the problem (2.3) are stated. Let us firstly formulate the necessary conditions via the calculus of variations.

Let $\mathbf{u}^*$ be a control that provides a local minimum of (2.2) for all piecewise continuous controls $\mathbf{u}$, i.e., $J(\mathbf{u}^*) \leq J(\mathbf{u})$. Let $\mathbf{x}^*$ be a corresponding optimal trajectory. Let $\mathbf{u}$ be a perturbed optimal control:

$$\mathbf{u}(t, \alpha) = \mathbf{u}^*(t) + \alpha\boldsymbol{\xi}(t), \tag{2.4}$$

where $\alpha \in \mathbb{R}$ and $\boldsymbol{\xi}$ is a piecewise continuous function from $\mathbb{T}$ to $\mathbb{R}^m$. The perturbed optimal trajectory $\mathbf{x}$ corresponding to the perturbed control $\mathbf{u}$ is defined as follows:

$$\mathbf{x}(t, \alpha) = \mathbf{x}^*(t) + \alpha\boldsymbol{\eta}(t) + \mathbf{o}(\alpha), \tag{2.5}$$

where $\mathbf{o}(\alpha)$ represents higher order terms of the Taylor expansion, i.e., $\lim_{\alpha\to 0} \frac{\mathbf{o}(\alpha)}{\alpha} = \mathbf{0}$. Observe that $\boldsymbol{\eta}(0) = \mathbf{0}$ since the initial conditions do not change. In addition, observe that:

$$\forall t \in \mathbb{T},\ \left.\frac{\partial \mathbf{x}}{\partial \alpha}\right|_{\alpha=0} = \boldsymbol{\eta}(t). \tag{2.6}$$

By differentiation of Eq. (2.6) with respect to time we obtain:

$$\begin{aligned} \dot{\boldsymbol{\eta}}(t) = \left.\frac{\partial \dot{\mathbf{x}}}{\partial \alpha}\right|_{\alpha=0} &= \frac{\partial \mathbf{f}}{\partial \mathbf{x}}(\mathbf{x}(t,0), \mathbf{u}^*(t), \boldsymbol{\gamma}(t))\ \left.\frac{\partial \mathbf{x}}{\partial \alpha}\right|_{\alpha=0} + \frac{\partial \mathbf{f}}{\partial \mathbf{u}}(\mathbf{x}(t,0), \mathbf{u}^*(t), \boldsymbol{\gamma}(t))\boldsymbol{\xi}(t) \\ &= \frac{\partial \mathbf{f}}{\partial \mathbf{x}}(\mathbf{x}(t,0), \mathbf{u}^*(t), \boldsymbol{\gamma}(t))\boldsymbol{\eta}(t) + \frac{\partial \mathbf{f}}{\partial \mathbf{u}}(\mathbf{x}(t,0), \mathbf{u}^*(t), \boldsymbol{\gamma}(t))\boldsymbol{\xi}(t) \\ &= \frac{\partial \mathbf{f}}{\partial \mathbf{x}}\left(\mathbf{x}^*(t), \mathbf{u}^*(t), \boldsymbol{\gamma}(t)\right)\boldsymbol{\eta}(t) + \frac{\partial \mathbf{f}}{\partial \mathbf{u}}(\mathbf{x}^*(t), \mathbf{u}^*(t), \boldsymbol{\gamma}(t))\boldsymbol{\xi}(t). \end{aligned} \tag{2.7}$$

Let us now rewrite the performance functional (2.2):

$$J(\mathbf{u}) = \int_0^{T_f} \left(L(\mathbf{x}(t), \mathbf{u}(t)) + \mathbf{p}^T(t)\left[\dot{\mathbf{x}}(t) - \mathbf{f}(\mathbf{x}(t), \mathbf{u}(t), \boldsymbol{\gamma}(t))\right]\right)\,\mathrm{d}t, \tag{2.8}$$

where $\mathbf{p} : \mathbb{T} \mapsto \mathbb{R}^n$ is a so-called *costate* function to be defined later. Observe that, because $\dot{\mathbf{x}}(t) \equiv \mathbf{f}(\mathbf{x}(t), \mathbf{u}(t), \boldsymbol{\gamma}(t))$, the addition of the term $\mathbf{p}^T(t)\left[\dot{\mathbf{x}}(t) - \mathbf{f}(\mathbf{x}(t), \mathbf{u}(t), \boldsymbol{\gamma}(t))\right]$ does not alter the value of J defined as in (2.2). In addition, let us define the Hamiltonian H:

$$H(\mathbf{x}, \mathbf{p}, \mathbf{u}, \boldsymbol{\gamma}) = \mathbf{p}^T\mathbf{f}(\mathbf{x}, \mathbf{u}, \boldsymbol{\gamma}) - L(\mathbf{x}, \mathbf{u}). \tag{2.9}$$

The performance functional can be now formulated in terms of this Hamiltonian:

$$J(\mathbf{u}) = \int_0^{T_f} \left(-H(\mathbf{x}(t), \mathbf{p}(t), \mathbf{u}(t), \boldsymbol{\gamma}(t)) + \mathbf{p}^T(t)\dot{\mathbf{x}}(t)\right) \mathrm{d}t, \tag{2.10}$$

We would like to analyse the first variation of the performance functional J at the optimal control $\mathbf{u}^*$, denoted by $\delta J|_{\mathbf{u}^*}$, which is equal to the first-order term with respect to α of the difference between the perturbed cost and the optimal cost:

$$J(\mathbf{u}) - J(\mathbf{u}^*) = J(\mathbf{u}^* + \alpha\boldsymbol{\xi}) - J(\mathbf{u}^*) = \alpha\, \delta J(\boldsymbol{\xi})|_{\mathbf{u}^*} + o(\alpha). \tag{2.11}$$

According to the Eq. (2.10), the difference (2.11) can be expanded as follows:

$$\begin{aligned} J(\mathbf{u}) - J(\mathbf{u}^*) = \int_0^{T_f} \big(&H(\mathbf{x}^*(t), \mathbf{p}(t), \mathbf{u}^*(t), \boldsymbol{\gamma}(t)) - H(\mathbf{x}(t), \mathbf{p}(t), \mathbf{u}(t), \boldsymbol{\gamma}(t)) \\ &+ \mathbf{p}^T \left[\dot{\mathbf{x}}(t) - \dot{\mathbf{x}}^*(t)\right]\big) \, \mathrm{d}t. \end{aligned} \tag{2.12}$$

Let us expand the difference of the Hamiltonians:

$$\begin{aligned} H(\mathbf{x}, \mathbf{p}, \mathbf{u}, \boldsymbol{\gamma}) - H(\mathbf{x}^*, \mathbf{p}, \mathbf{u}^*, \boldsymbol{\gamma}) = &\left.\frac{\partial H(\mathbf{x}, \mathbf{p}, \mathbf{u}^*, \boldsymbol{\gamma})}{\partial \mathbf{x}}\right|_{\mathbf{x}=\mathbf{x}^*(t)} \alpha\boldsymbol{\eta} \\ &+ \left.\frac{\partial H(\mathbf{x}^*, \mathbf{p}, \mathbf{u}, \boldsymbol{\gamma})}{\partial \mathbf{u}}\right|_{\mathbf{u}=\mathbf{u}^*} \alpha\boldsymbol{\xi} + o(\alpha). \end{aligned} \tag{2.13}$$

The second difference in the integral (2.12) can be expanded with via the integration by parts:

$$\begin{aligned} \int_0^{T_f} \mathbf{p}^T(t) \left[\dot{\mathbf{x}}(t) - \dot{\mathbf{x}}^*(t)\right] \mathrm{d}t &= \left(\mathbf{p}^T(t) \left[\mathbf{x}(t) - \mathbf{x}^*(t)\right]\right)\Big|_0^{T_f} - \int_0^{T_f} \dot{\mathbf{p}}^T(t) \left[\mathbf{x}(t) - \mathbf{x}^*(t)\right] \mathrm{d}t \\ &= \left(\mathbf{p}^T(T_f) \left[\mathbf{x}(T_f) - \mathbf{x}^*(T_f)\right]\right) - \left(\mathbf{p}^T(0) \left[\mathbf{x}(0) - \mathbf{x}^*(0)\right]\right) \\ &\quad - \int_0^{T_f} \dot{\mathbf{p}}^T(t)\alpha\boldsymbol{\eta}(t) \, \mathrm{d}t + o(\alpha). \end{aligned} \tag{2.14}$$

Observe that, because the starting point $\mathbf{x}_0$ is fixed, the term $\mathbf{p}^T(0) \left[\mathbf{x}(0) - \mathbf{x}^*(0)\right] \equiv 0$ for any function $\mathbf{p}(t)$ and $\mathbf{p}^T(T_f) \left[\mathbf{x}(T_f) - \mathbf{x}^*(T_f)\right] = \alpha\mathbf{p}^T(T_f)\boldsymbol{\eta}(T_f) + o(\alpha)$.

Finally, we obtain:

$$\begin{aligned} J(\mathbf{u}) - J(\mathbf{u}^*) = \alpha\mathbf{p}^T(T_f)\boldsymbol{\eta}(T_f) + \alpha \int_0^{T_f} \Bigg(&\left[\dot{\mathbf{p}}^T(t) + \left.\frac{\partial H(\mathbf{x}, \mathbf{p}, \mathbf{u}^*, \boldsymbol{\gamma})}{\partial \mathbf{x}}\right|_{\mathbf{x}=\mathbf{x}^*(t)}\right] \boldsymbol{\eta}(t) \\ &+ \left.\frac{\partial H(\mathbf{x}^*, \mathbf{p}, \mathbf{u}, \boldsymbol{\gamma})}{\partial \mathbf{u}}\right|_{\mathbf{u}=\mathbf{u}^*} \boldsymbol{\xi}(t)\Bigg) \, \mathrm{d}t + o(\alpha). \end{aligned} \tag{2.15}$$

The first variation is then as follows:

$$\begin{aligned} \delta J(\boldsymbol{\xi})|_{\mathbf{u}^*} = \mathbf{p}^T(T_f)\boldsymbol{\eta}(T_f) + \int_0^{T_f} \Bigg(&\left[\dot{\mathbf{p}}^T(t) + \left.\frac{\partial H(\mathbf{x}, \mathbf{p}, \mathbf{u}^*, \boldsymbol{\gamma})}{\partial \mathbf{x}}\right|_{\mathbf{x}=\mathbf{x}^*(t)}\right] \boldsymbol{\eta}(t) \\ &+ \left.\frac{\partial H(\mathbf{x}^*, \mathbf{p}, \mathbf{u}, \boldsymbol{\gamma})}{\partial \mathbf{u}}\right|_{\mathbf{u}=\mathbf{u}^*} \boldsymbol{\xi}(t)\Bigg) \, \mathrm{d}t, \end{aligned} \tag{2.16}$$

where the dependence of $\boldsymbol{\eta}$ on $\boldsymbol{\xi}$ is defined in Eq. (2.7).

The first-order necessary condition for optimality states that $\delta J(\boldsymbol{\xi})|_{\mathbf{u}^*} \equiv 0$. This condition is valid for optimal control $\mathbf{u}^*$ for any *costate* function $\mathbf{p}$, but is particularly interesting with the special choice of $\mathbf{p}$. Let us choose the function $\mathbf{p}^* : \mathbb{T} \mapsto \mathbb{R}^n$, such that it is a solution to the final value problem:

$$\dot{\mathbf{p}}^*(t) = -\left.\frac{\partial H^T(\mathbf{x}, \mathbf{p}^*(t), \mathbf{u}^*(t), \boldsymbol{\gamma}(t))}{\partial \mathbf{x}}\right|_{\mathbf{x}=\mathbf{x}^*(t)}, \quad \mathbf{p}^*(T_f) = \mathbf{0}. \tag{2.17}$$

As a consequence, the first-order necessary condition takes the form:

$$\delta J(\boldsymbol{\xi})|_{\mathbf{u}^*} = \int_0^{T_f} \left.\frac{\partial H(\mathbf{x}^*, \mathbf{p}^*, \mathbf{u}, \boldsymbol{\gamma})}{\partial \mathbf{u}}\right|_{\mathbf{u}=\mathbf{u}^*} \boldsymbol{\xi}\, \mathrm{d}t = 0. \tag{2.18}$$

Because Eq. (2.18) holds for any function $\boldsymbol{\xi}$, the condition (2.18) can be stated as follows:

$$\left.\frac{\partial H(\mathbf{x}^*, \mathbf{p}^*, \mathbf{u}, \boldsymbol{\gamma})}{\partial \mathbf{u}}\right|_{\mathbf{u}=\mathbf{u}^*} = 0,\ \forall t \in \mathbb{T}. \tag{2.19}$$

The first-order necessary condition for optimality can be now summarized:

$$\begin{aligned} H(\mathbf{x}, \mathbf{p}, \mathbf{u}, \boldsymbol{\gamma}) &= \mathbf{p}^T \mathbf{f}(\mathbf{x}, \mathbf{u}, \boldsymbol{\gamma}) - L(\mathbf{x}, \mathbf{u}), & \left.\frac{\partial H(\mathbf{x}^*, \mathbf{p}^*, \mathbf{u}, \boldsymbol{\gamma})}{\partial \mathbf{u}}\right|_{\mathbf{u}=\mathbf{u}^*} &= 0,\ \forall t \in \mathbb{T}, \\ \dot{\mathbf{x}}(t) &= \mathbf{f}(\mathbf{x}(t), \mathbf{u}(t), \boldsymbol{\gamma}(t)), & \mathbf{x}(0) &= \mathbf{x_0}, \\ \dot{\mathbf{p}}^*(t) &= -\left.\frac{\partial H^T(\mathbf{x}, \mathbf{p}^*(t), \mathbf{u}^*(t), \boldsymbol{\gamma}(t))}{\partial \mathbf{x}}\right|_{\mathbf{x}=\mathbf{x}^*(t)}, & \mathbf{p}^*(T_f) &= \mathbf{0}. \end{aligned} \tag{2.20}$$

The variational approach stated above has several limitations, such as assumption, that the values of $\mathbf{u}^*(t)$ lay in the interior of the control set $\mathcal{U}$ and that the Hamiltonian H is differentiable with respect to $\mathbf{u}$. A more general necessary condition for optimality that is not affected by these limitations and also considers a more general class of control perturbations is stated via the Maximum Principle, formulated by L. Pontryagin [53]. The variant of the Maximum Principle for the problem (2.3) is presented below:

Maximum Principle for Fixed-time Free-endpoint Problem. *Let $\mathbf{u}^* : \mathbb{T} \mapsto \mathcal{U}$ be an optimal control and let $\mathbf{x}^* : \mathbb{T} \mapsto \mathbb{R}^n$ be the corresponding optimal state trajectory. Then there exists a function $\mathbf{p}^* : \mathbb{T} \mapsto \mathbb{R}^n$ such that, for almost every $t \in \mathbb{T}$:*

$$\begin{aligned} H(\mathbf{x}, \mathbf{u}, \mathbf{p}^*, \boldsymbol{\gamma}) &= \mathbf{p}^{*T} \mathbf{f}(\mathbf{x}, \mathbf{u}, \boldsymbol{\gamma}) - L(\mathbf{x}, \mathbf{u}), \\ \dot{\mathbf{x}}(t) &= \mathbf{f}(\mathbf{x}(t), \mathbf{u}(t), \boldsymbol{\gamma}(t)), \\ \dot{\mathbf{p}}^* &= -\left.\frac{\partial H^T(\mathbf{x}, \mathbf{p}^*(t), \mathbf{u}^*(t), \boldsymbol{\gamma}(t))}{\partial \mathbf{x}}\right|_{\mathbf{x}=\mathbf{x}^*(t)}, \\ H(\mathbf{x}^*(t), \mathbf{p}^*(t), \mathbf{u}^*(t), \boldsymbol{\gamma}(t)) &= \max_{u \in \mathcal{U}} H(\mathbf{x}^*(t), \mathbf{p}^*(t), \mathbf{u}, \boldsymbol{\gamma}(t)), \\ \mathbf{x}(0) &= \mathbf{x_0}, \\ \mathbf{p}^*(T_f) &= \mathbf{0}. \end{aligned} \tag{2.21}$$

For the rigorous formulation of the Maximum Principle for more general optimal control problems, see for example [52] and [54]. The formulation of the discrete Maximum Principle for dynamical systems governed by difference equations is presented in [55].

The focus of this Thesis is on control methods that are of the feedback form, i.e., $\mathbf{u} = \mathbf{g}(t, \mathbf{x})$. The optimal controls in this form and the sufficient conditions for optimality are provided by the dynamic programming principle and the solution to the Hamilton-Jacobi-Bellman (HJB) equation [56]. Let us redefine the performance criterion (2.2) such that it corresponds to the *remaining* cost associated with the control $\mathbf{u}(t)$ and initial conditions $\mathbf{x}_0$:

$$J(\tau, \mathbf{x}_0, \mathbf{u}) = \int_{\tau}^{T_f} L(\mathbf{x}(t), \mathbf{u}(t))\, \mathrm{d}t, \quad \tau \in \mathbb{T}, \quad \mathbf{x}(\tau) = \mathbf{x_0}. \tag{2.22}$$

Observe, that $J(T_f, \mathbf{x}, \mathbf{u}) = 0$, $\forall \mathbf{x} \in \mathbb{R}^n$ and that $J(0, \mathbf{x}_0, \mathbf{u})$ corresponds to the performance criterion (2.2). Let us also define the optimal *cost-to-go* as a value of the performance criterion associated with an optimal control:

$$V(\tau, \mathbf{x}_0) = \min_{\mathbf{u}(\cdot)} J(\tau, \mathbf{x}_0, \mathbf{u}). \tag{2.23}$$

Sufficient Conditions for Optimality. *Let $V(t, \mathbf{x}) : \mathbb{T} \times \mathbb{R}^n \mapsto \mathbb{R}^+$ be a Lipschitz-continuous function that is a viscosity solution of the boundary value problem:*

$$-\frac{\partial V}{\partial t} = \min_{\mathbf{u}(t) \in \mathcal{U}} \left[L(\mathbf{x}(t), \mathbf{u}(t)) + \frac{\partial V(t, \mathbf{x})}{\partial \mathbf{x}} \mathbf{f}(\mathbf{x}(t), \mathbf{u}(t), \boldsymbol{\gamma}(t)) \right], \quad V(T_f, \mathbf{x}) = 0, \, \forall \mathbf{x} \in \mathbb{R}^n. \tag{2.24}$$

Then V is the optimal cost-to-go (2.23)*, $V(0, \mathbf{x_0})$ is the optimal value of the performance index* (2.3) *and the control law:*

$$\mathbf{u}^*(t, \mathbf{x}) = \arg\min_{\mathbf{u} \in \mathcal{U}} \left(L(\mathbf{x}(t), \mathbf{u}) + \frac{\partial V(t, \mathbf{x})}{\partial \mathbf{x}} \mathbf{f}(\mathbf{x}(t), \mathbf{u}, \boldsymbol{\gamma}(t)) \right) \tag{2.25}$$

is an optimal control law.

For the definition of the notion of the viscosity solution and the discussion on the sufficient conditions for optimality, see [54, Chapters 7, 8].

Observe that both the necessary conditions provided by the Maximum Principle and the sufficient conditions obtained via the dynamic programming employ functions that depend on the future behaviour of the dynamical system:

- The costate function $\mathbf{p}^*$ of the Maximum Principle is defined by the ordinary dynamical equation that depends on $\mathbf{f}$ with final value $\mathbf{p}^*(T_f) = 0$.
- The optimal *cost-to-go* function $V(t, \mathbf{x})$ of the HJB equation is defined by the partial differential equation that depends on $\mathbf{f}$ with the final boundary condition $V(T_f, \mathbf{x}) = 0$.

To obtain the solution of the optimal control problem (2.3) via the Maximum Principle or the HJB equation, the trajectories of the functions $\mathbf{p}^*$ and V have to be computed *backward in time*, that is, their values in time T depend on future values of the function $\mathbf{f}(\cdot, \cdot, \boldsymbol{\gamma}(t))$, $t \geq T$. Because the control problem (2.3) considered in this work assumes that the mechanical system is affected by unpredictable disturbances and change of the parameters, that is, the future values of the function $\boldsymbol{\gamma}(t)$ are not known at the time $t = 0$, the optimal control for such a case cannot be established. Instead, the near-optimal control based on the adaptation to changing working conditions is proposed.

2.2 Adaptive near-optimal control method

As stated above, the optimal control problem for the systems subjected to an unpredictable change or disturbance cannot be solved in a real-life application. This work focuses on near-optimal control methods that provide approximate solutions to a series of optimal control problems based on a frequently updated approximations of the problem (2.3).

The main idea of the proposed approach is to transform the unsolvable optimal control problem (2.3) into the series of simpler and approachable formulations. The new formulations depend on temporary working conditions of the system and can be solved either in the optimal or near-optimal sense. Reformulations of the control problem are attained via frequent measurements of the varying parameter $\boldsymbol{\gamma}(t)$ that represents changes occurring in the stabilized system. These measurements trigger the adaptation of the control problem formulation that corresponds to the current condition of the system. The adaptation is performed sequentially with constant time period h.

The general approach can be formulated in a Model Predictive Control framework presented in Algorithm 2.1.

Algorithm 2.1 The main loop of the MPC-based control methods

1: At the time $t_i = h \cdot i$, based on real-time measurements, establish the new dynamical model defined by function $\mathbf{f}_i$ of the system (2.1).
2: Compute the control law $\mathbf{u}_i^*(\mathbf{x})$ that is optimal or near-optimal with respect to the performance criterion J_i for dynamical model $\mathbf{f}_i$.
3: Apply the control according to the measured state, $\mathbf{u}_i^*(\mathbf{x}(t_i))$.
4: Increment $t_{i+1} \leftarrow t_i + h$.

To provide low computational complexity of the control law update, this work proposes the model $\mathbf{f}_i$ to be restricted to a function independent of time, i.e.,

$$\dot{\tilde{\mathbf{x}}}(t) = \mathbf{f}_i(\tilde{\mathbf{x}}(t), \mathbf{u}(t)), \quad \tilde{\mathbf{x}}(t_i) = \tilde{\mathbf{x}}_i, \tag{2.26}$$

where $\tilde{\mathbf{x}} \in \mathbb{R}^{\tilde{n}}$ is a state vector of the approximation of the original model (2.1). The initial conditions $\tilde{\mathbf{x}}_i \in \mathbb{R}^{\tilde{n}_i}$ depend on the measured state of the system $\mathbf{x}$ and the measurements of the disturbance signal $\boldsymbol{\gamma}$. Observe that the order of the approximation $\tilde{n}_i$ is not necessarily equal to the order n of the unmodified system. In addition, the receding horizon of the control method is assumed to be infinite:

$$J_i(\mathbf{u}) = \int_{t_i}^{\infty} L_i(\tilde{\mathbf{x}}(t), \mathbf{u}(t))\,\mathrm{d}t. \tag{2.27}$$

These two modifications (2.26) and (2.27) reduce the dimensionality of the original optimal control problem (2.3), as the solution to the modified problem is independent of time. The typical MPC computation algorithms have a complexity linear with respect to time. The proposed approach significantly lower the computational burden of the control method, as they rely on the stationary control problem formulation. The modified optimal control

problem can be then summarized in a similar fashion to (2.3):

$$\begin{aligned}
&\textbf{Find } \mathbf{u}_i^* : \mathbb{R}^{\tilde{n}_i} \mapsto \mathcal{U} \subset \mathbb{R}^m, \\
&\textbf{such that: } \mathbf{u}_i^*(\tilde{\mathbf{x}}) = \underset{\mathbf{u}(\tilde{\mathbf{x}}(t)) \in \mathcal{U},\ \forall t \in \mathbb{T}_i}{\arg\min} J_i(\mathbf{u}) = \int_{t_i}^{\infty} L_i(\tilde{\mathbf{x}}(t), \mathbf{u}(\tilde{\mathbf{x}}(t)))\,\mathrm{d}t, \\
&\textbf{subject to: } \dot{\tilde{\mathbf{x}}}(t) = \mathbf{f}_i(\tilde{\mathbf{x}}(t), \mathbf{u}(\tilde{\mathbf{x}}(t))), \\
&\qquad \tilde{\mathbf{x}}(t_i) = \tilde{\mathbf{x}}_i, \\
&\qquad \mathbb{T}_i = [t_i, \infty) \\
&\qquad t_i = h \cdot i, \\
&\qquad i = 0,\, 1,\, \ldots,\, N-1, \\
&\qquad t_N = T_f.
\end{aligned} \tag{2.28}$$

The modified optimal control problem is solved sequentially with equal time shifts $t_i = h \cdot i$, $i = 0,\, 1,\, \ldots,\, N-1$ to adapt the solution to the changing working conditions denoted by the $\boldsymbol{\gamma}(t)$ in the original formulation (2.1). Observe that the proposed method employs the Model Predictive Control framework: the control function $\mathbf{u}_i^*$ computed at the time instance t_i is applied to the system only on the first time interval $t \in [t_i,\, t_{i+1})$. After that, the optimal control is recomputed for the shifted time horizon of the performance index, $\mathbb{T}_i \to \mathbb{T}_{i+1}$.

Because the proposed approach relies on the infinite time-horizon formulation, a special focus has to be kept on a well-posedness of the modified optimal control problem, i.e., the existence of the admissible controls for which the performance criterion (2.28) exists. In this work, the considered control problems are characterized by linear and bilinear dynamical systems. For such systems, it is showed that this well-posedness is closely linked to the notions of stability and stabilizability. The well-posedness of this modified control problem is individually considered for each proposed control method and, in general, is guaranteed by the intrinsic properties of the system's dynamics or the special modification L_i of the function L.

2.3 Specific control problems considered in Thesis

This work is focused on the mechanical systems governed by the differential equations of the two independent forms:

- The case of mechanical system subjected to an external disturbance:

$$\mathbf{M}\ddot{\mathbf{q}}(t) + \mathbf{C}\dot{\mathbf{q}}(t) + \mathbf{K}\mathbf{q}(t) = \mathbf{F}(\mathbf{u}(t), \mathbf{q}(t), \dot{\mathbf{q}}(t)) + \mathbf{D}z(t), \quad \begin{bmatrix} \mathbf{q}(0) \\ \dot{\mathbf{q}}(0) \end{bmatrix} = \begin{bmatrix} \mathbf{q}_0 \\ \dot{\mathbf{q}}_0 \end{bmatrix}. \tag{2.29}$$

- The case of a mechanical system subjected to a change of its parameters:

$$\mathbf{M}(t)\ddot{\mathbf{q}}(t) + \mathbf{C}(t)\dot{\mathbf{q}}(t) + \mathbf{K}(t)\mathbf{q}(t) = \mathbf{F}(\mathbf{u}(t), \mathbf{q}(t), \dot{\mathbf{q}}(t)), \quad \begin{bmatrix} \mathbf{q}(0) \\ \dot{\mathbf{q}}(0) \end{bmatrix} = \begin{bmatrix} \mathbf{q}_0 \\ \dot{\mathbf{q}}_0 \end{bmatrix}, \tag{2.30}$$

where $\mathbf{q} \in \mathbb{R}^{n_q}$ is the vector of the generalized coordinates of the system, $\dot{\mathbf{q}}$ and $\ddot{\mathbf{q}}$ are the first and second derivatives of these coordinates, respectively. The vectors $\mathbf{q}_0$ and $\dot{\mathbf{q}}_0$ corresponds to the initial conditions. The matrix $\mathbf{M} \in \mathbb{R}^{n_q \times n_q}$ is the mass matrix of the system, $\mathbf{K} \in \mathbb{R}^{n_q \times n_q}$ is the stiffness matrix, $\mathbf{C} \in \mathbb{R}^{n_q \times n_q}$ is the damping matrix and $\mathbf{F}(\mathbf{u}(t), \mathbf{q}(t), \dot{\mathbf{q}}(t)) \in \mathbb{R}^{n_q}$ defines the dependence of the force generated by actuators on the control $\mathbf{u} \in \mathbb{R}^m$ and the system's state $\mathbf{q}$, $\dot{\mathbf{q}}$. In the first considered case, the additional term $z(t) \in \mathbb{R}$ represents the disturbance affecting the system and the matrix $\mathbf{D} \in \mathbb{R}^n$ represents the impact of the disturbance on the system. In the second, the variation of the internal parameters is realised by the varying matrices, $\mathbf{M}(t)$, $\mathbf{K}(t)$, $\mathbf{C}(t)$. We restrict our focus to the cases with $\mathbf{M}(t)$, $\mathbf{Z}(t)$, $\mathbf{K}(t)$, $\mathbf{C}(t)$ being piecewise continuous on the considered time interval $\mathbb{T} = [0,\, T_f]$.

We consider two independent types of actuation: active and semi-active. They are realised by two different forms of the vector function $\mathbf{F}$:

- For the active control, the force depends linearly on the control value:

$$\mathbf{F}(\mathbf{u}(t), \mathbf{q}(t), \dot{\mathbf{q}}(t)) = \mathbf{F}(\mathbf{u}) = \mathbf{E}_F \mathbf{u}. \tag{2.31}$$

- For the semi-active control, the force depends linearly on the control and the state of the system:

$$\mathbf{F}(\mathbf{u}(t), \mathbf{q}(t), \dot{\mathbf{q}}(t)) = \sum_{i=1}^{m} u_i \left(\mathbf{E}_{K,\,i}\mathbf{q} + \mathbf{E}_{C,\,i}\dot{\mathbf{q}}\right), \quad i = 1,\, 2,\, \ldots,\, m. \tag{2.32}$$

The matrix $\mathbf{E}_F \in \mathbb{R}^{n_q \times m}$ defines the relation between the force generated by actuators and the control value and $\mathbf{E}_{K,\,i} \in \mathbb{R}^{n_q \times n_q}$, $\mathbf{E}_{C,\,i} \in \mathbb{R}^{n_q \times n_q}$, $i = 1,\, 2,\, \ldots,\, m$ represent the assumption, that the forces generated by semi-active devices depend linearly not only on the control value but also on the generalized coordinates (deflections) and/or their derivatives (velocities), respectively.

With the substitution $\mathbf{x} = \begin{bmatrix}\mathbf{q}^T & \dot{\mathbf{q}}^T\end{bmatrix}^T$, $\mathbf{x} \in \mathbb{R}^n$, $n = 2n_q$, all considered control scenarios can be summarized via three independent first-order dynamical equations with initial conditions:

1. active control and an external disturbance:

$$\dot{\mathbf{x}}(t) = \mathbf{A}\mathbf{x}(t) + \mathbf{B}\mathbf{u}(t) + \mathbf{B}_z z(t), \quad \mathbf{x}(0) = \mathbf{x_0}, \tag{2.33}$$

with:

$$\begin{aligned} \mathbf{A} &= \begin{bmatrix} \mathbf{0} & \mathbb{I} \\ -\mathbf{M}^{-1}\mathbf{K} & -\mathbf{M}^{-1}\mathbf{C} \end{bmatrix}, \quad \mathbf{B}_z = \begin{bmatrix} \mathbf{0} \\ \mathbf{M}^{-1}\mathbf{D} \end{bmatrix}, \\ \mathbf{B} &= \begin{bmatrix} \mathbf{0} \\ \mathbf{M}^{-1}\mathbf{E_F} \end{bmatrix}, \qquad\qquad \mathbf{x_0} = \begin{bmatrix} \mathbf{q}_0 \\ \dot{\mathbf{q}}_0 \end{bmatrix} \end{aligned} \tag{2.34}$$

2. active control and a change of internal parameters:

$$\dot{\mathbf{x}}(t) = \mathbf{A}(t)\mathbf{x}(t) + \mathbf{B}\mathbf{u}, \quad \mathbf{x}(0) = \mathbf{x_0}, \tag{2.35}$$

with $\mathbf{B}$ as in (2.34) and:

$$\mathbf{A}(t) = \begin{bmatrix} \mathbf{0} & \mathbb{I} \\ -\mathbf{M}^{-1}(t)\mathbf{K}(t) & -\mathbf{M}^{-1}(t)\mathbf{C}(t) \end{bmatrix}, \quad \mathbf{x_0} = \begin{bmatrix} \mathbf{q}_0 \\ \dot{\mathbf{q}}_0 \end{bmatrix}. \tag{2.36}$$

Observe that the varying matrix $\mathbf{M}(t)$ is assumed restricted such that the matrix $\mathbf{B}$ remains constant in time, i.e., $\mathbf{M}^{-1}(t)\mathbf{E}_F = \text{const}$.

3. semi-active control and an external disturbance

$$\dot{\mathbf{x}}(t) = \mathbf{A}\mathbf{x}(t) + \sum_{j=1}^{m} u_j(t)\mathbf{B}_j\mathbf{x}(t) + \mathbf{B}_z z(t), \quad \mathbf{x}(0) = \mathbf{x_0}, \tag{2.37}$$

with $\mathbf{A}$, $\mathbf{B}_z$, $\mathbf{x_0}$ defined as in (2.34) and:

$$\mathbf{B}_j = \begin{bmatrix} \mathbf{0} & \mathbf{0} \\ \mathbf{M}^{-1}\mathbf{E}_{K,j} & \mathbf{M}^{-1}\mathbf{E}_{C,j} \end{bmatrix}, \quad j = 1, 2, \ldots, m, \tag{2.38}$$

We focus our attention on performance criteria (2.2) that have the form:

$$J(\mathbf{u}) = \int_0^{T_f} \left[\mathbf{x}^T(t)\mathbf{Q}\mathbf{x}(t) + \mathbf{u}^T(t)\mathbf{R}\mathbf{u}(t)\right] \mathrm{d}t, \tag{2.39}$$

where $\mathbf{Q} \in \mathbb{R}^{n\times n}$, $\mathbf{Q} \succ 0$ and $\mathbf{R} \in \mathbb{R}^{m\times m}$ and $\mathbf{R} \succ 0$ or $\mathbf{R} = \mathbf{0}$. Such a choice of performance criteria corresponds to the goal of minimization of the deviation of the system's state $\mathbf{x}$ on the whole time interval $\mathbb{T}$. In addition, the matrix $\mathbf{Q}$ can be defined in such a way, that it reflects the internal energy of the controlled system. In that case, the goal of the control would be to optimally dissipate energy accumulated in the system. The term associated with the matrix $\mathbf{R}$ reflects the cost of the control. Large value of $\mathbf{R}$ in relation to $\mathbf{Q}$ corresponds to the case with control being expensive. The case with $\mathbf{R}$ small or equal to $\mathbf{0}$ is associated with the control that is cheap or has no cost at all. The latter is especially common in the structural control with semi-active devices, which can generate forces of a large magnitude with a minimal energy consumption.

The adaptive control methods for the particular control problems characterized by dynamical models (2.33)–(2.38) and the performance criterion (2.39) are formulated in details in Chapters 3 and 4.

Chapter 3

Adaptive control in presence of changing disturbance

In this chapter, the adaptive control method for mechanical systems affected by an auxiliary disturbance is formulated and presented. The attention is focused on active and semi-active dynamical models presented in Eqs. (2.33) and (2.37):

$$\dot{\mathbf{x}}(t) = \mathbf{A}\mathbf{x}(t) + \mathbf{B}\mathbf{u}(t) + \mathbf{B}_z z(t), \quad \mathbf{x}(0) = \mathbf{x_0}, \tag{3.1}$$

$$\dot{\mathbf{x}}(t) = \mathbf{A}\mathbf{x}(t) + \sum_{j=1}^{m} u_j(t)\mathbf{B}_j\mathbf{x}(t) + \mathbf{B}_z z(t), \quad \mathbf{x}(0) = \mathbf{x_0}. \tag{3.2}$$

The goal of the control is to stabilize these systems with minimization of the performance index:

$$J(\mathbf{u}) = \int_0^{T_f} \left[\mathbf{x}^T(t)\mathbf{Q}\mathbf{x}(t) + \mathbf{u}^T(t)\mathbf{R}\mathbf{u}(t)\right] \mathrm{d}t. \tag{3.3}$$

The aim of the adaptive approach formulated in Section 2.2 is to sequentially approximate systems (3.1), (3.2) by the dynamical models that do not depend explicitly on time. Observe that the only element of the systems' dynamical equations (3.1), (3.2) that depends explicitly on time (besides the control) is the term associated with the external disturbance, $z(t)$. As a consequence, the goal of the time-invariant approximation is achieved by approximating the disturbance $z(t)$ at the time interval $[t_i,\, t_{i+1})$ by the linear time-invariant system:

$$\begin{aligned} \dot{\mathbf{x}}_{z,i}(t) &= \mathbf{A}_{z,i}\mathbf{x}_{z,i}(t), \quad \mathbf{x}_{z,\,i}(t_i) = \mathbf{x}_{z0,i}, \\ \tilde{z}_i(t) &= \mathbf{C}_{z,i}\mathbf{x}_{z,i}(t), \quad \text{such that: } \tilde{z}_i(t) \approx z(t), \end{aligned} \tag{3.4}$$

where $\mathbf{x}_{z,i}(t) \in \mathbb{R}^{n_{z,i}}$ is the state of the approximation model, $\tilde{z}_i(t) \in \mathbb{R}$ is the approximation of the disturbance signal and $\mathbf{A}_{z,i} \in \mathbb{R}^{n_{z,i}\times n_{z,i}}$, $\mathbf{C}_{z,i} \in \mathbb{R}^{1\times n_{z,i}}$ are state and output matrices of the approximation to be calculated by the identification procedure. Observe that the matrices $\mathbf{A}_{z,i}$ and $\mathbf{C}_{z,i}$ and their sizes $n_{z,i}$ are allowed change in every iteration of the adaptation, denoted here by the index i.

The approximation (3.4) is then incorporated into the active model (3.1) as follows:

$$\dot{\tilde{\mathbf{x}}}(t) = \begin{bmatrix} \dot{\mathbf{x}}_i(t) \\ \dot{\mathbf{x}}_{z,i}(t) \end{bmatrix} = \begin{bmatrix} \mathbf{A} & \mathbf{B}_z\mathbf{C}_{z,i} \\ \mathbf{0} & \mathbf{A}_{z,i} \end{bmatrix} \begin{bmatrix} \mathbf{x}_i(t) \\ \mathbf{x}_{z,i}(t) \end{bmatrix} + \begin{bmatrix} \mathbf{B} \\ \mathbf{0} \end{bmatrix} \mathbf{u}(t), \quad \begin{bmatrix} \mathbf{x}_i(t_i) \\ \mathbf{x}_{z,i}(t_i) \end{bmatrix} = \begin{bmatrix} \mathbf{x}(t_i) \\ \mathbf{x}_{z0,i} \end{bmatrix} \tag{3.5}$$

and into the semi-active model (3.2):

$$\begin{aligned}\dot{\tilde{\mathbf{x}}}_i(t) = \begin{bmatrix}\dot{\mathbf{x}}_i(t)\\ \dot{\mathbf{x}}_{z,i}(t)\end{bmatrix} = \begin{bmatrix}\mathbf{A} & \mathbf{B}_z\mathbf{C}_{z,i}\\ \mathbf{0} & \mathbf{A}_{z,i}\end{bmatrix}\begin{bmatrix}\mathbf{x}_i(t)\\ \mathbf{x}_{z,i}(t)\end{bmatrix} + \sum_{j=1}^{m}\left(u_j(t)\begin{bmatrix}\mathbf{B}_j & \mathbf{0}\\ \mathbf{0} & \mathbf{0}\end{bmatrix}\right)\begin{bmatrix}\mathbf{x}_i(t)\\ \mathbf{x}_{z,i}(t)\end{bmatrix},\\ \begin{bmatrix}\mathbf{x}_i(t_i)\\ \mathbf{x}_{z,i}(t_i)\end{bmatrix} = \begin{bmatrix}\mathbf{x}(t_i)\\ \mathbf{x}_{z0,i}\end{bmatrix},\end{aligned} \tag{3.6}$$

where $\tilde{\mathbf{x}}_i \in \mathbb{R}^{\tilde{n}}$, $\tilde{n} = n + n_{z,i}$ is the state vector of the i-th time-invariant model of a disturbed system, $\mathbf{x}_i \in \mathbb{R}^n$ is the state of the i-th approximation corresponding to the state of the mechanical system and $\mathbf{x}_{z,i} \in \mathbb{R}^{n_{z,i}}$ is the state of the i-th approximation of the auxiliary disturbance process. The initial conditions for this approximation consist of the direct measurement of the actual state of the controlled system, $\mathbf{x}(t_i)$ and the initial condition of the disturbance model $\mathbf{x}_{z0,i}$ that is defined separately for each disturbance identification scheme. Observe that resulting models (3.5), (3.6) are linear and bilinear, respectively and both do not depend explicitly on time.

The performance index for the approximated systems (3.5) and (3.6) can be formulated in such a way that retains the value of the original performance index (3.3):

$$J_i(\mathbf{u}) = \int_0^{T_f}\left[\tilde{\mathbf{x}}_i^T(t)\begin{bmatrix}\mathbf{Q} & \mathbf{0}\\ \mathbf{0} & \mathbf{0}\end{bmatrix}\tilde{\mathbf{x}}_i(t) + \mathbf{u}^T(t)\mathbf{R}\mathbf{u}(t)\right]\mathrm{d}t. \tag{3.7}$$

In the next section, two methods of the disturbance identification that are employed in the proposed control methods are formulated.

3.1 Methods of disturbance identification

The identification of the system based on the measurements can be conducted in many distinctive ways. The approaches are divided into the parametric identification, where the structure of the identified model is known *a priori* and only its parameters are tuned up and *black box* identification, where the internal structure of the model gives no physical insights about the identified process. For the comprehensive review of the system identification methods, see [57].

Autoregressive identification

The first identification approach employed in the proposed control methods is autoregressive (AR) identification. Autoregressive models are linear and the computation of their weights has low complexity, which makes them suitable for fast calculation of the disturbance model (3.4). It is important to point out that the AR models are discrete with respect to time and the identified model is the discrete equivalent of the continuous model (3.4):

$$\begin{aligned}\mathbf{x}_{z,i}(k+1) &= \mathbf{A}_{z,i}\mathbf{x}_{z,i}(k), \quad \mathbf{x}_{z,i}(i) = \mathbf{x}_{z0,i},\\ \tilde{z}_i(k) &= \mathbf{C}_{z,i}\mathbf{x}_{z,i}(k), \quad \text{such that: } \tilde{z}_i(k) \approx z(t_k),\end{aligned} \tag{3.8}$$

It is then assumed that the continuous dynamics of the controlled system (3.1), (3.2) can be successfully approximated by the discrete model.

Let

$$\begin{bmatrix} z_{i-S+1} & z_{i-S+2} & \cdots & z_i \end{bmatrix} \tag{3.9}$$

be the time series of the disturbance z_k sampled with the equidistant times t_k, $k = i-S+1, i-S+2, \ldots, i$, i.e., $z_k = z(t_k)$. The length of the series is S. To obtain this vector, one can use measurements of the past S values of the disturbance or employ an external signal extrapolator which provides forecasts of the future values of the disturbance. The design of such an extrapolator does not fall within the scope of this work, and it is assumed that the disturbance approximation is based on the past values of the perturbation.

The deterministic AR model of order $n_{z,i}$ has the following form

$$z(k+1) = \sum_{j=1}^{n_{z,i}} \theta_{j,i} z(k+1-j) = \begin{bmatrix} z(k) & z(k-1) & \cdots & z(k-n_{z,i}+1) \end{bmatrix} \cdot \boldsymbol{\Theta}_i, \tag{3.10}$$

where $\boldsymbol{\Theta}_i$ denotes the vector of weights of the AR model at the i-th iteration of the identification process:

$$\boldsymbol{\Theta}_i = \begin{bmatrix} \theta_{1,i} & \theta_{2,i} & \cdots & \theta_{n_{z,i},i} \end{bmatrix}^T. \tag{3.11}$$

The weights vector is computed such that it minimizes the quadratic estimation error R_{LSE} based on the past S measurements of the signal $z(t)$:

$$\begin{aligned} \boldsymbol{\Theta}_i &= \underset{\boldsymbol{\Theta} \in \mathbb{R}^{n_{z,i}}}{\arg\min}\, R_{\mathrm{LSE}} \\ &= \underset{\boldsymbol{\Theta} \in \mathbb{R}^{n_{z,i}}}{\arg\min} \sum_{k=i+n_{z,i}-S+1}^{i} \left(z_k - \begin{bmatrix} z_i(k-1) & z_i(k-2) & \cdots & z_i(k-n_{z,i}) \end{bmatrix} \boldsymbol{\Theta} \right)^2. \end{aligned} \tag{3.12}$$

The minimization problem (3.12) reduces to the matrix equation:

$$\mathbf{H}_i \boldsymbol{\Theta}_i = \sum_{k=i+n_{z,i}-S+1}^{i} z_k \begin{bmatrix} z_{k-1} \\ z_{k-2} \\ \vdots \\ z_{k-n_{z,i}} \end{bmatrix}, \tag{3.13}$$

where matrix $\mathbf{H}_i \in \mathbb{R}^{n_{z,i} \times n_{z,i}}$ is defined as follows:

$$\mathbf{H}_i = \sum_{k=i+n_{z,i}-S+1}^{i} \begin{bmatrix} z_{k-1} \\ z_{k-2} \\ \vdots \\ z_{k-n_{z,i}} \end{bmatrix} \cdot \begin{bmatrix} z_{k-1} & z_{k-2} & \cdots & z_{k-n_{z,i}} \end{bmatrix}. \tag{3.14}$$

Observe that the matrix $\mathbf{H}_i$ and the right-hand-side of the Eq. (3.13) consist of only elements of the measurement vector (3.9).

The solution to the equation (3.13) in the least-square sense is as follows:

$$\boldsymbol{\Theta}_i = \mathbf{H}_i^{+} \begin{bmatrix} z_{i-S+n_{z,i}+1} \\ z_{i-S+2} \\ \vdots \\ z_i \end{bmatrix}, \tag{3.15}$$

where $\mathbf{H}_i^+$ denotes the Moore-Penrose pseudoinverse of the matrix $\mathbf{H}_i$. It is easy to conclude that the number of the considered values (the size of the signal window) S and the order of the model $n_{z,i}$ have to satisfy the inequality

$$S \geq n_{z,i} + 1. \tag{3.16}$$

The AR model (3.10) can be reformulated in the discrete state-space representation

$$\begin{bmatrix} z(k+1) \\ z(k) \\ \vdots \\ z(k-n_{z,i}+2) \end{bmatrix} = \begin{bmatrix} \theta_{1,i} & \theta_{2,i} & \cdots & \theta_{n_{z,i}-1,i} & \theta_{n_{z,i},i} \\ 1 & 0 & \cdots & 0 & 0 \\ 0 & 1 & \ddots & 0 & 0 \\ \vdots & \ddots & \ddots & \ddots & \vdots \\ 0 & 0 & \cdots & 1 & 0 \end{bmatrix} \cdot \begin{bmatrix} z(k) \\ z(k-1) \\ \vdots \\ z(k-n_{z,i}+1) \end{bmatrix}. \tag{3.17}$$

Observe, that the difference equation (3.17) represents the desired model of the disturbance of the form defined in Eq. (3.8) with:

$$\begin{aligned} \mathbf{A}_{z,i} &= \begin{bmatrix} \theta_{1,i} & \theta_{2,i} & \cdots & \theta_{n_{z,i}-1,i} & \theta_{n_{z,i},i} \\ 1 & 0 & \cdots & 0 & 0 \\ 0 & 1 & \ddots & 0 & 0 \\ \vdots & \ddots & \ddots & \ddots & \vdots \\ 0 & 0 & \cdots & 1 & 0 \end{bmatrix}, \quad \mathbf{C}_{z,i} = \begin{bmatrix} 1 & 0 & \cdots & 0 \end{bmatrix}, \\ \mathbf{x}_{z0,i} &= \begin{bmatrix} z(t_i) \\ z(t_{i-1}) \\ \vdots \\ z(t_{i-n_{z,i}+1}) \end{bmatrix} \end{aligned} \tag{3.18}$$

and the state of the disturbance model $\mathbf{x}_{z,i}(k)$ consists of the consecutive measurements of the disturbance z. Such a choice of the state vector is particularly beneficial because the state vector in this form can be directly measured without the employment of any state estimation scheme.

If the approximation of the disturbance is based on the preceding values of the signal, it is obvious that the control scheme cannot be initiated until the number of the available past values of the disturbance is not less than some set parameter $S_{\min}$ ($n_{z,i}+1 \leq S_{\min} \leq S$). If the dynamic equation governing the evolution of the disturbance $z(t)$ in time is nonlinear and/or varies in time, it is highly recommended to choose relatively small values of S and $S_{\min}$. Otherwise, the past measurements that correspond to the previous character of the disturbance will dominate the measurement vector (3.9) over the new measurements. Because the approximation of the disturbance calculated by Eq. (3.15) depends on the whole measurement vector, it would be biased towards the outdated character of the load. It is important to observe that the measurements that reflect the former behaviour of the load will still appear in the measurement vector until the next S values of the disturbance are measured.

It must be emphasized that in some cases the dynamics of the disturbance has a different order than the order of the approximation $n_{z,i}$. In such a case, the autoregressive approximation may provide a model that does not provide the best approximation of the disturbance, with the forecasted trajectory of the disturbance significantly diverging from the actual one. As a consequence, the use of such an overfitted or underfitted model can result in the worse performance of the control law and even lead to instability of the control system. This situation can be avoided for example if we compute the series of AR models with orders ranging from 1 to some set parameter $n_{\max}$ and choose the best one according to some criterion. In [58], the authors propose the criterion called *final prediction error* (FPE) that is of the form:

$$\mathrm{FPE}_j = \left(1 + \frac{j+1}{S}\right) \frac{S}{S-1-j} R_{\mathrm{LSE}}, \tag{3.19}$$

where j is the order of the AR model. We propose to introduce this scheme into the identification method, that is, at every iteration of the method compute the series of AR models and pick the best according to the criterion (3.19).

The identification method is summarized in Algorithm 3.1. Observe that the compu-

Algorithm 3.1 The autoregressive identification of the disturbance

Require: The range of the order of the approximation $n_{\max}$, maximal and minimal size of the measurement vector S, $S_{\min}$.

1: At the time t_i, measure the disturbance value $z_i = z(t_i)$ and add it to the vector of past measurements $\begin{bmatrix} z_1 & z_2 & \dots & z_{i-1} \end{bmatrix}$.
2: **if** Size of the measurement vector is smaller than $S_{\min}$ **then**
3: Wait for the next measurement $i \leftarrow i + 1$.
4: **else**
5: **if** Size of the measurement vector is larger than S **then**
6: Trim the vector such that it consists of only last S measurements.
7: **end if**
8: $n_{z,i} = 1$
9: **while** $n_{z,i} \leq n_{\max}$ **do**
10: Build the matrix H_i according to Eq. (3.14).
11: Compute the Moore-Penrose pseudoinverse matrix $\mathbf{H}_i^+$.
12: Find the weights of the approximation $\mathbf{\Theta}_i$ by computing the equation (3.15).
13: Compute the error R_{LSE} according to Eq. (3.12).
14: Compute the FPE_j criterion according to Eq. (3.19).
15: $n_{z,i} \leftarrow n_{z,i} + 1$
16: **end while**
17: Pick the optimal AR model.
18: Build matrices $\mathbf{A}_{z,i}$, $\mathbf{C}_{z,i}$ with weights of the optimal AR model as in Eq. (3.18).
19: **end if**

tational complexity of the Algorithm 3.1 is clearly dominated by the calculation of the matrix $\mathbf{H}_i$ and its pseudoinverse $\mathbf{H}_i^+$ on lines 10 and 11. Both operations have complexity $\mathcal{O}(Sn_{z,i}^2)$ and $\mathcal{O}(n_{z,i}^3)$ respectively. The example of the pseudoinverse algorithm of such complexity is proposed in [57]. The loop starting at line 9 is executed $n_{\max}$ times and with the assumption that the length of the measurement window S is fixed, the final complexity

of the algorithm 3.1 with respect to the parameter $n_{\max}$ is $\mathcal{O}(n_{\max}^4)$. The AR identification is employed in adaptive control methods presented in Sections 3.2 and 3.3.

Parametric identification

The autoregressive identification method can be used when there is no knowledge about the intrinsic process governing the disturbance $z(t)$. In this section, we focus on a situation when the disturbance $z(t)$ is not directly measurable, but rather the dynamical model of the disturbance (3.4) is known and it depends on the set of measurable parameters $\boldsymbol{\gamma}_i = \boldsymbol{\gamma}(t_i)$, $\boldsymbol{\gamma}_i \in \mathbb{R}^p$:

$$\begin{aligned} \dot{\mathbf{x}}_{z,i}(t) &= \mathbf{A}_{z,i}(\boldsymbol{\gamma}_i)\mathbf{x}_{z,i}(t), \quad \mathbf{x}_{z,\,i}(t_i) = \mathbf{x}_{z0,i}(\boldsymbol{\gamma}_i), \\ \tilde{z}_i(t) &= \mathbf{C}_{z,i}(\boldsymbol{\gamma}_i)\mathbf{x}_{z,i}(t), \quad \text{such that: } \tilde{z}_i(t) \approx z(t). \end{aligned} \tag{3.20}$$

Typical examples of such a scenario are: a moving load with measurements of its mass, velocity and position or a sinusoidal disturbance with measurements of its frequency and phase. In such a case, the identification procedure is straightforward and consists only of the computation of matrices $\mathbf{A}_{z,i}(\boldsymbol{\gamma}_i)$, $\mathbf{C}_{z,i}(\boldsymbol{\gamma}_i)$ and the initial state vector $\mathbf{x}_{z0,i}(\boldsymbol{\gamma}_i)$. The procedure is summarized in Algorithm 3.2. If we assume that the values of elements of

Algorithm 3.2 The parametric identification of the disturbance

Require: Functions $\mathbf{A}_{z,i}(\boldsymbol{\gamma}_i)$, $\mathbf{C}_{z,i}(\boldsymbol{\gamma}_i)$ and $\mathbf{x}_{z0,i}(\boldsymbol{\gamma}_i)$.

1: At the time t_i, measure the parameters value $\boldsymbol{\gamma}_i = \boldsymbol{\gamma}(t_i)$.
2: Calculate matrices $\mathbf{A}_{z,i}(\boldsymbol{\gamma}_i)$, $\mathbf{C}_{z,i}(\boldsymbol{\gamma}_i)$ and vector $\mathbf{x}_{z0,i}(\boldsymbol{\gamma}_i)$.

matrices $\mathbf{A}_{z,i}(\boldsymbol{\gamma}_i)$, $\mathbf{C}_{z,i}(\boldsymbol{\gamma}_i)$ and the vector $\mathbf{x}_{z0,i}(\boldsymbol{\gamma}_i)$ that depend the measured parameters $\boldsymbol{\gamma}_i$ can be calculated in constant time (e.g., when this dependence is stated via basic arithmetic operations, such as addition and multiplication), then the computational complexity of Algorithm 3.2 is $\mathcal{O}\left(n_{z,i}^2 \cdot p\right)$. This simple identification scheme is employed in Section 3.4.

3.2 Finite horizon LQR with autoregressive identification of disturbance

The novel control method formulated in Section 3.3 is based on the control approach firstly introduced in [9]. The authors of the aforementioned paper propose the adaptive seismic stabilization method employing the AR disturbance identification and finite horizon LQR. The brief formulation of this control method is presented in this section. In addition, the comprehensive numerical analysis of the scheme that examines the impact of the method's parameters on the performance of the controller is presented in Section 5.1. The contents of this section have been originally presented in the author's paper [47].

Let the active control system with an auxiliary disturbance be defined via the linear time-variant differential Eq. (3.1). The discrete equivalent of the continuous model (3.1) with the sampling time h is defined as follows:

$$\mathbf{x}(k+1) = \mathbf{A}_D\mathbf{x}(k) + \mathbf{B}_D\mathbf{u}(k) + \mathbf{B}_{zD}z(k), \quad \mathbf{x}(0) = \mathbf{x}_0 \tag{3.21}$$

where the matrices $\mathbf{A}_D$, $\mathbf{B}_D$, $\mathbf{B}_{zD}$ of the discrete model are determined from the matrices $\mathbf{A}$, $\mathbf{B}$, $\mathbf{D}$ of the continuous model (3.1) by employing one of the system discretization methods. If the zero-order hold method is used, then the matrices are computed as follows:

$$\begin{aligned} \mathbf{A}_D &= e^{\mathbf{A}h}, \quad \mathbf{B}_D = \int_0^h e^{\mathbf{A}t}\,\mathrm{d}t\,\mathbf{B}, \\ \mathbf{B}_{zD} &= \int_0^h e^{\mathbf{A}t}\,\mathrm{d}t\,\mathbf{B}_z. \end{aligned} \tag{3.22}$$

The discrete finite horizon performance index that is analogous to the continuous index (3.3) is for the time horizon $T = h \cdot i_T$ defined as follows:

$$J = \sum_{k=0}^{i_T} \left(\mathbf{x}^T(k)\mathbf{Q}\mathbf{x}(k) + \mathbf{u}^T(k)\mathbf{R}\mathbf{u}(k) \right). \tag{3.23}$$

The goal of the control method is to stabilize the system (3.1) with the prescribed integral quadratic performance index (3.3). In every time instance t_i, the disturbance $z(t)$ is approximated by the autoregressive model according to Algorithm 3.1. As a result, the i-th discrete approximation of the whole system that consists of the autoregressive disturbance model established at the time instant $t_i = h \cdot i$ is as follows:

$$\begin{aligned} \tilde{\mathbf{x}}_i(k+1) &= \begin{bmatrix} \mathbf{x}_i(k+1) \\ \mathbf{x}_{z,i}(k+1) \end{bmatrix} = \begin{bmatrix} \mathbf{A}_D & \mathbf{B}_{zD}\mathbf{C}_{z,i} \\ \mathbf{0} & \mathbf{A}_{z,i} \end{bmatrix} \begin{bmatrix} \mathbf{x}_i(k) \\ \mathbf{x}_{z,i}(k) \end{bmatrix} + \begin{bmatrix} \mathbf{B}_D \\ \mathbf{0} \end{bmatrix} \mathbf{u}(k), \quad \mathbf{x}_i(i) = \mathbf{x}(t_i), \\ \mathbf{x}_{z,i}(i) &= \begin{bmatrix} z(t_i) \\ z(t_{i-1}) \\ \vdots \\ z(t_{i-n_{z,i}+1}) \end{bmatrix}. \end{aligned} \tag{3.24}$$

The receding-horizon discrete performance index can be now stated analogously to (3.7) in the Model Predictive Control fashion:

$$J_i(\mathbf{u}) = \sum_{k=i}^{i+i_T} \left[\tilde{\mathbf{x}}_i^T(k) \begin{bmatrix} \mathbf{Q} & \mathbf{0} \\ \mathbf{0} & \mathbf{0} \end{bmatrix} \tilde{\mathbf{x}}_i(k) + \mathbf{u}^T(k)\mathbf{R}\mathbf{u}(k) \right]. \tag{3.25}$$

The sequence of modified optimal control problems for the approximations (3.24) and the performance index (3.25) in the general form (2.28) is defined as follows:

$$\begin{aligned} &\textbf{Find: } \mathbf{u}_i^* : \mathbb{T}_i \times \mathbb{R}^{\tilde{n}} \mapsto \mathcal{U} \subset \mathbb{R}^m, \\ &\textbf{such that: } \mathbf{u}_i^*(k, \tilde{\mathbf{x}}_i) = \underset{\mathbf{u}(k,\tilde{\mathbf{x}}_i(k)) \in \mathcal{U},\ k \in \mathbb{T}_i}{\arg\min} J_i(\mathbf{u}) = \\ &\qquad \sum_{k \in \mathbb{T}_i} \left[\tilde{\mathbf{x}}_i^T(k) \begin{bmatrix} \mathbf{Q} & \mathbf{0} \\ \mathbf{0} & \mathbf{0} \end{bmatrix} \tilde{\mathbf{x}}_i(k) + \mathbf{u}^T(k)\mathbf{R}\mathbf{u}(k) \right], \\ &\textbf{subject to: } \textbf{difference equation and initial conditions } (3.24), \\ &\qquad t_i = h \cdot i, \\ &\qquad \mathbb{T}_i = \{i,\, i+1,\, \ldots,\, i+i_T\}. \end{aligned} \tag{3.26}$$

The magnitude of the positive definite matrix $\mathbf{R}$ is assumed chosen in such a way, that the resulting optimal control $\mathbf{u}_i^*$ belongs to the interior of the control set $\mathcal{U}$ for the considered range of excitations, that is, the constraints of the control value do not have to be treated explicitly.

For the finite control horizon - that is for $i_T < \infty$, the solution to (3.26) exists for any dynamics (3.24). In this case, the solution to (3.26) is represented by the linear state-feedback control of the form:

$$\mathbf{u}_i^*(k) = -\mathbf{K}_i(k)\tilde{\mathbf{x}}_i(k), \tag{3.27}$$

where $\mathbf{K}_i(k) \in \mathbb{R}^{m\times\tilde{n}}$ is the time-varying gain matrix depending on the temporary approximation of the disturbance and is computed backwards by solving the discrete dynamic Riccati equation with final conditions:

$$\begin{aligned}
\mathbf{K}_i(k) =& \left(\mathbf{R} + \begin{bmatrix}\mathbf{B}_D\\ \mathbf{0}\end{bmatrix}^T \mathbf{P}_i(k+1)\begin{bmatrix}\mathbf{B}_D\\ \mathbf{0}\end{bmatrix}\right)^{-1}\begin{bmatrix}\mathbf{B}_D\\ \mathbf{0}\end{bmatrix}^T \mathbf{P}_i(k+1)\begin{bmatrix}\mathbf{A}_D & \mathbf{B}_{zD}\mathbf{C}_{z,i}\\ \mathbf{0} & \mathbf{A}_{z,i}\end{bmatrix},\\
\mathbf{P}_i(k) =& \begin{bmatrix}\mathbf{Q} & \mathbf{0}\\ \mathbf{0} & \mathbf{0}\end{bmatrix} + \begin{bmatrix}\mathbf{A}_D & \mathbf{B}_{zD}\mathbf{C}_{z,i}\\ \mathbf{0} & \mathbf{A}_{z,i}\end{bmatrix}^T \mathbf{P}_i(k+1)\begin{bmatrix}\mathbf{A}_D & \mathbf{B}_{zD}\mathbf{C}_{z,i}\\ \mathbf{0} & \mathbf{A}_{z,i}\end{bmatrix}\\
&- \begin{bmatrix}\mathbf{A}_D & \mathbf{B}_{zD}\mathbf{C}_{z,i}\\ \mathbf{0} & \mathbf{A}_{z,i}\end{bmatrix}^T \mathbf{P}_i(k+1)\begin{bmatrix}\mathbf{B}_D\\ \mathbf{0}\end{bmatrix}\\
&\cdot\left(\mathbf{R} + \begin{bmatrix}\mathbf{B}_D\\ \mathbf{0}\end{bmatrix}^T \mathbf{P}_i(k+1)\begin{bmatrix}\mathbf{B}_D\\ \mathbf{0}\end{bmatrix}\right)^{-1}\begin{bmatrix}\mathbf{B}_D\\ \mathbf{0}\end{bmatrix}^T \mathbf{P}_i(k+1)\begin{bmatrix}\mathbf{A}_D & \mathbf{B}_{zD}\mathbf{C}_{z,i}\\ \mathbf{0} & \mathbf{A}_{z,i}\end{bmatrix},\\
\mathbf{P}_i(i+i_T) =& \mathbf{0},
\end{aligned} \tag{3.28}$$

where $\mathbf{P}_i(k) \in \mathbb{R}^{\tilde{n}\times\tilde{n}}$, $k = i,\, i+1,\, \ldots,\, i+i_T$ is the positive-definite Riccati matrix. For the full derivation of the LQR for the systems that are not disturbed, the reader is referred to [5]. The performance of the control (3.27) depends on the approximation of the disturbance dynamics, as represented by the matrices $\mathbf{A}_{z,i}$, $\mathbf{C}_{z,i}$.

In the case when there is an insufficient number of the measurements of the signal $z(t)$, that is, $i < S_{\min}$ and the model of the disturbance cannot be established, it is proposed to calculate the control law with the simplifying assumption that the disturbance does not affect the system:

$$\begin{aligned}
\mathbf{K}_i(k) =& \left(\mathbf{R} + \mathbf{B}_D^T\mathbf{P}_i(k+1)\mathbf{B}_D\right)^{-1}\mathbf{B}_D^T\mathbf{P}_i(k+1)\mathbf{A}_D,\\
\mathbf{P}_i(k) =& \mathbf{Q} + \mathbf{A}_D^T\mathbf{P}_i(k+1)\mathbf{A}_D\\
&- \mathbf{A}_D^T\mathbf{P}_i(k+1)\mathbf{B}_D\left(\mathbf{R} + \mathbf{B}_D^T\mathbf{P}_i(k+1)\mathbf{B}_D\right)^{-1}\\
&\cdot \mathbf{B}_D^T\mathbf{P}_i(k+1)\mathbf{A}_D,\\
\mathbf{P}_i(i+i_T) =& \mathbf{0}, \quad \mathbf{P}_i(k) \in \mathbb{R}^{n\times n},\ k = i,\, i+1,\, \ldots,\, i+i_T.
\end{aligned} \tag{3.29}$$

In that case, the optimal control law is affine with respect to only the measured state:

$$\mathbf{u}_i^*(k) = -\mathbf{K}_i(k)\mathbf{x}(t_k). \tag{3.30}$$

Observe that this situation occurs only at the very beginning of the control and is believed not to play any crucial role on the overall performance of the proposed method.

The benefit of the finite horizon formulation of the optimal control problem (3.26) is that the optimal control can be established without imposing any restrictions on the system matrices of the approximation (3.24). However, because the value of the control at the time instant t_i, $\mathbf{u}_i^*(i)$, depends on the all future values of matrix $\mathbf{P}_i(k)$, the computation burden of the iterative scheme (3.28) grows linearly with the horizon i_T. If we assume that the operations of the multiplication and the inversion of a square matrix have complexity proportional to the cube of a matrix's size[1] then the computational complexity of the scheme (3.28) is $\mathcal{O}\left(i_T \cdot \tilde{n}^3\right)$.

The final finite horizon adaptive method proposed in [9], consisting of the identification of the disturbance and the computation of the LQR feedback control law can be summarized in the form of Algorithm 2.1: The computational complexity of the one iteration of the control

Algorithm 3.3 The main loop of the finite horizon active control method

Require: LQR horizon i_T, the range of the order of the AR approximation $n_{\max}$, maximal and minimal size of the measurement vector S, $S_{\min}$

1: At the time $t_i = h \cdot i$, measure state of the system $\mathbf{x}(t_i)$, value of the disturbance $z(t_i)$.
2: Execute the autoregressive identification procedure described in Algorithm 3.1.
3: **if** $i \geq S_{\min}$ and the identification procedure computed the matrices $\mathbf{A}_{z,i}$, $\mathbf{C}_{z,i}$ **then**
4: Compute the optimal gain matrix $\mathbf{K}_i(i)$, by solving the equation (3.28).
5: Apply the control according to the measured state and the disturbance, $\mathbf{u}_i^*(i) = -\mathbf{K}_i(i)\tilde{\mathbf{x}}_i(i)$, with the state of the approximation $\tilde{\mathbf{x}}_i$ defined as in (3.24).
6: **else**
7: Compute $\mathbf{K}_i(i) \in \mathbb{R}^{m \times n}$, by solving the Riccati equation without the AR model, Eq. (3.29).
8: Apply the control according to just the measured state, $\mathbf{u}_i^*(i) = -\mathbf{K}_i(i)\mathbf{x}(t_i)$.
9: **end if**
10: Increment $i \leftarrow i + 1$.

method presented in Algorithm 3.3 is equal to $\mathcal{O}\left(i_T \cdot \tilde{n}^3 + n_{max}^4\right)$. With the reasonable assumptions that $\tilde{n}^3 \gg n_{max}^4$ and $i_T \gg n_{max}$, the computational complexity of Algorithm 3.3 reduces to $\mathcal{O}\left(i_T \cdot \tilde{n}^3\right)$. This finite horizon adaptive control method is validated and analysed numerically in Section 5.1.

3.3 Alpha-shift and infinite horizon modification

In this section, the novel adaptive control method based on the controller defined in Section 3.2 is presented. It is based on the Author's paper [51] (to be published). The development of this approach has been motivated by two drawbacks of the finite horizon method:

- Since the computational complexity of the finite horizon method is linear with respect to the time horizon i_T, the choice of a large horizon makes the computation time

[1] The complexity $\mathcal{O}\left(\tilde{n}^3\right)$ corresponds to *naive* divide-and-conquer algorithm for matrix multiplication and inversion. There exists a number of sub-cubic algorithms, e.g., [59] of complexity $\mathcal{O}\left(\tilde{n}^{\log_2 7}\right)$ that exhibit better performance for very large matrices. In the context of this work, we assume that the order $\tilde{n}$ is not large enough to justify the use of these algorithms.

of the method proportionally longer. With a horizon too large, the computation time may exceed the period of the adaptation loop h, which would make the method infeasible to use in real-time operation.

- Contrarily, an MPC control method can guarantee global stability of the control system only when a finite horizon is large enough, see theoretical results in [60, Theorem 4.2]. The phenomenon of instability caused by a too small horizon is also presented in this thesis, in the numerical analysis of the finite horizon method, see Figure 5.18. The figure presents the situation in which the method fails to stabilize the system for the finite horizon $T_{\text{horizon}} = i_T h < 0.5\,\text{s}$.

These two problems are especially significant in a case when the variation of the disturbance signal is considerably faster than the responsiveness of the controlled object. A very common example of such a scenario is a large structure subjected to an earthquake. The rapidity of an earthquake imposes a small discretization period h. On the other hand, natural frequencies of a large-mass structure are significantly lower than those typical to earthquakes. To accommodate a large inertia of a system and maintain good performance and stability of the controller, the finite horizon $T_{\text{horizon}} = i_T h$ has to be set appropriately long. As a consequence, the horizon of the discrete LQR scheme i_T is large and may prevent a real-time application of the method. To tackle these computation and performance problems here the use of the infinite horizon variant of the LQR controller is proposed.

For the discrete dynamical system with the disturbance model defined as in Eq. (3.24) and the infinite horizon performance index:

$$J_i(\mathbf{u}) = \sum_{k=i}^{\infty} \left[\tilde{\mathbf{x}}_i^T(k) \begin{bmatrix} \mathbf{Q} & \mathbf{0} \\ \mathbf{0} & \mathbf{0} \end{bmatrix} \tilde{\mathbf{x}}_i(k) + \mathbf{u}^T(k)\mathbf{R}\mathbf{u}(k) \right] \tag{3.31}$$

the infinite horizon optimal control problem can be formulated as follows:

$$\begin{aligned}
&\textbf{Find: } \mathbf{u}_i^* : \mathbb{R}^{\tilde{n}} \mapsto \mathcal{U} \subset \mathbb{R}^m, \\
&\textbf{such that: } \mathbf{u}_i^*(\tilde{\mathbf{x}}_i) = \underset{\mathbf{u}(\tilde{\mathbf{x}}_i(k)) \in \mathcal{U},\ k \in \mathbb{T}_i}{\arg\min} J_i(\mathbf{u}) = \\
&\qquad \sum_{k \in \mathbb{T}_i} \left[\tilde{\mathbf{x}}_i^T(k) \begin{bmatrix} \mathbf{Q} & \mathbf{0} \\ \mathbf{0} & \mathbf{0} \end{bmatrix} \tilde{\mathbf{x}}_i(k) + \mathbf{u}^T(k)\mathbf{R}\mathbf{u}(k) \right], \\
&\textbf{subject to: } \textbf{difference equation and initial conditions } (3.24), \\
&\qquad t_i = h \cdot i, \\
&\qquad \mathbb{T}_i = \{i,\, i+1,\, i+2,\, \ldots\}\,.
\end{aligned} \tag{3.32}$$

Observe that the formulation of the optimal control problem (3.32) is analogous to the general adaptive control problem stated in Eq. (2.28). The resulting optimal infinite horizon control law is similar to the control defined for finite horizon LQR, but the feedback matrix $\mathbf{K}$ is in this case constant and the Riccati equation is not dynamic, but algebraic. The control takes the form:

$$\mathbf{u}_i^*(k) = -\mathbf{K}_i \tilde{\mathbf{x}}_i(k), \tag{3.33}$$

where $\mathbf{K}_i \in \mathbb{R}^{m\times\tilde{n}}$ is the constant gain matrix that is computed by solving the discrete algebraic Riccati equation:

$$\begin{aligned}
\mathbf{K}_i &= \left(\mathbf{R} + \begin{bmatrix}\mathbf{B}_D\\ \mathbf{0}\end{bmatrix}^T \mathbf{P}_i \begin{bmatrix}\mathbf{B}_D\\ \mathbf{0}\end{bmatrix}\right)^{-1} \begin{bmatrix}\mathbf{B}_D\\ \mathbf{0}\end{bmatrix}^T \mathbf{P}_i \begin{bmatrix}\mathbf{A}_D & \mathbf{B}_{zD}\mathbf{C}_{z,i}\\ \mathbf{0} & \mathbf{A}_{z,i}\end{bmatrix},\\
\mathbf{P}_i &= \begin{bmatrix}\mathbf{Q} & \mathbf{0}\\ \mathbf{0} & \mathbf{0}\end{bmatrix} + \begin{bmatrix}\mathbf{A}_D & \mathbf{B}_{zD}\mathbf{C}_{z,i}\\ \mathbf{0} & \mathbf{A}_{z,i}\end{bmatrix}^T \mathbf{P}_i \begin{bmatrix}\mathbf{A}_D & \mathbf{B}_{zD}\mathbf{C}_{z,i}\\ \mathbf{0} & \mathbf{A}_{z,i}\end{bmatrix}\\
&\quad - \begin{bmatrix}\mathbf{A}_D & \mathbf{B}_{zD}\mathbf{C}_{z,i}\\ \mathbf{0} & \mathbf{A}_{z,i}\end{bmatrix}^T \mathbf{P}_i \begin{bmatrix}\mathbf{B}_D\\ \mathbf{0}\end{bmatrix} \left(\mathbf{R} + \begin{bmatrix}\mathbf{B}_D\\ \mathbf{0}\end{bmatrix}^T \mathbf{P}_i \begin{bmatrix}\mathbf{B}_D\\ \mathbf{0}\end{bmatrix}\right)^{-1}\\
&\quad \cdot \begin{bmatrix}\mathbf{B}_D\\ \mathbf{0}\end{bmatrix}^T \mathbf{P}_i \begin{bmatrix}\mathbf{A}_D & \mathbf{B}_{zD}\mathbf{C}_{z,i}\\ \mathbf{0} & \mathbf{A}_{z,i}\end{bmatrix},
\end{aligned} \tag{3.34}$$

where $\mathbf{P}_i$ is the positive-definite solution to the Riccati equation. The Riccati equation (3.34) can be solved very efficiently, e.g., with the use of the Shur method [6]. The computational complexity of the algorithm presented in the aforementioned paper is equal to $\mathcal{O}\left(\tilde{n}^3\right)$, where $\tilde{n}^3$ is the order of the problem. Observe that, as a consequence of the infinite horizon formulation, this complexity depends solely on the size of the system. When compared to the complexity of the finite horizon LQR presented in (3.28), we conclude that the infinite horizon method surpasses the finite horizon approach for large values of the horizon i_T.

This statement was computationally verified by comparison of the computation time of both finite and infinite LQR controllers for different orders of the system $\tilde{n}$ and different values of the finite horizon i_T. Results are presented in Figure 3.1. The blue colour

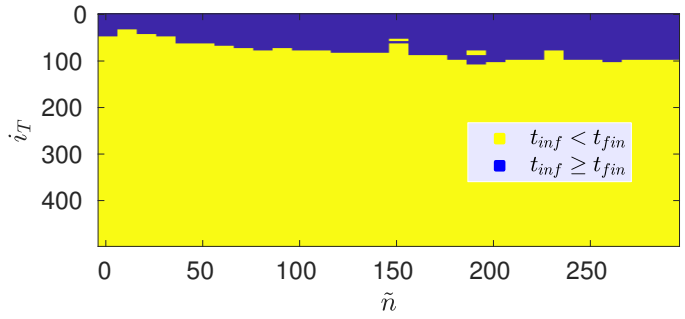

Figure 3.1: Comparison of the calculation times of finite (t_{fin}) and infinite horizon (t_{inf}) LQR for different values of the system order $\tilde{n}$ and the finite horizon N.

corresponds to such a pair of the parameters i_T and $\tilde{n}$ for which the computation time of the finite horizon LQR t_{fin} is smaller than the computation time of the infinite LQR t_{inf}. The yellow colour represents the opposite, i.e., situations, where t_{inf} is smaller than t_{fin}. Observe that the plot is divided into two coloured regions. With the growing size of the system's order $\tilde{n}$, the boundary between these regions is clearly limited from below, that is, it does not exceed finite horizon $i_T = 100$. We then conclude that for finite horizons i_T larger than 100, the infinite horizon approach will result in faster computation, despite the order $\tilde{n}$. The boundary $i_T = 100$ is easily exceeded in applications. For the control problem

analysed in Section 5.2, with a model of the order $n = 60$, the smallest finite horizon that has been found to provide acceptable performance is $i_T \approx 5000$. The computation time for this case was $0.2933 \pm 0.0299\,\mathrm{s}$. In contrast, the infinite horizon LQR for the same problem is computed in $0.0085 \pm 0.0013\,\mathrm{s}$ and gives superior control results to the finite horizon variant. Observe also that the finite horizon method stabilizes the drilling system in Section 5.1 only when i_T is larger than 100.

However, for the solution to the infinite horizon control problem (3.32) to exist, further assumptions for the structure of the control system have to be made:

Assumption 3.1. *The pair of the matrices of the controlled system*

$$\left(\begin{bmatrix} \mathbf{A}_D & \mathbf{B}_{zD}\mathbf{C}_{z,i} \\ \mathbf{0} & \mathbf{A}_{z,i} \end{bmatrix}, \begin{bmatrix} \mathbf{B}_D \\ \mathbf{0} \end{bmatrix} \right) \tag{3.35}$$

is stabilizable.

In addition, the optimal feedback defined in Eq. (3.33) stabilizes the controlled system if and only if the next assumption holds:

Assumption 3.2. *The pair of the matrices of the controlled system and the performance index*

$$\left(\begin{bmatrix} \mathbf{A}_D & \mathbf{B}_{zD}\mathbf{C}_{z,i} \\ \mathbf{0} & \mathbf{A}_{z,i} \end{bmatrix}, \begin{bmatrix} \mathbf{Q}^{\frac{1}{2}} & \mathbf{0} \end{bmatrix} \right), \tag{3.36}$$

where $\mathbf{Q}^{\frac{1}{2}}$ denotes the positive semi-definite square root of a matrix $\mathbf{Q}$ is detectable[2]*.*

The sufficiency of these conditions for the existence of infinite horizon LQR solution is proven in [61]. Stabilizability and detectability criteria can be stated in many equivalent forms. One exemplary criterion is: the pair $(\mathbf{A}, \mathbf{B})$ of the discrete dynamical system is stabilizable if and only if there exists a feedback control matrix $\mathbf{K}$ which makes the system asymptotically stable, i.e, the matrix $(\mathbf{A} - \mathbf{BK})$ has moduli of all its eigenvalues smaller than 1. An analogous condition can be stated for detectability: a pair $(\mathbf{A}, \mathbf{C})$ is detectable if and only if there exists a Luenberger observer matrix $\mathbf{L}$ which makes the error of a state estimation reach asymptotically 0, i.e., $(\mathbf{A} - \mathbf{LC})$ has moduli of all its eigenvalues smaller than 1. Observe that $(\mathbf{A}, \mathbf{B})$ is stabilizable if and only if $\left(\mathbf{A}^T, \mathbf{B}^T\right)$ is detectable. The stabilizability of the pair $(\mathbf{A}, \mathbf{B})$ can be then rigorously stated via checking if the next condition holds:

$$|\lambda| \geq 1 \;\Rightarrow\; \operatorname{rank}\left(\begin{bmatrix} \lambda\mathbb{I} - \mathbf{A} & \mathbf{B} \end{bmatrix} \right) = n, \quad \forall \lambda \in \mathbb{C}, \tag{3.37}$$

where n is the size of the square matrix $\mathbf{A}$. For the in-depth definitions of stabilizability, detectability and their stronger forms, controllability and observability for continuous systems, see for example [62, Appendix B]. The discrete equivalents of these criteria are discussed in [63, Chapter 6.2].

[2]The existence of the principal square root of a matrix $\mathbf{Q}$ is assured by the positive semi-definiteness property of this matrix.

Because of the changing and unpredictable value of the AR approximation $\mathbf{A}_{z,i}$, the fulfilment of detectability and stabilizability conditions is a non-trivial task. To ensure the existence of the solution of optimal control problem (3.32), we use the theory of LQR with *the alpha shift* [12]. In the aforementioned work, the authors added the exponential term α^{2k}, $\alpha > 1$ to the quadratic performance index (3.31) to increase the degree of stability of a completely controllable system. In the present work, we propose an opposite application, that is, we assume the modified performance criterion:

$$J_i(\mathbf{u}) = \sum_{k=i}^{\infty} \alpha_i^{2(k-i)} \left[\tilde{\mathbf{x}}_i^T(k) \begin{bmatrix} \mathbf{Q} & \mathbf{0} \\ \mathbf{0} & \mathbf{0} \end{bmatrix} \tilde{\mathbf{x}}_i(k) + \mathbf{u}^T(k)\mathbf{R}\mathbf{u}(k) \right] \tag{3.38}$$

with $\alpha_i < 1$, which relax stabilizability and detectability conditions. For the rest of this paper we also make standard assumptions about the controlled mechanical system:

Assumption 3.3. *The pair* $(\mathbf{A}_D, \mathbf{B}_D)$ *of the unaugmented control system* (3.21) *is stabilizable.*

Assumption 3.4. *The pair* $\left(\mathbf{A}_D, \mathbf{Q}^{\frac{1}{2}}\right)$ *of the unaugmented control system* (3.21) *and the matrix* $\mathbf{Q}$ *as in* (3.31) *is detectable.*

These assumptions are fulfilled by a majority of structural systems that display internal damping. In particular, the work [64] presents the necessary and sufficient conditions for asymptotic stability of an autonomous continuous mechanical system analogous to the system (2.29):

$$\mathbf{M}\ddot{\mathbf{q}}(t) + \mathbf{C}\dot{\mathbf{q}}(t) + \mathbf{K}\mathbf{q}(t) = \mathbf{0}, \quad \mathbf{q}(t) \in \mathbb{R}^{n_q}. \tag{3.39}$$

Theorem 3.1 ([64, Theorem 1, Corollary 2])**.** *Suppose the matrices of the system* (3.39) *have properties:* $\mathbf{K} \succ 0$ *and* $\mathbf{C} \succeq 0$*. Then the mechanical system* (3.39) *is asymptotically stable if and only if*

$$\operatorname{rank} \begin{bmatrix} \mathbf{C} \\ \mathbf{C}\left(\mathbf{M}^{-1}\mathbf{K}\right) \\ \mathbf{C}\left(\mathbf{M}^{-1}\mathbf{K}\right)^2 \\ \vdots \\ \mathbf{C}\left(\mathbf{M}^{-1}\mathbf{K}\right)^{n_q-1} \end{bmatrix} = n_q, \tag{3.40}$$

where n_q *is the number of the generalized coordinates of the system.*

Observe that the stability of the continuous autonomous system (3.39) directly implies the stability of its zero-order hold approximation[3] and, as a consequence, the stabilizability and detectability of the discrete system pairs presented in Assumptions 3.3 and 3.4. The

[3] A continuous linear autonomous system defined by a matrix $\mathbf{A}$ is asymptotically stable if and only if all eigenvalues λ_i of the matrix $\mathbf{A}$ have negative real part. A zero-order hold approximation of this system, defined by the matrix $\mathbf{A}_D = e^{\mathbf{A}h}$, has eigenvalues of the form $e^{\lambda_i h}$. If $\forall \lambda_i$, $\Re\lambda_i < 0$, then $\left|e^{\lambda_i h}\right| < 1$, which is a sufficient condition for the discrete linear autonomous to be asymptotically stable.

modified optimal control problem can be now stated as follows:

$$
\begin{aligned}
\textbf{Find: } & \mathbf{u}_i^* : \mathbb{R}^{\tilde{n}} \mapsto \mathcal{U} \subset \mathbb{R}^m, \\
\textbf{such that: } & \mathbf{u}_i^*(\tilde{\mathbf{x}}_i) = \underset{\mathbf{u}(\tilde{\mathbf{x}}_i(k)) \in \mathcal{U},\ k \in \mathbb{T}_i}{\arg\min} J_i(\mathbf{u}) = \\
& \sum_{k \in \mathbb{T}_i} \alpha_i^{2(k-i)} \left[\tilde{\mathbf{x}}_i^T(k) \begin{bmatrix} \mathbf{Q} & \mathbf{0} \\ \mathbf{0} & \mathbf{0} \end{bmatrix} \tilde{\mathbf{x}}_i(k) + \mathbf{u}^T(k) \mathbf{R} \mathbf{u}(k) \right], \qquad (3.41) \\
\textbf{subject to: } & \textbf{difference equation and initial conditions } (3.24), \\
& t_i = h \cdot i, \\
& \mathbb{T}_i = \{i,\, i+1,\, i+2,\, \ldots\}\,.
\end{aligned}
$$

As described above, the unique stabilizing solution to the infinite horizon LQR problem exists only for the linear systems and performance indices that fulfil the stabilizability and detectability criteria. However, in the presence of the varying matrix $\mathbf{A}_{z,i}$, fulfilment of these criteria is not guaranteed. Even if the measured disturbance $z(t)$ is asymptotically stable, its intrinsic nonlinearities and the presence of measurement errors may result in an unstable approximation $\mathbf{A}_{z,i}$.

When the disturbance model is unstable, there is no control $\mathbf{u}(k)$ that can prevent exponential growth of the state of the system with AR approximation (3.24) (because the control $\mathbf{u}(k)$ cannot affect the disturbance $\mathbf{x}_{z,i}(k)$). Consequently, the quadratic terms of the performance index (3.31) grow exponentially for every possible control and the infinite-horizon optimal control problem has no solution.

Nonetheless, if we introduce sufficiently small α_i into the performance index, the contracting exponential term $\alpha_i^{2(k-i)}$ will dominate the growth of the quadratic terms and allow the performance index to have a finite limit on the infinite time horizon, even if the system itself cannot be stabilized. Let us now formally state and prove the necessary value of the decay parameter α_i that guarantees well-posedness of the modified optimal control problem (3.41).

The exponential term α_i^k obviously varies with k, which transforms the original time independent formulation of performance index into an undesirable time-dependent one. To again get the time-independent optimal control problem, let us redefine the state of the approximated model $\tilde{\mathbf{x}}$ and the control $\mathbf{u}$ as the virtual state and control $\mathbf{y}$ and $\mathbf{w}$:

$$
\mathbf{y}(k) = \alpha_i^{k-i} \tilde{\mathbf{x}}(k), \quad \mathbf{w}(k) = \alpha_i^{k-i} \mathbf{u}(k). \qquad (3.42)
$$

Then the performance index (3.38) and the dynamics (3.24) takes the form:

$$
J_i = \sum_{k=i}^{\infty} \left[\mathbf{y}(k)^T \begin{bmatrix} \mathbf{Q} & \mathbf{0} \\ \mathbf{0} & \mathbf{0} \end{bmatrix} \mathbf{y}(k) + \mathbf{w}^T(k) \mathbf{R} \mathbf{w}(k) \right], \qquad (3.43)
$$

$$\mathbf{y}(k+1) = \alpha_i \begin{bmatrix} \mathbf{A}_D & \mathbf{B}_{zD}\mathbf{C}_{z,i} \\ \mathbf{0} & \mathbf{A}_{z,i} \end{bmatrix} \mathbf{y}(k) + \alpha_i \begin{bmatrix} \mathbf{B}_D \\ \mathbf{0} \end{bmatrix} \mathbf{w}(k), \quad \mathbf{y}(i) = \tilde{\mathbf{x}}(i) = \begin{bmatrix} \mathbf{x}(t_i), \\ z(t_i) \\ z(t_{i-1}) \\ \vdots \\ z(t_{i-n_{z,i}+1}) \end{bmatrix}. \tag{3.44}$$

It is apparent that the matrices of the system (3.44) and the performance index (3.43) do not explicitly depend on the time step k and, therefore, the solution of the infinite horizon LQR can be considered again. If this solution exists, then it is of the feedback form

$$\mathbf{w}^*(k) = -\mathbf{K}_i \mathbf{y}(k), \tag{3.45}$$

where the matrix $\mathbf{K}_i$ is computed via the algebraic Riccati equation with the incorporation of the exponential term α_i. The equation is defined as follows:

$$\begin{aligned} \mathbf{K}_i =& \alpha_i^2 \left(\mathbf{R} + \alpha_i^2 \begin{bmatrix} \mathbf{B}_D \\ \mathbf{0} \end{bmatrix}^T \mathbf{P}_i \begin{bmatrix} \mathbf{B}_D \\ \mathbf{0} \end{bmatrix} \right)^{-1} \begin{bmatrix} \mathbf{B}_D \\ \mathbf{0} \end{bmatrix}^T \mathbf{P}_i \begin{bmatrix} \mathbf{A}_D & \mathbf{B}_{zD}\mathbf{C}_{z,i} \\ \mathbf{0} & \mathbf{A}_{z,i} \end{bmatrix}, \\ \mathbf{P}_i =& \begin{bmatrix} \mathbf{Q} & \mathbf{0} \\ \mathbf{0} & \mathbf{0} \end{bmatrix} + \alpha_i^2 \begin{bmatrix} \mathbf{A}_D & \mathbf{B}_{zD}\mathbf{C}_{z,i} \\ \mathbf{0} & \mathbf{A}_{z,i} \end{bmatrix}^T \mathbf{P}_i \begin{bmatrix} \mathbf{A}_D & \mathbf{B}_{zD}\mathbf{C}_{z,i} \\ \mathbf{0} & \mathbf{A}_{z,i} \end{bmatrix} \\ & - \alpha_i^4 \begin{bmatrix} \mathbf{A}_D & \mathbf{B}_{zD}\mathbf{C}_{z,i} \\ \mathbf{0} & \mathbf{A}_{z,i} \end{bmatrix}^T \mathbf{P}_i \begin{bmatrix} \mathbf{B}_D \\ \mathbf{0} \end{bmatrix} \left(\mathbf{R} + \alpha_i^2 \begin{bmatrix} \mathbf{B}_D \\ \mathbf{0} \end{bmatrix}^T \mathbf{P}_i \begin{bmatrix} \mathbf{B}_D \\ \mathbf{0} \end{bmatrix} \right)^{-1} \\ & \cdot \begin{bmatrix} \mathbf{B}_D \\ \mathbf{0} \end{bmatrix}^T \mathbf{P}_i \begin{bmatrix} \mathbf{A}_D & \mathbf{B}_{zD}\mathbf{C}_{z,i} \\ \mathbf{0} & \mathbf{A}_{z,i} \end{bmatrix}. \end{aligned} \tag{3.46}$$

Observe that the transformation from the virtual optimal control $\mathbf{w}^*(k)$ to the actual control $\mathbf{u}^*(k)$ is straightforward:

$$\mathbf{u}^*(k) = \alpha^{i-k}\mathbf{w}^*(k) = -\alpha^{i-k}\mathbf{K}_i\mathbf{y}(k) = -\mathbf{K}_i\tilde{\mathbf{x}}(k). \tag{3.47}$$

Let us now proceed with basic remarks from control theory and matrix algebra. Spectrum σ and spectral radius ρ of a triangular block matrix $\mathbf{A} = \begin{bmatrix} \mathbf{A}_{11} & \mathbf{A}_{12} \\ 0 & \mathbf{A}_{22} \end{bmatrix}$ depend only on its diagonal sub-matrices:

$$\sigma_{\mathbf{A}} = \sigma_{\mathbf{A}_{11}} \cup \sigma_{\mathbf{A}_{22}} \Rightarrow \rho(\mathbf{A}) = \max\{\rho(\mathbf{A}_{11}); \rho(\mathbf{A}_{22})\}. \tag{3.48}$$

The following is also true for every square matrix $\mathbf{A}$

$$\forall \alpha \in \mathbb{R}^+, \quad \rho(\alpha\mathbf{A}) = \alpha\rho(\mathbf{A}). \tag{3.49}$$

Every triple $(\mathbf{A}, \mathbf{B}, \mathbf{C})$ that describes a discrete linear control system $\mathbf{x}(k+1) = \mathbf{A}\mathbf{x}(k) + \mathbf{B}\mathbf{u}(k)$, $\mathbf{y}(k) = \mathbf{C}\mathbf{x}(k)$ can be decomposed into the Kalman canonical form

$$\begin{aligned}
\begin{bmatrix} \mathbf{x}_{RU}(k+1) \\ \mathbf{x}_{RO}(k+1) \\ \mathbf{x}_{UU}(k+1) \\ \mathbf{x}_{UO}(k+1) \end{bmatrix} &= \begin{bmatrix} \mathbf{A}_{11} & \mathbf{A}_{12} & \mathbf{A}_{13} & \mathbf{A}_{14} \\ 0 & \mathbf{A}_{22} & 0 & \mathbf{A}_{24} \\ 0 & 0 & \mathbf{A}_{33} & \mathbf{A}_{34} \\ 0 & 0 & 0 & \mathbf{A}_{44} \end{bmatrix} \begin{bmatrix} \mathbf{x}_{RU}(k) \\ \mathbf{x}_{RO}(k) \\ \mathbf{x}_{UU}(k) \\ \mathbf{x}_{UO}(k) \end{bmatrix} + \begin{bmatrix} \mathbf{B}_1 \\ \mathbf{B}_2 \\ \mathbf{0} \\ \mathbf{0} \end{bmatrix} \mathbf{u}(k), \\
\mathbf{y}(k) &= \begin{bmatrix} \mathbf{0} & \mathbf{C}_1 & \mathbf{0} & \mathbf{C}_2 \end{bmatrix} \begin{bmatrix} \mathbf{x}_{RU}(k) \\ \mathbf{x}_{RO}(k) \\ \mathbf{x}_{UU}(k) \\ \mathbf{x}_{UO}(k) \end{bmatrix}
\end{aligned} \tag{3.50}$$

where $\mathbf{x}_{RU}$, $\mathbf{x}_{RO}$, $\mathbf{x}_{UU}$, $\mathbf{x}_{UO}$ represents respectively, reachable and unobservable, reachable and observable, unreachable and unobservable, unreachable and observable parts of the system state. This decomposition can be defined as a similarity transformation by a transformation matrix $\mathbf{T}$

$$\begin{aligned}
&\begin{bmatrix} \mathbf{A}_{11} & \mathbf{A}_{12} & \mathbf{A}_{13} & \mathbf{A}_{14} \\ 0 & \mathbf{A}_{22} & 0 & \mathbf{A}_{24} \\ 0 & 0 & \mathbf{A}_{33} & \mathbf{A}_{34} \\ 0 & 0 & 0 & \mathbf{A}_{44} \end{bmatrix} = \mathbf{T}^{-1}\mathbf{A}\mathbf{T}, \\
&\begin{bmatrix} \mathbf{B}_1^T & \mathbf{B}_2^T & \mathbf{0} & \mathbf{0} \end{bmatrix}^T = \mathbf{T}^{-1}\mathbf{B}, \quad \begin{bmatrix} \mathbf{0} & \mathbf{C}_1 & \mathbf{0} & \mathbf{C}_2 \end{bmatrix} = \mathbf{C}\mathbf{T}.
\end{aligned} \tag{3.51}$$

The Kalman decomposition exists for every discrete linear system; for the proof, the reader is referred to [65]. The original proof for continuous systems is presented in [66].

The Kalman canonical form is very convenient to test for stabilizability and detectability. The system (3.50) is stabilizable if and only if the unreachable part of the system; that is, governed by $\begin{bmatrix} \mathbf{A}_{33} & \mathbf{A}_{34} \\ \mathbf{0} & \mathbf{A}_{44} \end{bmatrix}$ has spectral radius $\rho < 1$. The pair $(\mathbf{A}, \mathbf{C})$ is detectable if and only if the pair $\left(\mathbf{A}^T, \mathbf{C}^T\right)$ is stabilizable, that is, $\begin{bmatrix} \mathbf{A}_{11} & \mathbf{A}_{13} \\ \mathbf{0} & \mathbf{A}_{33} \end{bmatrix}$ has spectral radius $\rho < 1$.

Let us now define the matrix

$$\mathbf{T} = \begin{bmatrix} \mathbf{T}_{11} & \mathbf{T}_{12} & \mathbf{T}_{13} & \mathbf{T}_{14} \\ \mathbf{T}_{21} & \mathbf{T}_{22} & \mathbf{T}_{23} & \mathbf{T}_{24} \\ \mathbf{T}_{31} & \mathbf{T}_{32} & \mathbf{T}_{33} & \mathbf{T}_{34} \\ \mathbf{T}_{41} & \mathbf{T}_{42} & \mathbf{T}_{43} & \mathbf{T}_{44} \end{bmatrix}, \quad \mathbf{T} \in \mathbb{R}^{n \times n}, \tag{3.52}$$

such that it transforms the triple $\left(\alpha_i \mathbf{A}_D, \alpha_i \mathbf{B}_D, \mathbf{Q}^{\frac{1}{2}}\right)$ of the model (3.44) to the Kalman canonical form:

$$\begin{aligned}
\mathbf{T}^{-1}\alpha_i \mathbf{A}_D \mathbf{T} &= \alpha_i \begin{bmatrix} \mathbf{A}_{D,11} & \mathbf{A}_{D,12} & \mathbf{A}_{D,13} & \mathbf{A}_{D,14} \\ \mathbf{0} & \mathbf{A}_{D,22} & \mathbf{0} & \mathbf{A}_{D,24} \\ \mathbf{0} & \mathbf{0} & \mathbf{A}_{D,33} & \mathbf{A}_{D,34} \\ \mathbf{0} & \mathbf{0} & \mathbf{0} & \mathbf{A}_{D,44} \end{bmatrix}, \quad \mathbf{T}^{-1}\alpha_i \mathbf{B}_D = \alpha_i \begin{bmatrix} \mathbf{B}_{D,1} \\ \mathbf{B}_{D,2} \\ \mathbf{0} \\ \mathbf{0} \end{bmatrix} \\
\mathbf{Q}^{\frac{1}{2}}\mathbf{T} &= \begin{bmatrix} \mathbf{0} & \mathbf{Q}_1 & \mathbf{0} & \mathbf{Q}_2 \end{bmatrix}.
\end{aligned} \tag{3.53}$$

Observe that if we transform the triple corresponding to the whole model that incorporates the AR approximation:

$$\left(\alpha_i \begin{bmatrix} \mathbf{A}_D & \mathbf{B}_{zD}\mathbf{C}_{z,i} \\ \mathbf{0} & \mathbf{A}_{z,i} \end{bmatrix}, \alpha_i \begin{bmatrix} \mathbf{B}_D \\ \mathbf{0} \end{bmatrix}, \begin{bmatrix} \mathbf{Q}^{\frac{1}{2}} & \mathbf{0} \end{bmatrix}\right) \tag{3.54}$$

via the transformation matrix that has been built with the use of the matrix $\mathbf{T}$:

$$\hat{\mathbf{T}} = \begin{bmatrix} \mathbf{T}_{11} & \mathbf{T}_{12} & \mathbf{T}_{13} & \mathbf{T}_{14} & \mathbf{0} \\ \mathbf{T}_{21} & \mathbf{T}_{22} & \mathbf{T}_{23} & \mathbf{T}_{24} & \mathbf{0} \\ \mathbf{T}_{31} & \mathbf{T}_{32} & \mathbf{T}_{33} & \mathbf{T}_{34} & \mathbf{0} \\ \mathbf{T}_{41} & \mathbf{T}_{42} & \mathbf{T}_{43} & \mathbf{T}_{44} & \mathbf{0} \\ \mathbf{0} & \mathbf{0} & \mathbf{0} & \mathbf{0} & \mathbb{I} \end{bmatrix} \cdot \begin{bmatrix} \mathbb{I} & \mathbf{0} & \mathbf{0} & \mathbf{0} & \mathbf{0} \\ \mathbf{0} & \mathbb{I} & \mathbf{0} & \mathbf{0} & \mathbf{0} \\ \mathbf{0} & \mathbf{0} & \mathbb{I} & \mathbf{0} & \mathbf{0} \\ \mathbf{0} & \mathbf{0} & \mathbf{0} & \mathbf{0} & \mathbb{I} \\ \mathbf{0} & \mathbf{0} & \mathbf{0} & \mathbb{I} & \mathbf{0} \end{bmatrix}, \tag{3.55}$$

then the resulting matrices will also be in the Kalman form:

$$\begin{aligned} &\hat{\mathbf{T}}^{-1}\alpha_i \begin{bmatrix} \mathbf{A}_D & \mathbf{B}_{zD}\mathbf{C}_{z,i} \\ \mathbf{0} & \mathbf{A}_{z,i} \end{bmatrix} \hat{\mathbf{T}} = \alpha_i \begin{bmatrix} \mathbf{A}_{D,11} & \mathbf{A}_{D,12} & \mathbf{A}_{D,13} & \mathbf{Z}_1 & \mathbf{A}_{D,14} \\ \mathbf{0} & \mathbf{A}_{D,22} & \mathbf{0} & \mathbf{Z}_2 & \mathbf{A}_{D,24} \\ \mathbf{0} & \mathbf{0} & \mathbf{A}_{D,33} & \mathbf{Z}_3 & \mathbf{A}_{D,34} \\ \mathbf{0} & \mathbf{0} & \mathbf{0} & \mathbf{A}_z & \mathbf{0} \\ \mathbf{0} & \mathbf{0} & \mathbf{0} & \mathbf{Z}_4 & \mathbf{A}_{D,44} \end{bmatrix}, \\ &\begin{bmatrix} \mathbf{Z}_1 \\ \mathbf{Z}_2 \\ \mathbf{Z}_3 \\ \mathbf{Z}_4 \end{bmatrix} = \mathbf{T}^{-1}\mathbf{B}_{zD}\mathbf{C}_{z,i}, \quad \hat{\mathbf{T}}\alpha_i \begin{bmatrix} \mathbf{B}_D \\ \mathbf{0} \end{bmatrix} = \alpha_i \begin{bmatrix} \mathbf{B}_{D,1} \\ \mathbf{B}_{D,2} \\ \mathbf{0} \\ \mathbf{0} \\ \mathbf{0} \end{bmatrix}, \\ &\begin{bmatrix} \mathbf{Q}^{\frac{1}{2}} & \mathbf{0} \end{bmatrix} \hat{\mathbf{T}} = \begin{bmatrix} \mathbf{0} & \mathbf{Q}_1 & \mathbf{0} & \mathbf{0} & \mathbf{Q}_2 \end{bmatrix}. \end{aligned} \tag{3.56}$$

The particular position of $\mathbf{A}_{z,i}$ in the canonical Kalman form (3.56) emphasizes the fact that the state of a disturbance is both unreachable and unobservable. Let us now prove that the special choice of the decay parameter α_i guarantees the stabilizability and detectability of the system with decay (3.44).

Lemma 3.1. *If Assumption 3.3 holds and* $\alpha_i < \min\left\{1; \left(\rho\left(\mathbf{A}_{z,i}\right)\right)^{-1}\right\}$, *then the system* (3.44) *is stabilizable.*

Proof. Let

$$\mathbf{A}_{\text{stab.}} = \alpha_i \begin{bmatrix} \mathbf{A}_{D,33} & \mathbf{Z}_3 & \mathbf{A}_{D,34} \\ \mathbf{0} & \mathbf{A}_{z,i} & \mathbf{0} \\ \mathbf{0} & \mathbf{Z}_4 & \mathbf{A}_{D,44} \end{bmatrix} \tag{3.57}$$

denote the unreachable part of the dynamics (3.56). Then

$$\rho\left(\mathbf{A}_{\text{stab.}}\right) = \alpha_i \max\left\{\rho\left(\mathbf{A}_{D,33}\right); \rho\left(\mathbf{A}_{D,44}\right); \rho\left(\mathbf{A}_{z,i}\right)\right\}. \tag{3.58}$$

From Assumption 3.3 and property (3.48) we know that the unreachable part of the matrix $\mathbf{A}_D$ is stable:

$$\max\left\{\rho\left(\mathbf{A}_{D,33}\right); \rho\left(\mathbf{A}_{D,44}\right)\right\} < 1. \tag{3.59}$$

Two cases may occur:

$$\begin{cases} \rho\left(\mathbf{A}_{\text{stab.}}\right) < \alpha_i, & \text{if } \rho\left(\mathbf{A}_{z,i}\right) < 1, \\ \rho\left(\mathbf{A}_{\text{stab.}}\right) < \alpha_i \rho\left(\mathbf{A}_{z,i}\right), & \text{if } \rho\left(\mathbf{A}_{z,i}\right) \geq 1. \end{cases} \tag{3.60}$$

Observe that by substituting $\alpha_i < \min\left\{1; \left(\rho\left(\mathbf{A}_{z,i}\right)\right)^{-1}\right\}$ these two cases reduces to:

$$\forall \mathbf{A}_{z,i} \in \mathbb{R}^{n_{z,i} \times n_{z,i}} \quad \rho\left(\mathbf{A}_{\text{stab.}}\right) < 1, \tag{3.61}$$

which fulfils the stabilizability condition. □

Lemma 3.2. *If Assumption 3.4 holds and* $\alpha_i < \min\left\{1; \left(\rho\left(\mathbf{A}_{z,i}\right)\right)^{-1}\right\}$*, then the system* (3.44) *is detectable.*

Proof. The proof is parallel to the stabilizability proof. Let

$$\mathbf{A}_{\text{det.}} = \alpha_i \begin{bmatrix} \mathbf{A}_{D,11} & \mathbf{A}_{D,13} & \mathbf{Z}_1 \\ \mathbf{0} & \mathbf{A}_{D,33} & \mathbf{Z}_3 \\ \mathbf{0} & \mathbf{0} & \mathbf{A}_{z,i} \end{bmatrix} \tag{3.62}$$

denote the unobservable part of system (3.56) dynamics. Then from Assumption 3.4, we know that

$$\begin{cases} \rho\left(\mathbf{A}_{\text{det.}}\right) < \alpha_i, & \text{if } \rho\left(\mathbf{A}_{z,i}\right) < 1, \\ \rho\left(\mathbf{A}_{\text{det.}}\right) < \alpha_i \rho\left(\mathbf{A}_{z,i}\right), & \text{if } \rho\left(\mathbf{A}_{z,i}\right) \geq 1. \end{cases} \tag{3.63}$$

The same substitution $\alpha_i < \min\left\{1; \left(\rho\left(\mathbf{A}_{z,i}\right)\right)^{-1}\right\}$ provides that

$$\forall \mathbf{A}_{z,i} \in \mathbb{R}^{n_{z,i} \times n_{z,i}}, \quad \rho\left(\mathbf{A}_{\text{Det.}}\right) < 1, \tag{3.64}$$

which fulfils the detectability criterion. □

Let us now collect the preceding findings into the final result.

Theorem 3.2. *Let the discrete system* (3.21) *fulfil Assumptions 3.3, 3.4. If the parameter* α_i *is selected such that* $\alpha_i < \min\left\{1; \left(\rho\left(\mathbf{A}_{z,i}\right)\right)^{-1}\right\}$*, where* $\rho\left(\mathbf{A}_{z,i}\right)$ *denotes a spectral radius of the matrix* $\mathbf{A}_{z,i}$*, then the modified optimal control problem* (3.41) *has a stabilizing solution.*

Proof. The proof emerges directly from Lemmas 3.1 and 3.2. If we choose α_i such that it is smaller than $\min\left\{1; \left(\rho\left(\mathbf{A}_{z,i}\right)\right)^{-1}\right\}$, then the system (3.44) is stabilizable and detectable. This is a sufficient condition for the existence of a stabilizing solution of the infinite-horizon linear quadratic regulator problem, as can be deducted from [61].

Remark 3.1. *Observe that the solution to the modified optimal control problem with decay* α_i *defined in Eq.* (3.41) *is stabilizing for the modified system* (3.44)*, that is, there exists* $\gamma \in (0,\, 1)$ *and constant* $\Gamma \in \mathbb{R}^+$ *such that*

$$\|\mathbf{y}(k)\| \leq \Gamma \|\mathbf{y}(i)\| \gamma^{k-i}. \tag{3.65}$$

Unfortunately, when the AR model is unstable, the resulting optimal control law $\mathbf{u}^*$ *does not stabilize the original dynamical system defined in Eq.* (3.24) *but rather guarantee that the rate of destabilization does not exceed the magnitude of destabilization provided by the spectral radius* $\rho\left(\mathbf{A}_{z,i}\right)$*:*

$$\|\tilde{\mathbf{x}}(k)\| \leq \Gamma \|\tilde{\mathbf{x}}(i)\| \gamma^{k-i} \alpha^{i-k} < \Gamma \|\tilde{\mathbf{x}}(i)\| \rho\left(\mathbf{A}_{z,i}\right)^{k-i}, \quad \text{if } \rho\left(\mathbf{A}_{z,i}\right) \geq 1. \tag{3.66}$$

□

Remark 3.2. *A more aggressive control strategy may be established if we enforce*

$$\alpha_i < \min\left\{\rho\left(\mathbf{A}_{D,11}\right)^{-1}; \rho\left(\mathbf{A}_{D,33}\right)^{-1}; \rho\left(\mathbf{A}_{D,44}\right)^{-1}; \rho\left(\mathbf{A}_{z,i}\right)^{-1}\right\}. \tag{3.67}$$

In a case when $\rho\left(\mathbf{A}_{z,i}\right) < 1$*, the parameter* α_i *takes values larger than* 1*, which adds a degree of stability to the control. Unfortunately, such a reformulation requires prior knowledge of spectral radii of these specific submatrices of* $\mathbf{A}_D$*.*

Remark 3.3. *We assume that the time of computing* $\rho\left(\mathbf{A}_{z,i}\right)$ *is insignificant in the comparison to the solution time of the algebraic Riccati equation. This is a case when the order of the approximation* $n_{z,i}$ *is smaller than the order of the system* n*. In a case when there is a need to make computation even faster, one can use Gelfand's formula [67]:*

$$\rho\left(\mathbf{A}_{z,i}\right) = \lim_{k\to\infty} \left\|\mathbf{A}_{z,i}^k\right\|^{\frac{1}{k}}. \tag{3.68}$$

This sequence converges to $\rho\left(\mathbf{A}_{z,i}\right)$ from the above*; that is,* $\forall k \in \mathbb{N}, \quad \left\|\mathbf{A}_{z,i}^k\right\|^{\frac{1}{k}} > \rho\left(\mathbf{A}_{z,i}\right)$*. Using even the first iteration of* (3.68) *ensures that Lemmas 3.1 and 3.2 are fulfilled. The computational complexity of Gelfand's formula is* $\mathcal{O}\left(\log k \cdot n_{z,i}^3\right)$[4]*.*

The final infinite horizon adaptive control method is stated in Algorithm 3.4 via the procedure similar to Algorithm 3.3. The computational complexity of one iteration of the control method presented in Algorithm 3.4 is equal to $\mathcal{O}\left(\tilde{n}^3 + n_{max}^4 + \log k \cdot n_{z,i}^3\right)$, where k denotes the number of iteration of Gelfand's formula. Observe that $n_{z,i} \leq n_{max}$. With the reasonable assumptions that $\tilde{n}^3 \gg n_{max}^4$ and $k \ll 2^{n_{max}}$, the computational complexity of Algorithm 3.3 reduces to $\mathcal{O}\left(\tilde{n}^3\right)$. This infinite horizon adaptive control method is validated and analysed numerically in Section 5.2.

[4]With assumptions that the multiplication of a matrix has complexity equal to $\mathcal{O}\left(n_{z,i}^3\right)$ and the power of a matrix is computed via exponentiation by squaring.

Algorithm 3.4 The main loop of the infinite horizon active control method

Require: The range of the order of the AR approximation $n_{\max}$, maximal and minimal size of the measurement vector S, $S_{\min}$

At the time $t_i = h \cdot i$, measure state of the system $\mathbf{x}(t_i)$, value of the disturbance $z(t_i)$.
Execute the autoregressive identification procedure described in Algorithm 3.1.
if $i \geq S_{\min}$ and the identification procedure computed the matrices $\mathbf{A}_{z,i}$, $\mathbf{C}_{z,i}$ **then**
    $\alpha_i \leftarrow 1$
    Compute the spectral radius of the matrix $\rho(\mathbf{A}_{z,i})$.
    if $\rho(\mathbf{A}_{z,i}) > 1$ **then**
        $\alpha_i \leftarrow \rho^{-1}(\mathbf{A}_{z,i})\,\beta, \quad \beta < 1$
    end if
    Compute $\mathbf{K}_i$, by solving the algebraic Riccati equation with decay (3.46).
    Apply the control $\mathbf{u}_i^*(i) = -\mathbf{K}_i\tilde{\mathbf{x}}_i(i)$, with $\tilde{\mathbf{x}}_i$ defined in (3.24).
else
    Compute $\mathbf{K}_i \in \mathbb{R}^{m\times n}$, by solving the algebraic Riccati equation without the AR model.
    Apply the control according to just the measured state, $\mathbf{u}_i^*(i) = -\mathbf{K}_i\mathbf{x}(t_i)$.
end if
Increment $i \leftarrow i + 1$.

3.4 Semi-active system – Lyapunov switching control

In this section, a semi-active adaptive stabilization method for systems affected by a disturbance is proposed. The method, as the active control methods that have been defined in Sections 3.2 and 3.3, employs the linear time-invariant approximation of the disturbance that affects the controlled system. The quadratic performance criterion is defined on an infinite time horizon, similarly to the LQR-based control method proposed in Section 3.3. The *alpha shift* is also introduced as a guarantee that the control problem has a solution. Unlike the active control approaches, this method does not rely on explicit optimal solutions such as LQR. The proposed control law takes the extremal values of the control set and is characterised by a switching behaviour. It is showed that this control law is near-optimal and exceeds the performance of passive, constant control.

Let the semi-active control system subjected to an external disturbance be defined as in Eq. (3.2):

$$\dot{\mathbf{x}}(t) = \mathbf{A}\mathbf{x}(t) + \sum_{j=1}^{m} u_j(t)\mathbf{B}_j\mathbf{x}(t) + \mathbf{B}_z z(t), \quad \mathbf{x}(0) = \mathbf{x}_0, \quad \mathbf{u}(t) \in [u_{\min}, u_{\max}]^m, \quad (3.69)$$

where $\mathbf{x}(t) \in \mathbb{R}^n$ denotes the state of the system, $\mathbf{u}(t) \in \mathbb{R}^m$ is the control signal, $\mathbf{A} \in \mathbb{R}^{n\times n}$ is a state-transition matrix, the matrices $\mathbf{B}_j \in \mathbb{R}^{n\times n}$, $j = 1, 2, \ldots, m$ denote the set of the control matrices and the matrix $\mathbf{B}_z \in \mathbb{R}^n$ defines the impact of the disturbance $z(t) \in \mathbb{R}$ on the system.

Each entry of the vector of the control signal $\mathbf{u}(t)$ is assumed constrained within the interval $[u_{\min}, u_{\max}]$, $u_{\max} > u_{\min}$. Observe that with the affine transformation of the control

$$\hat{\mathbf{u}} = \frac{2}{u_{\max} - u_{\min}}\mathbf{u} - \frac{u_{\max} + u_{\min}}{u_{\max} - u_{\min}}\mathbf{1}, \quad (3.70)$$

the semi-active control system (3.69) is defined via a more generic control set:

$$\dot{\mathbf{x}}(t) = \mathbf{A}\mathbf{x}(t) + \sum_{j=1}^{m} \hat{u}_j(t)\mathbf{B}_j\mathbf{x}(t) + \mathbf{B}_z z(t), \quad \mathbf{x}(0) = \mathbf{x}_0, \quad \hat{\mathbf{u}}(t) \in [-1,1]^m. \tag{3.71}$$

Any control set defined as in Eq. (3.69) can be transformed into the form defined in Eq. (3.71). Thus, for simplicity and without loss of generality it is assumed that the control set for $\mathbf{u}(t)$ equals to $[-1,1]^m$.

The similar condition to the stabilizability of active systems defined in Assumption 3.1 is imposed on the system (3.69).

Assumption 3.5. *For the matrices* $\mathbf{A}$ *and* $\mathbf{B}_j$, $j = 1, 2, \ldots, m$ *there exists a known constant control* $\mathbf{u}_0 = \begin{bmatrix} u_{01} & u_{02} & \cdots & u_{0m} \end{bmatrix}^T$, $\mathbf{u}_0 \in [-1,1]^m$ *for which the closed-loop state-transition matrix*

$$\left(\mathbf{A} + \sum_{j=1}^{m} u_{0j}\mathbf{B}_j \right) \tag{3.72}$$

is stable.

Observe that in the special case of the matrix $\mathbf{A}$ being stable, this assumption is trivially satisfied by the constant control $\mathbf{u}_0 = \begin{bmatrix} 0 & \cdots & 0 \end{bmatrix}^T$.

The performance of the stabilization is measured by the quadratic performance index

$$J = \int_0^{T_f} \mathbf{x}(t)\mathbf{Q}\mathbf{x}(t)\,\mathrm{d}t, \tag{3.73}$$

where T_f denotes the horizon of the control and $\mathbf{Q}$ is such a positive semi-definite matrix that Assumption 3.6 holds.

Assumption 3.6. *The matrix* $\mathbf{Q}$ *and matrices* $\mathbf{A}$, $\mathbf{B}_j$, $j = 1, 2, \ldots, m$ *are such that all pairs*

$$\left(\left(\mathbf{A} + \sum_{j=1}^{m} u_j\mathbf{B}_j \right), \mathbf{Q} \right) : \quad \mathbf{u} \in [-1,1]^m \tag{3.74}$$

are observable.

Notice that, unlike the criteria for the active control methods, this performance criterion does not depend explicitly on the value of the control. Such a formulation corresponds to the fact, that the power consumption of the semi-active devices is very often negligible. From the analysis of the HJB equation (2.24) and Maximum Principle (2.21), it can be easily showed that the optimal control in the case of the performance criterion (3.73) takes only the extremal values[5], i.e. $\mathbf{u}^*(t) \in \{-1,1\}^m$.

The semi-active control method employs the same approach towards the disturbance as the active controllers described in Sections 3.2 and 3.3. In every iteration i of the

[5]This statement holds only if the optimal control is not subjected to singular arcs.

adaptive method, the disturbance signal $z(t)$ is approximated by the linear time-invariant and continuous system of the order $n_{z,i}$ defined similarly as the system in Eq. (3.20),

$$\begin{aligned} \dot{\mathbf{x}}_{z,i}(t) &= \mathbf{A}_{z,i}(\boldsymbol{\gamma}_i)\mathbf{x}_{z,i}(t), \quad \mathbf{x}_{z,\,i}(t_i) = \mathbf{x}_{z0,i}(\boldsymbol{\gamma}_i), \\ \tilde{z}_i(t) &= \mathbf{C}_{z,i}(\boldsymbol{\gamma}_i)\mathbf{x}_{z,i}(t), \quad \text{such that: } \tilde{z}_i(t) \approx z(t), \end{aligned} \tag{3.75}$$

where $\boldsymbol{\gamma}_i$ is the vector of the disturbance parameters identified by an identification procedure in every iteration of the adaptation, $\mathbf{x}_{z,i}(t) \in \mathbb{R}^{n_{z,i}}$ is the state of the model of the disturbance, $\tilde{z}_i(t) \in \mathbb{R}$ is the approximated signal of the disturbance, $\mathbf{x}_{z0,i}(\boldsymbol{\gamma}_i)$ denotes the initial conditions and matrices $\mathbf{A}_{z,i}$, $\mathbf{C}_{z,i}$ are computed via the vector $\boldsymbol{\gamma}_i$. Both systems (3.69) and (3.75) can be combined as follows:

$$\begin{aligned} \dot{\tilde{\mathbf{x}}}(t) &= \begin{bmatrix} \dot{\mathbf{x}}(t) \\ \dot{\mathbf{x}}_{z,i}(t) \end{bmatrix} = \begin{bmatrix} \mathbf{A} & \mathbf{B}_z\mathbf{C}_{z,i}(\boldsymbol{\gamma}_i) \\ \mathbf{0} & \mathbf{A}_{z,i}(\boldsymbol{\gamma}_i) \end{bmatrix} \begin{bmatrix} \mathbf{x}(t) \\ \mathbf{x}_{z,i}(t) \end{bmatrix} + \sum_{j=1}^{m} u_j(t) \begin{bmatrix} \mathbf{B}_j & \mathbf{0} \\ \mathbf{0} & \mathbf{0} \end{bmatrix} \tilde{\mathbf{x}}(t), \\ \tilde{\mathbf{x}}(t_i) &= \begin{bmatrix} \mathbf{x}(t_i) \\ \mathbf{x}_{z,i}(t_i) \end{bmatrix} = \begin{bmatrix} \mathbf{x}_i \\ \mathbf{x}_{z0,i}(\boldsymbol{\gamma}_i) \end{bmatrix}, \end{aligned} \tag{3.76}$$

where $\tilde{\mathbf{x}}(t) \in \mathbb{R}^{\tilde{n}_i}$, $\tilde{n}_i = n + n_{z,i}$ is the state of the system consisting of the controlled object and the model of the disturbance and $\mathbf{x}_i \in \mathbb{R}^n$ is the state of the mechanical system measured in the ith iteration of the adaptation.

The performance criterion for the new control system (3.76) that maintains the value of the performance criterion (3.73) is defined as

$$J = \int_0^{T_f} \tilde{\mathbf{x}}^T(t) \begin{bmatrix} \mathbf{Q} & \mathbf{0} \\ \mathbf{0} & \mathbf{0} \end{bmatrix} \tilde{\mathbf{x}}(t)\,\mathrm{d}t. \tag{3.77}$$

Similarly to the active adaptive control methods defined in Sections and 3.2, 3.3, the operation of the semi-active controller is also based on the iterative solution to the receding horizon control problem:

$$\begin{aligned} &\textbf{Find: } \mathbf{u}_i^* : \mathbb{R}^{\tilde{n}_i} \mapsto [-1,1]^m, \\ &\textbf{such that: } \mathbf{u}_i^*(\tilde{\mathbf{x}}_i(t)) = \underset{\mathbf{u}(t)\in[-1,1]^m,\ t\in\mathbb{T}_i}{\arg\min} J_i(\mathbf{u}) = \int_{t_i}^{\infty} \tilde{\mathbf{x}}^T(t) \begin{bmatrix} \mathbf{Q} & \mathbf{0} \\ \mathbf{0} & \mathbf{0} \end{bmatrix} \tilde{\mathbf{x}}(t)\,\mathrm{d}t, \\ &\textbf{subject to: } \textbf{differential equation and initial conditions } (3.76), \\ &\qquad t_i = h \cdot i, \\ &\qquad \mathbb{T}_i = [t_i, \infty), \end{aligned} \tag{3.78}$$

where h denotes the period of the iteration of the adaptative controller.

Observe that the infinite horizon formulation of the control problem and time invariance of the system matrices implies that the resulting optimal control law does not depend explicitly on time. Similarly to the discussion in Section 3.3, the existence of the solution to the problem (3.78) has to be addressed. Because the state-transition matrix $\mathbf{A}_{z,i}(\boldsymbol{\gamma}_i)$ is not guaranteed to be stable, the performance integral in (3.78) may not exist. To guarantee that the performance criterion exists for the augmented system (3.76) controlled via the

stabilizing control $\mathbf{u}_0$, a continuous variant of the *alpha shift* is introduced:

$$\begin{aligned}
\textbf{Find: } & \mathbf{u}_i^* : \mathbb{R}^{\tilde{n}_i} \mapsto [-1,1]^m, \\
\textbf{such that: } & \mathbf{u}_i^*(\tilde{\mathbf{x}}_i(t)) = \underset{\mathbf{u}(t)\in[-1,1]^m,\ t\in\mathbb{T}_i}{\arg\min} J_i(\mathbf{u}) = \int_{t_i}^{\infty} e^{2\alpha_i(t-t_i)} \tilde{\mathbf{x}}^T(t) \begin{bmatrix} \mathbf{Q} & \mathbf{0} \\ \mathbf{0} & \mathbf{0} \end{bmatrix} \tilde{\mathbf{x}}(t)\,\mathrm{d}t, \\
\textbf{subject to: } & \textbf{differential equation and initial conditions } (3.76), \\
& t_i = h \cdot i, \\
& \mathbb{T}_i = [t_i, \infty).
\end{aligned} \tag{3.79}$$

Next, it is shown that the special choice of the parameter α_i guarantees that the performance criterion with *alpha shift* exists when the augmented system (3.76) is controlled via constant control $\mathbf{u}_0$.

Theorem 3.3. *Let the augmented dynamical model consisting of the controlled system and the disturbance approximation be defined as in Eq.* (3.76) *and let the Assumption 3.5 hold. Let* $\mathbf{u}_0 \in \mathbb{R}^m$, $\mathbf{u}_0 = const.$ *be any constant control for which the Assumption 3.5 holds. Let* λ_j, $j = 1, 2, \ldots, n_{z,i}$ *denote the eigenvalues of the state-transition matrix of the disturbance approximation,* $\mathbf{A}_{z,i}$*. Then if the parameter* α_i *of the modified control problem* (3.79) *is chosen such that* $\alpha_i < -\max\left\{0, \Re(\lambda_1), \Re(\lambda_2), \ldots, \Re\left(\lambda_{n_{z,i}}\right)\right\}$*, then the modified performance criterion for the augmented system controlled via constant control* $\mathbf{u}_0$*,* $J(\mathbf{u}_0)$*, defined in Eq.* (3.79) *exists.*

Proof. Let $\tilde{\mathbf{x}}(t)$ be a trajectory of the augmented system (3.76) controlled via the constant control $\mathbf{u}_0$. Define $\mathbf{y}(t) = e^{\alpha_i(t-t_i)}\tilde{\mathbf{x}}(t)$. Observe that $\mathbf{y}(t)$ is the trajectory of the linear time-invariant dynamical system:

$$\begin{aligned}
\dot{\mathbf{y}}(t) &= \alpha_i \mathbf{y}(t) + \begin{bmatrix} \mathbf{A} & \mathbf{B}_z\mathbf{C}_{z,i}(\boldsymbol{\gamma}_i) \\ \mathbf{0} & \mathbf{A}_{z,i}(\boldsymbol{\gamma}_i) \end{bmatrix} \mathbf{y}(t) + \sum_{j=1}^{m} u_{0j} \begin{bmatrix} \mathbf{B}_j & \mathbf{0} \\ \mathbf{0} & \mathbf{0} \end{bmatrix} \mathbf{y}(t) \\
&= \left(\begin{bmatrix} \mathbf{A} + \sum_{j=1}^{m} u_{0j}\mathbf{B}_j & \mathbf{B}_z\mathbf{C}_{z,i}(\boldsymbol{\gamma}_i) \\ \mathbf{0} & \mathbf{A}_{z,i}(\boldsymbol{\gamma}_i) \end{bmatrix} + \alpha_i \mathbb{I} \right) \mathbf{y}(t), \quad \mathbf{y}(t_i) = \tilde{\mathbf{x}}(t_i).
\end{aligned} \tag{3.80}$$

The performance criterion with *alpha shift* defined in Eq. (3.79) can be reformulated with the use of the new state trajectory $\mathbf{y}(t)$:

$$J_i(\mathbf{u}_0) = \int_{t_i}^{\infty} e^{2\alpha_i(t-t_i)} \tilde{\mathbf{x}}^T(t) \begin{bmatrix} \mathbf{Q} & \mathbf{0} \\ \mathbf{0} & \mathbf{0} \end{bmatrix} \tilde{\mathbf{x}}(t)\,\mathrm{d}t \equiv \int_{t_i}^{\infty} \mathbf{y}^T(t)(t) \begin{bmatrix} \mathbf{Q} & \mathbf{0} \\ \mathbf{0} & \mathbf{0} \end{bmatrix} \mathbf{y}(t)\,\mathrm{d}t. \tag{3.81}$$

Observe that these performance criteria are finite if the linear time-invariant system (3.80) is exponentially stable. Since the matrix

$$\left(\begin{bmatrix} \mathbf{A} + \sum_{j=1}^{m} u_{0j}\mathbf{B}_j & \mathbf{B}_z\mathbf{C}_{z,i}(\boldsymbol{\gamma}_i) \\ \mathbf{0} & \mathbf{A}_{z,i}(\boldsymbol{\gamma}_i) \end{bmatrix} + \alpha_i \mathbb{I} \right) = \begin{bmatrix} \mathbf{A} + \sum_{j=1}^{m} u_{0j}\mathbf{B}_j + \alpha_i\mathbb{I} & \mathbf{B}_z\mathbf{C}_{z,i}(\boldsymbol{\gamma}_i) \\ \mathbf{0} & \mathbf{A}_{z,i}(\boldsymbol{\gamma}_i) + \alpha_i\mathbb{I} \end{bmatrix} \tag{3.82}$$

is a triangular block matrix, its spectrum is a sum of the spectra of the matrices $\left(\mathbf{A}+\sum_{j=1}^{m} u_{0j}\mathbf{B}_j+\alpha_i\mathbb{I}\right)$ and $(\mathbf{A}_{z,i}(\boldsymbol{\gamma}_i)+\alpha_i\mathbb{I})$. Notice also that if λ is an eigenvalue of a matrix $\mathbf{M}$, then $(\lambda+\alpha)$ is an eigenvalue of a matrix $(\mathbf{M}+\alpha\mathbb{I})$.

Since Assumption 3.5 holds, all eigenvalues of the matrix $\left(\mathbf{A}+\sum_{j=1}^{m} u_{0j}\mathbf{B}_j\right)$ have a negative real part. Observe that the parameter α_i defined as in the body of the theorem is negative and ultimately the eigenvalues of the matrix $\left(\mathbf{A}+\sum_{j=1}^{m} u_{0j}\mathbf{B}_j+\alpha_i\mathbb{I}\right)$ also have a negative real part.

Because α_i is smaller than the maximal real part of the eigenvalues of the matrix $(\mathbf{A}_{z,i}(\boldsymbol{\gamma}_i))$, all eigenvalues of the matrix $(\mathbf{A}_{z,i}(\boldsymbol{\gamma}_i)+\alpha_i\mathbb{I})$ also have a negative real part. All eigenvalues of the matrix (3.82) have a negative real part and the modified linear dynamical system (3.80) is exponentially stable. As a conclusion, such a choice of the parameter α_i guarantees the existence of the performance criterion $J(\mathbf{u}_0)$. The criterion has the explicit value

$$J(\mathbf{u}_0)=\tilde{\mathbf{x}}^T(t_i)\mathbf{P}_i(\mathbf{u}_0)\tilde{\mathbf{x}}(t_i), \tag{3.83}$$

where $\mathbf{P}_i(\mathbf{u}_0)\succeq 0$, $\mathbf{P}_i(\mathbf{u}_0)\in\mathbb{R}^{\tilde{n}_i\times\tilde{n}_i}$ is the solution to the Lyapunov equation:

$$\begin{aligned}\mathbf{0}=&\begin{bmatrix}\mathbf{A}+\sum_{j=1}^{m} u_{0j}\mathbf{B}_j+\alpha_i\mathbb{I} & \mathbf{B}_z\mathbf{C}_{z,i}(\boldsymbol{\gamma}_i)\\ \mathbf{0} & \mathbf{A}_{z,i}(\boldsymbol{\gamma}_i)+\alpha_i\mathbb{I}\end{bmatrix}^T\mathbf{P}_i(\mathbf{u}_0)\\ &+\mathbf{P}_i(\mathbf{u}_0)\begin{bmatrix}\mathbf{A}+\sum_{j=1}^{m} u_{0j}\mathbf{B}_j+\alpha_i\mathbb{I} & \mathbf{B}_z\mathbf{C}_{z,i}(\boldsymbol{\gamma}_i)\\ \mathbf{0} & \mathbf{A}_{z,i}(\boldsymbol{\gamma}_i)+\alpha_i\mathbb{I}\end{bmatrix}+\begin{bmatrix}\mathbf{Q} & \mathbf{0}\\ \mathbf{0} & \mathbf{0}\end{bmatrix}.\end{aligned} \tag{3.84}$$

The existence of this solution is guaranteed by the stability of the matrix defined in Eq. (3.82). □

Remark 3.4. *Since the matrix* $\left[\begin{smallmatrix}\mathbf{Q} & \mathbf{0}\\ \mathbf{0} & \mathbf{0}\end{smallmatrix}\right]$ *is not positive definite and the pair*

$$\left(\begin{bmatrix}\mathbf{A}+\sum_{j=1}^{m} u_{0j}\mathbf{B}_j+\alpha_i\mathbb{I} & \mathbf{B}_z\mathbf{C}_{z,i}(\boldsymbol{\gamma}_i)\\ \mathbf{0} & \mathbf{A}_{z,i}(\boldsymbol{\gamma}_i)+\alpha_i\mathbb{I}\end{bmatrix},\begin{bmatrix}\mathbf{Q} & \mathbf{0}\\ \mathbf{0} & \mathbf{0}\end{bmatrix}\right) \tag{3.85}$$

is not observable, the matrix $\mathbf{P}_i(\mathbf{u}_0)$ *is positive semi-definite.*

Observe that the optimal control problem (3.79) is formulated for a nonlinear dynamical system and with the explicit control constraints. Therefore, it lacks explicit analytical solutions, similar to the LQR for the unconstrained linear-quadratic optimal control problem. In the present work, the approximate, near-optimal control method is proposed that has low computational complexity and has a simple and closed form of the feedback law.

The near-optimal control method proposed in this section guarantees improvement of the performance in comparison to the stabilizing constant control $\mathbf{u}_0$. If there are many constant controls that stabilizes the controlled system, then it is preferable to choose such a control $\mathbf{u}_0^*$ that is not only stabilizing but also provides the best performance. The possible ways of computing the optimal constant control are discussed below.

The Optimal Passive Control

For brevity, let the state-transition matrix of the system with *alpha shift* (3.80) stabilized via the control $\mathbf{u}$ be defined as:

$$\tilde{\mathbf{A}}_i(\mathbf{u}) = \begin{bmatrix} \mathbf{A} + \sum_{j=1}^{m} u_j \mathbf{B}_j + \alpha_i \mathbb{I} & \mathbf{B}_z \mathbf{C}_{z,i}(\boldsymbol{\gamma}_i) \\ \mathbf{0} & \mathbf{A}_{z,i}(\boldsymbol{\gamma}_i) + \alpha_i \mathbb{I} \end{bmatrix}. \tag{3.86}$$

and

$$\tilde{\mathbf{Q}} = \begin{bmatrix} \mathbf{Q} & \mathbf{0} \\ \mathbf{0} & \mathbf{0} \end{bmatrix} \tag{3.87}$$

According to Theorem 3.3, if for the constant control $\mathbf{u}_0$ the autonomous part of the mechanical system defined in Eq. (3.69) is stable, then the constant matrix $\tilde{\mathbf{A}}_i(\mathbf{u}_0)$ is also stable and the performance of the constant control has a quadratic form:

$$\begin{aligned} J(\mathbf{u}_0) &= \tilde{\mathbf{x}}^T(t_i)\mathbf{P}_i(\mathbf{u}_0)\tilde{\mathbf{x}}(t_i), \\ \mathbf{0} &= \tilde{\mathbf{A}}_i(\mathbf{u}_0)^T\mathbf{P}_i(\mathbf{u}_0) + \mathbf{P}_i(\mathbf{u}_0)\tilde{\mathbf{A}}_i(\mathbf{u}_0) + \tilde{\mathbf{Q}}. \end{aligned} \tag{3.88}$$

Now, the aim of this section is to find the constant control $\mathbf{u}_0^*$ that minimizes the objective (3.88). The corresponding optimization problem can be regarded as a minimization of the performance index for a given initial state $\tilde{\mathbf{x}}_0$:

$$\mathbf{u}_0^* = \underset{\mathbf{u}_0 \in [-1;1]^m}{\arg\min}\ F_1(\mathbf{u}_0), \quad F_1(\mathbf{u}_0) = \tilde{\mathbf{x}}_0^T \mathbf{P}_i(\mathbf{u}_0)\tilde{\mathbf{x}}_0. \tag{3.89}$$

Alternatively, in the case when the passive control is expected to provide a fair result for a wide range of the initial states, one can consider optimizing the expected value of the performance index, i.e.

$$\mathbf{u}_0^* = \underset{\mathbf{u}_0 \in [-1;1]^m}{\arg\min}\ F_2(\mathbf{u}_0), \quad F_2(\mathbf{u}_0) = \mathbb{E}\left(\tilde{\mathbf{x}}_0^T \mathbf{P}_i(\mathbf{u}_0)\tilde{\mathbf{x}}_0\right). \tag{3.90}$$

The expected value in Eq. (3.90) is equal to

$$\mathbb{E}\left(\tilde{\mathbf{x}}_0^T \mathbf{P}_i(\mathbf{u}_0)\tilde{\mathbf{x}}_0\right) = \operatorname{tr}\left(\mathbf{P}_i(\mathbf{u}_0)\boldsymbol{\Sigma}\right) + \boldsymbol{\mu}^T \mathbf{P}_i(\mathbf{u}_0)\boldsymbol{\mu}, \tag{3.91}$$

where $\boldsymbol{\Sigma} \in \mathbb{R}^{\tilde{n}_i \times \tilde{n}_i}$, $\boldsymbol{\mu} \in \mathbb{R}^{\tilde{n}_i}$ are the covariance matrix and the mean value vector of a random initial state $\tilde{\mathbf{x}}_0$, respectively. Assuming that the initial states are uniformly distributed on a unit sphere, the optimization criterion for (3.90) can be written as follows

$$F_2(\mathbf{u}_0) = \frac{1}{\tilde{n}_i} \operatorname{tr}\left(\mathbf{P}_i(\mathbf{u}_0)\right). \tag{3.92}$$

Below, the nonlinear programming problems for both considered criteria are formulated. Firstly, it is demonstrated that the dependence of $\mathbf{P}_i(\mathbf{u}_0)$ on $\mathbf{u}_0$ can be described using the Kronecker product. Let

$$\operatorname{vec}\mathbf{M} = \begin{bmatrix} m_{11} & \dots & m_{1n} & m_{21} & \dots & m_{2n} & \dots & m_{nn} \end{bmatrix}^T \in \mathbb{R}^{n^2} \tag{3.93}$$

be an operator that stacks vertically the columns of a matrix $\mathbf{M} \in \mathbb{R}^{n\times n}$ and $\mathbf{M_1} \otimes \mathbf{M_2}$ denote the Kronecker product of the matrices $\mathbf{M_1}$ and $\mathbf{M_2}$. Let also define the matrix $\mathbf{X} \in \mathbb{R}^{\tilde{n}_i^2 \times \tilde{n}_i^2}$ such that

$$\mathbf{X}\left(\mathbf{u}_0\right) = \left(\mathbb{I} \otimes \tilde{\mathbf{A}}_i\left(\mathbf{u}_0\right) + \tilde{\mathbf{A}}_i^{\,T}\left(\mathbf{u}_0\right) \otimes \mathbb{I}\right). \tag{3.94}$$

Then

$$\operatorname{vec} \mathbf{P}_i(\mathbf{u}_0) = -\mathbf{X}^{-1}\left(\mathbf{u}_0\right) \operatorname{vec} \tilde{\mathbf{Q}}. \tag{3.95}$$

The nonlinear programming problem for (3.89) and (3.90) can be stated as follows:

$$\begin{aligned} \textbf{Find: } \mathbf{u}_0^* = & \underset{\mathbf{u}_0 \in [-1;1]^m}{\arg\min} -\mathbf{c}_k^T \mathbf{X}^{-1}\left(\mathbf{u}_0\right) \operatorname{vec} \tilde{\mathbf{Q}}, \\ \textbf{subject to: } & \begin{bmatrix} \mathbb{I} \\ -\mathbb{I} \end{bmatrix} \mathbf{u}_0 \leq \begin{bmatrix} \mathbb{I} \\ \mathbb{I} \end{bmatrix}. \end{aligned} \tag{3.96}$$

The constant vector $\mathbf{c}_k \in \mathbb{R}^{\tilde{n}_i}$ depends on the choice of the minimization criteria $F_1(\mathbf{u}_0)$ or $F_2(\mathbf{u}_0)$. In the case of the first optimization criterion (3.89), the vector $\mathbf{c_1}$ depends on the given initial condition $\tilde{\mathbf{x}}_0$, i.e.

$$\mathbf{c_1} = \operatorname{vec} \tilde{\mathbf{x}}_0 \tilde{\mathbf{x}}_0^T. \tag{3.97}$$

For the second criterion (3.90), the vector $\mathbf{c_2}$ is defined as follows:

$$\mathbf{c_2} = \operatorname{vec} \mathbb{I}. \tag{3.98}$$

The search for the exact solution to the problem (3.96) is computationally complex. One of the reasons is that the computation of the gradient of the criterion (3.96) involves the calculation of the inverse of the matrix $\mathbf{X} \in \mathbb{R}^{\tilde{n}_i^2 \times \tilde{n}_i^2}$. This procedure has complexity $\mathcal{O}\left(n_i^6\right)$. Thus, it is advised to compute an approximate solution to (3.96), e.g. by the use of the Fixed Step Random Search. For a good number of the semi-active structures, the optimal passive control can also be established based on the practical experience. As an example, in the majority of the damping controlled structures, the optimal passive strategy relies on the maximal admissible value, i.e. $\mathbf{u}_0^* = \mathbf{1}$.

The Near-optimal Switched Control

Assume that the optimal or heuristic constant control $\mathbf{u}_0^* = \begin{bmatrix} u_{0,1}^* & u_{0,2}^* & \dots & u_{0,m}^* \end{bmatrix}$ is known. For the system (3.80), the state-feedback control function $\hat{\mathbf{u}}(\mathbf{y}) = [\hat{u}_1(\mathbf{y}), \hat{u}_2(\mathbf{y}), ..., \hat{u}_m(\mathbf{y})]$ is defined as follows:

$$\begin{aligned} \hat{u}_j(\mathbf{y}) &= -\operatorname{sgn}\left(\mathbf{y}^T \mathbf{P}_i(\mathbf{u}_0^*) \tilde{\mathbf{B}}_j \mathbf{y}\right), \\ \mathbf{0} &= \tilde{\mathbf{A}}_i^{\,T}(\mathbf{u}_0^*) \mathbf{P}_i(\mathbf{u}_0^*) + \mathbf{P}_i(\mathbf{u}_0^*) \tilde{\mathbf{A}}_i(\mathbf{u}_0^*) + \tilde{\mathbf{Q}}, \\ \tilde{\mathbf{B}}_j &= \begin{bmatrix} \mathbf{B}_j & \mathbf{0} \\ \mathbf{0} & \mathbf{0} \end{bmatrix}. \end{aligned} \tag{3.99}$$

This switching control law based on the Lyapunov equation has been introduced in [23]. In the present work, the control law formulation is extended to include the analysis of its near-optimality properties.

Observe that the differential equation that governs the system controlled via the switching control law (3.99):

$$\begin{aligned}\dot{\mathbf{y}}(t) &= \begin{bmatrix} \mathbf{A} + \alpha_i \mathbb{I} - \sum_{j=1}^{m} \operatorname{sgn}\left(\mathbf{y}^T \mathbf{P}_i(\mathbf{u}_0^*)\tilde{\mathbf{B}}_j \mathbf{y}\right) \mathbf{B}_j & \mathbf{B}_z \mathbf{C}_{z,i}(\boldsymbol{\gamma}_i) \\ \mathbf{0} & \mathbf{A}_{z,i}(\boldsymbol{\gamma}_i) + \alpha_i \mathbb{I} \end{bmatrix} \mathbf{y}(t), \\ \mathbf{y}(t_i) &= \tilde{\mathbf{x}}(t_i)\end{aligned} \tag{3.100}$$

is discontinuous. Thus, the trajectory $\mathbf{y}(t)$ is not a solution to (3.100) in the classical sense. The solution to (3.100) is considered in the Filippov sense [68, Chapter 2.], i.e. an absolutely continuous function that almost everywhere satisfies:

$$\dot{\mathbf{y}}(t) \in \mathbf{F}(\mathbf{y}), \tag{3.101}$$

where the differential inclusion is a set-valued function $\mathbf{F}(\mathbf{y})$ constructed as a convex hull of the right-hand side of Eq. (3.100):

$$\begin{aligned}\mathbf{F}(\mathbf{y}) &= \left\{ \begin{bmatrix} \mathbf{A} + \alpha_i \mathbb{I} + \sum_{j=1}^{m} u_j \mathbf{B}_j & \mathbf{B}_z \mathbf{C}_{z,i}(\boldsymbol{\gamma}_i) \\ \mathbf{0} & \mathbf{A}_{z,i}(\boldsymbol{\gamma}_i) + \alpha_i \mathbb{I} \end{bmatrix} \mathbf{y}(t) : \; u_j \in U_j(\mathbf{y}),\, j = 1,\, 2,\, \ldots,\, m \right\}, \\ U_j(\mathbf{y}) &= \begin{cases} -1, & \text{if } \mathbf{y}^T \mathbf{P}_i(\mathbf{u}_0^*)\tilde{\mathbf{B}}_j \mathbf{y} > 0, \\ [-1, 1] & \text{if } \mathbf{y}^T \mathbf{P}_i(\mathbf{u}_0^*)\tilde{\mathbf{B}}_j \mathbf{y} = 0, \\ 1, & \text{if } \mathbf{y}^T \mathbf{P}_i(\mathbf{u}_0^*)\tilde{\mathbf{B}}_j \mathbf{y} < 0, \end{cases}\end{aligned} \tag{3.102}$$

Observe that the set $\mathbf{F}(\mathbf{y})$ in Eq. (3.102) is nonempty, bounded, closed and convex for any $\mathbf{y} \in \mathbb{R}^{\tilde{n}_i}$ and the function $\mathbf{F}$ is upper semicontinuous on $\mathbb{R}^{\tilde{n}_i}$. Thus, from [68, Theorem 1, p. 77] it can be concluded that there exists a solution to this differential equation in the Filippov sense.

Firstly, it is proven that the feedback control law (3.99) is asymptotically stable.

Theorem 3.4. *The switched suboptimal controller defined as in* (3.99) *stabilizes asymptotically the system* (3.80).

Proof. Let $\mathbf{P}_z$ be a solution to the Lyapunov equation

$$\tilde{\mathbf{A}}_i^T(\mathbf{u}_0^*)\mathbf{P}_z + \mathbf{P}_z \tilde{\mathbf{A}}_i(\mathbf{u}_0^*) + \begin{bmatrix} \mathbf{0} & \mathbf{0} \\ \mathbf{0} & \mathbb{I} \end{bmatrix} = \mathbf{0}, \tag{3.103}$$

where $\mathbb{I} \in \mathbb{R}^{n_{z,i} \times n_{z,i}}$. The stability of the matrix $\tilde{\mathbf{A}}_i(\mathbf{u}_0^*)$ guarantees the existence of the solution $\mathbf{P}_z$. Since the matrix $\tilde{\mathbf{A}}_i(\mathbf{u}_0^*)$ is upper triangular, the matrix $\mathbf{P}_z$ has a special block form:

$$\mathbf{P}_z = \begin{bmatrix} \mathbf{0} & \mathbf{0} \\ \mathbf{0} & \mathbf{X} \end{bmatrix}, \tag{3.104}$$

where $\mathbf{X} \in \mathbb{R}^{n_{z,i} \times n_{z,i}}$ is a positive definite matrix.

Observe that the sum $(\mathbf{P}_i(\mathbf{u}_0^*) + \mathbf{P}_z)$ is positive definite because the pair

$$\left(\begin{bmatrix} \mathbf{A} + \sum_{j=1}^{m} u_{0j} \mathbf{B}_j + \alpha_i \mathbb{I} & \mathbf{B}_z \mathbf{C}_{z,i}(\boldsymbol{\gamma}_i) \\ \mathbf{0} & \mathbf{A}_{z,i}(\boldsymbol{\gamma}_i) + \alpha_i \mathbb{I} \end{bmatrix}, \begin{bmatrix} \mathbf{Q} & \mathbf{0} \\ \mathbf{0} & \mathbb{I} \end{bmatrix} \right) \tag{3.105}$$

is observable and the Lyapunov equation

$$\tilde{\mathbf{A}}_i^T(\mathbf{u}_0^*)\left(\mathbf{P}_i(\mathbf{u}_0^*)+\mathbf{P}_z\right)+\left(\mathbf{P}_i(\mathbf{u}_0^*)+\mathbf{P}_z\right)\tilde{\mathbf{A}}_i(\mathbf{u}_0^*)+\begin{bmatrix}\mathbf{Q} & \mathbf{0}\\ \mathbf{0} & \mathbb{I}\end{bmatrix}=\mathbf{0} \tag{3.106}$$

holds.

Let the Lyapunov candidate function be defined as follows:

$$V(\mathbf{y})=\mathbf{y}^T\left(\mathbf{P}_i(\mathbf{u}_0^*)+\mathbf{P}_z\right)\mathbf{y}. \tag{3.107}$$

Notice that $V(\mathbf{y})$ is a positive definite function. The upper derivative with respect to time

$$\dot{V}=\sup_{\dot{\mathbf{y}}\in\mathbf{F}(\mathbf{y})}\frac{\partial V(\mathbf{y})}{\partial \mathbf{y}}\dot{\mathbf{y}} \tag{3.108}$$

along the trajectories of the system controlled via the feedback control (3.99) is as follows:

$$\dot{V}(\mathbf{y}(t))=\sup_{u_j\in U_j(\mathbf{y})}2\mathbf{y}^T(t)\left(\mathbf{P}_i(\mathbf{u}_0^*)+\mathbf{P}_z\right)\begin{bmatrix}\mathbf{A}+\sum_{j=1}^m u_j\mathbf{B}_j+\alpha_i\mathbb{I} & \mathbf{B}_z\mathbf{C}_{z,i}(\boldsymbol{\gamma}_i)\\ \mathbf{0} & \mathbf{A}_{z,i}(\boldsymbol{\gamma}_i)+\alpha_i\mathbb{I}\end{bmatrix}\mathbf{y}(t). \tag{3.109}$$

Since $u_j=u_{0j}^*+u_j-u_{0j}^*$,

$$\begin{aligned}\dot{V}(\mathbf{y}(t))&=2\mathbf{y}^T(t)\left(\mathbf{P}_i(\mathbf{u}_0^*)+\mathbf{P}_z\right)\begin{bmatrix}\mathbf{A}+\sum_{j=1}^m u_{0j}^*\mathbf{B}_j+\alpha_i\mathbb{I} & \mathbf{B}_z\mathbf{C}_{z,i}(\boldsymbol{\gamma}_i)\\ \mathbf{0} & \mathbf{A}_{z,i}(\boldsymbol{\gamma}_i)+\alpha_i\mathbb{I}\end{bmatrix}\mathbf{y}(t)\\ &\quad+\sup_{u_j\in U_j(\mathbf{y})}2\mathbf{y}^T(t)\left(\mathbf{P}_i(\mathbf{u}_0^*)+\mathbf{P}_z\right)\sum_{j=1}^m(u_j-u_{0j}^*)\tilde{\mathbf{B}}_j\mathbf{y}(t)\\ &=2\mathbf{y}^T(t)\left(\mathbf{P}_i(\mathbf{u}_0^*)+\mathbf{P}_z\right)\tilde{\mathbf{A}}_i(\mathbf{u}_0^*)\mathbf{y}(t)\\ &\quad+\sup_{u_j\in U_j(\mathbf{y})}2\mathbf{y}^T(t)\left(\mathbf{P}_i(\mathbf{u}_0^*)+\mathbf{P}_z\right)\sum_{j=1}^m(u_j-u_{0j}^*)\tilde{\mathbf{B}}_j\mathbf{y}(t).\end{aligned} \tag{3.110}$$

Since the matrix $\mathbf{P}_z$ has the particular form (3.104), the identity

$$\mathbf{P}_z\tilde{\mathbf{B}}_j\equiv\mathbf{0},\quad j=1,\,2,\,\ldots,\,m \tag{3.111}$$

holds and as a result,

$$\begin{aligned}\dot{V}(\mathbf{y}(t))&=2\mathbf{y}^T(t)\left(\mathbf{P}_i(\mathbf{u}_0^*)+\mathbf{P}_z\right)\tilde{\mathbf{A}}_i(\mathbf{u}_0^*)\mathbf{y}(t)\\ &\quad+\sup_{u_j\in U_j(\mathbf{y})}\sum_{j=1}^m(u_j-u_{0j}^*)2\mathbf{y}^T(t)\mathbf{P}_i(\mathbf{u}_0^*)\tilde{\mathbf{B}}_j\mathbf{y}(t).\end{aligned} \tag{3.112}$$

Notice that

$$\begin{aligned}\sup_{u_j\in U_j(\mathbf{y})}u_j\mathbf{y}^T\mathbf{P}_i(\mathbf{u}_0^*)\tilde{\mathbf{B}}_j\mathbf{y}&=-\operatorname{sgn}\left(\mathbf{y}^T\mathbf{P}_i(\mathbf{u}_0^*)\tilde{\mathbf{B}}_j\mathbf{y}\right)\mathbf{y}^T\mathbf{P}_i(\mathbf{u}_0^*)\tilde{\mathbf{B}}_j\mathbf{y}\\ &=\hat{u}_j\mathbf{y}^T\mathbf{P}_i(\mathbf{u}_0^*)\tilde{\mathbf{B}}_j\mathbf{y}\end{aligned} \tag{3.113}$$

and

$$\begin{aligned}\dot{V}(\mathbf{y}(t))&=2\mathbf{y}^T(t)\left(\mathbf{P}_i(\mathbf{u}_0^*)+\mathbf{P}_z\right)\tilde{\mathbf{A}}_i(\mathbf{u}_0^*)\mathbf{y}(t)\\ &\quad+\sum_{j=1}^m(\hat{u}_j-u_{0j}^*)2\mathbf{y}^T(t)\mathbf{P}_i(\mathbf{u}_0^*)\tilde{\mathbf{B}}_j\mathbf{y}(t).\end{aligned} \tag{3.114}$$

Observe that the time derivative of the Lyapunov function (3.114) is a sum of two separate terms:

$$\begin{aligned} \text{the first term: } & 2\mathbf{y}^T(t)\left(\mathbf{P}_i(\mathbf{u}_0^*)+\mathbf{P}_z\right)\tilde{\mathbf{A}}_i(\mathbf{u}_0^*)\mathbf{y}(t), \\ \text{the second term: } & \sum_{j=1}^{m}\left[\left(\hat{u}_j-u_{0j}^*\right)\mathbf{y}^T(t)\mathbf{P}_i(\mathbf{u}_0^*)\tilde{\mathbf{B}}_j\mathbf{y}(t)\right]. \end{aligned} \tag{3.115}$$

Consider the sign of the first term. Recall from the Lyapunov equation (3.106) that

$$2\mathbf{y}^T(t)\left(\mathbf{P}_i(\mathbf{u}_0^*)+\mathbf{P}_z\right)\tilde{\mathbf{A}}_i(\mathbf{u}_0^*)\mathbf{y}(t) = -\mathbf{y}^T(t)\begin{bmatrix}\mathbf{Q} & \mathbf{0}\\ \mathbf{0} & \mathbb{I}\end{bmatrix}\mathbf{y}(t). \tag{3.116}$$

Since the matrix $\left[\begin{smallmatrix}\mathbf{Q} & \mathbf{0}\\ \mathbf{0} & \mathbb{I}\end{smallmatrix}\right]$ is positive semi-definite, the term (3.116) is non-positive.

Since the switching control law $\hat{\mathbf{u}}(\mathbf{y})$ is defined as in (3.99), each summand of the second term is as follows:

$$\begin{aligned} &\left(\hat{u}_j-u_{0j}^*\right)\mathbf{y}^T(t)\mathbf{P}_i(\mathbf{u}_0^*)\tilde{\mathbf{B}}_j\mathbf{y}(t) \\ &\qquad = \left(-\operatorname{sgn}\left(\mathbf{y}^T(t)\mathbf{P}_i(\mathbf{u}_0^*)\tilde{\mathbf{B}}_j\mathbf{y}\right)-u_{0j}^*\right)\cdot\mathbf{y}^T(t)\mathbf{P}_i(\mathbf{u}_0^*)\tilde{\mathbf{B}}_j\mathbf{y}(t). \end{aligned} \tag{3.117}$$

Observe that

$$-\operatorname{sgn}\left(\mathbf{y}^T\mathbf{P}_i(\mathbf{u}_0^*)\tilde{\mathbf{B}}_j\mathbf{y}\right)\mathbf{y}^T\mathbf{P}_i(\mathbf{u}_0^*)\tilde{\mathbf{B}}_j\mathbf{y} = -\left|\mathbf{y}^T\mathbf{P}_i(\mathbf{u}_0^*)\tilde{\mathbf{B}}_j\mathbf{y}\right| \tag{3.118}$$

and

$$-u_{0j}^*\mathbf{y}^T\mathbf{P}_i(\mathbf{u}_0^*)\tilde{\mathbf{B}}_j\mathbf{y}(t) = -u_{0j}^*\operatorname{sgn}\left(\mathbf{y}^T\mathbf{P}_i(\mathbf{u}_0^*)\tilde{\mathbf{B}}_j\mathbf{y}\right)\left|\mathbf{y}^T\mathbf{P}_i(\mathbf{u}_0^*)\tilde{\mathbf{B}}_j\mathbf{y}\right|. \tag{3.119}$$

From these observations follows that the second term of $\dot{V}$ is equal to

$$\begin{aligned} &2\sum_{j=1}^{m}\left[\left(\hat{u}_j-u_{0j}^*\right)\mathbf{y}^T\mathbf{P}_i(\mathbf{u}_0^*)\tilde{\mathbf{B}}_j\mathbf{y}\right] \\ &\qquad = -2\sum_{j=1}^{m}\left[1+u_{0j}^*\operatorname{sgn}\left(\mathbf{y}^T\mathbf{P}_i(\mathbf{u}_0^*)\tilde{\mathbf{B}}_j\mathbf{y}\right)\right]\left|\mathbf{y}^T\mathbf{P}_i(\mathbf{u}_0^*)\tilde{\mathbf{B}}_j\mathbf{y}\right|. \end{aligned} \tag{3.120}$$

By definition, $u_{0j}^* \in [-1,1]$, $j = 1, 2, \ldots, m$ and

$$1+u_{0j}^*\operatorname{sgn}\left(\mathbf{y}^T\mathbf{P}_i(\mathbf{u}_0^*)\tilde{\mathbf{B}}_j\mathbf{y}\right) \in [0,2]. \tag{3.121}$$

As a consequence, the sum (3.120) is non-positive.

Because the derivative $\dot{V}$ is a sum of the non-positive terms, it is also non-negative. The derivative $\dot{V}$ is equal to 0 on the whole trajectory of the system only if the first term denoted in Eq. (3.116) is equal to 0. Since the pair

$$\left(\begin{bmatrix}\mathbf{A}+\sum_{j=1}^{m}u_{0j}\mathbf{B}_j+\alpha_i\mathbb{I} & \mathbf{B}_z\mathbf{C}_{z,i}(\boldsymbol{\gamma}_i)\\ \mathbf{0} & \mathbf{A}_{z,i}(\boldsymbol{\gamma}_i)+\alpha_i\mathbb{I}\end{bmatrix},\begin{bmatrix}\mathbf{Q} & \mathbf{0}\\ \mathbf{0} & \mathbb{I}\end{bmatrix}\right) \tag{3.122}$$

is observable, there is no trajectory $\mathbf{y}(t)$ except trivial $\mathbf{y}(t) = \mathbf{0}$, for which $\dot{V}$ remains 0.

From LaSalle's invariance principle for discontinuous systems (see [69, Theorem 1 and Proposition 2]) it follows that the closed-loop system (3.80) controlled via the switching control law defined in (3.89) is asymptotically stable. □

The next theorem shows that the switching control law defined in (3.89) results in a non-greater value of the performance criterion than the optimal constant control $\mathbf{u}_0^*$.

Theorem 3.5. *Let $V_0(\mathbf{y}_0)$ and $\hat{V}(\mathbf{y}_0)$ stand for the performance cost* (3.81) *from the initial state $\mathbf{y}(t_i) = \mathbf{y}_0$ generated via the optimal passive control and suboptimal switched control, respectively. Then the relation $V_0(\mathbf{y}_0) \geq \hat{V}(\mathbf{y}_0)$ is satisfied for every initial condition $\mathbf{y}_0$.*

Proof. Observe that for the constant control, the value function is $V_0(\mathbf{y}_0) = \mathbf{y}_0^T \mathbf{P}_i(\mathbf{u}_0^*)\mathbf{y}_0$. Let $\mathbf{y}(t)$ be a trajectory of the system (3.80) controlled via the switching control law $\hat{\mathbf{u}}(\mathbf{y})$ defined in (3.89) with the initial state $\mathbf{y}_0$.

Since $\mathbf{y}(t)$ and consequently $V_0(\mathbf{y}(t)) = \mathbf{y}(t)^T \mathbf{P}_i(\mathbf{u}_0^*)\mathbf{y}(t)$ are absolutely continuous, the following relation holds (see [70, Theorem 20.8]):

$$V_0(\mathbf{y}(t)) - V_0(\mathbf{y}_0) = \int_{t_i}^{t} \dot{V}_0(\mathbf{y}(\tau))\,\mathrm{d}\tau. \tag{3.123}$$

Theorem 3.4 guarantees that the considered system with the switching control law is asymptotically stable and $\lim_{t\to\infty} \mathbf{y}(t) = \mathbf{0}$. As a result,

$$\lim_{t\to\infty} \left(V_0(\mathbf{y}(t)) - V_0(\mathbf{y}_0)\right) = -V_0(\mathbf{y}_0) = \int_{t_i}^{\infty} \dot{V}_0(\mathbf{y}(\tau))\,\mathrm{d}\tau. \tag{3.124}$$

In the similar fashion to Eqs. (3.109)–(3.116) it can be showed that

$$\begin{aligned} \dot{V}_0(\mathbf{y}(t)) = &-\mathbf{y}(t)^T \tilde{\mathbf{Q}} \mathbf{y}(t) \\ &+ 2\sum_{j=1}^{m} \left[\left(\hat{u}_j - u_{0j}^*\right) \mathbf{y}^T(t) \mathbf{P}_i(\mathbf{u}_0^*) \tilde{\mathbf{B}}_j \mathbf{y}(t) \right]. \end{aligned} \tag{3.125}$$

From the definition of the performance index (3.81), it follows that

$$\hat{V}(\mathbf{y}_0) = \int_{t_i}^{\infty} \mathbf{y}(\tau)^T \tilde{\mathbf{Q}} \mathbf{y}(\tau)\,\mathrm{d}\tau. \tag{3.126}$$

Compare values of $\hat{V}(\mathbf{y}_0)$ and $V_0(\mathbf{y}_0)$:

$$V_0(\mathbf{y}_0) - \hat{V}(\mathbf{y}_0) = -\int_{t_i}^{\infty} 2\sum_{j=1}^{m} \left[\left(\hat{u}_j - u_{0j}^*\right) \mathbf{y}^T(t) \mathbf{P}_i(\mathbf{u}_0^*) \tilde{\mathbf{B}}_j \mathbf{y}(t) \right] \mathrm{d}\tau. \tag{3.127}$$

Observe that the integrand in (3.127) is equivalent to the derivative of the Lyapunov function (3.114) defined in the proof of Theorem 3.4. Recall from Eq. (3.120) that this integrand is non-positive and as a result for all $\mathbf{y}_0 \in \mathbb{R}^{\tilde{n}_i}$, $V_0(\mathbf{y}_0) - \hat{V}(\mathbf{y}_0) \geq 0$. □

Theorem 3.5 shows that the performance of the proposed switching control $\hat{\mathbf{u}}(\mathbf{y})$ is bounded above by the performance of the constant control $\mathbf{u}_0^*$. Next theorem provides conditions that guarantee the strict improvement, i.e. that there exists $\mathbf{y}_0 \in \mathbb{R}^{\tilde{n}_i}$ such that $V_0(\mathbf{y}_0) > \hat{V}(\mathbf{y}_0)$.

Theorem 3.6. *Let $V_0(\mathbf{y}_0)$ and $\hat{V}(\mathbf{y}_0)$ be defined as in Theorem 3.5. Then $\hat{V}(\mathbf{y}_0)$ is equal to $V_0(\mathbf{y}_0)$ on whole domain $\mathbf{y}_0 \in \mathbb{R}^{\tilde{n}_i}$ if and only if the constant control $\mathbf{u}_0^*$ is the optimal control for the problem* (3.79).

Proof. Assume that $\mathbf{u}_0^*$ is the optimal control for the problem (3.79). The associated value function with the constant control is $V_0(\mathbf{y}_0) = \mathbf{y}_0^T \mathbf{P}_i(\mathbf{u}_0^*)\mathbf{y}_0$. The control $\mathbf{u}_0^*$ is optimal if and only if both $V_0(\mathbf{y}_0)$ and $\mathbf{u}_0^*$ satisfy the sufficient and necessary conditions of optimality, denoted by the infinite horizon variant of the HJB equation (2.24):

$$0 = \mathbf{y}^T \tilde{\mathbf{Q}}\mathbf{y} + \frac{\partial V_0(\mathbf{y})}{\partial \mathbf{y}} \tilde{\mathbf{A}}_i(\mathbf{u}_0^*)\mathbf{y}, \quad V_0(\mathbf{0}) = 0 \tag{3.128}$$

and

$$\begin{aligned} \mathbf{u}_0^* &= \underset{\mathbf{u}(\mathbf{y})\in[-1,1]^m}{\arg\min} \left[\mathbf{y}^T \tilde{\mathbf{Q}}\mathbf{y} + \frac{\partial V_0(\mathbf{y})}{\partial \mathbf{y}} \tilde{\mathbf{A}}_i(\mathbf{u})\mathbf{y} \right] \\ &= \underset{\mathbf{u}(\mathbf{y})\in[-1,1]^m}{\arg\min} \left[\mathbf{y}^T \mathbf{P}_i(\mathbf{u}_0^*) \tilde{\mathbf{A}}_i(\mathbf{u})\mathbf{y} \right] = \underset{\mathbf{u}(\mathbf{y})\in[-1,1]^m}{\arg\min} \left[\mathbf{y}^T \mathbf{P}_i(\mathbf{u}_0^*) \sum_{j=1}^{m} u_j \tilde{\mathbf{B}}_j \mathbf{y} \right]. \end{aligned} \tag{3.129}$$

Since the Lyapunov equation (3.99) holds, equation (3.128) is trivially satisfied:

$$\begin{aligned} \mathbf{y}^T \tilde{\mathbf{Q}}\mathbf{y} + \frac{\partial V_0(\mathbf{y})}{\partial \mathbf{y}} \tilde{\mathbf{A}}_i(\mathbf{u}_0^*)\mathbf{y} &= \mathbf{y}^T \tilde{\mathbf{Q}}\mathbf{y} + 2\mathbf{y}^T \mathbf{P}_i(\mathbf{u}_0^*) \tilde{\mathbf{A}}_i(\mathbf{u}_0^*)\mathbf{y} \\ &= \mathbf{y}^T \left(\tilde{\mathbf{Q}} + \mathbf{P}_i(\mathbf{u}_0^*) \tilde{\mathbf{A}}_i(\mathbf{u}_0^*) + \tilde{\mathbf{A}}_i^T(\mathbf{u}_0^*) \mathbf{P}_i(\mathbf{u}_0^*) \right) \mathbf{y} = 0. \end{aligned} \tag{3.130}$$

Let us analyse the minimum denoted in Eq. (3.129). Two cases are possible.

$$\underset{\mathbf{u}_j(\mathbf{y})\in[-1,1]}{\arg\min} \left[u_j \mathbf{y}^T \mathbf{P}_i(\mathbf{u}_0^*) \tilde{\mathbf{B}}_j \mathbf{y} \right] \in \begin{cases} \left\{ -\operatorname{sgn}\left(\mathbf{y}^T \mathbf{P}_i(\mathbf{u}_0^*) \tilde{\mathbf{B}}_j \mathbf{y} \right) \right\}, & \left(\mathbf{y}^T \mathbf{P}_i(\mathbf{u}_0^*) \tilde{\mathbf{B}}_j \mathbf{y} \right) \neq 0, \\ [-1, 1], & \left(\mathbf{y}^T \mathbf{P}_i(\mathbf{u}_0^*) \tilde{\mathbf{B}}_j \mathbf{y} \right) = 0. \end{cases} \tag{3.131}$$

From that follows that the constant control $\mathbf{u}_0^* \in [-1, 1]^m$ is optimal if and only if

$$\forall \mathbf{y} \in \mathbb{R}^{\tilde{n}_i} : \mathbf{y}^T \mathbf{P}_i(\mathbf{u}_0^*) \tilde{\mathbf{B}}_j \mathbf{y} \neq 0, \quad u_{0j}^* = -\operatorname{sgn}\left(\mathbf{y}^T \mathbf{P}_i(\mathbf{u}_0^*) \tilde{\mathbf{B}}_j \mathbf{y} \right). \tag{3.132}$$

Observe that this condition holds only if each of the matrix products $\mathbf{P}_i(\mathbf{u}_0^*)\tilde{\mathbf{B}}_j$, $j = 1, 2, \ldots, m$ is positive or negative semi-definite. Recall the assumed form of the switching control law:

$$\hat{u}_j(\mathbf{y}) = -\operatorname{sgn}\left(\mathbf{y}^T \mathbf{P}_i(\mathbf{u}_0^*) \tilde{\mathbf{B}}_j \mathbf{y} \right). \tag{3.133}$$

The constant control $\mathbf{u}_0^*$ is optimal if and only if

$$\forall \mathbf{y} \in \mathbb{R}^{\tilde{n}_i}, \quad u_{0j}^* = \hat{u}_j(\mathbf{y}) \quad \vee \quad \mathbf{y}^T \mathbf{P}_i(\mathbf{u}_0^*) \tilde{\mathbf{B}}_j \mathbf{y} = 0. \tag{3.134}$$

Equivalently, the constant control $\mathbf{u}_0^*$ is the optimal control if and only if the next condition holds:

$$\forall \mathbf{y} \in \mathbb{R}^{\tilde{n}_i}, \quad (u_{0j}^* - \hat{u}_j(\mathbf{y})) \mathbf{y}^T \mathbf{P}_i(\mathbf{u}_0^*) \tilde{\mathbf{B}}_j \mathbf{y} = 0. \tag{3.135}$$

Notice that the left-hand side of Eq. (3.135) is the same as the integrand that characterizes the difference of $\hat{V}(\mathbf{y}) - V_0(\mathbf{y})$ in Eq. (3.127). Observe that if (3.135) holds, then $\hat{V}(\mathbf{y}) \equiv V_0(\mathbf{y})$.

Let us prove the opposite implication, i.e., if $\hat{V}(\mathbf{y}) \equiv V_0(\mathbf{y})$ then (3.135) holds. From Theorem 3.4 it follows that the integrand in Eq. (3.127) is non-positive. Thus the

equivalence $\hat{V}(\mathbf{y}) \equiv V_0(\mathbf{y})$ can be achieved only if this integrand is equal to 0 almost everywhere on $[t_i, \infty)$. Observe that this integrand function in Eq. (3.127) is continuous with respect to t. From that follows that $\hat{V}(\mathbf{y}) \equiv V_0(\mathbf{y})$ only if the integrand function is equal to 0 on the whole interval $[t_i, \infty)$. Because the initial conditions $\mathbf{y}_0$ are arbitrary, it follows that if $\hat{V}(\mathbf{y}) \equiv V_0(\mathbf{y})$ then (3.135) holds. As a conclusion, the constant control $\mathbf{u}_0^*$ is optimal if and only if $\hat{V}(\mathbf{y}) \equiv V_0(\mathbf{y})$. □

Remark 3.5. *If for some $j = 1, 2, \ldots, m$ the matrix product $\mathbf{P}_i(\mathbf{u}_0^*)\tilde{\mathbf{B}}_j$ is indefinite, then there exists $\tilde{\mathbf{y}} \in \mathbb{R}^{\tilde{n}_i}$ such that $\hat{V}(\tilde{\mathbf{y}}) < V_0(\tilde{\mathbf{y}})$*

Proof. Because $\mathbf{P}_i(\mathbf{u}_0^*)\tilde{\mathbf{B}}_j$ is indefinite, there exist $\mathbf{y}_1, \mathbf{y}_2 \in \mathbb{R}^{\tilde{n}_i}$ for which

$$\mathbf{y}_1^T \mathbf{P}_i(\mathbf{u}_0^*)\tilde{\mathbf{B}}_j \mathbf{y}_1 > 0 \quad \wedge \quad \mathbf{y}_2^T \mathbf{P}_i(\mathbf{u}_0^*)\tilde{\mathbf{B}}_j \mathbf{y}_2 < 0 \tag{3.136}$$

and the switching control $\hat{\mathbf{u}}(\mathbf{y})$ takes both values -1 and 1 on domain $\mathbb{R}^{\tilde{n}_i}$. Since $\mathbf{u}_0$ is constant, it cannot satisfy the condition (3.135) and via Theorem 3.6 there exists $\tilde{\mathbf{y}} \in \mathbb{R}^{\tilde{n}_i}$ such that $\hat{V}(\tilde{\mathbf{y}}) \neq V_0(\tilde{\mathbf{y}})$. From the result of Theorem 3.4 it follows that $\hat{V}(\tilde{\mathbf{y}}) < V_0(\tilde{\mathbf{y}})$. □

The resulting switching control law asymptotically stabilizes the system and guarantees bounded performance. In fact, the improvement of the overall performance is guaranteed for all possibilities except the special case, when the constant control is already the optimal control. Because the control problem is formulated on the infinite time horizon, the near-optimal feedback law is established via a computationally efficient procedure of solution to the algebraic Lyapunov equation.

The semi-active adaptive control method formulated in this section is summarized in Algorithm 3.5. It is assumed that the computation of the eigenvalues of the matrix $\mathbf{A}_{z,i}$ has a computational complexity of $\mathcal{O}\left(n_{z,i}^2\right)$. The procedure that solves the Lyapunov equation (3.99) [71] has complexity $\mathcal{O}\left(n_i^3\right)$. Since $n_i > n_{z,i}$, the computational complexity of the one iteration of the proposed control method is $\mathcal{O}\left(n_i^3\right)$.

Algorithm 3.5 The main loop of the infinite horizon semi-active control method

Require: The initial stabilizing (and preferably optimal) constant control $\mathbf{u}_0^*$.

1: At the time $t_i = h \cdot i$, measure state of the system $\mathbf{x}(t_i)$ and parameters of the disturbance $\boldsymbol{\gamma}_i$.
2: Execute the parametric identification procedure described in Algorithm 3.2 and compute matrices $\mathbf{A}_{z,i}$, $\mathbf{C}_{z,i}$ and the initial state of the disturbance $\mathbf{x}_{z0,i}$.
3: Compute eigenvalues λ_j, $j = 1, 2, \ldots, n_{z,i}$ of the matrix $\mathbf{A}_{z,i}$.
4: Pick $\alpha_i : \alpha_i < -\max\left\{0, \Re\left(\lambda_1\right), \Re\left(\lambda_2\right), \ldots, \Re\left(\lambda_{n_{z,i}}\right)\right\}$.
5: Compute solution $\mathbf{P}_i(\mathbf{u}_0^*)$ of the Lyapunov equation (3.99).
6: Apply switching control $\hat{\mathbf{u}} = (\hat{u}_j)_1^m$, $\hat{u}_j = -\operatorname{sgn} \mathbf{y}^T(t_i)\mathbf{P}_i(\mathbf{u}_0^*)\tilde{\mathbf{B}}_j\mathbf{y}(t_i)$, where $\mathbf{y}(t_i) = \begin{bmatrix}\mathbf{x}^T(t_i) & \mathbf{x}_{z0,i}^T\end{bmatrix}^T$.
7: Increment $i \leftarrow i + 1$.

Chapter 4

Adaptive control in presence of change of system parameters

In this chapter, the adaptive control method for mechanical systems affected by a change of their intrinsic parameters is proposed. The content of this chapter has been published in the Author's paper [46].

The attention is focused on the active model presented firstly in Eq. (2.35):

$$\dot{\mathbf{x}}(t) = \mathbf{A}(t)\mathbf{x}(t) + \mathbf{B}\mathbf{u}(t), \quad \mathbf{x}(0) = \mathbf{x_0}, \tag{4.1}$$

where $\mathbf{x}(t) \in \mathbb{R}^n$ is the state of the system, $\mathbf{u}(t) \in \mathbb{R}^m$ is the control vector, $\mathbf{x_0} \in \mathbb{R}^n$ denotes the initial condition, $\mathbf{A}(t) \in \mathbb{R}^{n\times n}$ is the varying state-transition matrix that represents changes of the system's parameters and $\mathbf{B} \in \mathbb{R}^{n\times m}$ is the control matrix. The goal of the control is to stabilize this system with minimization of the performance index:

$$J(\mathbf{u}) = \int_0^{T_f} \left[\mathbf{x}^T(t)\mathbf{Q}\mathbf{x}(t) + \mathbf{u}^T(t)\mathbf{R}\mathbf{u}(t)\right] \, \mathrm{d}t, \tag{4.2}$$

where $\mathbf{Q} \in \mathbb{R}^{n\times n}$ and $\mathbf{R} \in \mathbb{R}^{m\times m}$ are positive definite. It is also assumed that the changing parameters of these systems and, as a consequence, changing matrix $\mathbf{A}(t)$, vary *slow enough*, that is, they allow to approximate them by a series of parameters that are constant on each adaptation interval, $t \in [t_i, t_i + h)$. In particular, we assume that the system's actual parameters are piecewise constant and are affected only by jump changes. Example of such a situation is a sudden damage of a structure. In every iteration i of the adaptation, it is then assumed that the matrix $\mathbf{A}_i$ which approximates the matrix $\mathbf{A}(t)$ is constant in time.

The adaptive control problem considered in this section can be now stated as follows:

$$\begin{aligned}
\textbf{Find: } & \mathbf{u}_i^* : \mathbb{R}^n \mapsto \mathcal{U} \subset \mathbb{R}^m, \\
\textbf{such that: } & \mathbf{u}_i^*(\mathbf{x}(t)) = \underset{\mathbf{u}(\mathbf{x}(t))\in\mathcal{U},\ t\in\mathbb{T}_i}{\arg\min} J_i(\mathbf{u}) = \\
& \int_{t_i}^{\infty} \left[\mathbf{x}^T(t)\mathbf{Q}\mathbf{x}(t) + \mathbf{u}^T(t)\mathbf{R}\mathbf{u}(t)\right] \mathrm{d}t, \\
\textbf{subject to: } & \dot{\mathbf{x}}(t) = \mathbf{A}_i\mathbf{x}(t) + \mathbf{B}\mathbf{u}(t), \\
& \mathbf{x}(t_i) = \mathbf{x}_i, \\
& t_i = ih, \\
& \mathbb{T}_i = [t_i,\, \infty)\,.
\end{aligned} \tag{4.3}$$

Observe that the adaptive MPC formulation (4.3) represents an optimal control problem that is independent of time. In the case of an active control system, the solution to the problem (4.3) takes the form of the infinite horizon LQR. The goal of the adaptive control method is to, based on measurements, find approximations $\mathbf{A}_i$ of the matrix $\mathbf{A}(t)$. In this work, the proposed approach is to identify matrix $\mathbf{A}_i$ indirectly, via the approximation of the associated value function, similar to the value function V of the HJB equation (2.23). This method is based on the control methods presented in the series of works [72, 73, 74].

4.1 Policy iteration method

Let the linear active control system with unknown state-transition matrix $\mathbf{A}_i$ be defined as in control problem (4.3):

$$\dot{\mathbf{x}}(t) = \mathbf{A}_i\mathbf{x}(t) + \mathbf{B}\mathbf{u}(t), \quad \mathbf{x}(t_i) = \mathbf{x}_i. \tag{4.4}$$

The performance of the control is measured by the quadratic performance index defined on an infinite time horizon, as defined in adaptive control problem (4.3):

$$J_i(\mathbf{u}) = \int_{t_i}^{\infty} (\mathbf{x}^T(t)\mathbf{Q}\mathbf{x}(t) + \mathbf{u}^T(t)\mathbf{R}\mathbf{u}(t))\,\mathrm{d}t. \tag{4.5}$$

Within the considered problem it is assumed that the pair $(\mathbf{A}_i, \mathbf{B})$ is stabilizable for every adaptation iteration i.

Define the value function $V^{\boldsymbol{\mu}_i}(\mathbf{x}_0) : \mathbb{R}^n \mapsto \mathbb{R}^+$ associated with a closed-loop control law $\boldsymbol{\mu}_i(\mathbf{x})$ as the value of the performance index $J_i(\boldsymbol{\mu}_i(\mathbf{x}))$ for the initial point $\mathbf{x}_0$:

$$\begin{aligned}
V^{\boldsymbol{\mu}_i}(\mathbf{x}_i) &= \int_{t_i}^{\infty} \left(\mathbf{x}^T(t)\mathbf{Q}\mathbf{x}(t) + \boldsymbol{\mu}_i^T(\mathbf{x}(t))\mathbf{R}\boldsymbol{\mu}_i(\mathbf{x}(t))\right) \mathrm{d}t, \quad \mathbf{x}(t_i) = \mathbf{x}_0, \\
\dot{\mathbf{x}}(t) &= \mathbf{A}_i\mathbf{x}(t) + \mathbf{B}\boldsymbol{\mu}_i(\mathbf{x}(t)).
\end{aligned} \tag{4.6}$$

Let now define an admissible control law for the system (4.4).

Definition 4.1 (Admissible control, based on [75, Definition 1.])**.** *A control law $\boldsymbol{\mu}_i(\mathbf{x})$ is defined admissible for the system* (4.4) *on some compact set $\Omega \subseteq \mathbb{R}^n$, $\mathbf{0} \in \operatorname{int}\Omega$ if:*

1. $\boldsymbol{\mu}_i(\mathbf{x})$ *is differentiable on* Ω,

2. $\boldsymbol{\mu}_i(\mathbf{0}) = \mathbf{0}$,

3. *the closed-loop system* $\dot{\mathbf{x}}(t) = \mathbf{A}_i\mathbf{x}(t) + \mathbf{B}\boldsymbol{\mu}_i(\mathbf{x}(t))$ *is asymptotically stable on* Ω,

4. *the value function* $V^{\boldsymbol{\mu}_i}(\mathbf{x})$ *is finite on* Ω.

Notice that for the admissible control $\boldsymbol{\mu}_i(\mathbf{x})$, the value function $V^{\boldsymbol{\mu}_i}(\mathbf{x})$ is differentiable on Ω. Observe important property of the infinite horizon value function defined for admissible control law $\boldsymbol{\mu}_i(\mathbf{x})$:

$$V^{\boldsymbol{\mu}_i}(\mathbf{x}(t_i)) = V^{\boldsymbol{\mu}_i}(\mathbf{x}(t_i + t)) + \int_{t_i}^{t_i+t} \left(\mathbf{x}^T(\tau)\mathbf{Q}\mathbf{x}(\tau) + \boldsymbol{\mu}_i^T(\mathbf{x}(\tau))\mathbf{R}\boldsymbol{\mu}_i(\mathbf{x}(\tau))\right) \mathrm{d}\tau. \tag{4.7}$$

Differentiating Eq. (4.7) with respect to t, a partial differential equation is obtained:

$$0 = \frac{\partial V^{\boldsymbol{\mu}_i}(\mathbf{x})}{\partial \mathbf{x}} \left(\mathbf{A}_i\mathbf{x} + \mathbf{B}\boldsymbol{\mu}_i(\mathbf{x})\right) + \mathbf{x}^T\mathbf{Q}\mathbf{x} + \boldsymbol{\mu}_i^T(\mathbf{x})\mathbf{R}\boldsymbol{\mu}_i(\mathbf{x}), \quad V^{\boldsymbol{\mu}_i}(\mathbf{0}) = 0. \tag{4.8}$$

Notice the similarity between the partial differential equation (4.8) that defines the cost associated with an admissible control $\boldsymbol{\mu}_i(\mathbf{x})$ and the HJB equation (2.24) that defines the cost associated with the *optimal* control $\boldsymbol{\mu}^*(\mathbf{x})$:

$$0 = \min_{\boldsymbol{\mu}_i(\mathbf{x})} \left\{ \frac{\partial V^*(\mathbf{x})}{\partial \mathbf{x}} \left(\mathbf{A}_i\mathbf{x} + \mathbf{B}\boldsymbol{\mu}_i(\mathbf{x})\right) + \mathbf{x}^T\mathbf{Q}\mathbf{x} + \boldsymbol{\mu}_i^T(\mathbf{x})\mathbf{R}\boldsymbol{\mu}_i(\mathbf{x}) \right\}, \quad V^*(\mathbf{0}) = 0. \tag{4.9}$$

The main difference between both equation is that the Eq. (4.8) is linear, where the HJB equation is not.

In the present section of the work, the focus is on the admissible control law that is affine with respect to the system state,

$$\boldsymbol{\mu}_i(\mathbf{x}) = \mathbf{K}_i\mathbf{x}, \quad \mathbf{K}_i \in \mathbb{R}^{m\times n}, \quad i = 1, 2, \ldots. \tag{4.10}$$

Recall from the discussion in Section 3.3 that the linear system (4.4) is stabilizable if and only if there exists such a linear feedback control law $\boldsymbol{\mu}_i(\mathbf{x}) = \mathbf{K}_i\mathbf{x}$ for which the system (4.4) is stable. Observe that with such an affine control law, the system (4.4) has the linear autonomous form

$$\dot{\mathbf{x}}(t) = \left(\mathbf{A}_i + \mathbf{B}\mathbf{K}_i\right)\mathbf{x}(t), \quad \mathbf{x}(t_i) = \mathbf{x}_i. \tag{4.11}$$

As a consequence, the resulting closed-loop control system is exponentially stable and the value function $V^{\boldsymbol{\mu}_i}(\mathbf{x})$ is finite on $\mathbb{R}^n$. In fact, for the asymptotically stable linear system the value function $V^{\boldsymbol{\mu}_i}(\mathbf{x})$ has the explicit formula

$$V^{\boldsymbol{\mu}_i}(\mathbf{x}) = \mathbf{x}^T\mathbf{P}_i\mathbf{x}, \tag{4.12}$$

where the matrix $\mathbf{P}_i \in \mathbb{R}^{n\times n}$ is the solution to the algebraic Lyapunov equation:

$$\left(\mathbf{A}_i + \mathbf{B}\mathbf{K}\right)^T\mathbf{P}_i + \mathbf{P}_i\left(\mathbf{A}_i + \mathbf{B}\mathbf{K}_i\right) + \left(\mathbf{Q} + \mathbf{K}_i^T\mathbf{R}\mathbf{K}_i\right) = \mathbf{0}. \tag{4.13}$$

Notice that the linear stabilizing control law (4.10) is then an admissible control defined by Definition 4.1. Observe also, that the optimal value function V^* and the optimal control

law $\boldsymbol{\mu}^*(\mathbf{x})$ for the linear dynamical system (4.4) and the quadratic performance index (4.5) are defined similarly, i.e.

$$V^*(\mathbf{x}) = \mathbf{x}^T\mathbf{P}_i^*\mathbf{x},\ \boldsymbol{\mu}_i^*(\mathbf{x}) = \mathbf{K}_i^*\mathbf{x}, \quad \mathbf{K}_i^* = -\mathbf{R}^{-1}\mathbf{B}^T\mathbf{P}_i^*\mathbf{x}, \tag{4.14}$$

where $\mathbf{P}_i^*$ is the solution to the algebraic Riccati equation

$$\mathbf{0} = \mathbf{A}_i^T\mathbf{P}_i^* + \mathbf{P}_i^*\mathbf{A}_i - \mathbf{P}_i^*\mathbf{B}\mathbf{R}^{-1}\mathbf{B}^T\mathbf{P}_i^* + \mathbf{Q}. \tag{4.15}$$

Because the state-transition matrix $\mathbf{A}_i$ is not known, this Riccati equation cannot be solved in the direct way.

The idea of the present control algorithm is to calculate the series of admissible control laws $\boldsymbol{\mu}_i(\mathbf{x}) = \mathbf{K}_i\mathbf{x}$, $i = 1, 2, \ldots$, which guarantee improvement of the control, i.e.

$$\forall i = 1, 2, \ldots, \quad \forall \mathbf{x} \in \Omega,\ V^{\boldsymbol{\mu}_{i+1}}(\mathbf{x}) \leq V^{\boldsymbol{\mu}_i}\mathbf{x}). \tag{4.16}$$

The new control law is computed via minimization of the infinitesimal Eq. (4.8) for the value function of the previous admissible control:

$$\begin{aligned}\boldsymbol{\mu}_{i+1}(\mathbf{x}) &= \arg\min_{\boldsymbol{\mu}(\mathbf{x})}\left\{\frac{\partial V^{\boldsymbol{\mu}_i}(\mathbf{x})}{\partial \mathbf{x}}\left(\mathbf{A}_i\mathbf{x} + \mathbf{B}\boldsymbol{\mu}(\mathbf{x})\right) + \mathbf{x}^T\mathbf{Q}\mathbf{x} + \boldsymbol{\mu}^T(\mathbf{x})\mathbf{R}\boldsymbol{\mu}(\mathbf{x})\right\} \\ &= -\frac{1}{2}\mathbf{R}^{-1}\mathbf{B}^T\frac{\partial V^{\boldsymbol{\mu}_i}(\mathbf{x})}{\partial \mathbf{x}} = -\mathbf{R}^{-1}\mathbf{B}^T\mathbf{P}_i\mathbf{x}.\end{aligned} \tag{4.17}$$

Notice that, if the matrix $\mathbf{P}_i$ is known, then the new control is computed without the knowledge of the matrix $\mathbf{A}_i$. Next two Lemmas show that the new control $\boldsymbol{\mu}_{i+1}(\mathbf{x})$ is admissible and it results in a smaller performance cost than the previous control $\boldsymbol{\mu}_i(\mathbf{x})$.

Lemma 4.1. *Let $\boldsymbol{\mu}_i(\mathbf{x}) = \mathbf{K}_i\mathbf{x}$ denote an admissible control law for the system* (4.4) *and the performance index* (4.5) *and let the $V^{\boldsymbol{\mu}_i}(\mathbf{x}) = \mathbf{x}^T\mathbf{P}_i\mathbf{x}$ denote the associated value function. Then the new control law $\boldsymbol{\mu}_{i+1}(\mathbf{x}) = \mathbf{K}_{i+1}\mathbf{x}$ defined as in Eq.* (4.17) *is admissible.*

Proof. The control law $\boldsymbol{\mu}_{i+1}(\mathbf{x})$ is clearly differentiable with respect to $\mathbf{x}$ and $\boldsymbol{\mu}_{i+1}(\mathbf{0}) = \mathbf{0}$. The sufficient condition for admissibility is then the stability of the new control law. Recall that because $\left(\mathbf{Q} + \mathbf{K}_i^T\mathbf{R}\mathbf{K}_i\right)$ is positive definite, the solution to the Lyapunov equation corresponding to the previous closed-loop system:

$$\left(\mathbf{A}_i + \mathbf{B}\mathbf{K}_i\right)^T\mathbf{P}_i + \mathbf{P}_i\left(\mathbf{A}_i + \mathbf{B}\mathbf{K}_i\right) + \mathbf{Q} + \mathbf{K}_i^T\mathbf{R}\mathbf{K}_i = \mathbf{0} \tag{4.18}$$

is also a positive definite matrix $\mathbf{P}_i$. Consider a Lyapunov equation for the new closed-loop system and the matrix $\mathbf{P}_i$

$$\left(\mathbf{A}_i + \mathbf{B}\mathbf{K}_{i+1}\right)^T\mathbf{P}_i + \mathbf{P}_i\left(\mathbf{A}_i + \mathbf{B}\mathbf{K}_{i+1}\right) + \boldsymbol{\chi}_i = \mathbf{0}. \tag{4.19}$$

In this case, matrix $\mathbf{P}_i$ is known and the stability of the closed-loop system can be deduced from matrix $\boldsymbol{\chi}_i$: because $\mathbf{P}_i$ is a positive definite matrix, matrix $(\mathbf{A}_i + \mathbf{B}\mathbf{K}_{i+1})$ is stable if the matrix $\boldsymbol{\chi}_i$ is also positive definite, see [76, Lemma 7.1].

$$\boldsymbol{\chi}_i = -\mathbf{A}_i^T\mathbf{P}_i - \mathbf{P}_i\mathbf{A}_i - \mathbf{P}_i\mathbf{B}\mathbf{K}_{i+1} - \mathbf{K}_{i+1}^T\mathbf{B}^T\mathbf{P}_i. \tag{4.20}$$

Because the new feedback matrix is defined as $\mathbf{K}_{i+1} = -\mathbf{R}^{-1}\mathbf{B}^T\mathbf{P}_i$, then

$$\boldsymbol{\chi}_i = -\mathbf{A}_i^T\mathbf{P}_i - \mathbf{P}_i\mathbf{A}_i + 2\mathbf{K}_{i+1}^T\mathbf{R}\mathbf{K}_{i+1}. \tag{4.21}$$

From Lyapunov equation (4.18) it holds that

$$\begin{aligned} -\mathbf{A}_i^T\mathbf{P}_i - \mathbf{P}_i\mathbf{A}_i &= \mathbf{K}_i^T\mathbf{B}^T\mathbf{P}_i + \mathbf{P}_i\mathbf{B}\mathbf{K}_i + \mathbf{Q} + \mathbf{K}_i^T\mathbf{R}\mathbf{K}_i \\ &= -\mathbf{K}_i^T\mathbf{R}\mathbf{K}_{i+1} - \mathbf{K}_{i+1}^T\mathbf{R}\mathbf{K}_i + \mathbf{Q} + \mathbf{K}_i^T\mathbf{R}\mathbf{K}_i \end{aligned} \tag{4.22}$$

and

$$\begin{aligned} \boldsymbol{\chi}_i &= -\mathbf{K}_i^T\mathbf{R}\mathbf{K}_{i+1} - \mathbf{K}_{i+1}^T\mathbf{R}\mathbf{K}_i + \mathbf{Q} + \mathbf{K}_i^T\mathbf{R}\mathbf{K}_i + 2\mathbf{K}_{i+1}^T\mathbf{R}\mathbf{K}_{i+1} \\ &= \mathbf{Q} + \left(\mathbf{K}_i - \mathbf{K}_{i+1}\right)^T\mathbf{R}\left(\mathbf{K}_i - \mathbf{K}_{i+1}\right) + \mathbf{K}_{i+1}^T\mathbf{R}\mathbf{K}_{i+1} \end{aligned} \tag{4.23}$$

Because the matrix $\mathbf{Q}$ is positive definite and the matrices $\left(\mathbf{K}_i - \mathbf{K}_{i+1}\right)^T\mathbf{R}\left(\mathbf{K}_i - \mathbf{K}_{i+1}\right)$ and $\mathbf{K}_{i+1}^T\mathbf{R}\mathbf{K}_{i+1}$ are positive semi-definite, the matrix $\boldsymbol{\chi}_i$ is also positive definite. As a consequence, the new control $\boldsymbol{\mu}_{i+1}(\mathbf{x})$ is stabilizing and admissible. □

Lemma 4.2. *Let $\boldsymbol{\mu}_i(\mathbf{x}) = \mathbf{K}_i\mathbf{x}$ denote an admissible control law for the system* (4.4) *and performance index* (4.5) *and let the $V^{\boldsymbol{\mu}_i} = \mathbf{x}_i^T\mathbf{P}_i\mathbf{x}_i$ denote the associated value function. Then for the value function $V^{\boldsymbol{\mu}_{i+1}}(\mathbf{x}) = \mathbf{x}^T\mathbf{P}_{i+1}\mathbf{x}$ associated with the new control law $\boldsymbol{\mu}_{i+1}(\mathbf{x}) = \mathbf{K}_{i+1}\mathbf{x}$ defined as in Eq.* (4.17)*, the inequality*

$$\forall \mathbf{x} \in \Omega,\ V^{\boldsymbol{\mu}_{i+1}}(\mathbf{x}) \leq V^{\boldsymbol{\mu}_i}(\mathbf{x}). \tag{4.24}$$

holds.

Proof. Lemma 4.2 is proven by the comparison of matrices $\mathbf{P}_i$ and $\mathbf{P}_{i+1}$. Because Lemma 4.1 holds and new control is admissible, matrix $\mathbf{P}_{i+1}$ is defined as a positive definite solution to the Lyapunov equation:

$$\left(\mathbf{A}_i + \mathbf{B}\mathbf{K}_{i+1}\right)^T\mathbf{P}_{i+1} + \mathbf{P}_{i+1}\left(\mathbf{A}_i + \mathbf{B}\mathbf{K}_{i+1}\right) + \mathbf{Q} + \mathbf{K}_{i+1}^T\mathbf{R}\mathbf{K}_{i+1} = \mathbf{0}. \tag{4.25}$$

Recall from Eqs. (4.23) and (4.18) that

$$\begin{aligned} \mathbf{Q} + \mathbf{K}_{i+1}^T\mathbf{R}\mathbf{K}_{i+1} &= \boldsymbol{\chi}_i - \left(\mathbf{K}_i - \mathbf{K}_{i+1}\right)^T\mathbf{R}\left(\mathbf{K}_i - \mathbf{K}_{i+1}\right) \\ &= -\left(\mathbf{A}_i + \mathbf{B}\mathbf{K}_{i+1}\right)^T\mathbf{P}_i - \mathbf{P}_i\left(\mathbf{A}_i + \mathbf{B}\mathbf{K}_{i+1}\right) \\ &\quad - \left(\mathbf{K}_i - \mathbf{K}_{i+1}\right)^T\mathbf{R}\left(\mathbf{K}_i - \mathbf{K}_{i+1}\right). \end{aligned} \tag{4.26}$$

Combining Eqs. (4.25) and (4.26), we have

$$\begin{aligned} 0 &= \left(\mathbf{A}_i + \mathbf{B}\mathbf{K}_{i+1}\right)^T\mathbf{P}_{i+1} + \mathbf{P}_{i+1}\left(\mathbf{A}_i + \mathbf{B}\mathbf{K}_{i+1}\right) - \left(\mathbf{A}_i + \mathbf{B}\mathbf{K}_{i+1}\right)^T\mathbf{P}_i \\ &\quad - \mathbf{P}_i\left(\mathbf{A}_i + \mathbf{B}\mathbf{K}_{i+1}\right) - \left(\mathbf{K}_i - \mathbf{K}_{i+1}\right)^T\mathbf{R}\left(\mathbf{K}_i - \mathbf{K}_{i+1}\right) \\ &= \left(\mathbf{A}_i + \mathbf{B}\mathbf{K}_{i+1}\right)^T\left(\mathbf{P}_{i+1} - \mathbf{P}_i\right) + \left(\mathbf{P}_{i+1} - \mathbf{P}_i\right)\left(\mathbf{A}_i + \mathbf{B}\mathbf{K}_{i+1}\right) \\ &\quad - \left(\mathbf{K}_i - \mathbf{K}_{i+1}\right)^T\mathbf{R}\left(\mathbf{K}_i - \mathbf{K}_{i+1}\right). \end{aligned} \tag{4.27}$$

Since matrix $\left(\mathbf{K}_i - \mathbf{K}_{i+1}\right)^T\mathbf{R}\left(\mathbf{K}_i - \mathbf{K}_{i+1}\right)$ is positive semi-definite, then symmetric matrix $\left(\mathbf{P}_{i+1} - \mathbf{P}_i\right)$ is negative semi-definite. As a result, $\mathbf{P}_{i+1} \preceq \mathbf{P}_i$, which concludes the proof. □

Remark 4.1. *Observe that if the matrices* $\mathbf{K}_i$ $\mathbf{K}_{i+1}$ *are not equal, then* $\mathbf{P}_{i+1} \neq \mathbf{P}_i$. *As a result, there exists such an initial state* $\mathbf{x} \in \mathbb{R}^n$, *for which the new control law* $\boldsymbol{\mu}_{i+1}(\mathbf{x})$ *provides strict improvement, i.e.*

$$\exists \mathbf{x} \in \mathbb{R}^n : \quad V^{\boldsymbol{\mu}_{i+1}}(\mathbf{x}) < V^{\boldsymbol{\mu}_i}(\mathbf{x}). \tag{4.28}$$

The next theorem combines results of the Lemmas 4.1, 4.2 and defines policy iteration scheme.

Theorem 4.1. *Let* $\boldsymbol{\mu}_0(\mathbf{x}) = \mathbf{K}_0\mathbf{x}$ *denote the initial admissible control law for the system* (4.4) *and the performance index* (4.5). *Then the iteration between*

1. *computation of the value function*
   $V^{\boldsymbol{\mu}_i} = \mathbf{x}_i^T\mathbf{P}_i\mathbf{x}_i$*:* $(\mathbf{A}_i + \mathbf{B}\mathbf{K}_i)^T \mathbf{P}_i + \mathbf{P}_i (\mathbf{A}_i + \mathbf{B}\mathbf{K}_i) + \mathbf{Q} + \mathbf{K}_i^T\mathbf{R}\mathbf{K}_i = \mathbf{0}$ *and*

2. *computation of the new control law* $\boldsymbol{\mu}_{i+1}(\mathbf{x}) = \mathbf{K}_{i+1}\mathbf{x} = -\mathbf{R}^{-1}\mathbf{B}^T\mathbf{P}_i\mathbf{x}$

for $i = 1, 2, \ldots$ *converges to the optimal control* $\boldsymbol{\mu}^*(\mathbf{x})$ *and the optimal value function* $V^*(\mathbf{x})$.

Proof. [72, Theorem 1.] Sketch of the proof is as follows. From Lemma 4.1, the sequence of control laws $\boldsymbol{\mu}_i(\mathbf{x})$, $i = 1, 2, \ldots$ is admissible. From Lemma 4.2, the sequence of value functions $V^{\boldsymbol{\mu}_i}(\mathbf{x})$, $i = 1, 2, \ldots$ is monotonically decreasing and bounded from below by the optimal value function $V^*(\mathbf{x}) = \mathbf{x}^T\mathbf{P}_i^*\mathbf{x}$. Observe that for all $\mathbf{x} \in \mathbb{R}^n$, $V^*(\mathbf{x})$ is the infimum of the sequence $V^{\boldsymbol{\mu}_i}(\mathbf{x})$, $i = 1, 2, \ldots$.

Because Ω is compact, Dini's Theorem [77, Theorem 12.1] states that $V^{\boldsymbol{\mu}_i}$ converges uniformly to $V^*(\mathbf{x})$. $\mathbf{P}_i$ converges then to $\mathbf{P}_i^*$ and the control law $\boldsymbol{\mu}_i(\mathbf{x}) = \mathbf{R}^{-1}\mathbf{B}^T\mathbf{P}_i\mathbf{x}$ converges to the optimal control $\boldsymbol{\mu}_i^*(\mathbf{x}) = -\mathbf{R}^{-1}\mathbf{B}^T\mathbf{P}_i^*\mathbf{x}$ □

The policy iteration scheme defined in Theorem 4.1 guarantees that if the initial control is admissible, then every control law that has been computed in the policy iteration is also admissible and provides improvement of the controller's performance. To obtain these new control laws, only matrices $\mathbf{R}$, $\mathbf{B}$ and $\mathbf{P}_i$ are needed to be known. Because matrix $\mathbf{A}_i$ is assumed to be unknown, matrix $\mathbf{P}_i$ cannot be computed from the associated Lyapunov equation (4.13). In the present approach, the matrix $\mathbf{P}_i$ is evaluated via online measurements of the state of the system. The computation algorithm makes use of the fundamental property of the value function, denoted in Eq. (4.7).

4.2 Estimation of value function

The goal of this part of the section is to provide scheme that allows to compute the associated matrix $\mathbf{P}_i$. It is assumed that the state of the system $\mathbf{x}(t)$ can be directly measured. Let

$$\boldsymbol{\upsilon}_i(t) : [t_i, t_{i+1}) \times \mathbb{R}^n \mapsto \mathbb{R}^n, \quad t_{i+1} = t_i + h \tag{4.29}$$

denote the trajectory of the controlled system during the ith adaptation interval with the initial state $\mathbf{x}(t_i)$. The proposed scheme is based on the subsequent measurements of the state conducted within this adaptation interval. Let the set of N such measurements be defined as $\Upsilon_N(t_i) = \{\boldsymbol{\upsilon}_i(t_i + d_j),\, j = 1,\, 2,\, \ldots,\, N\}$ with $d_1 = 0$, $d_1 \leq d_2 \leq \ldots \leq d_N < h$.

From Eq. (4.7) it is known that for some $\Delta t > 0$

$$\begin{aligned}
&\mathbf{x}(t)^T \mathbf{P}_i \mathbf{x}(t) - \mathbf{x}(t+\Delta t)^T \mathbf{P}_i \mathbf{x}(t+\Delta t) \\
&= \int_t^{t+\Delta t} \left(\mathbf{x}(\tau)^T \mathbf{Q} \mathbf{x}(\tau) + \boldsymbol{\mu}_i^T(\mathbf{x}(\tau)) \mathbf{R} \boldsymbol{\mu}_i(\mathbf{x}(\tau)) \right) \mathrm{d}\tau \\
&= \int_t^{t+\Delta t} \mathbf{x}(\tau)^T \left(\mathbf{Q} + \mathbf{K}_i^T \mathbf{R} \mathbf{K}_i \right) \mathbf{x}(\tau)\, \mathrm{d}\tau.
\end{aligned} \tag{4.30}$$

Denote the right-hand side of the Eq. (4.30) by

$$q_{i,j}(t, \Delta t) = \int_{t+d_j}^{t+d_j+\Delta t} \mathbf{x}(\tau)^T \left(\mathbf{Q} + \mathbf{K}_i^T \mathbf{R} \mathbf{K}_i \right) \mathbf{x}(\tau)\, \mathrm{d}\tau, \quad j = 1,\, 2,\, \ldots,\, N. \tag{4.31}$$

Let $\Upsilon_N(t_i + \Delta t)$ denote the set of the measurements of the state that is shifted in time by Δt. The focus of the considered computation scheme is on the values of $q_{i,j}(t_i, \Delta t)$ that is, measured between the consecutive elements of $\Upsilon_N(t_i, \mathbf{x}(t_i))$ and $\Upsilon_N(t_i + \Delta t, \mathbf{x}(t_i + \Delta t))$. It is assumed that the values of the integrals $q_{i,j}$ can be obtained via online measurement of the state of the system.

Since the positive definite matrix

$$\mathbf{P}_i = \begin{bmatrix} p_{11}^{(i)} & p_{12}^{(i)} & \cdots & p_{1n}^{(i)} \\ p_{12}^{(i)} & p_{22}^{(i)} & \cdots & p_{2n}^{(i)} \\ \vdots & \vdots & \ddots & \vdots \\ p_{1n}^{(i)} & p_{2n}^{(i)} & \cdots & p_{nn}^{(i)} \end{bmatrix} \tag{4.32}$$

is symmetric, it is uniquely defined by only $\frac{(n+1)n}{2}$ entries, placed above or below the main diagonal. The quadratic form $\mathbf{x}^T \mathbf{P}_i \mathbf{x}$ can be then rewritten as a scalar equation

$$\mathbf{x}^T \mathbf{P}_i \mathbf{x} = \sum_{a=1}^{n} \sum_{b=1}^{a} x_a x_b p_{ab}^{(i)}, \quad \mathbf{x} = \begin{bmatrix} x_1 \\ x_2 \\ \vdots \\ x_n \end{bmatrix}. \tag{4.33}$$

Define the vector consisting of the entries of matrix $\mathbf{P}_i$ that have been used in Eq. (4.33)

$$\boldsymbol{\theta}_i = \begin{bmatrix} p_{11}^{(i)} & p_{21}^{(i)} & p_{22}^{(i)} & p_{31}^{(i)} & \cdots & p_{nn}^{(i)} \end{bmatrix}^T \in \mathbb{R}^{\frac{(n+1)n}{2}} \tag{4.34}$$

and the row vector function that consists of the corresponding polynomials:

$$\boldsymbol{\gamma}(\mathbf{x}) = \begin{bmatrix} x_1^2 & x_1 x_2 & x_2^2 & x_1 x_3 & \cdots & x_n^2 \end{bmatrix}. \tag{4.35}$$

Notice that

$$\boldsymbol{\gamma}(\mathbf{x}) \boldsymbol{\theta}_i = \mathbf{x}^T \mathbf{P}_i \mathbf{x}. \tag{4.36}$$

Let the number of measurements N in the set $\Upsilon_N(t_i)$ be equal to the number of the unknown parameters of the matrix $\mathbf{P}_i$, i.e. $N = \frac{(n+1)n}{2}$. Let the square matrix $\mathbf{\Gamma}(t)$ be built as follows:

$$\mathbf{\Gamma}(t) = \begin{bmatrix} \boldsymbol{\gamma}(\mathbf{x}(t+d_1)) \\ \boldsymbol{\gamma}(\mathbf{x}(t+d_2)) \\ \vdots \\ \boldsymbol{\gamma}(\mathbf{x}(t+d_N)) \end{bmatrix} \in \mathbb{R}^{\frac{(n+1)n}{2} \times \frac{(n+1)n}{2}}. \tag{4.37}$$

Observe that, according to Eqs. (4.36) and (4.30), the identity

$$(\mathbf{\Gamma}(t_i) - \mathbf{\Gamma}(t_i + \Delta t))\boldsymbol{\theta}_i = \begin{bmatrix} q_{i,1}(t_i, \Delta t) \\ q_{i,2}(t_i, \Delta t) \\ \vdots \\ q_{i,N}(t_i, \Delta t) \end{bmatrix}. \tag{4.38}$$

holds.

It is assumed that the initial state $\mathbf{x}(t_i)$ and the measurement times d_j, $j = 1, 2, \ldots, N$ are such that $\mathbf{\Gamma}(t_i)$ is invertible, i.e. the polynomial functions that the vector $\boldsymbol{\theta}_i$ (Eq. (4.34)) consists of are linearly independent on the set $\Upsilon_N(t_i)$. From [74, Lemma 3] it follows that there exists Δt such that the matrix $(\mathbf{\Gamma}(t_i) - \mathbf{\Gamma}(t_i + \Delta t))$ is invertible. The unknown matrix $\mathbf{P}_i$ defined by the vector $\boldsymbol{\theta}_i$ is then an unique solution of the equation

$$\boldsymbol{\theta}_i = (\mathbf{\Gamma}(t_i) - \mathbf{\Gamma}(t_i + \Delta t))^{-1} \begin{bmatrix} q_{i,1}(t_i, \Delta t) \\ q_{i,2}(t_i, \Delta t) \\ \vdots \\ q_{i,N}(t_i, \Delta t) \end{bmatrix}. \tag{4.39}$$

Notice that the convergence of the iteration scheme defined in Theorem 4.1 is guaranteed only if the initial control $\boldsymbol{\mu}_0(\mathbf{x}) = \mathbf{K}_0\mathbf{x}$ is stabilizing. When the matrix $\mathbf{A}_i$ is stable, this condition is trivially achieved with $\mathbf{K}_0 = \mathbf{0}$. Such a situation is very common when the controlled system represents a mechanical system with internal damping, see the discussion in Theorem 3.1. If the stability of the matrices $\mathbf{A}_i$ cannot be guaranteed, it is then assumed that the internal structure of the controlled mechanical system is known and allows for explicit formulation of the control law $\boldsymbol{\mu}_0(\mathbf{x})$ that it always stable. In particular, it is assumed that such a control law can be formulated as affine with respect to the velocities of the system, i.e. control that mimics internal damping.

The computation of the new control laws is continued until the assumed convergence criterion is not reached, i.e. $\|\boldsymbol{\theta}_i - \boldsymbol{\theta}_{i-1}\| \leq \epsilon_{\text{stop}}$, with $\epsilon_{\text{stop}} > 0$. Control law $\boldsymbol{\mu}_i(\mathbf{x})$ is then used as the initial control in the subsequent iterations of the adaptation scheme $i+1$, $i+2$, ..., i.e. $\boldsymbol{\mu}_{i+1}(\mathbf{x}) = \boldsymbol{\mu}_i(\mathbf{x})$, until the change of the parameters is not detected. This detection is conducted by checking whether the value function for the converged control law did not change, i.e. $\|\boldsymbol{\theta}_i - \boldsymbol{\theta}_{i-1}\| \geq \epsilon_{\text{start}}$ with $\epsilon_{\text{start}} > \epsilon_{\text{stop}}$. The initial stabilizing control law $\boldsymbol{\mu}_0(\mathbf{x}) = \mathbf{K}_0\mathbf{x}$ is applied to the system at the beginning of the control and whenever the change of the dynamics has been detected.

Algorithm 4.1 The main loop of the active policy iteration control method

Require: The times of measurements d_j, $j = 1, 2, \ldots, \frac{n(n+1)}{2}$, the time-shift Δt, the initial stabilizing policy $\boldsymbol{\mu}_0(\mathbf{x}) = \mathbf{K}_0$, matrices $\mathbf{Q}$, $\mathbf{R}$, $\mathbf{B}$, threshold values ϵ_{start} ϵ_{stop} for detection of the change and convergence of the iteration, respectively.

Control the system using the previously computed control $\boldsymbol{\mu}_i(\mathbf{x})$.
$j \leftarrow 1$
for $j \leq \frac{n(n+1)}{2}$ **do**
    Measure state $\mathbf{x}(t_i + d_j)$.
    Measure state $\mathbf{x}(t_i + d_j + \Delta t)$.
    Compute integral $q_{i,j}(t_i, \Delta t)$ according to Eq. (4.31).
    Increment $j \leftarrow j + 1$.
end for
Compute $\boldsymbol{\theta}_i$ according to Eq. (4.39).
if $\|\boldsymbol{\theta}_i - \boldsymbol{\theta}_{i-1}\| \geq \epsilon_{\text{start}}$ **then**
    $\boldsymbol{\mu}_{i+1}(\mathbf{x}) = \boldsymbol{\mu}_0(\mathbf{x})$
else
    if $\|\boldsymbol{\theta}_{i+1} - \boldsymbol{\theta}_i\| < \epsilon_{\text{stop}}$ **then**
        $\boldsymbol{\mu}_{i+1}(\mathbf{x}) = \boldsymbol{\mu}_i(\mathbf{x})$
    else
        Compute matrix $\mathbf{P}_i$ from $\boldsymbol{\theta}_i$
        Compute new control law $\boldsymbol{\mu}_{i+1}(\mathbf{x}) = -\mathbf{R}^{-1}\mathbf{B}\mathbf{P}_i\mathbf{x}$
    end if
end if
Increment $i \leftarrow i + 1$.

Presented adaptive control algorithm is summarized in Algorithm 4.1. The computational burden of the Algorithm 4.1 is dominated by the computation of the vector $\boldsymbol{\theta}_i$. For the dynamical system of the order n, the size of the vector to be found $\boldsymbol{\theta}_i$ is equal to $\frac{n(n+1)}{2}$ and the inversion of the matrix performed in Eq. (4.39) has complexity $\mathcal{O}\left(n^6\right)$. The proposed control method is tested numerically in Section 5.4 via simulation of the mechanical oscillator subjected to a sudden change of the stiffness parameters.

Chapter 5

Numerical analysis

In this chapter, the numerical analysis of the adaptive control methods formulated in Chapters 3 and 4 is presented. The performance of every control method is tested via numerical simulations of mechanical stabilization problems. The particular scenarios correspond to the practical engineering problems that commonly occur in the industry. The special attention is given to the analysis of the autoregressive identification of a disturbance, as it has a number of parameters that impacts the overall performance of the control method.

5.1 Active control of the drilling machine

In this Section, the adaptive control method that has been presented in Section 3.2 is tested numerically. The results of this section have been originally presented in the author's paper [47]. The method is based on the autoregressive identification of a disturbance and the finite-horizon LQR. It is validated and analysed numerically via simulation of the problem of vibration attenuation of a drilling system subjected to a change of the ground friction characteristics.

The friction is considered as a generalized resistance of the drilled ground to the drilling. It can be both smooth in time and stepwise variable and can contain a sudden jump of characteristics. It generates a resistive force that can change suddenly when the drill passes a layer of soil or rock or it meets rigid inclusions. The voltage supplying the electric motor is the control function and when applied to the system, it influences the dynamic response in a nonlinear way. A drill string used in drilling for gas and oil is an example of such a system. The string has a low diameter-to-length ratio. The sticking phase and the phase of slipping when the friction coefficient decreases may lead to instability of the system and to stick-slip flicker. Self-induced vibrations lower the effectiveness of the drilling process and may even damage the drill. The friction parameters depend on the rock formation, which means that the resulting friction varies with the depth of the drilling.

The control methods proposed in the literature for such problems can be divided into passive and active approaches. The passive solutions focus on optimization of the drilling bit parameters or drilling input parameters, such as the weight of the drill bit, the input torque,

and the rotary speed, to make stick-slip vibrations less likely to occur. This approach is presented in [78], where the authors proposed an increase of the torsional stiffness of the drill string and a redesign of the bit. In [79] the optimization of the bottom hole assembly (BHA) design is given.

One of the active methods for vibration attenuation is to optimize the aforementioned parameters in real time, based on measurements. In [80] an automated vibration detection system with guidelines for the machine operators is proposed. In another approach, active control systems are used. In [81], a sliding mode control scheme is proposed to attenuate stick-slip oscillations in oil drill strings. An active damping system based on a feedback control is developed in [82]. [83] presented an active strategy based on optimal state feedback control. An H_∞ controller for a drilling system is given in [84]. In [85] the control scheme based on the proportional-integral regulator for reduction of torsional vibration in a drill string is investigated. A comprehensive review of the literature concerning vibration suppression in drilling systems is given in [86].

The drilling machine can be treated as a special case of a more general drive system coupled with an elastic joint. There exist numerous examples of the vibration control algorithms for such systems that also deal with the disturbances explicitly. The sliding-mode control and the reconstruction of the disturbance value by the Kalman filtering are proposed in [20]. In [87], the authors formulate nonlinear fuzzy Luenberger observer that estimates the state of the system along with the present value of the disturbance load. Similar fuzzy disturbance observer is introduced in [21].

Model description

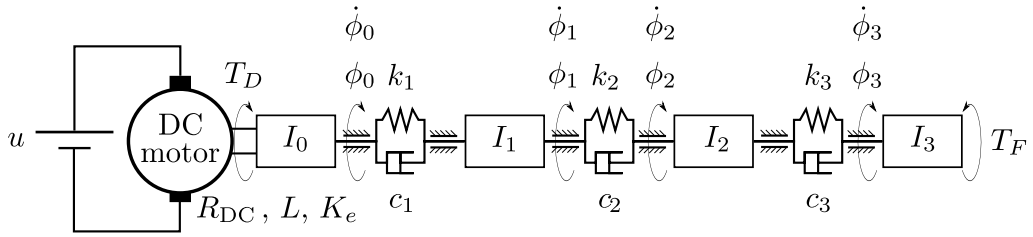

Figure 5.1: The scheme of the controlled object.

Let us consider the system depicted in Fig. 5.1. It consists of a DC motor with resistance R_{DC}, inductance L, and electromotive force constant K_e. The motor generates the torque T_D. Although the drill string part of the machine can be modelled as the dynamical system of distributed parameters that is then transformed into its lumped approximation (see [82], [88]), it is also common to model it directly by the system of lumped parameters (see [89], [84], [90], [81]). In this example, we employ the latter strategy and define the mechanical part of the system only by the means of a set of rigid bodies. The shaft of the motor is firmly connected to the first body. The moment of inertia of this coupling is I_0. The next three bodies are numbered from left to right and are characterized by the moments of inertia denoted by I_1, I_2, I_3, respectively. These bodies are interconnected by the use of torsion

springs of the stiffnesses k_1, k_2 and k_3, and torsion dampers with damping coefficients c_1, c_2, and c_3. The angular displacement and angular velocity of the i-th body are denoted by ϕ_i and $\dot{\phi}_i$, respectively. The disturbance torque, consisting of the changing torsional friction $T_F(t, \dot{\phi}_3)$ and other disturbances, modelled as the white noise, is assumed to excite the body I_3.

The friction torque is defined as in [88]:

$$T_F\left(\dot{\phi}_3\right) = \begin{cases} \left(T_C + [T_B - T_C]\, e^{-c_v|\dot{\phi}_3|}\right) \operatorname{sign}(\dot{\phi}_3) + f_T\dot{\phi}_3, & \text{if } \left|\dot{\phi}_3\right| \geq \dot{\phi}_c \\ \left(\frac{\dot{\phi}_3}{\dot{\phi}_c}\right)\left(T_C + [T_B - T_C]\, e^{-c_v\dot{\phi}_c} + f_T\dot{\phi}_c\right), & \text{if } \left|\dot{\phi}_3\right| < \dot{\phi}_c, \end{cases} \tag{5.1}$$

where T_C is the Coulomb friction torque, T_B is the static friction torque, c_v defines the steepness of the friction characteristics, and f_T is the viscous friction coefficient. The parameter $\dot{\phi}_c$ defines the length of the interval of the angular velocity on the friction characteristics on which the sticking phase (static friction) is approximated by a straight line.

The dynamics of the mechanical coupling is represented by the second-order nonlinear differential equation analogous to the general dynamical equation (2.29) of the mechanical object

$$\mathbf{M}\ddot{\mathbf{q}}(t) + \mathbf{C}\dot{\mathbf{q}}(t) + \mathbf{K}\mathbf{q}(t) = -\mathbf{F}_{\text{frict.}}T_F(t, \dot{\phi}_3) + \mathbf{F}_{\text{DC}}T_D(\dot{\mathbf{q}}(t), u(t)), \tag{5.2}$$

where $\mathbf{q} = \begin{bmatrix}\phi_0 & \cdots & \phi_3\end{bmatrix}^T$ is the vector of the angular positions of the bodies; $\dot{\mathbf{q}}$ and $\ddot{\mathbf{q}}$ are the vectors of angular velocities and accelerations of the bodies, respectively. The matrix $\mathbf{M} = \operatorname{diag}(I_0, I_1, I_2, I_3)$, $\mathbf{M} \in \mathbb{R}^{4\times4}$ is the mass matrix of the system, $\mathbf{K} \in \mathbb{R}^{4\times4}$ is the stiffness matrix, $\mathbf{C} \in \mathbb{R}^{4\times4}$ is the damping matrix and $\mathbf{F}_{\text{frict.}} = \begin{bmatrix}0 & 0 & 0 & 1\end{bmatrix}^T$ and $\mathbf{F}_{\text{DC}} = \begin{bmatrix}1 & 0 & 0 & 0\end{bmatrix}^T$ are the vectors allocating the nonlinear friction and motor torque on the mechanical part of the system, respectively. The dynamic behaviour of the DC motor is described by the first-order dynamical equation:

$$\dot{T}_D(t) = -\frac{K_e^2}{L}\mathbf{E}\dot{\mathbf{q}}(t) - \frac{R}{L}T_D(t) + \frac{K_e}{L}u(t), \tag{5.3}$$

where $\mathbf{E} = \begin{bmatrix}1 & 0 & 0 & 0\end{bmatrix}$ represents the impact of the angular velocity of the first body on the motor's torque (observe that $\mathbf{E}\dot{\mathbf{y}}(t) = \dot{\phi}_0(t)$). The voltage applied to the motor is the control input $u(t) \in \mathcal{U} \subset \mathbb{R}$. In this particular system the compact control set is defined by the lower and upper constraints on the control value, $\mathcal{U} = [u_{\min}; u_{\max}]$ with $u_{\min} < u_{\max}$, $u_{\min}$, $u_{\max} \in \mathbb{R}$.

Both equations (5.2) and (5.3) can be rewritten as the first-order differential equation of the form of Eq. (3.1) that links both mechanical and electric part of the considered system:

$$\dot{\mathbf{x}}(t) = \mathbf{A}\mathbf{x}(t) + \mathbf{B}u(t) + \mathbf{B}_z T_F(t, \dot{\phi}_3), \tag{5.4}$$

$$\mathbf{x}(t) = \begin{bmatrix}\mathbf{q}^T(t) & \dot{\mathbf{q}}^T(t) & T_D(t)\end{bmatrix}^T, \quad \mathbf{x}(t) \in \mathbb{R}^9, \tag{5.5}$$

where $\mathbf{x}(t)$ is the state of the system that is made up of the set of angular displacements and velocities of all rigid bodies, ϕ_{0-3} and $\dot{\phi}_{0-3}$, along with the torque generated by the DC motor T_D. The matrix

$$\mathbf{A} = \begin{bmatrix} \mathbf{0} & \mathbf{I} & \mathbf{0} \\ -\mathbf{M}^{-1}\mathbf{K} & -\mathbf{M}^{-1}\mathbf{C} & \mathbf{M}^{-1}\mathbf{F}_{\mathrm{DC}} \\ \mathbf{0} & -\frac{K_e^2}{L}\mathbf{E} & -\frac{R}{L} \end{bmatrix} \in \mathbb{R}^{9\times 9} \tag{5.6}$$

is the state-transition matrix of values defined by equations (5.2) and (5.3),

$$\mathbf{B} = \begin{bmatrix} 0 & \cdots & 0 & \frac{K_e}{L} \end{bmatrix}^T \in \mathbb{R}^9 \tag{5.7}$$

is the matrix allocating the control input in the system, defined in the equation (5.3) and

$$\mathbf{B}_z = \begin{bmatrix} \mathbf{0} \\ -\mathbf{M}^{-1}\mathbf{F}_{\mathrm{frict.}} \\ 0 \end{bmatrix} = \begin{bmatrix} 0 & \cdots & 0 & -\frac{1}{I_3} & 0 \end{bmatrix}^T \in \mathbb{R}^9 \tag{5.8}$$

represents the impact of the friction force.

The initial point of the system considered in the simulations is assumed to be at the origin of the state space

$$\mathbf{x}(0) = \begin{bmatrix} 0 & \cdots & 0 \end{bmatrix}^T. \tag{5.9}$$

The goal of the control is to control all bodies to yield constant angular velocity ω_d. The desired state of the system is achieved when all the bodies of the system rotate with an identical constant angular velocity ω_d. This condition is feasible only if the torque T_D generated by the motor is constant and equal to the friction torque corresponding to the velocity ω_d, i.e. $T_D = T_F(\omega_d)$. This means that the operating point to be tracked by the control

$$\mathbf{x}_d(t) = \begin{bmatrix} \phi_0^d(t) & \cdots & \phi_3^d(t) & \dot{\phi}_0^d(t) & \cdots & \dot{\phi}_3^d(t) & T_D^d(t) \end{bmatrix}^T, \tag{5.10}$$

fulfills the condition

$$\dot{\mathbf{x}}_d(t) = \begin{bmatrix} \omega_d & \omega_d & \omega_d & \omega_d & 0 & 0 & 0 & 0 & 0 \end{bmatrix}^T. \tag{5.11}$$

The trajectory $\mathbf{x}_d(t)$ and the value of the control at the operating point u_d are obtained from the algebraic solution of the equation:

$$\dot{\mathbf{x}}_d(t) = \mathbf{A}\mathbf{x}_d(t) + \mathbf{B}u_d + \mathbf{D}T_F(t, \omega_d). \tag{5.12}$$

with $\dot{\mathbf{x}}_d(t)$ and $\mathbf{x}_d(t)$ defined as in (5.11) and (5.10), respectively and u_d being the constant voltage for which the stationary DC torque and the friction torque at the angular velocity setpoint are equal. The solution to (5.12) is

$$\begin{aligned} \mathbf{x}_d(t) = &\begin{bmatrix} \omega_d t & \omega_d t + \xi_1 & \omega_d t + \xi_2 & \omega_d t + \xi_3 \\ & \omega_d & \omega_d & \omega_d & \omega_d & T_F(\omega_d) \end{bmatrix}^T, \\ u_d = &\frac{RT_F(\omega_d) + K_e^2\omega_d}{K_e}. \end{aligned} \tag{5.13}$$

Since the system of the bodies at the operating point acts under two opposite torques, the static stretch between the bodies appears. This phenomenon is reflected in the reference trajectory $\mathbf{x}_d(t)$ by the presence of the ξ_i terms. These terms are equal to the static difference between the angular position of the first body and the i-th body at the operating point and are equal to

$$\begin{aligned}\xi_1 &= -T_F(\omega_d)\frac{1}{k_1},\\ \xi_2 &= -T_F(\omega_d)\frac{k_1+k_2}{k_1k_2}\\ \xi_3 &= -T_F(\omega_d)\frac{k_1k_2+k_2k_3+k_3k_2}{k_1k_2k_3}.\end{aligned} \tag{5.14}$$

The error state-space representation of the system can be introduced:

$$\boldsymbol{\epsilon}(t) = \mathbf{x}(t) - \mathbf{x_d}(t). \tag{5.15}$$

It can be noticed that the error dynamical equation is analogous to the system equation (5.4):

$$\dot{\boldsymbol{\epsilon}}(t) = \dot{\mathbf{x}}(t) - \dot{\mathbf{x}}_d(t) = \mathbf{A}\boldsymbol{\epsilon}(t) + \mathbf{B}u_\epsilon(t) + \mathbf{B}_z T_F^\epsilon(t, \dot{\epsilon}_3), \tag{5.16}$$

$$u_\epsilon(t) = u(t) - u_d \tag{5.17}$$

$$\begin{aligned}\boldsymbol{\epsilon}(0) &= -\mathbf{x_d}(0)\\ &= \Big[0 \quad -\xi_1 \quad -\xi_2 \quad -\xi_3 \quad -\omega_d\\ &\quad -\omega_d \quad -\omega_d \quad -\omega_d \quad -T_F(t,\omega_d)\Big]^T,\end{aligned} \tag{5.18}$$

$$T_F^\epsilon(t, \dot{\epsilon}_3) = T_F(t, \dot{\epsilon}_3 + \omega_d) - T_F(t, \omega_d). \tag{5.19}$$

The goal of the control is to stabilize the system around the desired trajectory $\mathbf{x}_d(t)$. The performance index for this aim is constructed in terms of the error of the trajectory $\boldsymbol{\epsilon}(t)$ and the error of the control $u_\epsilon(t)$:

$$J = \int_0^{T_f} \left[\boldsymbol{\epsilon}^T(t)\mathbf{Q}\boldsymbol{\epsilon}(t) + u_\epsilon^2(t)R\right] \,\mathrm{d}t. \tag{5.20}$$

The convergence of the quadratic terms of the objective to 0 means that the control successfully steers the system to the desired angular velocity ω_d.

In this work, we assume that both the error state of the system $\boldsymbol{\epsilon}(t)$ and the friction torque $T_F^\epsilon(t, \dot{\epsilon}_3(t))$ are directly measurable. In addition, the friction torque $T_F^\epsilon(t, \dot{\epsilon}_3(t))$ is treated not as a function of the angular velocity $\dot{\epsilon}_3$ but rather as a disturbance that depends purely on time, $T_F^\epsilon(t)$. This approach bypasses the nonlinear dynamical formulation (5.16) and provides an approximate but desired linear model of the system's dynamics:

$$\dot{\boldsymbol{\epsilon}}(t) = \mathbf{A}\boldsymbol{\epsilon}(t) + \mathbf{B}u_\epsilon(t) + \mathbf{B}_z T_F^\epsilon(t). \tag{5.21}$$

Observe that the error dynamics (5.21) and the performance criterion (5.20) correspond to the general dynamics (3.1) and general performance index (3.3) proposed in the formulation of the adaptive control method described in Algorithm 3.3.

Let $\mathbf{A}_D$, $\mathbf{B}_D$, $\mathbf{B}_{zD}$ be the matrices of the discrete equivalent of the error model of the drilling system (5.21) computed by the zero-order-hold method defined in Eq. (3.22). The discrete model in the error space is then as follows:

$$\boldsymbol{\epsilon}(k+1) = \mathbf{A}_D\boldsymbol{\epsilon}(k) + \mathbf{B}_D u_\epsilon(k) + \mathbf{B}_{zD} T_F^\epsilon(k), \tag{5.22}$$

The adaptive control method presented in Section 3.2, in Algorithm 3.3 can be then straightforwardly employed for this stabilization problem.

Numerical Results

In this section, the numerical results are presented. The performance of the proposed control scheme is compared to the results established by the Linear-Quadratic-Gaussian (LQG) regulator.

The framework of the Linear-Quadratic-Gaussian controller employs a specific form of the dynamical equations of the system dynamics. It is assumed that in general not all states of the system can be measured by the sensors and that two Gaussian noises act on the system: a measurement noise w replicating the errors of the sensors and a system noise v corresponding to the disturbances affecting the system. The discrete dynamical model in the error space (5.21) adapted for the LQG framework is of the form

$$\begin{aligned} \boldsymbol{\epsilon}(k+1) &= \mathbf{A}_D\boldsymbol{\epsilon}(k) + \mathbf{B}_D u^\epsilon(k) + \mathbf{B}_{zD} w(k), \\ \mathbf{y}(k) &= \mathbf{L}\boldsymbol{\epsilon}(k) + \mathbf{v}(k), \end{aligned} \tag{5.23}$$

where $\mathbf{y}$ is the measured output vector, $\mathbf{L} = \mathbb{I} \in \mathbb{R}^{9\times 9}$ is the output matrix, $w \in \mathbb{R}$ is the Gaussian system noise with variance $W \in \mathbb{R}^+$ and $\mathbf{v} \in \mathbb{R}^9$ is the Gaussian measurement noise with covariance matrix $\mathbf{V} \in \mathbb{R}^{9\times 9}$.

The steady-state LQG regulator feedback matrix $\mathbf{K}_{\mathrm{LQG}}$ and the Kalman filter matrix $\mathbf{S}_{\mathrm{LQG}}$ are calculated as follows:

$$\begin{aligned} \mathbf{K}_{\mathrm{LQG}} &= \left(\mathbf{R} + \mathbf{B}_D^T\mathbf{P}_{\mathrm{LQG}}\mathbf{B}_D\right)^{-1}\mathbf{B}_D\mathbf{P}_{\mathrm{LQG}}\mathbf{A}_D, \quad \mathbf{K}_{\mathrm{LQG}} \in \mathbb{R}^{1\times 9}, \\ \mathbf{S}_{\mathrm{LQG}} &= \boldsymbol{\Sigma}_{\mathrm{LQG}}\mathbf{L}^T\left(\mathbf{V} + \mathbf{L}\boldsymbol{\Sigma}_{\mathrm{LQG}}\mathbf{L}^T\right)^{-1}, \quad \mathbf{S}_{\mathrm{LQG}} \in \mathbb{R}^{9\times 9} \end{aligned} \tag{5.24}$$

where $\mathbf{P}_{\mathrm{LQG}} \in \mathbb{R}^{9\times 9}$, $\boldsymbol{\Sigma}_{\mathrm{LQG}} \in \mathbb{R}^{9\times 9}$ are the solutions of the respective algebraic Riccati equations:

$$\begin{aligned} \mathbf{P}_{\mathrm{LQG}} =& \mathbf{A}_D^T\mathbf{P}_{\mathrm{LQG}}\mathbf{A}_D - \left(\mathbf{A}_D^T\mathbf{P}_{\mathrm{LQG}}\mathbf{B}_D\right) \\ & \cdot \left(\mathbf{R} + \mathbf{B}_D^T\mathbf{P}_{\mathrm{LQG}}\mathbf{B}_D\right)^{-1}\left(\mathbf{B}_D^T\mathbf{P}_{\mathrm{LQG}}\mathbf{A}_D\right) + \mathbf{Q}. \\ \boldsymbol{\Sigma}_{\mathrm{LQG}} =& \mathbf{A}_D\boldsymbol{\Sigma}_{\mathrm{LQG}}\mathbf{A}_D^T - \left(\mathbf{A}\boldsymbol{\Sigma}_{\mathrm{LQG}}\mathbf{L}^T\right) \\ & \cdot \left(\mathbf{V} + \mathbf{L}\boldsymbol{\Sigma}_{\mathrm{LQG}}\mathbf{L}^T\right)^{-1}\left(\mathbf{L}\boldsymbol{\Sigma}_{\mathrm{LQG}}\mathbf{A}_D^T\right) + \mathbf{B}_{zD}W\mathbf{B}_{zD}^T. \end{aligned} \tag{5.25}$$

For the steady-state solution of the LQR and Kalman estimation problems, it is assumed that the system's matrices $(\mathbf{A}_D, \mathbf{B}_D)$ are stabilizable and $(\mathbf{A}_D, \mathbf{L})$ detectable. For the full derivation of the steady-state Kalman filter, see [91, Chapter 2].

The matrices $\mathbf{K}_{\mathrm{LQG}}$ and $\mathbf{P}_{\mathrm{LQG}}$ are calculated with the employment of the same matrices $\mathbf{Q}$ and R as the feedback law of the adaptive scheme. The values of these matrices are presented in Eq. (5.28). The LQG regulator operates in the infinite loop defined in Algorithm 5.1.

Algorithm 5.1 LQG control loop

1: Measure the output of the system $\mathbf{y}(k) = \boldsymbol{\epsilon}(k)$ according to Eq. (5.23).
2: Update state estimation: $\hat{\mathbf{x}}(k) = \mathbf{A}_D\hat{\mathbf{x}}(k-1) + \mathbf{B}_D u(k-1) + \mathbf{S}_{\mathrm{LQG}}\left(\mathbf{y}(k) - \mathbf{L}\left[\mathbf{A}_D\hat{\mathbf{x}}(k-1) + \mathbf{B}_D u(k-1)\right]\right)$.
3: Update control: $u(k) = -\mathbf{K}_{\mathrm{LQG}}\hat{\mathbf{x}}(k)$.

Both the proposed adaptive control method defined in Section 3.2 and the LQG regulator were tested for the angular velocity stabilization problem with friction models of the form defined in Eq. (5.1) and different parameters depicted in Tables 5.2, 5.3, 5.4. The torque-angular velocity characteristics of each used friction model are depicted in respective sections concerning particular disturbance scenario. In addition, the spectral analysis of the considered control system is conducted and the dependence of the performance of the proposed scheme on various model and algorithm's parameters is being studied.

The performance of the adaptive and the LQG controllers is compared by the computation of the quadratic cost function

$$J_x(t) = \int_0^t \boldsymbol{\epsilon}^T(s)\mathbf{Q}\boldsymbol{\epsilon}(s)\,\mathrm{d}s. \tag{5.26}$$

Because the ultimate goal of the control is to steer the system to the reference trajectory $\mathbf{x}_d(t)$ despite the control expenditure, the function (5.26) does depend only on the error of the state of the system. The time horizon t varies for every simulation case and is equal to the simulation duration.

The analogous performance criterion for the error of the control u_ϵ is not considered as a proper measurement of the performance in the simulations, because it does not reflect the goal of the control. As a motivational example let us observe that the for the constant control $u_\epsilon = 0$ such a criterion $\int_0^t u_\epsilon(s)Ru_\epsilon(s)\,\mathrm{d}s$ will equal to 0, however, the trajectory of the considered system will diverge as a result of the self-induced oscillations.

The assessment of the control input performance is rather conducted by measurement of the energy used by the motor on the whole simulation interval,

$$E_u = \int_0^t \frac{u^2(s)}{R_{DC}}\,\mathrm{d}s. \tag{5.27}$$

The mechanical parameters of the considered system, as well as both the proposed adaptive and the LQG controllers' settings, are listed below. The values of the parameters of the considered drilling machine model (5.4) employed in the computations are summarized in Table 5.1. For every simulation case, it is assumed that the constraints of the input

Table 5.1: The values of the system parameters.

Parameter	Value
R_{DC}	$0.472\,\Omega$
L	$7.85\,\mathrm{mH}$
K_e	$4.9\,\mathrm{N\,m\,A^{-1}}$
I_0	$5.56 \cdot 10^{-2}\,\mathrm{kg\,m^2}$
I_{1-2}	$1 \cdot 10^{-1}\,\mathrm{kg\,m^2}$
I_3	$1.2114\,\mathrm{kg\,m^2}$
k_{1-3}	$200\,\mathrm{N\,m\,rad^{-1}}$
c_{1-3}	$1\,\mathrm{N\,m\,s\,rad^{-1}}$

defined are equal to $u_{\min} = -200$ V and $u_{\max} = 200$ V.

For the objective function (5.20), we assume

$$R = 10^{-4},$$
$$\mathbf{Q} = \begin{bmatrix} \mathbb{I}_8 & \mathbf{0} \\ \mathbf{0} & 0 \end{bmatrix}. \tag{5.28}$$

The assumed form of the matrix $\mathbf{Q}$ results from the fact that the goal of the control is to minimize only the error of the states representing the angle and angular velocity deflection of the system. Such value of R has been used to meet value constraints on the input $\mathcal{U} = [-200\,\mathrm{V}; 200\,\mathrm{V}]$.

The parameters of the adaptive control method defined in Algorithm 3.3 are defined as follows: the maximal order of the approximating autoregressive model of the adaptive control method was set to $n_{\max} = 3$. The size of the window was set to $S = 220$. The minimal size of the window was $S_{\min} = 40$ and the sample time chosen for the simulation was $h = 0.005\,\mathrm{s}$. The horizon of the LQR regulator is chosen $i_T = 300$. It can be emphasized that the time of execution of one call of the proposed control scheme for this system on a PC-class computer is approximately equal to $0.000259\,\mathrm{s}$, so the devised control method fulfils the requirements for real-time computing.

The LQG regulator was synthesized for various values of V and $\mathbf{W}$ and tested for the single friction case simulation scenario described below. The final values of these parameters were then chosen such that the performance index obtained in the control simulation was minimal and are as follows:

$$\mathbf{V} = 5.5 \cdot \mathbb{I}_9,$$
$$W = 1. \tag{5.29}$$

Such a LQG tuning strategy was used to assure that the potential improvement of the adaptive scheme in comparison to the LQG control is not caused by a poor choice of the LQG parameters.

The case with a single friction

In the first simulation, the goal of the controller is to steer the object from the initial state (5.9) to the reference trajectory (5.13) with the setpoint angular velocity $\omega_s = 10\,\mathrm{rad\,s^{-1}}$.

The time of the simulation was set to $T_F = 8\,\mathrm{s}$. The values of the friction parameters are given in Table 5.2. The characteristics of the friction torque are depicted in Fig. 5.2. For the first simulation scenario, it is assumed that the disturbance torque consists of friction torque only. The impact of random noise on the quality of control is analysed in the second scenario. The results of the simulation are compared to the result of the LQG control in

Table 5.2: The values of the friction parameters for the first scenario.

Parameter	Value
T_{C1}	$60\,\mathrm{N\,m}$
T_{B1}	$190\,\mathrm{N\,m}$
c_{v1}	$0.05\,\mathrm{s\,rad^{-1}}$
f_{T1}	$0.001\,\mathrm{N\,m\,s\,rad^{-1}}$
$\dot{\phi}_{c1}$	$0.0001\,\mathrm{rad\,s^{-1}}$

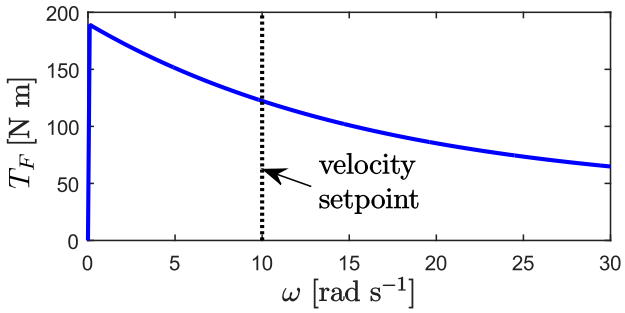

Figure 5.2: The torque–angular velocity characteristics of the friction torque model assumed for the first simulation scenario.

Figs. 5.3–5.4. As one can see, the control generated by the developed control method brings

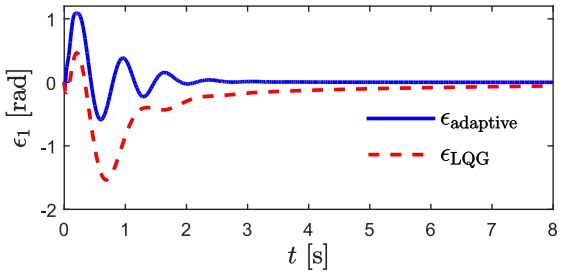

(a) The error of the angular displacement of the first mass controlled with the proposed method and LQG control.

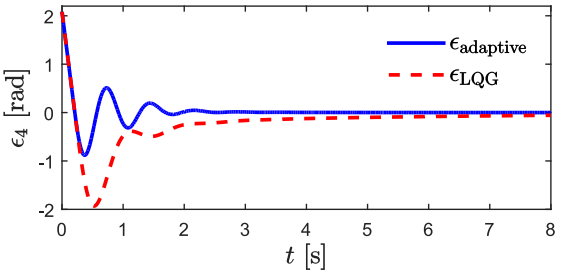

(b) The error of the angular displacement of the fourth mass controlled with the proposed method and LQG control.

Figure 5.3: The comparison of the numerical simulation of the adaptive controller Alg. 3.3 and the LQG regulator Alg. 5.1

the system to the reference trajectory in about two seconds (Fig. 5.3). Then the objective function (5.26) depicted in Fig. 5.4 stabilizes. This means that all the displacements of the angles and angular velocities of the bodies from the reference trajectory $\mathbf{x}_d$ approach zero. On the other hand, the LQG control results in a greater final value of the objective function. The performance objective (5.26) equals 91.73 for the proposed control scheme

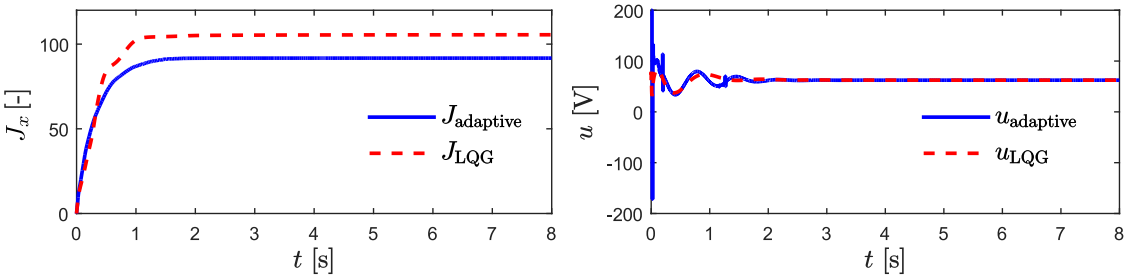

(a) The objective function values obtained by the proposed scheme and the LQG regulator.

(b) The control values generated by the adaptive controller and the LQG regulator.

Figure 5.4: The comparison of the numerical simulation of the adaptive controller Alg. 3.3 and the LQG regulator Alg. 5.1 in the first scenario.

and 105.5 for the LQG control, the improvement is 13 %.

The total energy consumed by the system for the LQG control is $E_u \approx 83000$ J, whereas the adaptive control scheme resulted in $E_u \approx 88000$ J. This 6% increase of the energy utilisation is a result of the sharp peaks of the control at the beginning of the simulation (see Fig. 5.4).

The LQG control provides greater absolute values of the system errors, which can be seen in Fig. 5.3. These simulation results prove the ability of the developed adaptive method to control the system under external disturbances with higher quality than the LQG control.

The case with single friction characteristics with a noise

In this section, the ability to control the system by the proposed method in the presence of Gaussian noise is tested. The parameters of the system and the proposed control algorithm are the same as in the previous section. The uniform signal noise with variance g and mean 0 is added to the friction model from the previous section. The simulation time was set to $T_F = 8\,\text{s}$. The resulting variation of the friction force over time for the two considered variances $g = 1\,\text{N}^2\,\text{m}^2$ and $g = 200\,\text{N}^2\,\text{m}^2$ is depicted in Fig. 5.5. A comparison of the

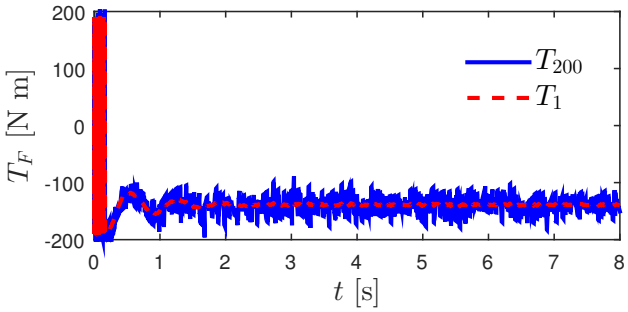

Figure 5.5: The friction torque values in the simulation for the noise variance $g = 1\,\text{N}^2\,\text{m}^2$ and $g = 200\,\text{N}^2\,\text{m}^2$. T_{200} stands for the friction torque generated in the simulation with noise variance $g = 200\,\text{N}^2\,\text{m}^2$ and T_1 stands for the simulation with $g = 1\,\text{N}^2\,\text{m}^2$.

objective function for different values of g is presented in Fig. 5.6. The objective function

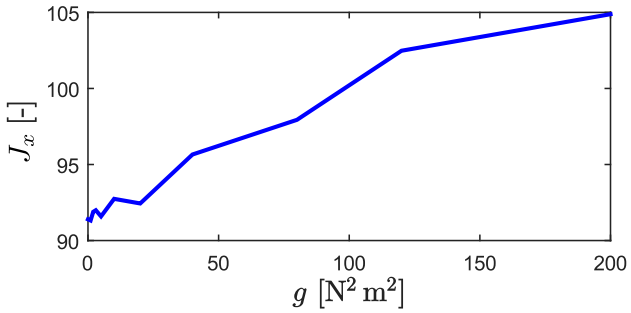

Figure 5.6: The objective function J_x achieved at the simulation time $t = 8\,\mathrm{s}$ for different variances of the noise g.

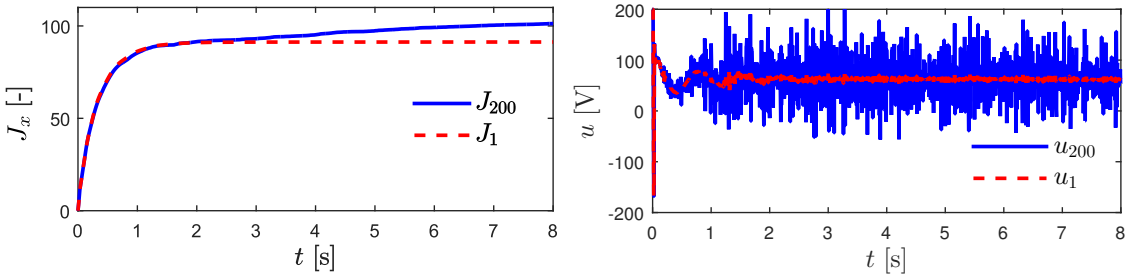

(a) The objective functions achieved with the control method.

(b) The control values generated by the Algorithm 3.3.

Figure 5.7: The comparison of the numerical simulation of the adaptive scheme 3.3 for the friction noise gain $g = 1\,\mathrm{N}^2\,\mathrm{m}^2$ and $g = 200\,\mathrm{N}^2\,\mathrm{m}^2$. J_{200} stands for the result of simulation governed with noise variance $g = 200\,\mathrm{N}^2\,\mathrm{m}^2$ and J_1 stands for the trajectory of simulation with the noise variance $g = 1\,\mathrm{N}^2\,\mathrm{m}^2$.

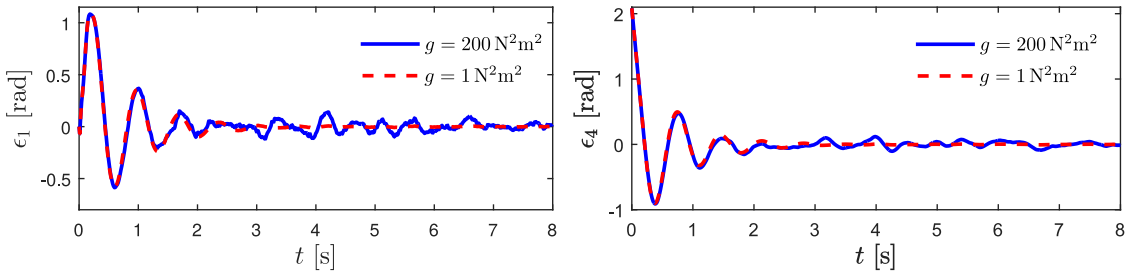

(a) The error of the angular displacement of the first body.

(b) The error of the angular displacement of the fourth body.

Figure 5.8: The comparison of the numerical simulation of the control scheme 3.3 for the friction noise gain $g = 1\,\mathrm{N}^2\,\mathrm{m}^2$ and $g = 200\,\mathrm{N}^2\,\mathrm{m}^2$.

obtained at the time 8 s of the simulation increases with an increase of the variance g. In addition, Fig. 5.7 (a) shows that the value of the objective function does not stabilize but increases with time. In fact, when $g \neq 0$, the objective function obviously diverges. However, even for a noise variance as high as $g = 200\,\mathrm{N}^2\,\mathrm{m}^2$, Fig. 5.8 shows that the values of the errors are bounded and have lower values than for the LQG control without noise, as depicted in Fig. 5.3. For $g = 1\,\mathrm{N}^2\,\mathrm{m}^2$, the value of the objective function is 91.3 and for $g = 200\,\mathrm{N}^2\,\mathrm{m}^2$ J_x it is equal to 101.3.

The case with varying friction characteristics

In this section, the scenario with a step change of the friction characteristic is studied. As in the previous case, the results are compared to the LQG control. The initial point and the angular velocity set point are the same as in the previous cases. In the first phase of the simulation, for $t \in [0\,\mathrm{s}, 1\,\mathrm{s})$, the friction torque has the parameters assumed as in the first column of Table 5.3 and at the time $t = 1\,\mathrm{s}$, the parameters of the friction changes to the second set of parameters, presented in the second column of Table 5.3. The simulation runs then until the final time $T_F = 9\,\mathrm{s}$. Both torque characteristics defined by the parameters in Table 5.3 are presented in Fig. 5.9. The sets of parameters were chosen to provide an unchanged friction torque value for ω_d. This property of the friction was chosen to avoid a sudden jump of the constant in the formula (5.17). It can be observed that the friction characteristics significantly change at the time 1 s.

Table 5.3: The values of the friction parameters for the second scenario.

Parameter	First stage	Second stage
T_{C2}	$200\,\mathrm{N\,m}$	$45\,\mathrm{N\,m}$
T_{B2}	$210\,\mathrm{N\,m}$	$310.5518\,\mathrm{N\,m}$
c_{v2}	$0.05\,\mathrm{s\,rad^{-1}}$	$0.05\,\mathrm{s\,rad^{-1}}$
f_{T2}	$0.001\,\mathrm{N\,m\,s\,rad^{-1}}$	$0.001\,\mathrm{N\,m\,s\,rad^{-1}}$
$\dot{\phi}_{c2}$	$0.0001\,\mathrm{rad\,s^{-1}}$	$0.0001\,\mathrm{rad\,s^{-1}}$

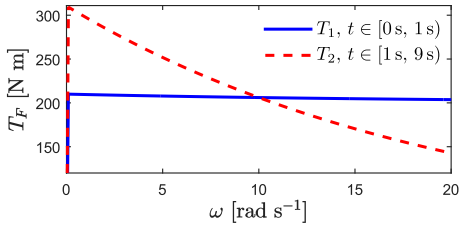

Figure 5.9: The friction torque vs. angular velocity characteristics for the second simulation scenario: T_1 - characteristics of the friction torque at the first stage of the simulation, $t \in [0\,\mathrm{s}, 1\,\mathrm{s})$; T_2 - characteristics of the friction torque at the second stage of the simulation, $t \in [1\,\mathrm{s}, 9\,\mathrm{s})$.

The results are depicted in Figs. 5.10 and 5.11. The curves depict the results for the LQG control method (dashed lines) and are compared with our adaptive control method (solid lines). In the first interval of the simulation $t \in [0\,\mathrm{s}; 1\,\mathrm{s})$ both the adaptive method and LQG regulator are stabilizing the system. In fact, the results obtained for the LQG control in the first interval are better than for the proposed control method. The initial peak of the error of the angular displacement for the first and the fourth masses is nearly 40% greater for the system controlled by the adaptive method than for the LQG. This is due to the fact that the number of measurements of the friction is small at the beginning of the simulation and the friction at this time is in the sticking phase. The generated AR model in such a case cannot be precise enough. Despite that, the objective functions (Fig. 5.10 (a)) achieved in the first interval by both control algorithms have similar values. In

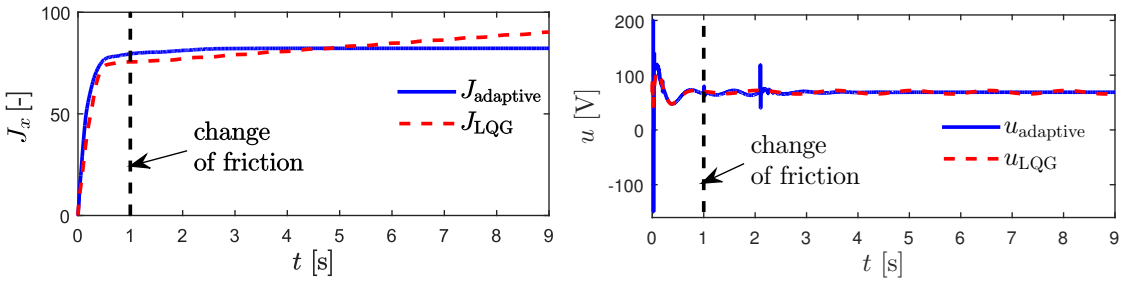

(a) The objective functions achieved by the control scheme and the LQG regulator.

(b) The control values generated by the adaptive controller and the LQG regulator.

Figure 5.10: The comparison of the numerical results of the simulation of the adaptive controller Alg. 3.3 and the LQG regulator Alg. 5.1 in the second scenario.

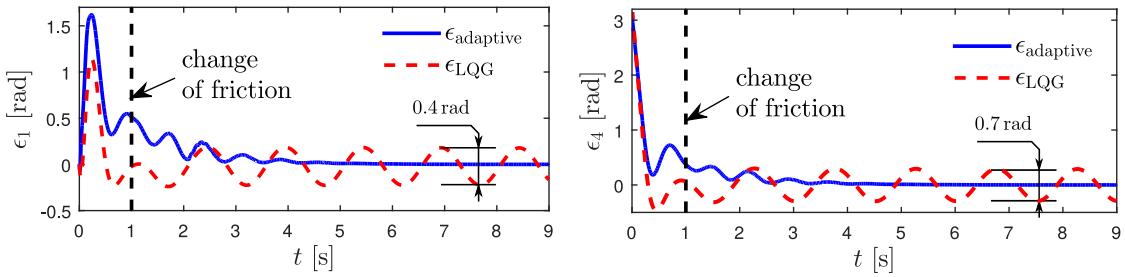

(a) The error of the angular displacement of the first mass controlled with the proposed control scheme and LQG control.

(b) The error of the angular displacement of the fourth mass controlled with the proposed control scheme and LQG control.

Figure 5.11: The comparison of the numerical results of the simulation of the adaptive controller Alg. 3.3 and the LQG regulator Alg. 5.1 in the second scenario.

the second stage of the simulation $t \in [1; 9]$ s, when the friction characteristics are changed, the LQG control destabilizes the system. The error trajectories (Fig. 5.11) for the LQG control exhibits undamped oscillations and the objective function does not converge.

The peak-to-peak amplitude of the angular displacement error of the first and the fourth body stabilise at 0.4 rad and 0.7 rad, respectively. In comparison, the proposed control method quickly achieves the goal of the control: in 1.5 seconds after the friction change the adaptive method generates smaller oscillation of the angular displacement than the LQG regulator and after approximately 3 s, the error trajectories of the system converge to 0. The final value of the objective function J_x obtained in the simulation is 82.25, that for LQG control is $J = 90.28$. The results of this simulation prove the efficiency of adaptation by the proposed algorithm to a sudden change of the disturbance.

The ultimate energy consumed by the adaptive and LQG controllers is approximately equal 95300 J and 93400 J, respectively. The small power increase (approximately 2%) for the adaptive scheme is caused mainly by the sharp peaks of the control. What is important, the system after $t = 2$ s has approximately the same energy consumption for both control algorithms but the LQG control fails to stabilize the system.

As can be noticed from Fig. 5.10 (b), the adaptive scheme yields two sharp peaks of the control at $t = 1$ s and $t = 2.1$ s. The first peak is observed at 1.05 s, right after the

step change of the friction characteristics. Because of the step change of the disturbance parameters, the time instant $t = 1\,\mathrm{s}$ marks not only the discontinuity of the friction signal but also the change of the signal's parameters such as amplitude and frequency. Because of that, the feedback vector of the measured disturbance $\mathbf{x}_{zi}$ is sharply changed. In addition, the change of the AR model caused by the introduction of new friction parameters results in a significantly different value of the feedback matrix $\mathbf{K}_i$. The observed peak in the control signal is a result of both aforementioned events.

In order to explain the second aberration, it is crucial to observe that the assumed disturbance measurement window $S = 220$ corresponds to the measurements interval $S \cdot T_s = 1.1\,\mathrm{s}$. For the time interval $t \in [1,\, 2.1)$, the AR model adjusts its parameters based on the measurements corresponding to both friction models with a gradual increase of the measurements of the second one. The instant $2.1\,\mathrm{s}$ marks the complete removal of the initial friction values from the measurement window. This event again triggers the change of the AR model parameters and, as a consequence, the change of the matrix $\mathbf{K}_i$ which explains the second peak.

It is important to emphasize that the presented simulation assumes rather an extreme scenario of the friction change, which is sudden and discontinuous. In practice, the friction character changes more smoothly. It has been validated that for such cases the control peaks does not occur.

The case with two friction characteristics

In this scenario, an additional friction torque $T_2(\omega)$ applied to the third body of the system is considered. The torque $T_1(\omega)$ is applied to the fourth body, as in the previous scenarios. The equation of motion (5.4) is now modified and it includes the additional friction

$$\dot{\mathbf{x}}(t) = \mathbf{A}\mathbf{x}(t) + \mathbf{B}u(t) + \mathbf{B}_{z2}\begin{bmatrix} T_2(\dot{\phi}_2) \\ T_1(\dot{\phi}_3) \end{bmatrix}, \tag{5.30}$$

$$\mathbf{B}_{z2} = \begin{bmatrix} 0 & \cdots & 0 & -\frac{1}{I_2} & 0 & 0 & 0 \\ 0 & \cdots & 0 & 0 & 0 & -\frac{1}{I_3} & 0 \end{bmatrix}^T. \tag{5.31}$$

The steady state angular displacements between the bodies that appear in the equation of the reference trajectory (5.14) are as follows:

$$\begin{aligned} \xi_1 &= -\left(T_1(\omega_d) + T_2(\omega_d)\right)\frac{1}{k_1}, \\ \xi_2 &= -\left(T_1(\omega_d) + T_2(\omega_d)\right)\frac{k_1 + k_2}{k_1 k_2}, \\ \xi_3 &= -T_1(\omega_d)\frac{k_1k_2 + k_2k_3 + k_3k_1}{k_1k_2k_3} - T_2(\omega_d)\frac{k_1 + k_2}{k_1k_2}. \end{aligned} \tag{5.32}$$

The setpoint angular velocity has the value $\omega_d = 10\,\mathrm{rad\,s^{-1}}$.

The algorithm is now modified to take into account the simultaneously measured friction torques, both T_1 and T_2. Two dynamic models are generated by the algorithm, one for each friction function, T_1 and T_2, given in Fig. 5.12. The respective parameters that are

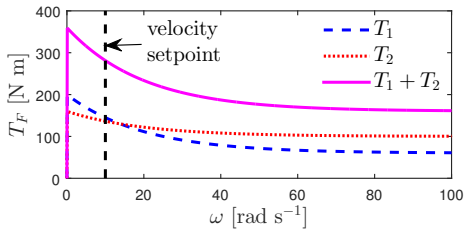

Figure 5.12: The friction torque–angular velocity characteristics for the third simulation scenario.

Table 5.4: Values of the friction parameters for the third scenario.

Parameter	T_1	T_2
T_{C3}	60 N m	100 N m
T_{B3}	200 N m	160 N m
c_{v3}	0.05 s rad^{-1}	0.05 s rad^{-1}
f_{T3}	0.001 N m s rad^{-1}	0.001 N m s rad^{-1}
$\dot{\phi}_{c3}$	0.0001 rad s^{-1}	0.0001 rad s^{-1}

used in both formulas are listed in Table 5.4. Figs. 5.13 and 5.14 depict the results of the simulation. Fig. 5.13 (a) shows the objective function in time. In the first second, it

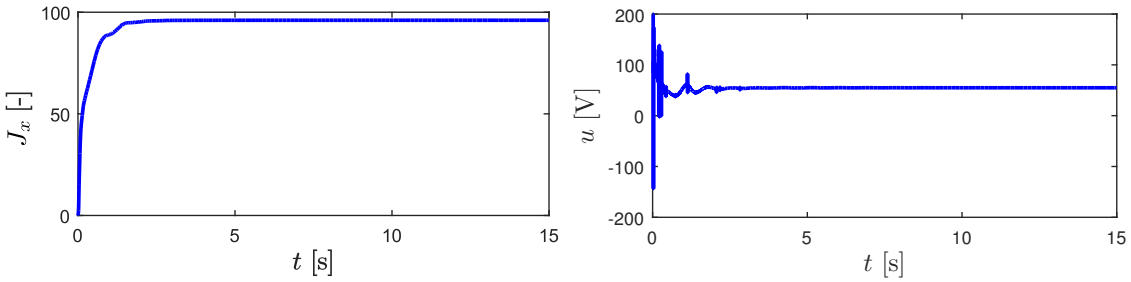

(a) The objective functions achieved by the method. (b) The control values generated by the method.

Figure 5.13: The results of the numerical simulation of the adaptive controller Alg. 3.3.

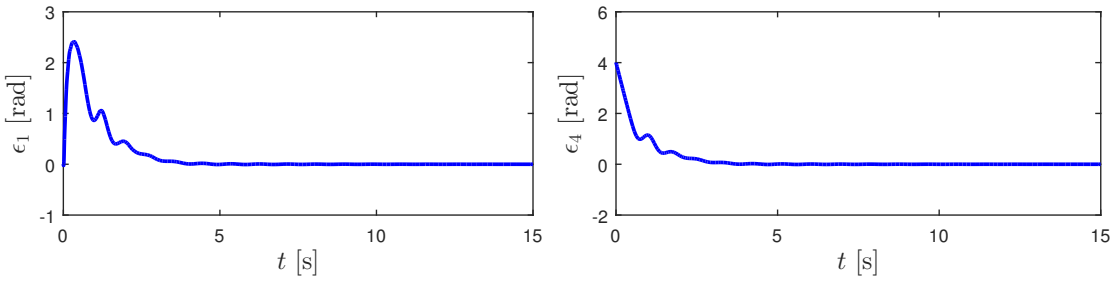

(a) The error of the angular displacement of the first mass under the algorithm control. (b) The error of the angular displacement of the fourth mass under the algorithm control.

Figure 5.14: The results of the numerical simulation of the adaptive controller Alg. 3.3.

increases and reaches the constant value 96.04. This means that the dynamical system is successfully steered to the reference trajectory. In the remaining period, it is practically

constant. The control function $u(t)$ is depicted in Fig. 5.13 (b). It varies significantly at the beginning of the process, then slightly improves the solution, and starting from $t = 2.5\,\mathrm{s}$ remains constant. The errors ϵ_1 and ϵ_4 of the angular displacements of the first and fourth masses are presented in Fig. 5.14. One can notice that the errors reduce to zero rapidly. The error ϵ_1 increases from zero to the value $2.4\,\mathrm{rad}$ at the beginning and then decreases. The reason for this is that the reference angular displacement to be tracked by the system is a linear function of time, i.e. $\phi_1^d = \omega_d t$, as in (5.10). At the beginning of the simulation all bodies are still, the angular error $\epsilon_1 = \phi_1^d - \dot{\phi}_1$ is increasing. This error reaches its peak at approximately $t = 0.8\,\mathrm{s}$, when the velocity of the first body $\dot{\phi}_1$ reaches the velocity setpoint ω_d. After that, the error decreases and converges to zero.

The results of this simulation are similar to the results achieved for the first simulation scenario. The derived control scheme effectively steers the system to the desired trajectory. A comparison with the results of the first scenario suggests that the proposed control method can be applied to complex disturbance configurations, such as two disturbances of different characteristics applied to the system.

Spectral analysis

To adequately verify adaptive controller's ability to counteract a load of wide-range frequency, the spectral analysis of the control system has been conducted. The dynamical model (5.4) governed by the proposed control scheme defined in Algorithm 3.2 has been subjected to the sinusoidal disturbance with frequency from the range $f \in [0.1,\, 20]$ Hz. The steady-state amplitudes of the dynamical system's state $\mathbf{x}(t)$ were then measured.

In this simulation scenario, the goal of the control is to steer the system to the origin and as a result, the algorithm can be formulated directly for the state-space formulation (5.4) rather than the error-space (5.16). The parameters of the algorithm remain the same as for the previous scenarios, i.e. $n_{\max} = 3$, $S = 220$, $S_{\min} = 40$ and $h = 0.005\,\mathrm{s}$ with $\mathbf{Q}$, R defined as in (5.28).

The amplitude spectra obtained with the adaptive control scheme have been compared to the results of the same analysis conducted for the LQG regulator. The values of the correlation matrices $\mathbf{V}$ and W remain the same as in the previous simulations.

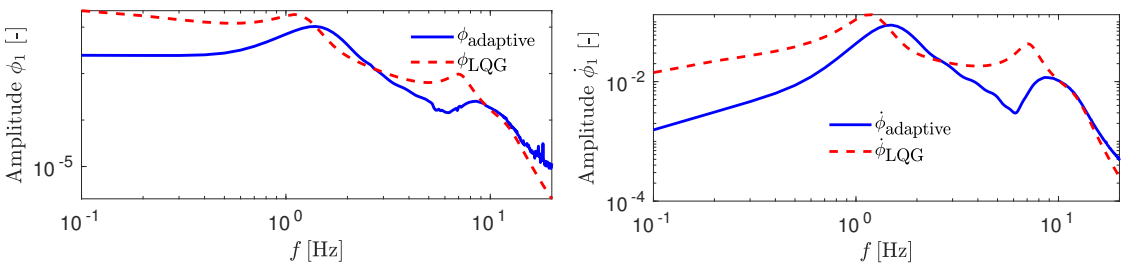

(a) The amplitude spectra of the angular deflection ϕ_1.

(b) The amplitude spectra of the angular velocity $\dot{\phi}_1$.

Figure 5.15: Amplitude spectra of the response of the body I_1. Results obtained with the adaptive controller Alg. 3.3 and the LQG regulator Alg. 5.1.

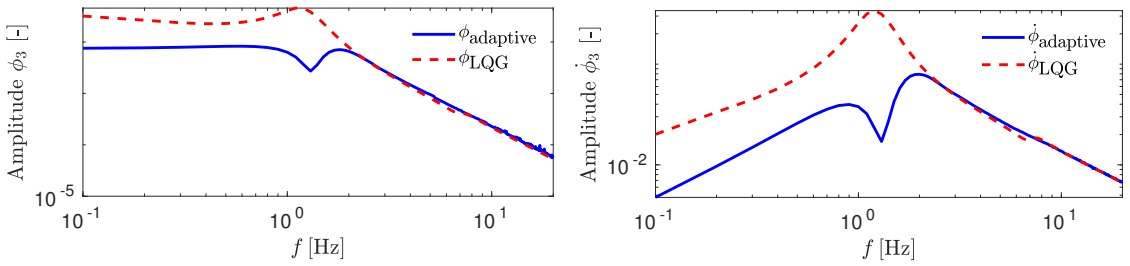

(a) The amplitude spectra of the angular deflection ϕ_3.

(b) The amplitude spectra of the angular velocity $\dot{\phi}_3$.

Figure 5.16: Amplitude spectra of the response of the body I_3. Results obtained with the adaptive controller Alg. 3.3 and the LQG regulator Alg. 5.1.

The results of the analysis are presented in Figs. 5.15–5.16 that depict amplitude spectra of the angular deflections and velocities of the bodies I_1 and I_3. It can be observed that the proposed scheme results in greater damping of the oscillations for almost the whole considered frequency spectrum. According to the results, the diagrams can be divided into three regions. For the frequencies lower than 1 Hz, the adaptive control method gives significantly better results than the LQG regulator. The improvement for this interval varies from 10-fold (see values depicted in Fig. 5.15 (b) for $f = 0.1$ Hz) to twofold. For the second interval, $f \in [1, 10]$ Hz, the difference between the amplitudes decreases and for the subinterval $f \in [1, 2.5]$ Hz the LQG regulator results in smaller amplitudes of movement of the body I_1 than in the case of the adaptive scheme. Nevertheless, the body I_3, to which the load is directly applied, still exhibits lower amplitudes for the adaptive control. For the last interval denoted by $f \in [10, 20]$ Hz, responses of both controllers coincide and the adaptive controller exhibits no improvement. The results for the remaining bodies $I_{0,2}$ are similar, but with the noticeable trend: the closer the body to the disturbance, the better the improvement. It may be then concluded that the transitional lack of improvement for the interval $f \in [1, 2.5]$ Hz for the bodies closer to the drive but farther from the disturbance is a result of the adaptive scheme controlling the motor aggressively to damp out oscillations of the bodies I_{2-3} that are more prone to the load.

Favourable results of the analysis for the proposed control scheme come from the fact that the adaptive scheme controls the system using the identification of the linear dynamic model of the load. In this case, the load is a sinusoidal function, which can be precisely approximated by the linear autoregressive model. The fact that time-variation of the disturbance is exactly reconstructed by the model makes the control generated by the adaptive scheme very close to the optimal one.

Impact of the algorithm parameters

In this section, the effectiveness of the proposed control method is tested for different values of the algorithm parameters: the sample time h, the size of the signal window $T_S = Sh$, the length of the LQR horizon $T_{\text{horizon}} = i_T h$, and the order of the model approximation n. To show the impact of the AR model's order on the controller's performance, it is assumed

in this section that the procedure of choosing the best order defined by Eq. (3.19) is not being used and the Algorithm 3.3 operates with the constant order $n_{z,i} = n$. The analysis was performed for the drilling system set as for the first simulation scenario.

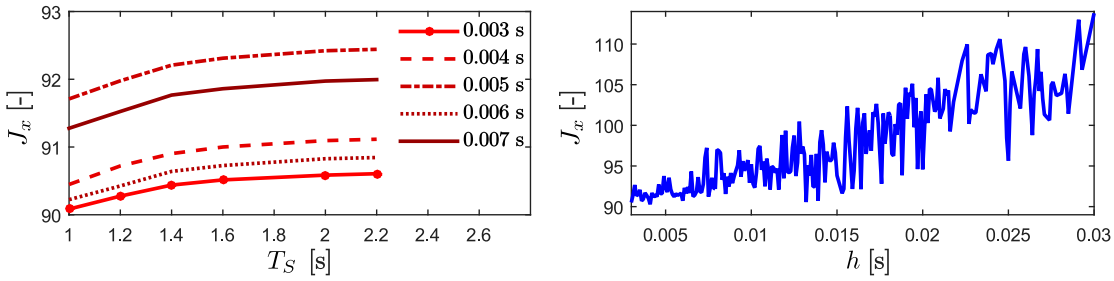

(a) The comparison of the objective functions achieved by the adaptive controller for different sampling periods h and different lengths of the window T_S (size of the LQR horizon is constant, $T_{\text{horizon}} = 1.5\,\text{s}$).

(b) The objective function as the function of the sampling period h (order of the disturbance model - $n = 3$, size of the window - $T_S = 1.5\,\text{s}$).

Figure 5.17: The dependence of the objective function achieved by the adaptive Algorithm 3.3 on the parameters.

In Fig. 5.17 (a), a comparison of the objective functions computed for different sampling times T_s and different sizes of the window S is presented. One can see that the objective function increases with S. This monotonicity is preserved for different sampling periods h. It is important that for $T_S < 1\,\text{s}$, the stabilization of the dynamic system fails. A signal horizon shorter than 1 s is not sufficient to calculate a good autoregressive approximation of the torque dynamics. This critical value of T_S is related to the system configuration described above. For a system governed by different dynamic equations or with frictions of different characteristics, this value naturally will be different. However, it appears that the value of J_x as a function of h does not change monotonically. The lowest characteristics presented in Fig. 5.17 (a) are computed for $h = 0.007\,\text{s}$. The next one is computed for the shorter sampling period $h = 0.006\,\text{s}$. This trend breaks as the characteristics for $h = 0.004\,\text{s}$ and $T_s = 0.003\,\text{s}$ show lower values of J_x than the characteristics computed for $h = 0.005\,\text{s}$. This phenomenon is presented in Fig. 5.17 (b), where the values of the objective function J_x are computed for a fixed length of the window T_S and different sampling periods h. One can notice that although the characteristics are not smooth (which explains the seeming randomness of the results in Fig. 5.17 (a)), the global trend is that the value of the objective function increases with an increase of the sampling period. However, a reduction of the sampling period h involves an increase of the window size S. This ensures acceptable control results in the unchanged horizon of the measurements $T_S = S \cdot h$. The increase of S results in a longer execution time of the proposed algorithm. This means that there is a critical value of h below which the execution time of the algorithm exceeds the sampling time and the algorithm fails to be useful in real time.

Fig. 5.18 (a) presents the influence of the value of the LQR horizon on the objective function. For short T_{horizon}, e.g., $T_{\text{horizon}} < 0.5\,\text{s}$, the algorithm fails. For longer simulation times, the value of the objective function calculated for $T_{\text{horizon}} < 0.5\,\text{s}$ will be higher, but

for $T_{\text{horizon}} \geq 0.5\,\text{s}$ will remain still, as the adaptive algorithm stabilizes the system in the simulation time. For $T_{\text{horizon}} > 0.5\,\text{s}$ one can observe that the value of the function stabilizes and for $T_{\text{horizon}} > 1\,\text{s}$ there is no profit in a further increase of the horizon.

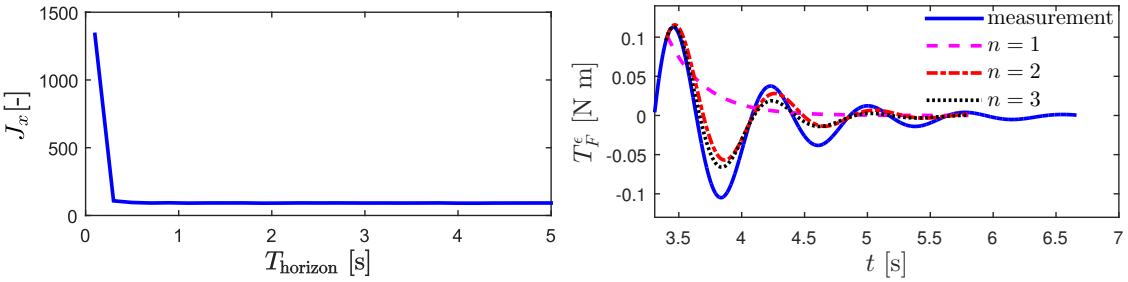

(a) The impact of the length of the horizon T_{horizon}.

(b) The ability of the disturbance prediction for different orders n of the model ($S = 220$).

Figure 5.18: The influence of selected parameters on the control quality.

In Fig. 5.18 (b) the ability of the prediction of the AR model used in the derived algorithm is presented. The reference signal of the friction torque (referred in Fig. 5.18 (b) to as "measurement") that was used to analyse the AR models was computed from the results of the first simulation case. The signal "measurement" is a friction torque generated by the model (5.1) represented in the error space defined in (5.19) with the use of the parameters from Table 5.2 and angular velocity of the last body $\dot{\phi}_3$ measured at the first simulation case, i.e. $\text{measurement}(t) = T_F^\epsilon(\dot{\phi}_3(t))$.

Then the AR models were generated with various values of the parameter n. The predicted future signals of these models are compared to the values of the torque calculated in the simulation. The other parameters of the proposed algorithm are as in the previous cases. One can see that the order of the autoregressive model $n = 1$ is too low to give a good prediction of the signal because dynamical models of order 1 cannot reproduce oscillations. With the order equal to $n = 2$ or larger, the oscillations are properly approximated by the model. However, the increase of the order to $n = 3$ provides a better approximation of the original signal, the overall change in comparison to $n = 2$ is small. In addition, further increase of the order to $n > 3$ does not provide a significant change in the quality of the approximation.

Impact of the number of elements

The developed control algorithm was tested on the drilling system consisting of four rigid bodies. However, a real drilling machine is comprised of a long drill string, which is an example of a distributed parameter dynamical system. To check if the control scheme can be successfully used in a real scenario, the efficiency of the control of the model with an increased number of elements is investigated. Such a modification provides a more accurate model of a real system.

The control algorithm is computed as previously by using the model (5.21). The control is then applied to the altered model, consisting of a greater number of interior elements.

The scheme of the model is presented in Fig. 5.19.

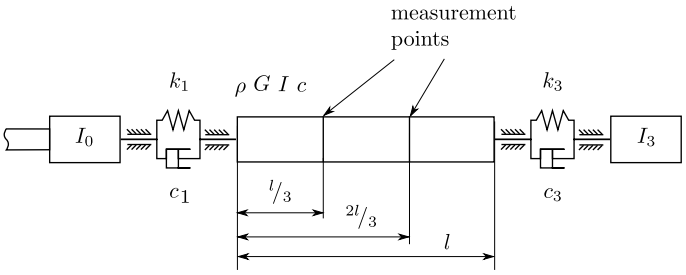

Figure 5.19: Scheme of the altered model with the points on which the measurements are conducted.

The parameters: linear density ρ, shear modulus G, torsion inertia moment I, torsional damping coefficient c and length l of the interior body were selected such that they correspond to the parameters I_1, I_2, k_1, k_2, c_1, c_2 of the simplified model described in Section 5.1. Measurements of the angular displacements and angular velocities corresponding to the interior bodies of the simplified model were made at the $^1/_3$ and $^2/_3$ of the length of the interior body.

The simulation scenario was then performed with the constant single friction torque described in the first simulation case for the interior body I discretized to 1-11 elements (the case with discretization to 1 element is identical to the model employed for the previous cases). To measure the performance of the scheme a quadratic performance index defined by (5.26) for the altered model was introduced. The indices of the diagonal matrix Q corresponding to the elements of the interior body are inversely proportional to the number of elements, to ensure normalization of the cost function. For all cases, the control scheme successfully steers the system to the angular velocity set point.

The final value of the cost function as the function of the number of elements is presented in Fig. 5.20. As can be observed, the initial increase up to the three elements causes worsening of the performance index. The peak corresponds to 150% of the performance index for only one element. However, the further increase of the elements causes the performance index to decrease. The final value for the choice of 11 elements is approximately 25% higher than for the one-element model. It has been validated that further increase of the number of elements does not affect significantly the value of the performance index. This result confirms that the developed control scheme can be successfully used in a real-world application with only two additional measurements of the displacement and velocity on the drill string.

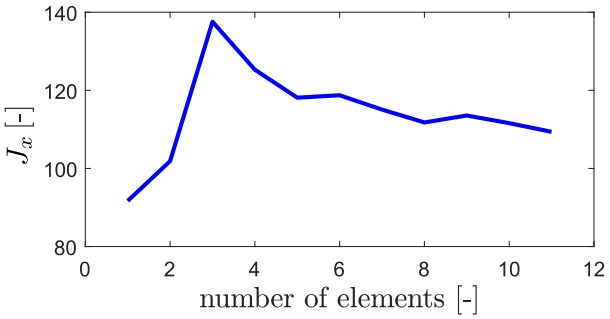

Figure 5.20: The value of the performance index J_x for a different number of elements in the model.

5.2 Active seismic stabilization of structure

In this Section, the adaptive infinite horizon control method that has been presented in Section 3.3 is tested numerically. The results of this section have been originally presented in the Author's paper [51] (to be published). The method is validated and analysed numerically via simulation of the problem of vibration attenuation of the structure subjected to a seismic excitation.

There are numerous examples of active control schemes that are used for seismic control. The application of the simple LQR method can be reviewed in [8, 92, 93]. Some improvements in the means of seismic reduction are provided by the linear-quadratic-Gaussian (LQG) regulator. In this formulation, the regulator still minimizes the quadratic index but it is also assumed that the control system is affected by the Gaussian-noise disturbance. The inclusion of the disturbance in the control problem setting is an evident contribution. Nevertheless, the variance and amplitude of the disturbance have to be set *a priori* and, as a result, the LQG regulator is not guaranteed to sustain good operation for a wide variety of the earthquake signals. For interesting results describing the use of LQG for earthquake attenuation, the reader is referred to [11, 10, 94].

The H_∞ controller is introduced for structural control in [95] and the experimental verification of this controller on the three-story test structure is presented in [96]. Another approach to H_∞ structural control is proposed in [97], where the authors use a more general and computationally efficient numerical scheme based on Linear Matrix Inequalities. The resulting control method is successfully tested against the LQG controller on the numerical simulation of the three-story building. In [98], the authors reformulate H_∞ controller so that it operates using only a sampled feedback information. Sliding-mode control is another robust control technique; its application for stabilization of the slender building by the means of an active tuned-mass damper is proposed in [99]. The use of active tuned-mass damper is also studied in [100], where a fuzzy logic based adaptive controller is implemented. In [101], a robust control method based on online neural network identification is successfully validated for an L-shaped structure. The MPC control scheme is universally applied to industrial process automation, but it also has a number of uses in seismic control, for example [13]. For a comprehensive state of the art review of the

structural control methods, the reader is referred to [102].

Model description

This section provides a description of the numerical dynamical model that is used for controller verification. We consider the problem of the vibration attenuation of a multi-store steel structure subjected to an earthquake. First the controlled structure is described. Its linear finite-element approximation is then obtained with the use of ANSYS software. This precise model, will be termed the reference model (RM) hereafter, serves as the basis for the simplified model and for ultimately testing the effectiveness of the proposed control scheme.

The simplified model (SM) with a reduced number of degrees of freedom is essential for a control law synthesis. In this model, we treat structure levels as lumped masses that are joined by springs and dampers. There are several ways to reduce the fully detailed finite-element model of the structure. The simplest and most commonly used is the dimensionality reduction scheme, such as the Guyan reduction [103]. A more precise dynamic synthesis method [104] can also be used. The Rayleigh-Ritz reduction enables generally good agreement of reduced model natural frequencies with a full modal response. However, in a multi-degree-of-freedom system, we are unsure if the reduced model has proper physical representation. In reality, we do not have a reliable numerical model. Instead, we have a physical system.

In this scenario, the RM model is treated as such real physical object, information about which can only be obtained through its excitation and measurements, as can be done in practice. An identification procedure has to be conducted to obtain an SM model. Obviously, the identification process results in inaccuracies of the model's parameters. However, this method of synthesis of the SM model is closer to the real-life scenario application of the control method, where the structure to be controlled is already built. In addition, extracting the system matrices from ANSYS commercial software can be burdensome. The parameters of the simplified model were determined based on the static and harmonic response of the reference model.

Reference model definition

The considered RM model is adapted from the work [105]. In this paper, the authors define the benchmark structure for seismic control problems, and they provide exact geometrical and physical properties of the object. The structure is 30.48 m by 36.58 m in plan and 80.77 m in height. Its outline and its geometric properties are depicted in Figure 5.21. The building consists of steel perimeter moment-resisting frames. The building has 22 levels (basement B-1, 20 above-ground floors and the roof). The columns are 345 MPa steel. The exterior columns have a box cross-section, while the interior columns have profiles that are defined according to the norm ASTM A6. The specific dimensions of the columns vary with the height of the structure.

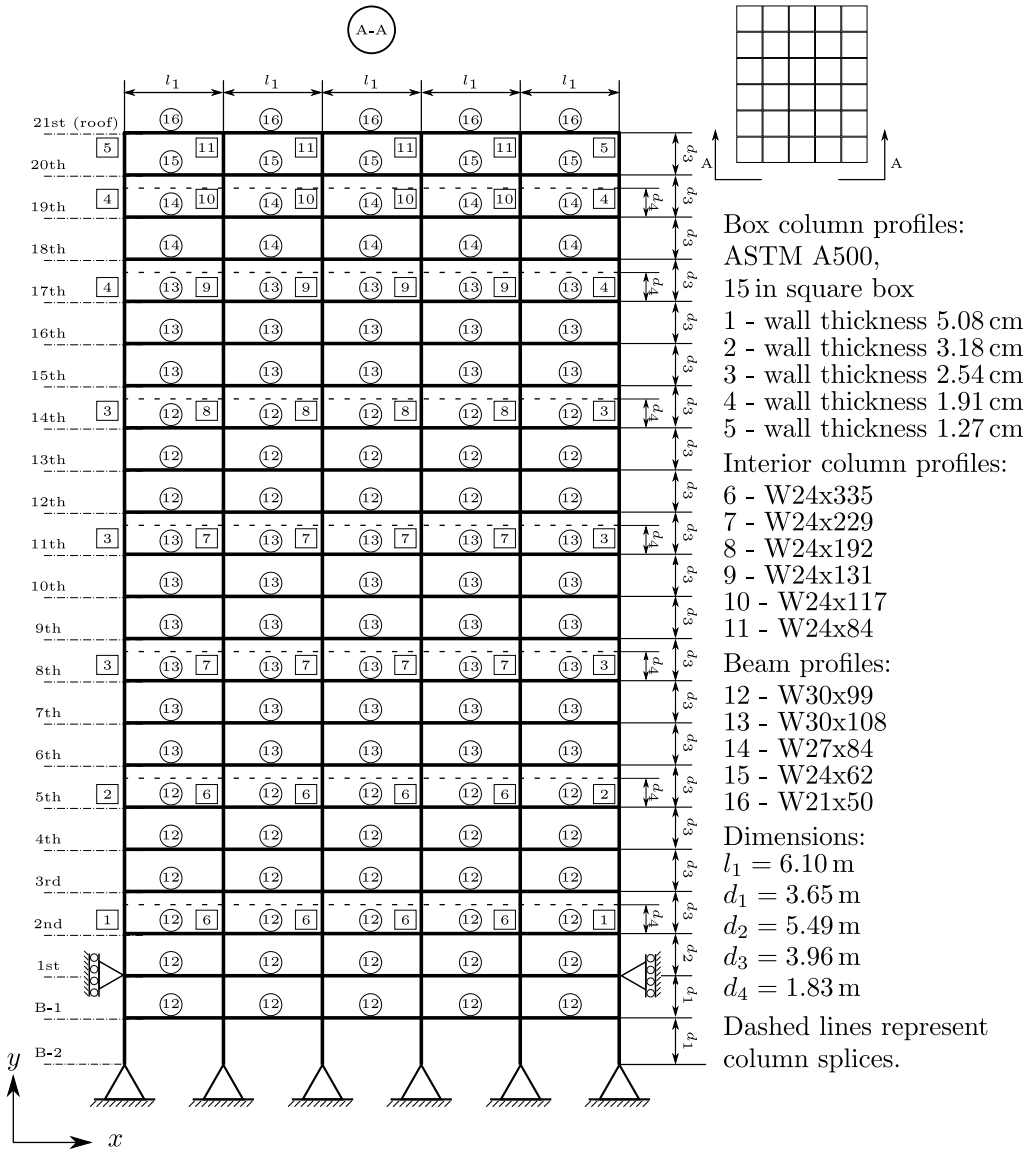

Figure 5.21: Scheme of the steel structure.

The level floors are comprised of 248 MPa steel wide-flange beams with dimensions according to the norm ASTM A6. Rigid connections are assumed between beams, columns, and columns and beams.

The column bases are fixed in the ground. The first floor is assumed to be restrained from horizontal movement, because of the presence of the foundation walls and the soil.

Apart from the mass of the steel framing itself, the structure is modelled to have an additional seismic mass that is distributed evenly on every above-ground level. For the first floor, this seismic mass is $5.08 \cdot 10^5\,\mathrm{kg}$. For the second floor, this mass is $5.4 \cdot 10^5\,\mathrm{kg}$. For the third to the 20th level, this mass is $5.26 \cdot 10^5\,\mathrm{kg}$. And for the roof, this mass is $5.58 \cdot 10^5\,\mathrm{kg}$. The summary mass of the entire structure is $1.16 \cdot 10^7\,\mathrm{kg}$.

In this work, as in the original paper [105], we focus on a 2-D analysis of the single frame of the entire structure. This frame is also depicted in Figure 5.21. We assume that the seismic acceleration of the ground is in the plane of this frame and that a chosen section

of the structure supports half of the seismic mass of the whole object; that is, $2.54 \cdot 10^5$ kg for the first floor, $2.7 \cdot 10^5$ kg for the second floor, $2.63 \cdot 10^5$ kg for the third to 20th floor and $2.79 \cdot 10^5$ kg for the roof. The mass of the steel frame is $5.80 \cdot 10^5$ kg.

This object is then modelled by the use of the finite element method in the ANSYS software. Each column and beam is divided evenly into four finite elements. The obtained finite-element model has 892 elements with 5040 degrees of freedom. The element BEAM188 that is obtained from the software's element database is used in the simulation. This is a linear element that is based on the Timoshenko's beam theory, which includes shear deformation effects. In this model, Rayleigh-type damping with coefficients $\alpha = 0.015277$ and $\beta = 0.12466$ is used. These coefficients correspond to the damping of the first two natural frequencies (respectively 0.205 Hz and 0.597 Hz) by the decay ratio $\zeta = 0.05$.

Although similar to the model synthesized in [105], our RM model differs in the much greater number of degrees of freedom and different damping coefficients. This difference manifests itself in a plot of the three mode shapes of the model, as depicted in Figure 5.22. Both the frequencies and the shapes differ from the model given in [105]. The first ten

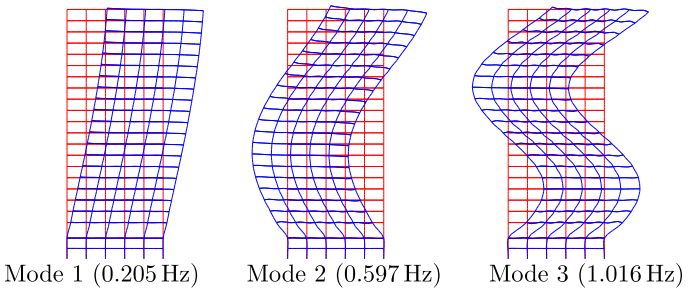

Figure 5.22: First three mode shapes of the RM model.

eigenfrequencies of the RM model are presented in Table 5.5.

Table 5.5: The first ten values of the RM model's eigenfrequencies.

Index	Eigenfrequency [Hz]
1	0.2050
2	0.5973
3	1.0158
4	1.1299
5	1.2334
6	1.5065
7	2.3849
8	3.1561
9	3.5264
10	3.6236

Simplified model

The SM model with a reduced number of degrees of freedom is used to synthesize the described control method. This is a set of 20 adjoined masses that are joined with dampers

and springs. The lumped masses correspond to the subsequent on-ground levels of the structure. The scheme of this model is presented in Figure 5.23.

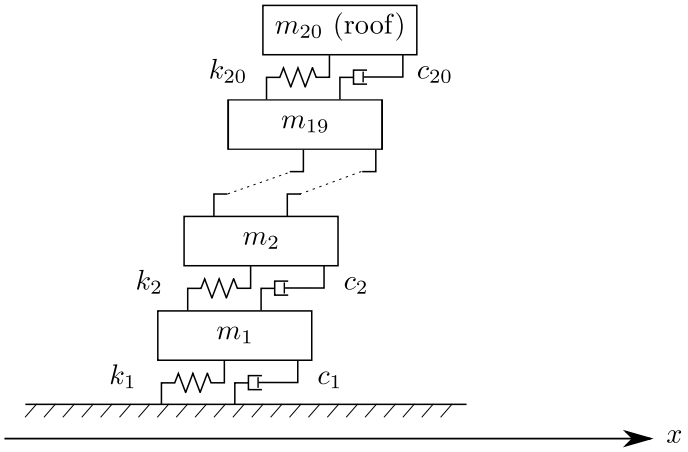

Figure 5.23: Scheme of the simplified model.

Due to the assumption that the first floor is horizontally fixed and due to the premise of the simplified model that there is no direct influence between non-adjacent floors, the floors below and above the first floor have to be treated as separate systems. From the modal analysis depicted in Figure 5.22 it can be concluded that the movement of the basement floor B-1 has a negligible impact on the whole structure. Thus, the basement floor and the first floor are not modelled by SM.

The SM model is defined by the motion equation analogous to the general equation (2.29):

$$\mathbf{M}\ddot{\mathbf{q}}(t) + \mathbf{K}\mathbf{q}(t) + \mathbf{C}\dot{\mathbf{q}}(t) = \mathbf{F}(\mathbf{u}(t)) + \mathbf{M}\mathbf{1}\ddot{x}_e(t), \tag{5.33}$$

where $\mathbf{q}(t) \in \mathbb{R}^{20}$ is a vector of level deflection ($\mathbf{q}(t) = \mathbf{0}$ refers to non-deflected, equilibrium state of the structure), $\mathbf{F}(\mathbf{u}(t)) \in \mathbb{R}^{20}$ is a vector of external forces applied to the subsequent floors, $\mathbf{1}$ denotes the column vector consisting of entries equal to 1, $\ddot{x}_e$ is an earthquake acceleration and matrices $\mathbf{M}$, $\mathbf{K}$, $\mathbf{C} \in \mathbb{R}^{20\times 20}$ are mass, stiffness and damping matrices, respectively.

These are built as follows:

$$\mathbf{M}(\boldsymbol{\kappa}) = \begin{bmatrix} m_1 & 0 & \cdots & \cdots & 0 \\ 0 & m_2 & \ddots & \ddots & 0 \\ \vdots & \ddots & \ddots & \ddots & \ddots \\ 0 & \cdots & \cdots & m_{19} & 0 \\ 0 & \cdots & \cdots & 0 & m_{20} \end{bmatrix},$$

$$\mathbf{K}(\boldsymbol{\xi}) = \begin{bmatrix} k_1 + k_2 & -k_2 & \cdots & \cdots & 0 \\ -k_2 & k_2 + k_3 & \ddots & \ddots & 0 \\ \vdots & \ddots & \ddots & \ddots & \ddots \\ 0 & \cdots & \cdots & k_{19} + k_{20} & -k_{19} \\ 0 & \cdots & \cdots & -k_{19} & k_{20} \end{bmatrix},$$

$$\mathbf{C}(\boldsymbol{\lambda}) = \begin{bmatrix} c_1 + c_2 & -c_2 & \cdots & \cdots & 0 \\ -c_2 & c_2 + c_3 & \ddots & \ddots & 0 \\ \vdots & \ddots & \ddots & \ddots & \ddots \\ 0 & \cdots & \cdots & c_{19} + c_{20} & -c_{19} \\ 0 & \cdots & \cdots & -c_{19} & c_{20} \end{bmatrix}, \tag{5.34}$$

where the tuples

$$\begin{aligned} &\boldsymbol{\kappa} = (m_1, m_2, \ldots, m_{20}), \quad \boldsymbol{\xi} = (k_1, k_2, \ldots, k_{20}), \\ &\boldsymbol{\lambda} = (c_1, c_2, \ldots, c_{20}) \end{aligned} \tag{5.35}$$

are introduced for readability.

The identification scheme for the simplified model has to determine a total of 60 parameters $\boldsymbol{\kappa}$, $\boldsymbol{\xi}$, $\boldsymbol{\lambda}$. The procedure and the final values of the parameters $\boldsymbol{\kappa}$, $\boldsymbol{\xi}$, $\boldsymbol{\lambda}$ are presented in Appendix A.

Actuators and sensors setting

The control forces, as in the example in [105] are induced by hydraulic actuators. Six actuators are placed between each level, starting from the ground floor, one each in every cell of the considered frame. In summary, the object is controlled by a set of 120 actuators. They are rigidly mounted horizontally between subsequent floors, as depicted in Figure 5.24. It is also assumed that parameters of all actuators are the same and that a group of six actuators placed on a certain floor realizes the same control strategy. This postulate reduces the control signal to just 20 inputs.

The dynamic behaviour of the hydraulic actuators is modelled as in [106]:

$$\dot{f}_{a_k} = a_1 (u_k - d_k) - a_2 \dot{d}_k - a_3 f_{a_k}, \tag{5.36}$$

where f_{a_k} stands for the force generated by the actuator on the kth floor, u_k is a control input of the actuator, d_k is the current position of the actuator, and a_1, a_2, a_3 are the

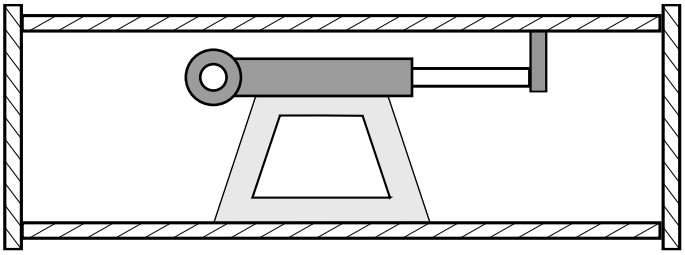

Figure 5.24: The scheme representing the idea of the active actuators mounting.

parameters of values similar to [105]:

$$a_1 = 5.813 \cdot 10^9\,\mathrm{Nm^{-1}s^{-1}}, \quad a_2 = 5.464 \cdot 10^7\,\mathrm{Nm^{-1}}, \quad a_3 = 1.621 \cdot 10^3\,\mathrm{s^{-1}}. \tag{5.37}$$

These parameters correspond to the hydraulic actuator of capacity equal to 897 kN. It is worth noting that the control devices have a servomechanism-type design; that is, the dynamic response of the actuator has negative feedback, as denoted by the term $a_1\,(u_k - d_k)$ in (5.36). In this case, the control input u_k is not an explicit power supply but rather the desired stroke of the actuator. This formulation agrees with the typical realization of the devices that are available on the market.

Because of the horizontal mounting of the servomechanisms between the floors, the position of the actuator is equal to the interstory drift of the structure:

$$d_k = q_k - q_{k-1}, \tag{5.38}$$

where q_k is a displacement of the kth level and d_k is a position of an actuator placed between kth and $(k-1)$th floor (we assume $q_0 \equiv 0 \Rightarrow d_1 = q_1$). Let us define the transformation matrix $\mathbf{Z}_1 \in \mathbb{R}^{20\times 20}$:

$$\mathbf{Z}_1 = \begin{bmatrix} 1 & 0 & 0 & \cdots & 0 \\ -1 & 1 & 0 & \cdots & 0 \\ 0 & -1 & 1 & \cdots & 0 \\ \vdots & \ddots & \ddots & \ddots & \vdots \\ 0 & 0 & \cdots & -1 & 1 \end{bmatrix}, \tag{5.39}$$

and

$$\dot{\mathbf{f}}_a(t) = \begin{bmatrix} \dot{f}_{a_1}(t) \\ \vdots \\ \dot{f}_{a_{20}}(t) \end{bmatrix} = -a_3\mathbf{f}_a(t) + \begin{bmatrix} -a_1\mathbf{Z}_1 & -a_2\mathbf{Z}_1 \end{bmatrix} \begin{bmatrix} \mathbf{q}(t) \\ \dot{\mathbf{q}}(t) \end{bmatrix} + a_1 \begin{bmatrix} u_1(t) \\ \vdots \\ u_{20}(t) \end{bmatrix}. \tag{5.40}$$

The summary force $\mathbf{f}$ acting on all levels of the structure (as in (5.33)) is a sum of the forces that are induced by all of the control devices that are directly above and below each floor:

$$\mathbf{f} = \begin{bmatrix} f_1 \\ \vdots \\ f_{20} \end{bmatrix} = \begin{bmatrix} 6f_{a_1} - 6f_{a_2} \\ \vdots \\ 6f_{a_{19}} - 6f_{a_{20}} \\ 6f_{a_{20}} \end{bmatrix} = 6\mathbf{Z}_2\mathbf{f_a}, \tag{5.41}$$

where

$$\mathbf{Z}_2 = \begin{bmatrix} 1 & -1 & 0 & \cdots & 0 \\ 0 & 1 & -1 & \cdots & 0 \\ \vdots & \ddots & \ddots & \ddots & \vdots \\ 0 & 0 & \cdots & 1 & -1 \\ 0 & 0 & \cdots & 0 & 1 \end{bmatrix}. \tag{5.42}$$

We assume that the weight of the actuators and their mounting is negligible when compared with the whole mass of the structure.

The measurement of the system state is done by the set of 20 accelerometers, which are placed on every above-ground floor. An additional accelerometer is attached to the ground and it provides the earthquake acceleration signal $\ddot{x}_e$ to the controller. The use of the base accelerometer fulfils the assumption of the disturbance measured in real-time. We assume idealized versions of accelerometers; that is, without the bias and the inertia. The time delay of measurement is assumed $\tau = h = 0.01\,\mathrm{s}$.

The whole time-continuous control model, combining control devices inputs $\mathbf{u}$, system state $\mathbf{x} = \begin{bmatrix} \mathbf{q}^T & \dot{\mathbf{q}}^T & \mathbf{f}_a^T \end{bmatrix}^T$, the earthquake acceleration $\ddot{x}_e$ and the measurement of the accelerometers $\mathbf{y} = \begin{bmatrix} \ddot{x}_1 & \cdots & \ddot{x}_{20} \end{bmatrix}^T$ can be presented in the general form of a linear system subjected to an external disturbance (2.33):

$$\dot{\mathbf{x}}(t) = \begin{bmatrix} \dot{\mathbf{q}}(t) \\ \ddot{\mathbf{q}}(t) \\ \dot{\mathbf{f}}_a(t) \end{bmatrix} = \mathbf{A}\mathbf{x}(t) + \mathbf{B}\mathbf{u}(t) + \mathbf{B}_z\ddot{x}_e(t), \quad \mathbf{y} = \mathbf{C}\mathbf{x}(t), \tag{5.43}$$

where

$$\mathbf{A} = \begin{bmatrix} \mathbf{0} & \mathbb{I} & \mathbf{0} \\ -\mathbf{M}^{-1}\mathbf{K} & -\mathbf{M}^{-1}\mathbf{C} & 6\mathbf{M}^{-1}\mathbf{Z}_2 \\ -a_1\mathbf{Z}_1 & -a_2\mathbf{Z}_1 & -a_3\mathbb{I} \end{bmatrix}, \quad \mathbf{B} = \begin{bmatrix} \mathbf{0} \\ \mathbf{0} \\ a_1\mathbb{I} \end{bmatrix}, \mathbf{B}_z = \begin{bmatrix} \mathbf{0} \\ \mathbf{1} \\ \mathbf{0} \end{bmatrix},$$

$$\mathbf{C} = \begin{bmatrix} -\mathbf{M}^{-1}\mathbf{K} & -\mathbf{M}^{-1}\mathbf{C} & 6\mathbf{M}^{-1}\mathbf{Z}_2 \end{bmatrix}. \tag{5.44}$$

The pair $(\mathbf{A}, \mathbf{B})$ of the system (5.43) is controllable (which can be proven by calculating the rank of a respective Kalman matrix) and, therefore, it fulfils Assumption 3.3 required for the existence of the solution to modified optimal control problem (3.41).

Because the described controller is discrete in time, a discrete equivalent of the system (5.43) in the form of Eq. (3.24) was determined via the zero-order hold method:

$$\mathbf{x}(k+1) = \mathbf{A}_D\mathbf{x}(k) + \mathbf{B}_D\mathbf{u}(k) + \mathbf{B}_{zD}\ddot{x}_e(k). \tag{5.45}$$

The period of the discretization was chosen as $h = 0.01\,\mathrm{s}$. It was assumed that period h corresponds to the measurement frequency of the accelerometers and the frequency of updating the control law. This period of time is short enough for the discrete system to sufficiently reproduce the response of the continuous plant. At the same time, the frequency of $1/h = 100\,\mathrm{Hz}$ is within the operating range of the numerous accelerometers available on the market.

Because the sensors that we have used do not measure the full state of the system, and because this full state information is necessary to determine the regulator input, a state estimator has to be used. One of the possibilities is the steady-state Kalman filter (for the formulation, see [107] and [91, Chapter 2]).

The steady-state Kalman estimation $\hat{\mathbf{x}}(k)$ is computed similarly to the estimation introduced in Algorithm 5.1, but with the explicit incorporation of the measured disturbance $\ddot{x}_e(k)$:

$$\hat{\mathbf{x}}(k+1) = \mathbf{A}_D \left[\mathbb{I} - \mathbf{S}_K \mathbf{C}\right] \hat{\mathbf{x}}(k) + \mathbf{B}_D \mathbf{u}(k) + \mathbf{B}_{zD} \ddot{x}_e(k) + \mathbf{A}_D \mathbf{S}_K \mathbf{y}(k+1), \tag{5.46}$$

where $\mathbf{S}_K$ is a constant gain matrix of the Kalman filter calculated for the discrete dynamical model (5.45) via the algebraic discrete Riccati equation:

$$\begin{aligned} \mathbf{S}_K =& \boldsymbol{\Sigma} \mathbf{C}^T \left(\mathbf{V} + \mathbf{C} \boldsymbol{\Sigma} \mathbf{C}^T\right)^{-1}, \\ \boldsymbol{\Sigma} =& \mathbf{A}_D \boldsymbol{\Sigma} \mathbf{A}_D^T - \left(\mathbf{A} \boldsymbol{\Sigma} \mathbf{C}^T\right) \\ & \cdot \left(\mathbf{V} + \mathbf{L} \boldsymbol{\Sigma} \mathbf{C}^T\right)^{-1} \left(\mathbf{C} \boldsymbol{\Sigma} \mathbf{A}_D^T\right) + \mathbf{W}. \end{aligned} \tag{5.47}$$

The incorporation of an earthquake $\ddot{x}_e(k)$ into the Kalman filter scheme is reasonable because $\ddot{x}_e(k)$ is directly measured by the accelerometer.

For the filter synthesis, we assume that the covariance matrices of the process noise $\mathbf{W}$ and the measurement noise $\mathbf{V}$ are as follows:

$$\mathbf{V} = \mathbb{I} \in \mathbb{R}^{20\times 20}, \quad \mathbf{W} = 10^{-6}\mathbb{I} \in \mathbb{R}^{60\times 60}. \tag{5.48}$$

For the full derivation of the Kalman filter for control purposes, the reader is referred to [108]. The state estimation (5.46) along with the measurement $\ddot{x}_e$ is then passed to the proposed control method.

The parameters of the adaptive control method, length of the measurement window S and the order of the AR model $n_{\max}$ were chosen as $S = 750$ and $n_{\max} = 9$, respectively.

The matrices of the assumed quadratic performance index (3.38) are defined as follows. The matrix

$$\mathbf{Q} = \begin{bmatrix} \frac{1}{2}\mathbf{K} & \mathbf{0} & \mathbf{0} \\ \mathbf{0} & \frac{1}{2}\mathbf{M} & \mathbf{0} \\ \mathbf{0} & \mathbf{0} & \mathbf{0} \end{bmatrix} \in \mathbb{R}^{60\times 60}, \quad \mathbf{Q} \succeq 0 \tag{5.49}$$

represents the internal energy that has accumulated in the structure (neglecting the energy of the actuators) and the matrix

$$\mathbf{R} = 5 \cdot 10^6 \cdot \mathbb{I}_{20} \tag{5.50}$$

was chosen by trial and error such that the forces generated by the actuators during the simulations do not exceed their capacity 897 kN. The pair $\left(\mathbf{A}, \mathbf{Q}^{\frac{1}{2}}\right)$ of the system (5.43) is detectable and, therefore, it fulfils the Assumption 3.4. The adaptive control method computes the desired control via the SM model formulation (5.45).

The simulation is conducted in online cooperation of two simulation environments: MATLAB and ANSYS. The exact scheme of the information exchange between both programs is outlined in Algorithm 5.2.

Algorithm 5.2 Simulation of seismic control.

ANSYS (A): Set initial and boundary conditions.
MATLAB (M): Set the initial state of the Kalman filter and hydraulic actuators. Set initial control value to 0.
$t = 0\,\mathrm{s}$
loop $t \leq T_f$
M: Measure the instantaneous floor and earthquake accelerations.
A: Apply earthquake acceleration $\ddot{x}_e(t)$ and forces generated by the actuators $\mathbf{f}$.
A: Conduct construction simulation on time interval $(t; t+h]$.
M: Conduct actuators simulation on time interval $(t; t+h]$ for the present control input $\mathbf{u}$ and the state of the construction.
$t \leftarrow t + h$
M: Update state estimator $\hat{\mathbf{x}}$.
M: Update controller state according to Algorithm 3.4 with the measurements of floor and earthquake accelerations.
M: Apply control signal $\mathbf{u}$ to the actuators.
end loop

Comparative controllers setting

For the sake of the comparative study, the same control scenarios are carried out employing two additional controllers, LQG and H_∞ regulators. The methodology that provided the parameters of these controllers is described below.

Both comparative controllers were determined under the same assumptions as the proposed adaptive method, namely:

1. All controllers use the direct measurements of the ground acceleration $\ddot{x}_e(t)$.
2. All controllers optimize the norm based on the quadratic functions of the state $\mathbf{x}^T\mathbf{Q}\mathbf{x}$ and the control $\mathbf{u}^T\mathbf{R}\mathbf{u}$.

In the case of the LQG regulator, for the performance index, we assume a combination of the quadratic functions and the infinite time horizon, similarly to performance index (3.31):

$$J_{\mathrm{LQG}} = \sum_{i=0}^{\infty} \left(\mathbf{x}_i^T \mathbf{Q} \mathbf{x}_i + \mathbf{u}_i^T \mathbf{R}_{\mathrm{LQG}} \mathbf{u}_i \right). \tag{5.51}$$

In the design of the H_∞ regulator, the continuous system defined in Eq. (5.43) is assumed and the control objective is defined in terms of the H_∞ norm:

$$J_{\mathrm{H}_\infty} = \sup_{\|\ddot{x}_e\|_2 \neq 0} \frac{\left\| \begin{bmatrix} \mathbf{Q}^{\frac{1}{2}} & \mathbf{0} \\ \mathbf{0} & \mathbf{R}_{\mathrm{H}_\infty}^{\frac{1}{2}} \end{bmatrix} \cdot \begin{bmatrix} \mathbf{x}(t) \\ \mathbf{u}(t) \end{bmatrix} \right\|_2}{\|\ddot{x}_e^2(t)\|_2}. \tag{5.52}$$

In (5.52), we use the following norm definition $\|\mathbf{z}(t)\|_2 = \left(\int_0^\infty \mathbf{z}^T(t)\mathbf{z}(t)\,\mathrm{d}t \right)^{\frac{1}{2}}$. Observe that this norm in the numerator in (5.52) is defined by analogy to (3.31) and (5.51):

$$\left\| \begin{bmatrix} \mathbf{Q}^{\frac{1}{2}} & \mathbf{0} \\ \mathbf{0} & \mathbf{R}_{\mathrm{H}_\infty}^{\frac{1}{2}} \end{bmatrix} \cdot \begin{bmatrix} \mathbf{x}(t) \\ \mathbf{u}(t) \end{bmatrix} \right\|_2 = \left(\int_0^\infty \left[\mathbf{x}^T(t)\mathbf{Q}\mathbf{x}(t) + \mathbf{u}^T(t)\mathbf{R}_{\mathrm{H}_\infty}\mathbf{u}(t) \right] \mathrm{d}t \right)^{\frac{1}{2}}. \tag{5.53}$$

The H_∞ controller's state is simulated with the use of the fourth order Runge-Kutta method, but both the measured values of the earthquake and the structure's state, which constitute the regulator's input, and the control value itself are updated with the same discretization period as the adaptive and LQG scheme, i.e., $h = 0.01$ s. To validate this choice, the simulation with tenfold smaller discretization period $h = 0.001$ s has been also conducted. For both $h = 0.01$ s and $h = 0.001$ s, the resulting control signals and the performance indices coincided.

For LQG and H_∞ regulators, the matrix $\mathbf{Q}$ is defined the same as for the adaptive method, see Eq. (5.49). The matrices $\mathbf{R}_{\mathrm{LQG}} \succ 0$, $\mathbf{R}_{\mathrm{H}_\infty} \succ 0$ vary for every considered simulation scenario and were selected such that the control expenditure measured as $\|\mathbf{u}(t)\|_2$ is equivalent for each controller. The equivalence in the energy expenditures for all controllers ensures that any improvement in the method's performance results from the intrinsic properties of the respective controller and not from more aggressive control signals. The values selected for $\mathbf{R}_{\mathrm{LQG}}$ and $\mathbf{R}_{\mathrm{H}_\infty}$ are summarized in Table 5.6.

Since the covariance matrices used for the LQG synthesis are as in (5.48), the resulting Kalman filter is analogous to the state observer used in the adaptive controller defined in Eq. (5.46). The control function of the LQG regulator is affine with respect to the state estimation:

$$\mathbf{u}_{\mathrm{LQG}}(k) = -\mathbf{K}_{\mathrm{LQG}} \begin{bmatrix} \hat{\mathbf{x}}(k) \\ \hat{\dot{\mathbf{x}}}(k) \\ \hat{\mathbf{f}}_a(k) \end{bmatrix}, \tag{5.54}$$

In Eq. (5.54), the gain matrix $\mathbf{K}_{\mathrm{LQG}}$ is assumed as the feedback matrix of the LQR regulator for the infinite horizon performance index (5.51), and is computed by solving the discrete algebraic Riccati equation:

$$\begin{cases} \mathbf{P}_{\mathrm{LQG}} &= \mathbf{A}_D^T \mathbf{P}_{\mathrm{LQG}} \mathbf{A}_D - \left(\mathbf{A}_D^T \mathbf{P}_{\mathrm{LQG}} \mathbf{B}_D\right) \left(\mathbf{R}_{\mathrm{LQG}} + \mathbf{B}_D^T \mathbf{P}_{\mathrm{LQG}} \mathbf{B}_D\right)^{-1} \left(\mathbf{B}_D^T \mathbf{P}_{\mathrm{LQG}} \mathbf{A}_D\right) \\ & \quad + \mathbf{Q} \\ \mathbf{K}_{\mathrm{LQG}} &= \left(\mathbf{R}_{\mathrm{LQG}} + \mathbf{B}_D^T \mathbf{P}_{\mathrm{LQG}} \mathbf{B}_D\right)^{-1} \left(\mathbf{B}_D^T \mathbf{P}_{\mathrm{LQG}} \mathbf{A}_D\right) \end{cases} \tag{5.55}$$

The continuous H_∞ regulator is defined in the state-space form as follows:

$$\begin{cases} \dot{\mathbf{x}}_{\mathrm{H}_\infty}(t) = \mathbf{A}_{\mathrm{H}_\infty} \mathbf{x}_{\mathrm{H}_\infty}(t) + \mathbf{B}_{\mathrm{H}_\infty} \begin{bmatrix} \mathbf{y}(t) \\ \ddot{x}_e(t) \end{bmatrix}, \\ \mathbf{u}_{\mathrm{H}_\infty}(t) = \mathbf{C}_{\mathrm{H}_\infty} \mathbf{x}_{\mathrm{H}_\infty}(t) + \mathbf{D}_{\mathrm{H}_\infty} \begin{bmatrix} \mathbf{y}(t) \\ \ddot{x}_e(t) \end{bmatrix}, \end{cases} \tag{5.56}$$

where $\mathbf{y}(t)$ is the vector of measurements defined in (5.43), $\ddot{x}_e(t)$ is the measurement of the earthquake acceleration, $\mathbf{u}_{\mathrm{H}_\infty}(t)$ is the control signal generated by the regulator H_∞ and $\mathbf{x}_{\mathrm{H}_\infty}(t)$ is the state of the regulator. The matrices $\mathbf{A}_{\mathrm{H}_\infty} \in \mathbb{R}^{60\times 60}$, $\mathbf{B}_{\mathrm{H}_\infty} \in \mathbb{R}^{60\times 21}$, $\mathbf{C}_{\mathrm{H}_\infty} \in \mathbb{R}^{20\times 60}$ and $\mathbf{D}_{\mathrm{H}_\infty} \in \mathbb{R}^{20\times 21}$ were established based on the numerical procedure suggested in [109, 110].

Numerical results

Excitation signals

The designed adaptive control method is tested and compared to LQG and H_∞ control for the reference model subjected to four different excitation signals. Two of these signals are stochastic and established by the exact seismic measurements of the historical earthquakes, in Kobe in 1995 and in El Centro in 1940. The following two excitations are periodic and correspond to the structures' eigenfrequencies. Here, for the first signal, we assume a sine function of the frequency that is equal to the first eigenfrequency of the reference model. The second signal is polyharmonic and consists of the first ten eigenfrequencies of the system. The values of the eigenfrequencies are summarized in Table 5.5. The aim of testing the adaptive controller for the periodic signals is to validate its performance not only for the earthquake conditions but also other possible vibration scenarios, such as those induced by periodic strong wind blows, passages of heavy vehicles or sea waves which may act on offshore platforms. Since the frequencies of the assumed periodic signals coincide with the natural frequencies of the structure, the structure's response is expected to be of large magnitudes. This gives a clear insight into whether the proposed method successfully stabilizes the structure for the deterministic excitation signal scenarios. The amplitudes of the periodic signals' components are selected in such a way that the amplitude spectrum of these signals corresponds to the amplitude spectrum of the El Centro earthquake. The time evolution of all four considered signals and their amplitude spectra are demonstrated in Figures 5.25–5.28.

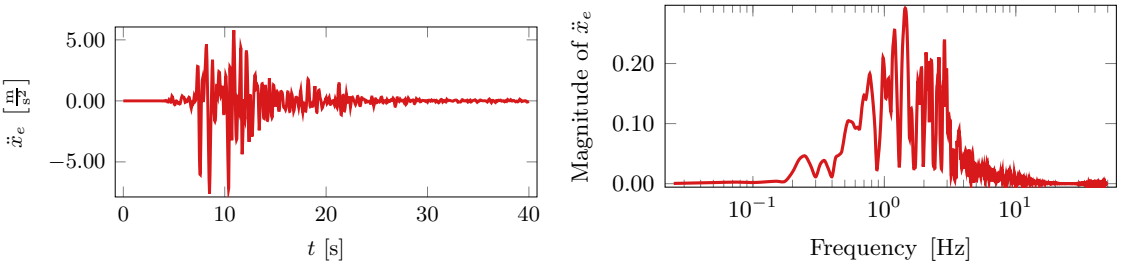

(a) Time evolution of the Kobe excitation signal. (b) The amplitude spectrum of the Kobe excitation signal.

Figure 5.25: Parameters of the Kobe signal.

The initial state of the system corresponds to its equilibrium state, that is,

$$\begin{bmatrix} \mathbf{x}(0) \\ \dot{\mathbf{x}}(0) \\ \mathbf{f_a}(0) \end{bmatrix} = \begin{bmatrix} \mathbf{0} \\ \mathbf{0} \\ \mathbf{0} \end{bmatrix}. \tag{5.57}$$

Starting with the initial condition, the simulations are conducted for $t \in [0; T_f]$, where the final time T_f varies for each scenario. The signal parameters of every scenario, consisting of the type of disturbance, the final time T_f and the assumed values for $\mathbf{R}_{\text{LQG}}$, $\mathbf{R}_{\text{H}_\infty}$ are presented in Table 5.6.

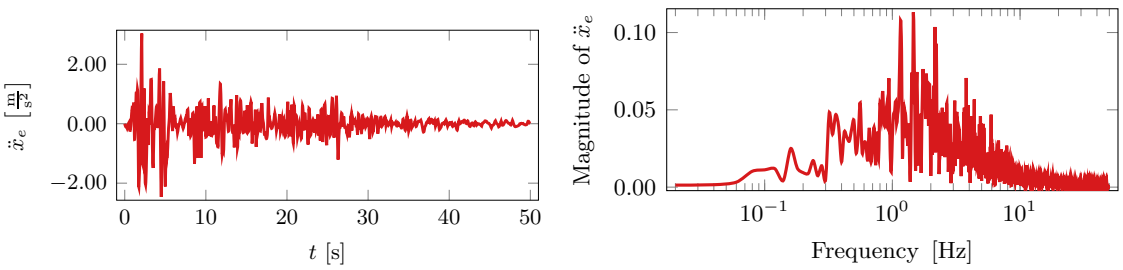

(a) Time evolution of the El Centro signal. (b) The amplitude spectrum of the El Centro signal.

Figure 5.26: Parameters of the El Centro signal.

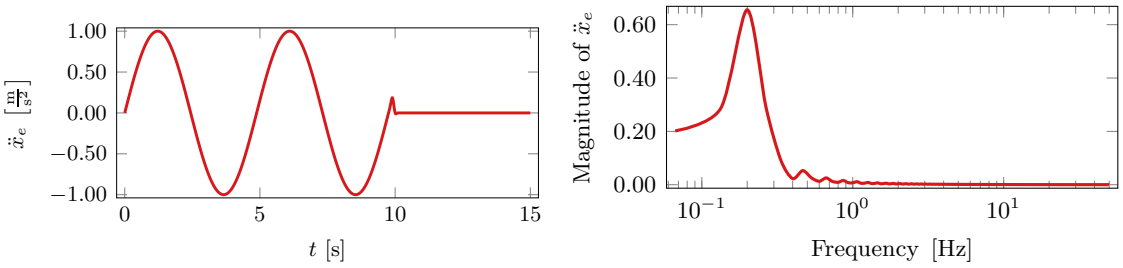

(a) Time evolution of the sine signal. (b) The amplitude spectrum of the sine signal.

Figure 5.27: Parameters of the sine signal.

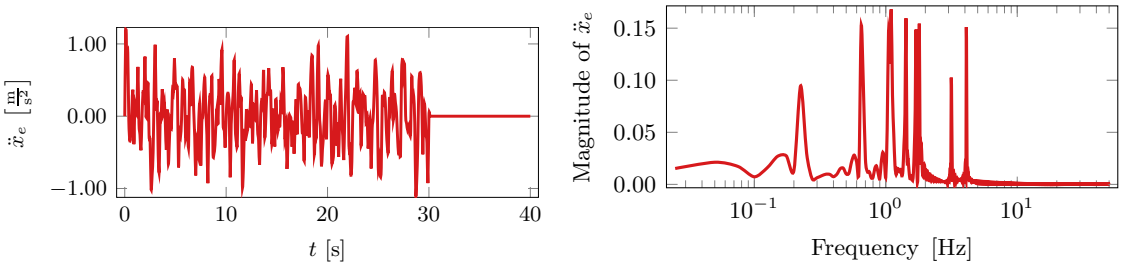

(a) Time evolution of the polyharmonic signal. (b) The amplitude spectrum of the polyharmonic signal.

Figure 5.28: Parameters of the polyharmonic signal.

Table 5.6: Parameters of the simulations.

Index	Disturbance	Final time T_f [s]	$\mathbf{R}_{\mathrm{LQG}}$	$\mathbf{R}_{\mathrm{H}_\infty}$
1	Kobe	40	$5.2356 \cdot 10^6\mathbb{I}$	$2.6240 \cdot 10^8\mathbb{I}$
2	El Centro	50	$3.7929 \cdot 10^6\mathbb{I}$	$1.8154 \cdot 10^8\mathbb{I}$
3	Sine signal	15	$4.8862 \cdot 10^5\mathbb{I}$	$2.3932 \cdot 10^7\mathbb{I}$
4	Polyharmonic signal	40	$6.0809 \cdot 10^6\mathbb{I}$	$3.3035 \cdot 10^8\mathbb{I}$

Control systems' responses

The results of the simulations are demonstrated on Figures: 5.29 and 5.33 (response to the Kobe earthquake), 5.30 and 5.34 (response to the El Centro earthquake), 5.31 and 5.35 (response to the sine disturbance) and 5.32 and 5.36 (response to the polyharmonic

excitation).

Figures 5.29(a), 5.30(a), 5.31(a), 5.32(a) depict the deflection of the tenth floor of the structure with respect to time. It can be observed that for the earthquake excitations, the proposed adaptive control method results in deflection amplitudes reduced by 18.0%–23.0% for the Kobe signal and 5.6%–22.2% for the El Centro signal. The improvement can be also observed for the periodic signals, where compared to the LQG and H_∞ controllers, the adaptive strategy results in the reduction of the deflection amplitudes by 11.8%–47.1% for the sine excitation and 2.2%–6.7% for the polyharmonic excitation.

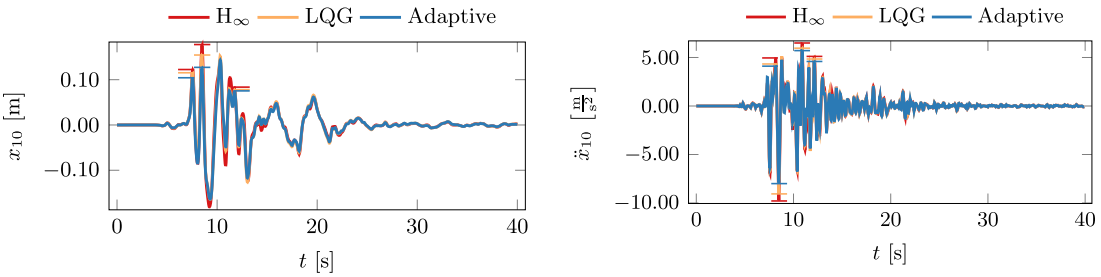

(a) Deflection of the tenth floor over time. (b) Acceleration of the tenth floor over time.

Figure 5.29: Floor deflections and accelerations under the Kobe signal for the considered controllers. To enhance readability, selected peak values are indicated by the horizontal dashes.

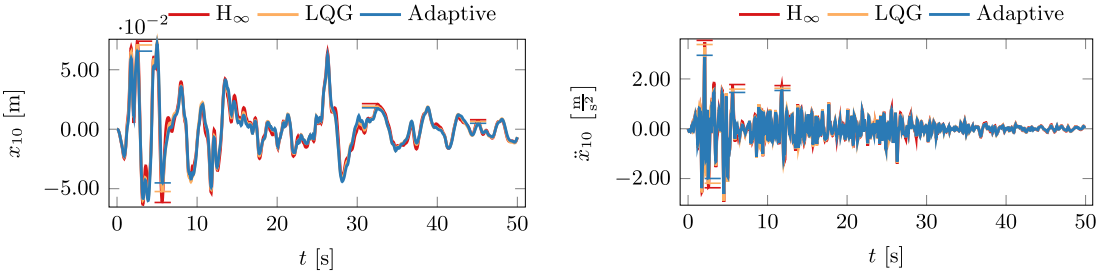

(a) Deflection of the tenth floor over time. (b) Acceleration of the tenth floor over time.

Figure 5.30: Floor deflections and accelerations for the El Centro signal for the considered controllers. To enhance readability, selected peak values are indicated by the horizontal dashes.

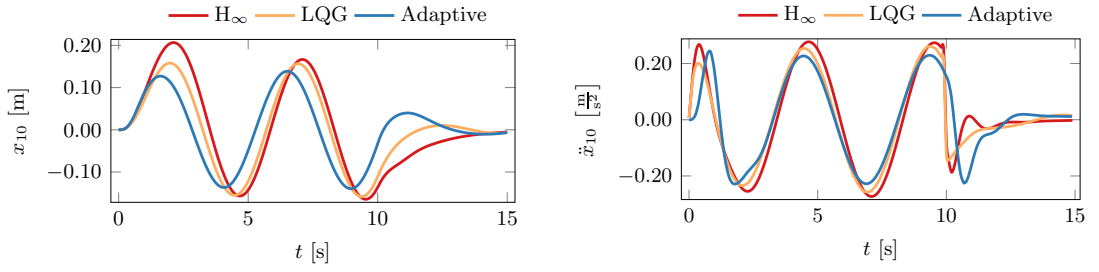

(a) Deflection of the tenth floor over time. (b) Acceleration of the tenth floor over time.

Figure 5.31: Floor deflections and accelerations under the Sine signal for the considered controllers.

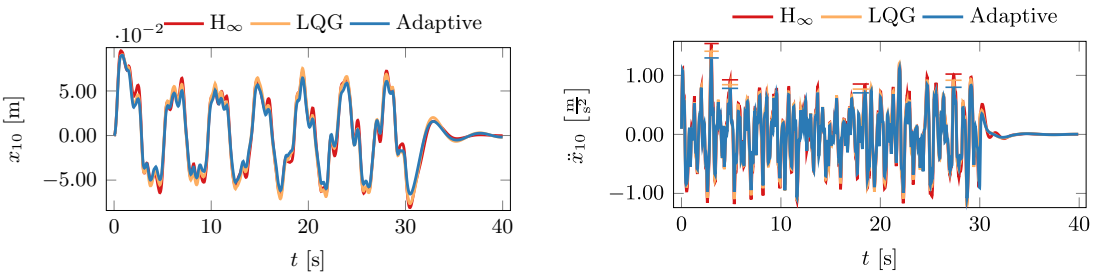

(a) Deflection of the tenth floor over time.

(b) Acceleration of the tenth floor over time.

Figure 5.32: Floor deflections and accelerations under the Polyharmonic signal for the considered controllers.

In addition to the deflection, we also examine the acceleration of the tenth floor. The acceleration measure relates to the safety and comfort of the humans that are inside the building. From Figures 5.29(b), 5.30(b), 5.31(b), 5.32(b), it can be noticed that the adaptive controller results in significantly lower accelerations for each considered disturbance. For Kobe and El Centro earthquakes, the peak values of the acceleration decrease by 11.1%–22.2% and 15.0%–27.1%, respectively. Regarding the sine and polyharmonic signals, the peak accelerations are respectively reduced by 5.1%–23.0% and 9.5%–19.0%.

Figures 5.33(a), 5.34(a), 5.35(a), 5.36(a) depict the time evolution of the performance index $J_x(t)$ corresponding to the total energy of the structure defined by

$$J_x(t) = \int_0^t \mathbf{x}(\tau)\mathbf{Q}\mathbf{x}(\tau)\,\mathrm{d}\tau. \tag{5.58}$$

Here the matrix $\mathbf{Q}$ is assumed as in Eq. (5.49). It can be noticed, that for every excitation signal, the lowest value of this index is obtained for the adaptive control scheme, which confirms that the use of the designed controller improves the structure's energy dissipation. From the evolution of $J_x(t)$, the reader can also observe that the improvement resulting from the use of the adaptive control increases in time which brings us to the conclusion that the proposed control scheme exhibit superior vibration attenuation capabilities throughout the whole simulation.

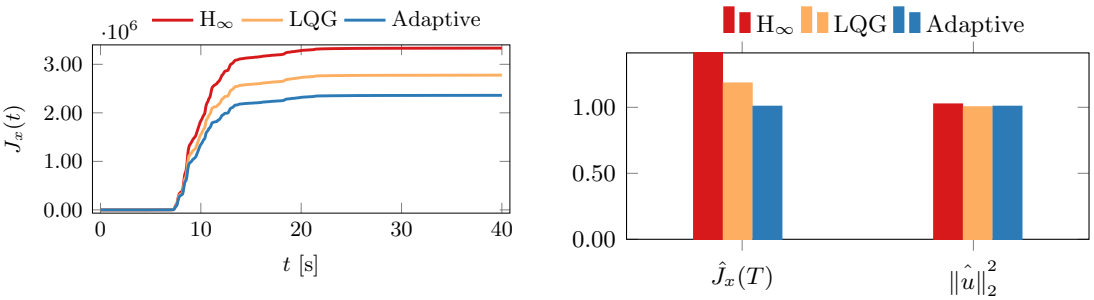

(a) Time evolution of the structure's energy performance index $J_x(t) = \int_0^t \mathbf{x}(\tau)\mathbf{Q}\mathbf{x}(\tau)\,\mathrm{d}\tau$.

(b) The final values of the performance index $\hat{J}_x(T) = J_x(T)/J_x^{\text{adapt.}}(T)$ and the control expenditure $\|\hat{u}\|_2^2 = \|u\|_2^2/\|u^{\text{adapt.}}\|_2^2$. All values are normalized to the adaptive control case.

Figure 5.33: Performance indices and energy expenditure of the control systems excited by the Kobe signal.

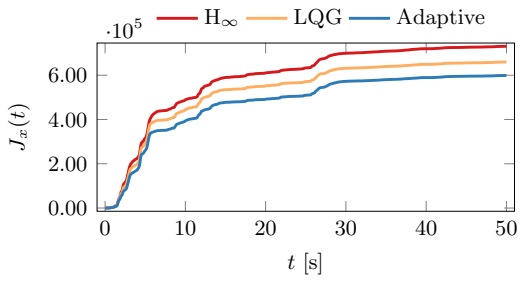

(a) Time evolution of the internal energy performance index $J_x(t) = \int_0^t \mathbf{x}(\tau)\mathbf{Q}\mathbf{x}(\tau)\,\mathrm{d}\tau$.

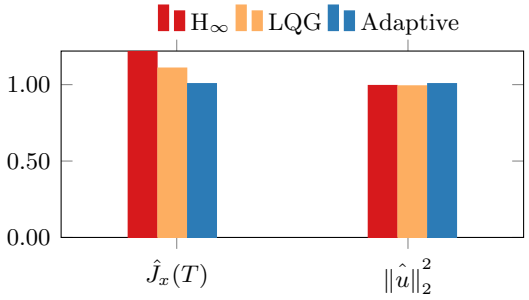

(b) The final values of the performance index $\hat{J}_x(T) = J_x(T)/J_x^{\text{adapt.}}(T)$ and the control expenditure $\|\hat{u}\|_2^2 = \|u\|_2^2/\left\|u^{\text{adapt.}}\right\|_2^2$. All values are normalized to the adaptive control case.

Figure 5.34: Performance indices and energy expenditure of the control systems excited by the El Centro signal.

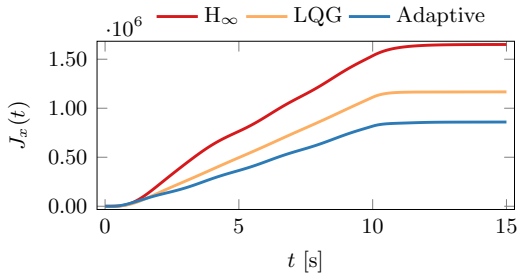

(a) Time evolution of the internal energy performance index $J_x(t) = \int_0^t \mathbf{x}(\tau)\mathbf{Q}\mathbf{x}(\tau)\,\mathrm{d}\tau$.

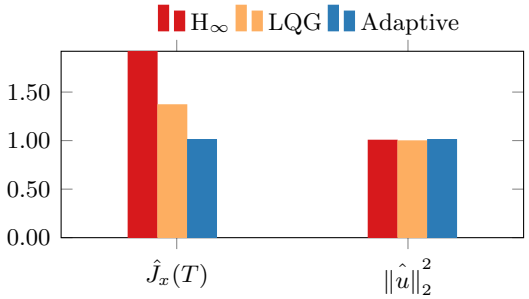

(b) The final values of the performance index $\hat{J}_x(T) = J_x(T)/J_x^{\text{adapt.}}(T)$ and the control expenditure $\|\hat{u}\|_2^2 = \|u\|_2^2/\left\|u^{\text{adapt.}}\right\|_2^2$. All values are normalized to the adaptive control case.

Figure 5.35: Performance indices and energy expenditure of the control systems excited by the Sine signal.

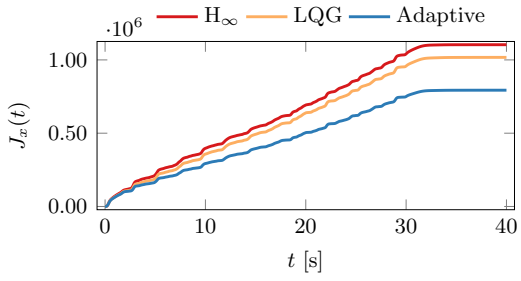

(a) Time evolution of the internal energy performance index $J_x(t) = \int_0^t \mathbf{x}(\tau)\mathbf{Q}\mathbf{x}(\tau)\,\mathrm{d}\tau$.

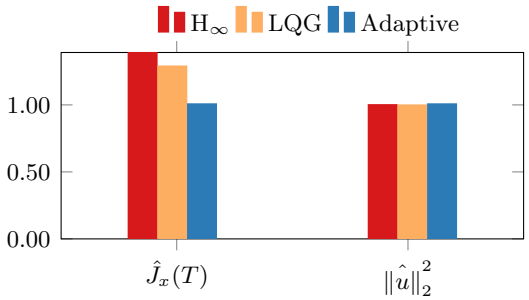

(b) The final values of the performance index $\hat{J}_x(T) = J_x(T)/J_x^{\text{adapt.}}(T)$ and the control expenditure $\|\hat{u}\|_2^2 = \|u\|_2^2/\left\|u^{\text{adapt.}}\right\|_2^2$. All values are normalized to the adaptive control case.

Figure 5.36: Performance indices and energy expenditure of the control systems excited by the Polyharmonic signal.

A similar conclusion can be also deduced from the analysis of Figures 5.33(b), 5.34(b), 5.35(b) and 5.36(b), where the final values of the performance index $J_x(T_f)$ are presented. All of the demonstrated values are normalized to those obtained via the adaptive control, i.e. $\hat{J}_x^{\text{adapt.}}(T_f) = 1$. The proposed adaptive control method outperforms both the LQG

and H_∞ for each of the considered scenarios. The improvement varies from 8.4% for the El Centro earthquake and comparison to the LQG control to 92.0% for the sine signal and comparison to the H_∞ regulator. The second part of the Figures 5.33(b), 5.34(b), 5.35(b), 5.36(b) presents the normalized norm of the control, $\|u\|_2^2 = \int_0^T \mathbf{u}^T(t)\mathbf{u}\,\mathrm{d}t$. The values of the regularization matrices $\mathbf{R}_{\mathrm{LQG}} \succ 0$, $\mathbf{R}_{\mathrm{H}_\infty} \succ 0$ have been picked in such a way that the control expenditure of all algorithms and all excitations is approximately equal. This means that the adaptive control more efficiently stabilizes the structure with the comparable control expenditure level.

It is also worth analyzing other criteria for the quality of stabilization, in particular, those related to the acceleration and the interstory drift. As mentioned before, acceleration corresponds directly to the safety and comfort of humans inside a building. The interstory drift, on the other hand, is linked to dangerous inelastic deformations of the structure. Such insightful performance criteria are introduced in [105]. The details of these criteria are presented in Table 5.7. Their values that have been obtained for all considered excitation

Table 5.7: Definition of the examined performance criteria.

Criterion	description
$J_1 = \max_{t,\,i} \lvert x_i(t)\rvert$	Floor Displacement
$J_2 = \max_{t,\,i} \frac{\lvert d_i(t)\rvert}{l_i}$	Interstory Drift
$J_3 = \max_{t,\,i} \lvert \ddot{x}_i(t)\rvert$	Floor Acceleration
$J_4 = \max_t \left\lvert \sum_{i=2}^{21} m_i \ddot{x}_i(t)\right\rvert$	Base Shear
$J_5 = \max_i \lVert x_i(t)\rVert$	Normalized Floor Displacement
$J_6 = \max_i \frac{\lVert d_i(t)\rVert}{l_i}$	Normalized Interstory Drift
$J_7 = \max_i \lVert \ddot{x}_i(t)\rVert$	Normalized Floor Acceleration
$J_8 = \left\lVert \sum_{i=2}^{21} m_i \ddot{x}_i(t)\right\rVert$	Normalized Base Shear

scenarios can be found in Tables 5.8, 5.9, 5.10 and 5.11.

Remark 5.1. *The masses that are used to compute the criteria J_4 and J_8 are the actual masses of the levels of the RM model and they are not the values that were identified for the SM model. The norm used for the criteria J_{5-8} is the L^2 norm that is computed with taking into account the whole simulation time, $\|x_i(t)\| = \sqrt{\int_0^{T_f} x_i^2(\tau)\,\mathrm{d}\tau}$.*

For the majority of the considered criteria, the designed adaptive method significantly outperforms the comparative LQG and H_∞ regulators. In particular, the reduction of the normalized base shear and the normalized interstory drift criteria ranges respectively by 8.1%–21.1% and 5.2%–50.1% when implementing the adaptive strategy. The criteria where the adaptive method does not exhibit the improvement are the maximal interstory drift and the base shear computed for the sine excitation. For the maximal interstory drift, the LQG controller outperforms the adaptive one by 0.7%. For the base shear index, the best performance is exhibited by H_∞ regulator which resulted in 14.2% improvement compared to the adaptive method. In the case of the sine excitation, the autoregressive scheme has the ability to ideally identify the disturbance model. As a result, the adaptive method transiently realizes more aggressive control than the LQG and H_∞ counterparts and the

Table 5.8: The performance criteria for the Kobe earthquake. Each value is normalized to the adaptive controller case.

Kobe			
Crit.	Adapt.	LQG	H_∞
J_1	1.0000	1.0148	1.0256
J_2	1.0000	1.3599	1.9983
J_3	1.0000	1.0772	1.2165
J_4	1.0000	1.1071	1.1793
J_5	1.0000	1.0398	1.0331
J_6	1.0000	1.0566	1.2102
J_7	1.0000	1.1106	1.2455
J_8	1.0000	1.0812	1.1197
$J_x(T)$	1.0000	1.1137	1.4121
Avg.	**1.000**	**1.1762**	**1.2669**

Table 5.9: The performance criteria for El Centro earthquake. Each value is normalized to the adaptive controller case.

El Centro			
Crit.	Adapt.	LQG	H_∞
J_1	1.000	1.0109	1.005
J_2	1.000	1.1224	1.6362
J_3	1.000	1.141	1.3143
J_4	1.000	1.1266	1.1365
J_5	1.000	1.0017	1.0104
J_6	1.000	1.0551	1.0518
J_7	1.000	1.1024	1.2307
J_8	1.000	1.0925	1.1251
$J_x(T)$	1.0000	1.0838	1.2199
Avg.	**1.000**	**1.0921**	**1.1922**

amplitudes of the force generated by the actuators are on some time intervals higher than when the comparative controllers are in use. For this reason, the amplitude of vibrations induced in the adaptively controlled structure is very quickly reduced to a small value, but the peak values of the structure's levels' deflection, velocity and acceleration can be high. Because of that, both the maximal interstory drift and the maximal base shear (which linearly depends on the accelerations) are larger for the adaptive control than for both remaining controllers. However, the criteria for normalized accelerations J_6 and base shears J_8, which take into account the whole simulation interval, clearly shows that the adaptive method gives better results.

Regarding the normalized interstory drift, the adaptive control results in 5.2%–50.1% range of improvement compared to the other two controllers. This confirms that the proposed control method can also reduce the risk of inelastic deformation of the structure which may be beneficial for preventing the structural damages.

In order to evaluate the overall stabilizing performance, mean values of the considered criteria are also investigated. Compared to the LQG controller, the adaptive method results in a 9.2% to 29.7% reduction of the mean value. When compared to the H_∞ controller this

Table 5.10: The performance criteria for the sine signal excitation. Each value is normalized to the adaptive controller case.

	Sine		
Crit.	Adapt.	LQG	H_∞
J_1	1.0000	1.3975	1.8881
J_2	1.0000	0.99319	1.1995
J_3	1.0000	1.4087	1.5358
J_4	1.0000	1.2054	0.85829
J_5	1.0000	1.4361	1.7241
J_6	1.0000	1.4026	1.5008
J_7	1.0000	1.318	1.4212
J_8	1.0000	1.1568	1.2114
$J_x(T)$	1.0000	1.3579	1.9204
Avg.	**1.0000**	**1.2974**	**1.4733**

Table 5.11: The performance criteria for the polyharmonic signal excitation. Each value is normalized to the adaptive controller case.

	Polyharmonic		
Crit.	Adapt.	LQG	H_∞
J_1	1.0000	1.0223	1.0862
J_2	1.0000	1.022	1.2661
J_3	1.0000	1.2507	1.2964
J_4	1.0000	1.4402	1.3507
J_5	1.0000	1.1285	1.1235
J_6	1.0000	1.1338	1.1444
J_7	1.0000	1.1015	1.2364
J_8	1.0000	1.0869	1.1223
$J_x(T)$	1.0000	1.2823	1.3912
Avg.	**1.0000**	**1.1631**	**1.2241**

reduction varies from 19.2% to 47.3%.

5.3 Semi-active stabilization of beam under moving load

In this section, the adaptive semi-active control method that has been presented in Section 3.4 is tested numerically. The method is employed to stabilise the beam subjected to a moving load.

The problem of the stabilisation of a structure under a moving load is widely recognized by the scientific community. In [111], the semi-active control of the beam under a moving load is introduced. The switching times are obtained via trial and error approach. Authors of [112] propose the active shape control of the railway track to minimize vibrations during the movement of a train. The control is applied to the system by the set of smart sleepers. After the separate procedure identifies the weight and mass of the train, the heuristic method computed the near-optimal control. [113] analyses the switching control strategy of the semi-active control of the beam under a moving load. The performance of the control is defined in the framework of the optimal control theory. The switching times are assumed as optimization parameters. This work shows that the switching strategy outperforms passive control. The extension of [113] is proposed in [30], where the stabilized system is the set of two coupled elastic beams subjected to the moving load. The optimal switching times of the dampers have been computed using the pattern search method. The heuristic distributed and semi-active control for the moving load problem is proposed in [114]. The simple but effective control law is based solely on the measurements of the velocity of the deflection of the beam above the damper. In [115], the stabilization of the plate subjected to two moving masses is considered. The control is realized via the smart damping layer. The proposed control strategy is developed via optimization of the switching hyperplane. [37] formulates closed-loop near-optimal control method based on sensitivity analysis for the problem of a beam subjected to the moving load. The method adapts the control signal to the change of the velocity of the load. The control signal is computed using measurements of the position, the velocity of the load and the state of the beam. Fast revaluation of the control is guaranteed by the use of the precomputed optimal trajectories for reference velocities of the load.

Model description

The scheme of the control system is depicted in Figure 5.37. The mechanical object to be stabilized is a simply supported, homogeneous and isotropic beam that has linear density μ, flexural rigidity EI and length L. It is assumed that the deflection $w(\xi, t)$ of the beam during excitation is elastic and that Hooke's law holds. The beam is excited via the concentrated constant force $P < 0$ moving with varying velocity $v(t) > 0$ along the structure. It is assumed that the value of the force P is known and the instantaneous value of the velocity $v(t)$ and the position of the load $p(t) = \int_0^t v(\tau)\,\mathrm{d}\tau$ can be measured online.

Four supports are placed below the beam at distances a_j, $j = 1, 2, 3, 4$ and consist of springs with stiffness k and controllable dampers with damping friction $c_j(u_j) \in [c_{\min}, c_{\max}]$, $j = 1, 2, 3, 4$, where $\mathbf{u} = \begin{bmatrix} u_1 & u_2 & u_3 & u_4 \end{bmatrix}^T$ is the vector of the control signal. The resultant

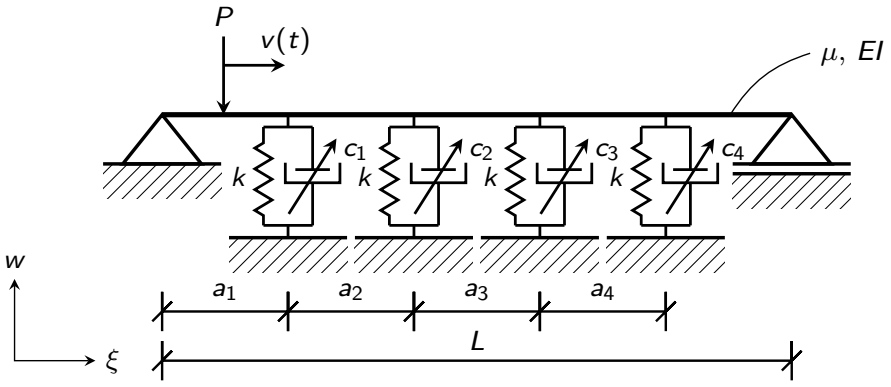

Figure 5.37: Scheme of the control system.

damping coefficient is assumed to depend linearly on the control value, i.e.

$$c_j(u_j) = \frac{c_{\max} - c_{\min}}{2} u_j + \frac{c_{\max} + c_{\min}}{2},\ u_j \in [-1, 1], \quad j = 1,\ 2,\ 3,\ 4. \tag{5.59}$$

The boundary conditions are assumed as:

$$\begin{aligned} w(0,t) = w(L,t) = 0, \quad & t \in [0, T_f], \\ \left.\frac{\partial^2 w(\xi,t)}{\partial \xi^2}\right|_{\xi=0} = \left.\frac{\partial^2 w(\xi,t)}{\partial \xi^2}\right|_{\xi=L} = 0, \quad & t \in [0, T_f], \\ w(\xi,0) = \dot{w}(\xi,0) = 0, \quad & \xi \in [0, L]. \end{aligned} \tag{5.60}$$

The goal of the control is to minimize the quadratic performance criterion J on the finite horizon T_f that depends on the overall deflection of the beam $w(\xi, t)$:

$$J = \frac{1}{2} \int_0^{T_f} \int_0^L w^2(\xi, t)\, \mathrm{d}\xi\, \mathrm{d}t. \tag{5.61}$$

The parameters of the system are summarized in Table 5.12. The mathematical model of

Table 5.12: The parameters of the model and the simulation.

Parameter	Value
μ	$1.38 \cdot 10^3\ \mathrm{kg/m}$
EI	$616 \cdot 10^6\ \mathrm{Nm}^2$
L	$120\ \mathrm{m}$
P	$5000 \cdot 9.81\ \mathrm{N}$
k	$0.05 \cdot 48EI \cdot 1/L^3$
$c_{\min}$	$8 \cdot 10^3\ \mathrm{Ns/m}$
$c_{\max}$	$8 \cdot 10^5\ \mathrm{Ns/m}$
a_1	$0.205L$
a_2	$0.205L$
a_3	$0.205L$
a_4	$0.205L$

the system is formulated via Euler-Bernoulli beam theory and is represented by the partial

differential equation with boundary conditions:

$$\begin{aligned}
\mu\frac{\partial^2 w(\xi,t)}{\partial t^2} + EI\frac{\partial^4 w(\xi,t)}{\partial \xi^4} &= -\sum_{j=1}^{4}\left[\left(kw(a_j,t) + c_j(u_j)\frac{\partial w(a_j,t)}{\partial t}\right)\delta\left(\xi - a_j\right)\right] \\
&\quad - P\delta\left(\xi - \int_0^t v(\tau)\,\mathrm{d}\tau\right), \\
(0,t) = w(L,t) &= 0, \quad t \in [0, T_f], \\
\left.\frac{\partial^2 w(\xi,t)}{\partial \xi^2}\right|_{\xi=0} &= \left.\frac{\partial^2 w(\xi,t)}{\partial \xi^2}\right|_{\xi=L} = 0, \quad t \in [0, T_f], \\
w(\xi,0) = \dot{w}(\xi,0) &= 0, \quad \xi \in [0, L].
\end{aligned} \tag{5.62}$$

The critical speed of the Euler-Bernoulli beam is calculated as follows:

$$v_{\text{crit.}} = \frac{\pi}{L}\sqrt{\frac{EI}{\mu}} \approx 17.49\,\frac{\text{m}}{\text{s}}. \tag{5.63}$$

State-space approximation

To obtain the preferable model in the state-space form, the spatial discretization of the formulation (5.62) is conducted. The weak formulation is developed with the employment of sine function as the orthogonal basis.

Let the deflection $w(\xi,t)$ of the system defined in Eq. (5.62) be expanded via Fourier series:

$$w(\xi,t) = \frac{2}{L}\sum_{l=1}^{\infty} V_l(t)\sin\left(\frac{l\pi\xi}{L}\right), \tag{5.64}$$

where V_l, $l = 1, 2, \ldots, \infty$ are series of functions to be determined and functions $\sin\left(\frac{l\pi\xi}{L}\right)$, $l = 1, 2, \ldots, \infty$ form the basis that respects the boundary conditions of (5.62).

After inserting (5.64) into (5.62), the result is:

$$\begin{aligned}
&\mu\frac{2}{L}\sum_{l=1}^{\infty}\ddot{V}_l(t)\sin\left(\frac{l\pi\xi}{L}\right) + EI\frac{2\pi^4}{L^5}\sum_{l=1}^{\infty} l^4 V_l(t)\sin\left(\frac{l\pi\xi}{L}\right) = \\
&\quad -\frac{2}{L}\sum_{j=1}^{4}\sum_{l=1}^{\infty}\left[\left(kV_l(t) + c_j(u_j)\dot{V}_l(t)\right)\sin\left(\frac{a_j l\pi}{L}\right)\right]\delta\left(\xi - a_j\right) \\
&\quad - P\delta\left(\xi - \int_0^t v(\tau)\,\mathrm{d}\tau\right), \\
&V_l(0) = \dot{V}_l(0) = 0, \quad l = 1, 2, \ldots, \infty.
\end{aligned} \tag{5.65}$$

By multiplying (5.65) by $\sin\left(\frac{p\pi\xi}{L}\right)$, $p = 1, 2, \ldots, \infty$ and integrating with respect to ξ

on the interval $[0, L]$, the weak formulation of (5.62) is obtained:

$$\begin{aligned}
&\frac{2\mu}{L}\sum_{l=1}^{\infty}\ddot{V}_l(t)\int_0^L \sin\left(\frac{l\pi\xi}{L}\right)\sin\left(\frac{p\pi\xi}{L}\right)\mathrm{d}\xi + EI\frac{2\pi^4}{L^5}\sum_{l=1}^{\infty} l^4 V_l(t)\int_0^L \sin\left(\frac{l\pi\xi}{L}\right)\sin\left(\frac{p\pi\xi}{L}\right)\mathrm{d}\xi \\
&= -\frac{2}{L}\sum_{j=1}^{4}\sum_{l=1}^{\infty}\left[\left(kV_l(t) + c_j(u_j)\dot{V}_l(t)\right)\sin\left(\frac{a_j l\pi}{L}\right)\right]\int_0^L \delta\left(\xi - a_j\right)\sin\left(\frac{p\pi\xi}{L}\right)\mathrm{d}\xi \\
&\quad - P\int_0^L \delta\left(\xi - \int_0^t v(\tau)\,\mathrm{d}\tau\right)\sin\left(\frac{p\pi\xi}{L}\right)\mathrm{d}\xi, \quad p = 1,\, 2,\, \ldots,\, \infty \\
&V_l(0) = \dot{V}_l(0) = 0, \quad l = 1,\, 2,\, \ldots,\, \infty.
\end{aligned} \tag{5.66}$$

Recall that:

$$\int_0^L \sin\left(\frac{l\pi\xi}{L}\right)\sin\left(\frac{p\pi\xi}{L}\right)\mathrm{d}\xi = \begin{cases} \frac{L}{2}, & \text{if } l = p, \\ 0, & \text{if } l \neq p \end{cases} \tag{5.67}$$

and

$$\int_0^L \delta\left(\xi - a\right) f(\xi)\,\mathrm{d}\xi = \begin{cases} f(a), & \text{if } a \in [0, L] \\ 0, & \text{if } a \notin [0, L] \end{cases}. \tag{5.68}$$

Eq. (5.66) reduces then to the set of dynamical equations:

$$\begin{aligned}
&\mu\ddot{V}_p(t) + EI\frac{\pi^4}{L^4}p^4 V_p(t) = \\
&\quad - \frac{2}{L}\sum_{j=1}^{4}\sum_{l=1}^{\infty}\left[\left(kV_l(t) + c_j(u_j)\dot{V}_l(t)\right)\sin\left(\frac{a_j l\pi}{L}\right)\right]\sin\left(\frac{a_j p\pi}{L}\right) \\
&\quad - P\sin\left(\frac{p\pi\int_0^t v(\tau)\,\mathrm{d}\tau}{L}\right), \quad p = 1,\, 2,\, \ldots,\, \infty \\
&V_p(0) = \dot{V}_p(0) = 0, \quad p = 1,\, 2,\, \ldots,\, \infty.
\end{aligned} \tag{5.69}$$

Observe that in terms of the weak formulation (5.69), the performance criterion (5.61) takes the form:

$$J = \frac{2}{L}\sum_{p=1}^{\infty}\int_0^{T_f} V_p^2(t)\,\mathrm{d}t. \tag{5.70}$$

In the subsequent sections, the approximate solution to the infinite formulation (5.69) is considered. The approximation is conducted by neglecting the impact of higher-order terms in Eqs. (5.69). Such an approximation strategy is commonly used in literature, e.g. in [30, 37, 116]. In the present case, only first $n = 5$ terms are considered. The resulting set of ordinary equations is as follows:

$$\begin{aligned}
&\mu\ddot{V}_p(t) + EI\frac{\pi^4}{L^4}p^4 V_p(t) = \\
&\quad - \frac{2}{L}\sum_{j=1}^{4}\sum_{l=1}^{5}\left[\left(kV_l(t) + c_j(u_j)\dot{V}_l(t)\right)\sin\left(\frac{a_j l\pi}{L}\right)\right]\sin\left(\frac{a_j p\pi}{L}\right) \\
&\quad - P\sin\left(\frac{p\pi\int_0^t v(\tau)\,\mathrm{d}\tau}{L}\right), \quad p = 1,\, 2,\, \ldots,\, n \\
&V_p(0) = \dot{V}_p(0) = 0, \quad p = 1,\, 2,\, \ldots,\, n.
\end{aligned} \tag{5.71}$$

For brevity, define the series of matrices

$$\mathbf{G}_j = \begin{bmatrix} \sin\left(\frac{a_j\pi}{L}\right) \\ \sin\left(\frac{2a_j\pi}{L}\right) \\ \vdots \\ \sin\left(\frac{na_j\pi}{L}\right) \end{bmatrix} \cdot \begin{bmatrix} \sin\left(\frac{a_j\pi}{L}\right) & \sin\left(\frac{2a_j\pi}{L}\right) & \dots & \sin\left(\frac{na_j\pi}{L}\right) \end{bmatrix}, \quad j = 1,\, 2,\, 3,\, 4 \tag{5.72}$$

and the matrix

$$\mathbf{H} = \operatorname{diag}(1,\, 2,\, \dots,\, n). \tag{5.73}$$

Notice that matrices $\mathbf{G}_j$, $j = 1,\, 2,\, 3,\, 4$ are positive semi-definite and the matrix $\mathbf{H}$ is positive definite. Eq. (5.71) can be rewritten in the state-space form as follows:

$$\dot{\mathbf{x}}(t) = \begin{bmatrix} \dot{V}_1 \\ \dot{V}_2 \\ \vdots \\ \ddot{V}_5 \\ \ddot{V}_1 \\ \ddot{V}_2 \\ \vdots \\ \ddot{V}_5 \end{bmatrix} = \mathbf{A}\mathbf{x}(t) + \sum_{j=1}^{4} u_j(t)\mathbf{B}_j\mathbf{x}(t) + \mathbf{F}(t, v(t)), \tag{5.74}$$

where the matrices $\mathbf{A} \in \mathbb{R}^{10\times10}$ and $\mathbf{B}_j \in \mathbb{R}^{10\times10}$, $j = 1,\, 2,\, 3,\, 4$ are built as follows:

$$\mathbf{A} = \begin{bmatrix} \mathbf{0} & \mathbb{I} \\ -\mathbf{M}^{-1}\mathbf{K} & -\mathbf{M}^{-1}\mathbf{C} \end{bmatrix}, \quad \mathbf{B}_j = \frac{c_{\max} - c_{\min}}{L} \begin{bmatrix} \mathbf{0} & \mathbf{0} \\ 0 & -\mathbf{M}^{-1}\mathbf{G}_j \end{bmatrix}, \tag{5.75}$$

with

$$\mathbf{M} = \mu\mathbb{I}, \quad \mathbf{K} = EI\frac{\pi^4}{L^4}\mathbf{H}^4 + \frac{2k}{L}\sum_{j=1}^{4}\mathbf{G}_j, \quad \mathbf{C} = \frac{c_{\max} + c_{\min}}{L}\sum_{j=1}^{4}\mathbf{G}_j. \tag{5.76}$$

The vector $\mathbf{F}(t, v(t))$ corresponding to the excitation by the moving load is defined as follows:

$$\mathbf{F}(t, v(t)) = -\frac{P}{\mu} \begin{bmatrix} 0 \\ 0 \\ \vdots \\ 0 \\ \sin\left(\frac{\pi\int_0^t v(\tau)\,\mathrm{d}\tau}{L}\right) \\ \sin\left(\frac{2\pi\int_0^t v(\tau)\,\mathrm{d}\tau}{L}\right) \\ \vdots \\ \sin\left(\frac{n\pi\int_0^t v(\tau)\,\mathrm{d}\tau}{L}\right) \end{bmatrix}. \tag{5.77}$$

The performance criterion (5.70) for the approximate model (5.74) takes the form:

$$J = \int_0^{T_f} \mathbf{x}^T(t)\mathbf{Q}\mathbf{x}(t)\,\mathrm{d}t, \tag{5.78}$$

where

$$\mathbf{Q} = \frac{2}{L}\begin{bmatrix} \mathbb{I} & \mathbf{0} \\ \mathbf{0} & \mathbf{0} \end{bmatrix} \tag{5.79}$$

Observe that matrix $\mathbf{K}$ is positive definite and matrix $\mathbf{C}$ is positive semi-definite. Since the rank of the matrix $\begin{bmatrix} \mathbf{C} \\ \mathbf{CM}^{-1}\mathbf{K} \end{bmatrix}$ is equal to n, Theorem 3.1 guarantees that the matrix $\mathbf{A}$ is stable. This implies that the constant zero control $\mathbf{u}_0 = \mathbf{0}$ stabilizes the system (5.74). Matrix $\mathbf{Q}$ of the performance criterion (5.78) is positive semi-definite. Observe that the matrix consisting of the first two terms of the observability matrix:

$$\begin{bmatrix} \mathbf{Q} \\ \mathbf{Q}\left(\mathbf{A} + \sum_{j=1}^{4} u_j(t)\mathbf{B}_j\right) \end{bmatrix} = \frac{2}{L}\begin{bmatrix} \mathbb{I} & \mathbf{0} \\ \mathbf{0} & \mathbf{0} \\ \mathbf{0} & \mathbb{I} \\ \mathbf{0} & \mathbf{0} \end{bmatrix} \tag{5.80}$$

has full rank and therefore the pair $\left(\mathbf{A} + \sum_{j=1}^{4} u_j(t)\mathbf{B}_j, \mathbf{Q}\right)$ is observable for any $\mathbf{u} \in [-1, 1]^m$. Both Assumptions 3.5 and 3.6 are satisfied and the adaptive semi-active control scheme formulated in Section 3.4 can be applied.

Controllers setting

Parametric identification

The semi-active adaptive control method described in Section 3.4 is verified via the simulation of the beam under a moving load. To operate, the control method needs the online procedure for the identification of the disturbance model:

$$\begin{aligned} \dot{\mathbf{x}}_{z,i}(t) &= \mathbf{A}_{z,i}(\boldsymbol{\gamma}_i)\mathbf{x}_{z,i}(t), \quad \mathbf{x}_{z,\,i}(t_i) = \mathbf{x}_{z0,i}(\boldsymbol{\gamma}_i), \\ \tilde{\mathbf{F}}_i(t) &= \mathbf{C}_{z,i}(\boldsymbol{\gamma}_i)\mathbf{x}_{z,i}(t), \quad \text{such that: } \tilde{\mathbf{F}}_i(t) \approx \mathbf{F}(t, v(t)). \end{aligned} \tag{5.81}$$

The proposed parametric identification scheme is based on a particular form of the disturbance defined in Eq. (5.77).

Observe that the measurement of the position of the load $p_i = p(t_i) = \int_0^{t_i} v(\tau)\,\mathrm{d}\tau$ at the adaptation time t_i fully identifies the vector $\mathbf{F}(t_i, v(t_i))$:

$$\mathbf{F}(t_i, v(t_i)) = -\frac{P}{\mu}\begin{bmatrix} 0 \\ 0 \\ \vdots \\ 0 \\ \sin\left(\frac{\pi p_i}{L}\right) \\ \sin\left(\frac{2\pi p_i}{L}\right) \\ \vdots \\ \sin\left(\frac{n\pi p_i}{L}\right) \end{bmatrix}. \tag{5.82}$$

At each iteration i of the adaptive scheme the simplifying assumption that the load moves with the constant velocity $v_i = v(t_i)$ is imposed, i.e.

$$p(t) \approx p_i + v_i(t - t_i), \quad \forall t \in [t_i, t_{i+1})\,. \tag{5.83}$$

Let $\hat{\mathbf{F}}(t, v(t)) \in \mathbb{R}^n$ denote the vector of non-zero components of $\mathbf{F}(t, v(t))$:

$$\hat{\mathbf{F}}(t, v(t)) = -\frac{P}{\mu} \begin{bmatrix} \sin\left(\frac{\pi p(t)}{L}\right) \\ \sin\left(\frac{2\pi p(t)}{L}\right) \\ \vdots \\ \sin\left(\frac{n\pi p(t)}{L}\right) \end{bmatrix}. \tag{5.84}$$

With the assumption of the piecewise constant velocity defined in Eq. (5.83), $\hat{\mathbf{F}}(t, v(t))$ takes the form:

$$\hat{\mathbf{F}}(t, v_i) = -\frac{P}{\mu} \begin{bmatrix} \sin\left(\frac{\pi(p_i + v_i(t-t_i))}{L}\right) \\ \sin\left(\frac{2\pi(p_i + v_i(t-t_i))}{L}\right) \\ \vdots \\ \sin\left(\frac{n\pi(p_i + v_i(t-t_i))}{L}\right) \end{bmatrix}, \quad \forall t \in [t_i, t_{i+1}). \tag{5.85}$$

Calculate the first and the second derivative of $\hat{\mathbf{F}}(t, v(t))$:

$$\begin{aligned} \dot{\hat{\mathbf{F}}}(t, v_i) &= -\frac{P}{\mu}\frac{\pi v_i}{L} \begin{bmatrix} \cos\left(\frac{\pi(p_i + v_i(t-t_i))}{L}\right) \\ 2\cos\left(\frac{2\pi(p_i + v_i(t-t_i))}{L}\right) \\ \vdots \\ n\cos\left(\frac{n\pi(p_i + v_i(t-t_i))}{L}\right) \end{bmatrix}, \quad \forall t \in [t_i, t_{i+1}) \\ \ddot{\hat{\mathbf{F}}}(t, v_i) &= \frac{P}{\mu}\frac{\pi^2 v_i^2}{L} \begin{bmatrix} \sin\left(\frac{\pi(p_i + v_i(t-t_i))}{L}\right) \\ 4\sin\left(\frac{2\pi(p_i + v_i(t-t_i))}{L}\right) \\ \vdots \\ n^2\sin\left(\frac{n\pi(p_i + v_i(t-t_i))}{L}\right) \end{bmatrix} \\ &= -\frac{\pi^2 v_i^2}{L^2}\mathbf{H}^2\hat{\mathbf{F}}(t, v_i), \quad \forall t \in [t_i, t_{i+1}), \end{aligned} \tag{5.86}$$

where $\mathbf{H}$ is defined as in Eq. (5.73).

Let the vector of the state of the excitation be defined as

$$\mathbf{x}_{z,i}(t) = \begin{bmatrix} \hat{\mathbf{F}}(t, v_i) \\ \dot{\hat{\mathbf{F}}}(t, v_i) \end{bmatrix}, \tag{5.87}$$

the initial conditions as:

$$\mathbf{x}_{z0,i}(p_i, v_i) = -\frac{P}{\mu}\begin{bmatrix} \hat{\mathbf{F}}(t_i, v_i) \\ \dot{\hat{\mathbf{F}}}(t_i, v_i) \end{bmatrix} = \begin{bmatrix} \sin\left(\frac{\pi p_i}{L}\right) \\ \sin\left(\frac{2\pi p_i}{L}\right) \\ \vdots \\ \sin\left(\frac{n\pi p_i}{L}\right) \\ \frac{\pi v_i}{L}\cos\left(\frac{\pi p_i}{L}\right) \\ \frac{2\pi v_i}{L}\cos\left(\frac{2\pi p_i}{L}\right) \\ \vdots \\ \frac{n\pi v_i}{L}\cos\left(\frac{n\pi p_i}{L}\right) \end{bmatrix} \tag{5.88}$$

and let the matrices $\mathbf{A}_{z,i}(p_i, v_i)$ and $\mathbf{C}_{z,i}$ be defined as follows:

$$\mathbf{A}_{z,i}(p_i, v_i) = \begin{bmatrix} \mathbf{0} & \mathbb{I} \\ \mathbf{0} & -\frac{\pi^2 v_i^2}{L^2}\mathbf{H}^2 \end{bmatrix}, \quad \mathbf{C}_{z,i} = \begin{bmatrix} \mathbf{0} & \mathbf{0} \\ \mathbb{I} & \mathbf{0} \end{bmatrix}, \mathbf{C}_{z,i} \in \mathbb{R}^{2n \times n}. \tag{5.89}$$

Then the trajectory of the excitation (5.77) with the assumption denoted in Eq. (5.83) can be approximated by the linear dynamical system:

$$\begin{aligned} \dot{\mathbf{x}}_{z,i}(t) &= \mathbf{A}_{z,i}(p_i, v_i)\mathbf{x}_{z,i}(t), \quad \mathbf{x}_{z,i}(t_i) = \mathbf{x}_{z0,i}(p_i, v_i) \\ \mathbf{F}(t, v(t)) &\approx \mathbf{C}_{z,i}\mathbf{x}_{z,i}(t). \end{aligned} \tag{5.90}$$

Observe that the only parameters that are needed for computation of the dynamical model of the moving load are the velocity v_i and position p_i.

As a conclusion, the stabilization of the beam subjected to the moving load is conducted via the semi-active control method summarized in Algorithm 3.5 with the measurement vector $\boldsymbol{\gamma}_i = \begin{bmatrix} p_i & v_i \end{bmatrix}$.

Remark 5.2. Observe that the proposed identification method is based solely on the special choice of the basis function of the weak formulation. If the boundary conditions of the partial differential equation (5.62) were chosen differently or the dynamical model of the beam was different, the sine functions could not be used. In that case, the vector $\mathbf{F}(t, v(t))$ corresponding to the impact of the load would have a different form that could not be transformed directly to the linear model (5.90).

However, the knowledge of the instantaneous values of the position p_i and velocity v_i would allow for exact determination of the future trajectory of $\mathbf{F}(t, v_i)$. It is believed that the linear autonomous model of the disturbance (5.90) could be then established using the continuous AR model analogous to the discrete method defined in Algorithm 3.1 that is fitted to the known signal $\mathbf{F}(t, v_i)$. For the review of the continuous autoregressive identification method, see [117].

Comparative controls

The adaptive method is compared to the results of two different types of control:

1. maximal constant control $\mathbf{u}_0 = \mathbf{1}$,
2. open-loop optimal control $\mathbf{u}^*(t)$.

The maximal constant control corresponds to the situation, where the supports of the beam generate the greatest damping ratio on the whole simulation interval.

The open-loop optimal control is computed separately for each considered excitation scenario. The optimization procedure is assumed to possess whole information about the future value of the disturbance, i.e, the exact trajectory of the moving load is known. The optimal control problem is assumed not in the MPC form defined in Eq. (3.78) but rather it corresponds to the explicit formulation defined in Eq. (2.3) without approximation of the disturbance. The optimal control is computed via a direct multiple shooting method

implemented using the CasADi package [118]. This open-loop optimal control could not be employed in a real-life scenario, because the movement of the load is in general nondeterministic. However, computation of such an optimal control and its performance gives theoretical lower bound on the semi-active performance and allows to assess the near-optimality of the proposed adaptive control method.

Numerical results

Excitation signals

The performance of the proposed control method is tested via four different excitation scenarios. The trajectory of the load i presented in Figures 5.38 and 5.39.

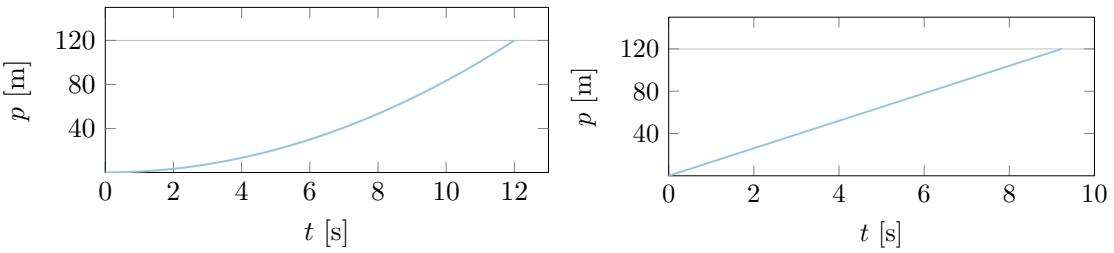

(a) First scenario. (b) Second scenario.

Figure 5.38: Movement of the load at the first and second scenario.

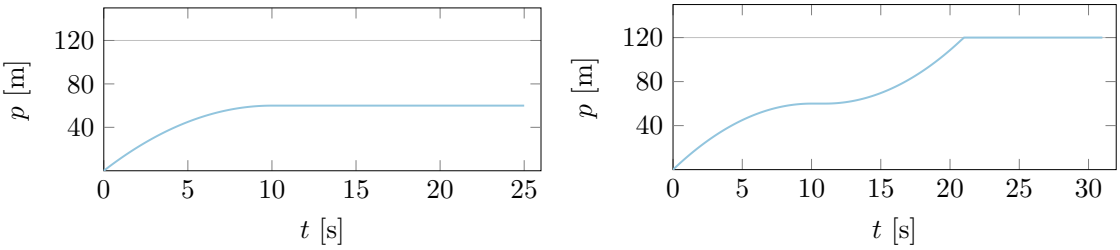

(a) Third scenario. (b) Fourth scenario.

Figure 5.39: Movement of the load at the third and fourth scenario.

The first excitation depicted in Figure 5.38(a) corresponds to the load moving with constant acceleration. The motion is defined as:

$$p_1(t) = \min\left\{L, \frac{5}{6}t^2\right\}, \quad t \in [0, \infty). \tag{5.91}$$

In the second scenario, presented in Figure 5.38(b), the velocity of the load remains constant,

$$p_2(t) = \min\{L, 13t\}, \quad t \in [0, \infty). \tag{5.92}$$

The decelerated movement corresponds to the third scenario, with the position of the load presented in Figure 5.38(b). The load has initial non-zero velocity and moves with constant deceleration until it stops at the centre of the beam. The equation of motion is as

follows:

$$p_3(t) = \begin{cases} 12t - \frac{3}{5}t^2, & t \in [0, 10)\,\mathrm{s} \\ \frac{1}{2}L, & t \in [10, \infty)\,\mathrm{s}. \end{cases} \tag{5.93}$$

In fourth scenario, the movement of the load consists of three distinctive parts: firstly, the load moves with constant deceleration, until it halts at the centre of the beam. It remains at the centre of the beam for 1 s. Finally, it starts to move with constant acceleration until it leaves the beam. The movement is described as follows:

$$p_4(t) = \begin{cases} 12t - \frac{3}{5}t^2, & t \in [0, 10)\,\mathrm{s} \\ \frac{1}{2}L, & t \in [10, 11)\,\mathrm{s} \\ \min\left\{L, \frac{1}{2}L + \frac{3}{5}(t-11)^2\right\}, & t \in [11, \infty) \end{cases} \tag{5.94}$$

The horizons of the simulations of the first and third scenario are equal to the times at which the loads arrive at the end of the beam, i.e. L. In the second scenario, the simulation time is equal to $T_f = 25\,\mathrm{s}$. In the fourth scenario, the simulation horizon is longer than the movement of the load, $T_f = 30\,\mathrm{s}$. Such a choice of the horizon allows to assess the performance of the control methods when no load acts on the structure, but the beam is not in its equilibrium state. The parameters of simulations are summarized in Table 5.13

Table 5.13: The parameters of the model and the simulation.

Scenario	Maximal velocity	Duration of movement	Duration of simulation T_f
1	$1.14v_{\mathrm{crit.}}$	12 s	12 s
2	$0.74v_{\mathrm{crit.}}$	9.23 s	9.23 s
3	$0.69v_{\mathrm{crit.}}$	–	25 s
4	$0.69v_{\mathrm{crit.}}$	21 s	30 s

Control systems' responses

Results of the simulations are presented in Figures 5.40–5.47 and in Table 5.14. Instantaneous deflection of the beam at two instances during the first simulation scenario is depicted in Figure 5.40. Observe that the deflection of the beam controlled via the adaptive method is close to the deflection of the beam that is stabilized optimally. Although the constant control results in smaller deflection on the first half of the movement, its performance is significantly worse on the next part of the simulation.

This statement is also visible in Figure 5.41(a), where the evolution of the quadratic performance criterion defined in Eq. (5.78) is presented. On the first 9 seconds of the simulation, the constant control outperforms the adaptive and optimal ones. Nonetheless, the constant control is not optimal, which is reflected by the significant increase of the performance criterion on the last 3 seconds of the movement.

Figure 5.41(b) shows the shape of the control of the adaptive and optimal controllers. Observe the similarity of both control signals, especially for the first three dampers. It can be argued that the proposed adaptive method generates near-optimal control but, in

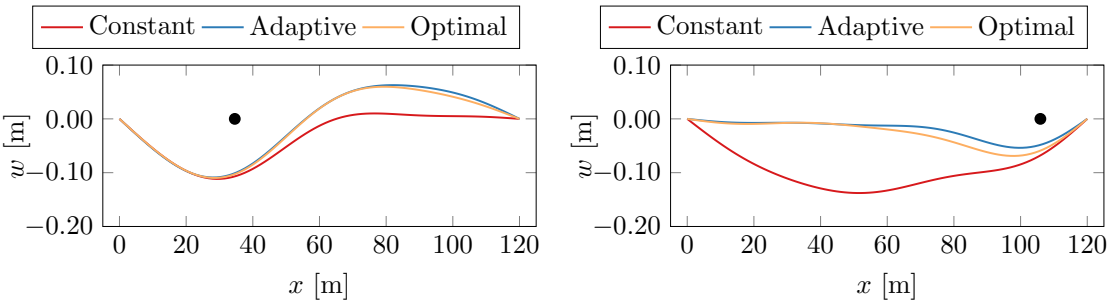

(a) $t = 4.77\,\mathrm{s}$ (b) $t = 11.67\,\mathrm{s}$

Figure 5.40: Deflection of the beam during first scenario. The black dot represents the position of the load.

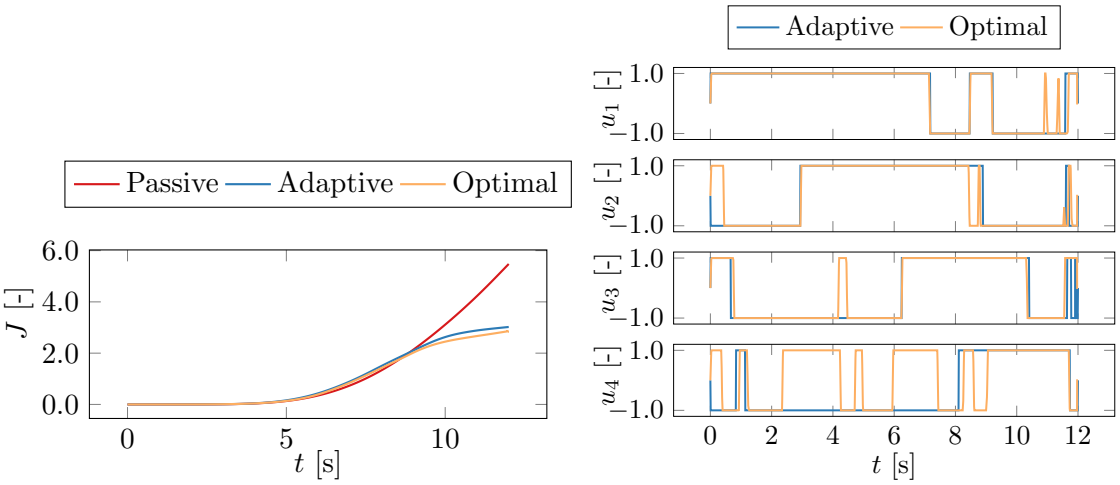

(a) Performance criterion. (b) Control signal.

Figure 5.41: Performance and control during the first simulation.

contrast to the optimal control, it is in the robust closed-loop form and its computation is of significantly lower computational complexity.

Figure 5.42 shows the deflection of the beam during the second simulation scenario. Similarly to the results of the first scenario, the beam controlled via adaptive method has deflection close to the optimal one. The constant control provides better performance on the first part of the simulation, but its overall performance is worse than for the adaptive and optimal control. Figure 5.43(a) presents the performance criterion associated with all three control methods. It proves that the adaptive controller provides near-optimal control. The final performance criterion associated with the constant control is approximately two times larger than for the adaptive and optimal cases. The control signal of the adaptive and optimal methods is presented in Figure 5.43(a). The shape of the adaptive control is close to the optimal for the first three dampers. The control of the fourth damper diverges on the first half of the simulation, but on the second half it behaves almost like the optimal one.

The third scenario corresponds to the load stopping at the centre of the beam. In

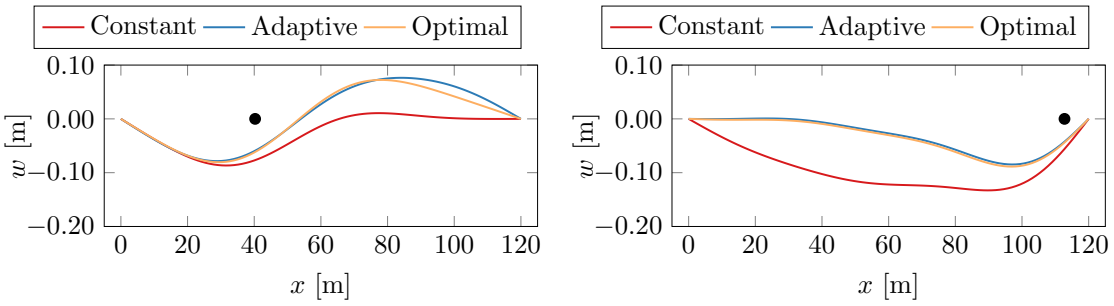

(a) $t = 3.70\,\mathrm{s}$ (b) $t = 8.62\,\mathrm{s}$

Figure 5.42: Deflection of the beam during the second scenario. The black dot represents the position of the load.

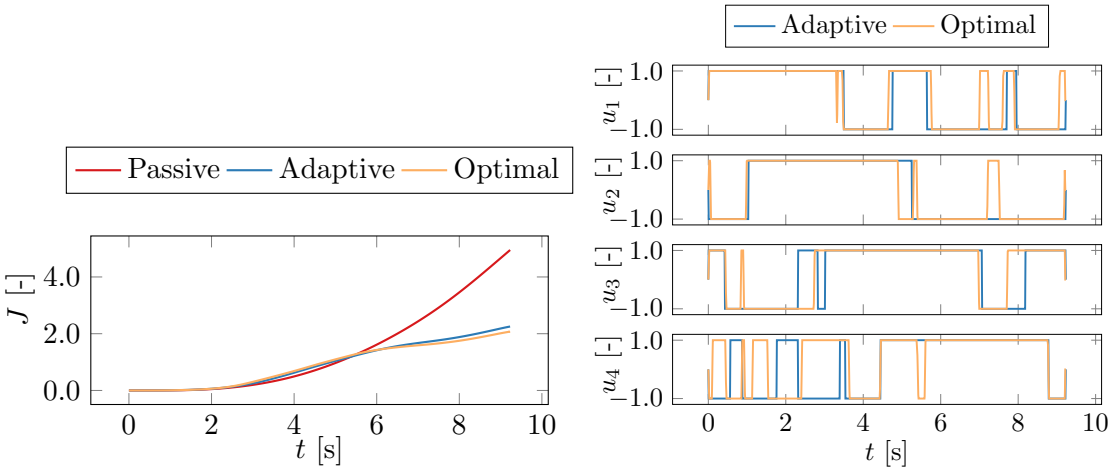

(a) Performance criterion. (b) Control signal.

Figure 5.43: Performance and control during the second simulation.

this case, the beam does not return to the initial state and its deflection grow over time. However, Figure 5.44(b) shows that the adaptive and optimal control results in smaller amplitude of deflection than the constant control. It is reflected also in Figure 5.45(a), where the performance criterion is depicted. Adaptive control provides near-optimal performance and smaller overall value of the criterion than passive control. The shape of the optimal control is constant and maximal on the majority of the simulation interval. The adaptive control is close to optimal on the second, third and fourth damper.

The optimal control of the first damper is minimal in the first part of the simulation. It causes the initial deflection of the optimally controlled beam to be directed upwards, which results in smaller downward deflection on the further stages of the simulation. This behaviour is not fully reproduced by the adaptive controller but the overall difference of the performance is not significant.

The results of the last simulation scenario are depicted in Figures 5.46 and 5.47. Deflections of the beam at $t = 6\,\mathrm{s}$ are presented in Figure 5.46(a). Observe that the upward deflection associated with the optimal case is greater than in the constant and adaptive case. Interesting results can be observed in Figure 5.46(b), where the deflection of the

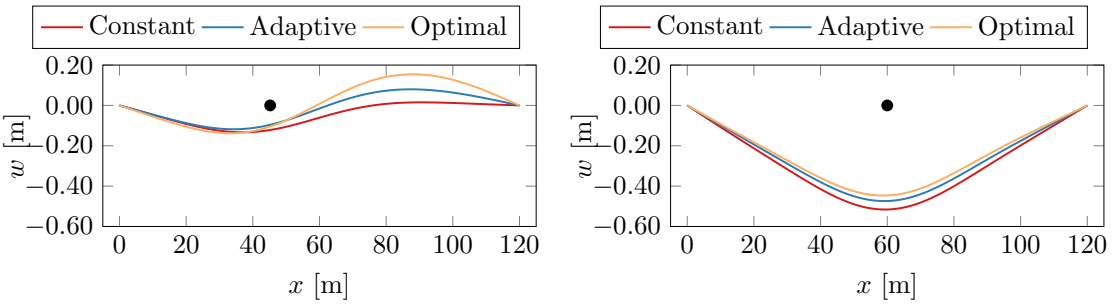

(a) $t = 6.67\,\mathrm{s}$ (b) $t = 25\,\mathrm{s}$

Figure 5.44: Deflection of the beam during the third scenario. The black dot represents the position of the load.

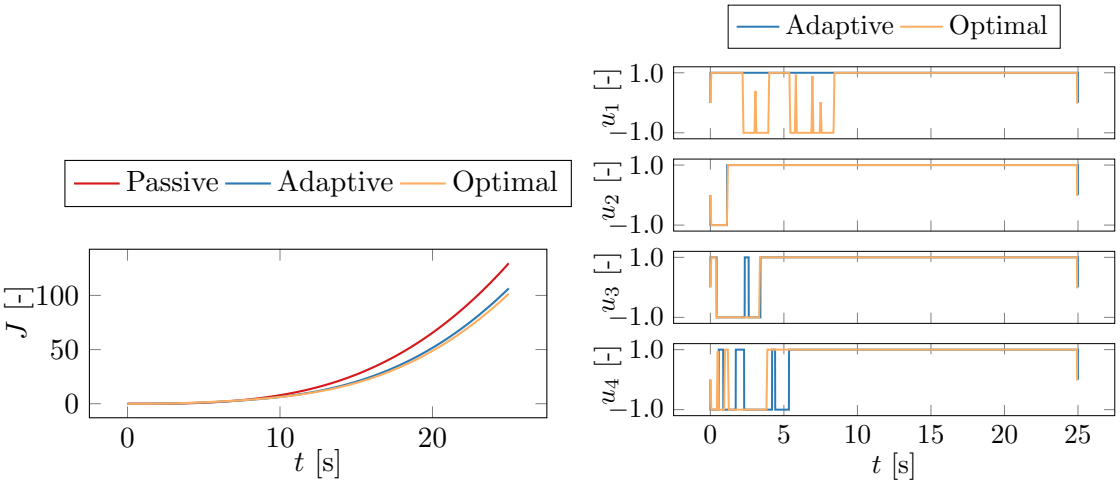

(a) Performance criterion. (b) Control signal.

Figure 5.45: Performance and control during the third simulation.

beam five seconds after the finish of the movement is depicted. The optimal control, in this case, is to generate the smallest damping force, which results in the fast return of the beam to its equilibrium state. The maximal constant control fails in this case to effectively stabilize the beam because large damping forces prevent the movement of the beam.

The evolution of the performance criterion is depicted in Figure 5.47(a). Observe that after the finish of the movement, both adaptive and optimal control quickly steers the system to its origin. At $t = 22\,\mathrm{s}$ the performance criterion stabilizes. On the other hand, the constant control fails to stabilize the beam and the associated criterion grows during the whole simulation interval.

The control signals are presented in Figure 5.47(b). As in the cases of previous simulations, the adaptive control is close to the optimal. It can be noticed, that the optimal control displays the chattering behaviour at the time interval $t \in (21, 26)\,\mathrm{s}$. This interval corresponds to the beam being close to its equilibrium state. The adaptive controller does not display such behaviour.

Final values of the performance criteria for all simulation scenarios are summarized in

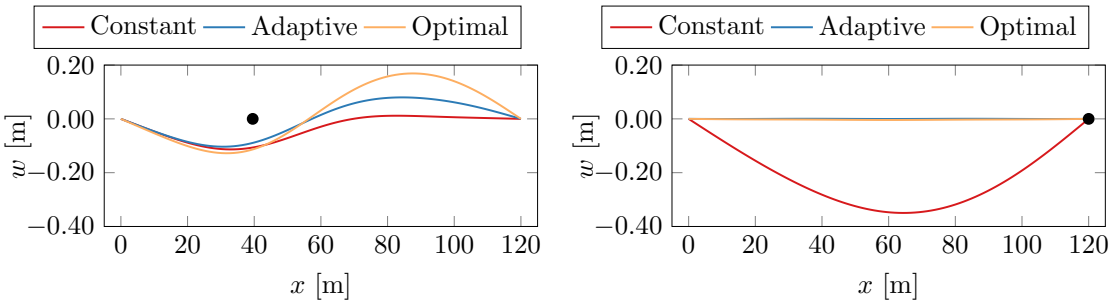

(a) $t = 6\,\mathrm{s}$ (b) $t = 30\,\mathrm{s}$

Figure 5.46: Deflection of the beam during the fourth scenario. The black dot represents the position of the load.

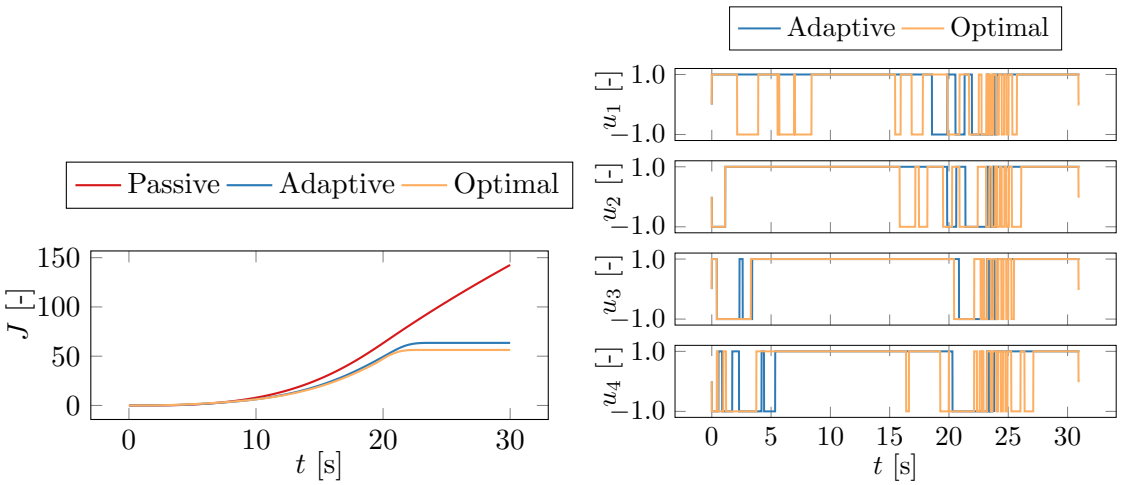

(a) Performance criterion. (b) Control signal.

Figure 5.47: Performance and control during the fourth simulation.

Table 5.14. The values of the criteria have been normalized to the values generated via the optimal control. It can be noticed that for each scenario, the adaptive control method results in the smaller value of the performance criterion than the constant control. The value of the criterion associated with the adaptive controller ranges from 1.071 to 1.185, while the criterion associated with the constant control ranges from 1.434 to 3.008. The average value of the performance of the adaptive controller is equal to 1.114 and mean performance of the constant control is equal to 2.226. The closeness of the performance of the adaptive controller to 1.000 proves the near-optimal property of the adaptive method.

Table 5.14: Normalized performances $J(T_f)$ of the controllers.

Scenario	Passive	Adaptive	Optimal
1	1.985	1.073	1.000
2	2.476	1.071	1.000
3	1.434	1.127	1.000
4	3.008	1.185	1.000
Avg.	2.226	1.114	1.000

5.4 Active stabilization of partially damaged structure

In this Section, the adaptive control method that has been presented in Section 4.1 is tested numerically. The results of this section have been originally presented in the Author's paper [46]. The method is employed to the problem of vibration attenuation of the mechanical system subjected to a sudden loss of its stiffness. Although the considered system is simple, it may represent many real-life control problems. The proposed control method is compared to the LQR controller.

The scheme of the considered object is presented in Figure 5.48. The controlled system

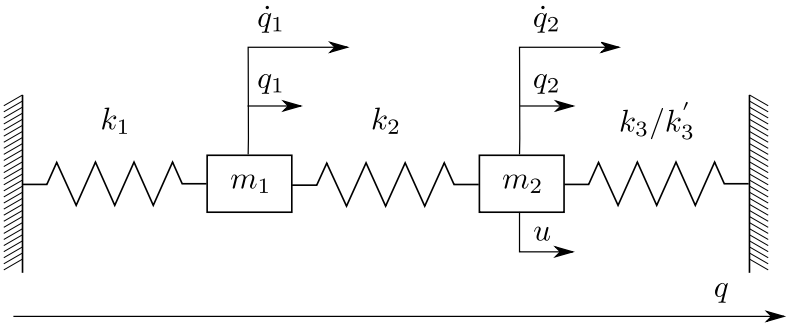

Figure 5.48: The scheme of the controlled system.

is composed of the two masses m_1 and m_2, linked to the rigid bases by the springs k_1 and k_3 and joined by the spring k_2. In the time instance T_s, the sudden degradation of the stiffness k_3 to k_3' occurs.

The object is controlled by the input force $u \in \mathbb{R}$ applied to the mass m_2. The state of the system consists of deflections q_1, q_2 and velocities $\dot{q}_1$, $\dot{q}_2$ of the masses m_1 and m_2, respectively. The dynamical equation that governs this mechanical system is formulated in the standard second-order form:

$$\begin{bmatrix} \ddot{q}_1(t) \\ \ddot{q}_2(t) \end{bmatrix} \mathbf{M} + \mathbf{K}(t) \begin{bmatrix} q_1(t) \\ q_2(t) \end{bmatrix} = \begin{bmatrix} 0 \\ 1 \end{bmatrix} u(t). \tag{5.95}$$

The matrices $\mathbf{K}(t)$ and $\mathbf{M}$ are defined as

$$\mathbf{K}(t) = \begin{bmatrix} k_1 + k_2 & -k_2 \\ -k_2 & k_2 + k_3 \mathbb{H}(T_s - t) + k_3' \mathbb{H}(t - T_s) \end{bmatrix}, \quad \mathbf{M} = \begin{bmatrix} m_1 & 0 \\ 0 & m_2 \end{bmatrix}, \tag{5.96}$$

where $\mathbb{H}(t)$ denotes the Heaviside step function:

$$\mathbb{H}(t) = \begin{cases} 0, & t < 0 \\ 1, & t \geq 0. \end{cases} \tag{5.97}$$

Observe that the spring k_3 is affected by the sudden change: during the time interval $[0, T_s)$ it has stiffness k_3 and for time after T_s this stiffness equals to k_3'.

The second-order system (5.95) is then transformed into the state-space form:

$$\dot{\mathbf{x}}(t) = \begin{bmatrix} \dot{q}_1(t) \\ \dot{q}_2(t) \\ \ddot{q}_1(t) \\ \ddot{q}_2(t) \end{bmatrix} = \mathbf{A}(t)\mathbf{x}(t) + \mathbf{B}u(t), \tag{5.98}$$

with

$$\mathbf{A}(t) = \begin{bmatrix} \mathbf{0} & \mathbb{I} \\ -\mathbf{M}^{-1}\mathbf{K}(t) & \mathbf{0} \end{bmatrix}, \quad \mathbf{B} = \begin{bmatrix} 0 \\ 0 \\ 0 \\ \frac{1}{m_2} \end{bmatrix}. \tag{5.99}$$

The goal of the control is to stabilize the mechanical system via minimization of the infinite horizon quadratic performance index

$$J = \int_0^\infty \left[\mathbf{x}^T(t)\mathbf{Q}\mathbf{x}(t) + u^2(t)R\right] \, \mathrm{d}t, \tag{5.100}$$

where $\mathbf{Q} \succ 0$ and $R > 0$. The simulation is conducted on time interval $[0, T_{\text{end}}]$.

The values of the parameters of the system (5.95) are presented in Table 5.15. The

Table 5.15: The parameters of the model and the simulation.

Parameter	Value
m_1	1 kg
m_2	1 kg
k_1	1 N/m
k_2	1 N/m
k_3	30 N/m
$k_3^{'}$	0.3 N/m
T_s	30 s
T_{end}	60 s

assumed initial condition corresponds to the deflection of the mass m_1 by $5 \cdot 10^{-2}$ m,

$$\mathbf{x}(0) = \begin{bmatrix} 5 \cdot 10^{-2} \\ 0 \\ 0 \\ 0 \end{bmatrix}. \tag{5.101}$$

The parameters of the performance criterion (5.100) are as follows:

$$\mathbf{Q} = \mathbb{I}, \quad R = 1. \tag{5.102}$$

At the time of the change of the stiffness k_3, $t = T_s$, the state of the system $\mathbf{x}$ is set back to the initial conditions (5.101). It allows for direct comparison of the performance of both the adaptive and LQR controllers before and after the damage of the stiffness.

Controllers setup

The adaptive control method employed in the considered simulation is described in Section 4.1. Required parameters of the method, stated in Algorithm 4.1, are defined as follows.

The number of the required measurements N is equal to 10. The adaptation period h is equal to 1.65 s. The measurement times d_j, $j = 1, 2, \ldots, N$ are picked equidistant, i.e. $d_j = 0.165j$ s. The time-shift Δt is equal to 0.165 s. Since the shifted measurement at time $d_j \Delta t$ is equal to d_{j+1}, only $N + 1 = 11$ measurements are being made during one adaptation interval.

Notice that, to maintain robustness of the control method against the system and measurement noise, the number of the measurements N can be extended. In such a case, the matrix $(\mathbf{\Gamma}(t_i) - \mathbf{\Gamma}(t_i + \Delta t))$ of Eq. (4.39) is rectangular and the unknown vector $\boldsymbol{\theta}_i$ is computed as a least-square solution of the linear equation,

$$\boldsymbol{\theta}_i = (\mathbf{\Gamma}(t_i) - \mathbf{\Gamma}(t_i + \Delta t))^+ \begin{bmatrix} q_{i,1}(t_i, \Delta t) \\ q_{i,2}(t_i, \Delta t) \\ \vdots \\ q_{i,N}(t_i, \Delta t) \end{bmatrix}, \tag{5.103}$$

where $(\cdot)^+$ denotes the pseudoinverse of a matrix.

The threshold values for the detection of the change and convergence of the iteration are equal to $\epsilon_{\text{start}} = 1$ $\epsilon_{\text{stop}} = 10^{-10}$, respectively. The initial stabilizing control law $\mu_0(\mathbf{x}) = \mathbf{K}_0\mathbf{x}$ has been chosen as

$$\mu_0(\mathbf{x}) = \begin{bmatrix} 0 & 0 & 0 & -4 \end{bmatrix} \mathbf{x}. \tag{5.104}$$

Observe that the control law $\mu_0(\mathbf{x})$ acts like a damping force for the mass m_2. For any k_1, k_2, $k_3 > 0$, this control law makes the system (5.95) asymptotically stable. This statement can be verified via Theorem 3.1.

The infinite horizon LQR controller is computed using the same performance matrices $\mathbf{Q}$, R as the adaptive method. The feedback matrix $\mathbf{K}_{\text{LQR}}$ of the LQ regulator is computed with explicit knowledge of the state-transition matrix $\mathbf{A}(0)$ with the initial value of the stiffness k_3 and the matrix $\mathbf{B}$, both defined in Eq. (5.99). The feedback matrix $\mathbf{K}_{\text{LQR}}$ is computed according to Eq. (4.14) and the algebraic Riccati equation (4.15). Notice that the initial control law of the LQR controller is optimal during the initial phase of the control, $t \in [0, T_s)$. Because the initial control law of the adaptive scheme is not optimal, it is expected to initially exhibit worse performance than the LQR.

Numerical results

The results of the simulation are presented in Figures 5.49–5.52. In Figures 5.49 and 5.50 the trajectories of the deflections and velocities of the system are presented.

In Figure 5.51 the values of the controls produced by both control method are provided. Figure 5.52 shows how the objective functional defined in Eq. (5.100) changes over time, i.e.

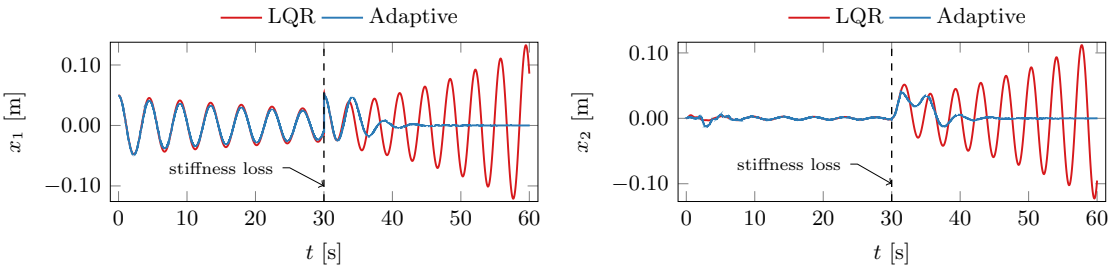

(a) The position of the first mass x_1.

(b) The position of the second mass x_2.

Figure 5.49: The comparison of the numerical results of the simulation of the adaptive controller and the LQR regulator.

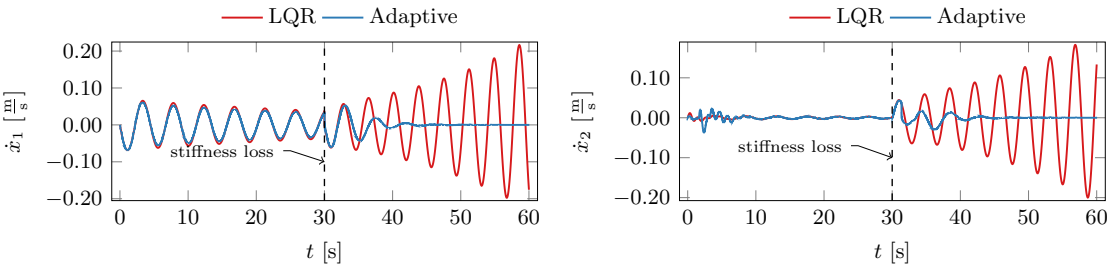

(a) The velocity of the first mass $\dot{x}_1$.

(b) The velocity of the second mass $\dot{x}_2$.

Figure 5.50: The comparison of the numerical results of the simulation of the adaptive controller and the LQR regulator.

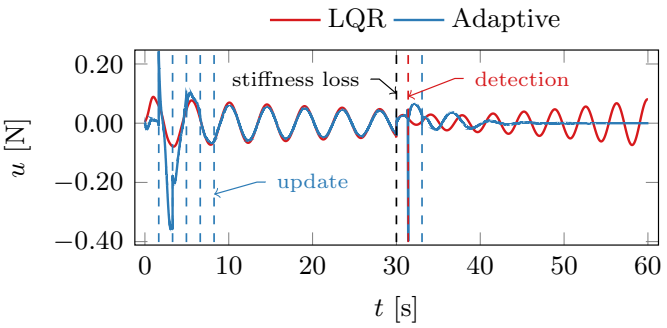

Figure 5.51: The control values generated by the adaptive controller and the LQR regulator. Dashed lines represents the change of the stiffness of the system, updates of the adaptive control law and detection of the change of the parameters.

$J(t) = \int_0^t \left(\mathbf{x}^T(\tau)\mathbf{Q}\mathbf{x}(\tau) + u^2(\tau)R\right) \mathrm{d}\tau$. One can see in the first part of simulation (when the stiffness between mass m_2 and the rigid base is equal to $k_3 = 30\,\mathrm{N/m}$) that the best performance is provided by the LQ regulator. This result is caused by the feedback matrix $\mathbf{K}_{\mathrm{LQR}}$ being calculated before simulation, with exact knowledge of the system dynamics. The adaptive method starts with no knowledge of the system and begin with the safe but not optimal "damping-like" control denoted by the feedback matrix $\mathbf{K}_0$. From $t = 1.65\,\mathrm{s}$ to $t \approx 8.5\,\mathrm{s}$ one can distinguish the transition phase of the adaptive controller, where the control law is updated at every adaptation interval. It is important to point out that after

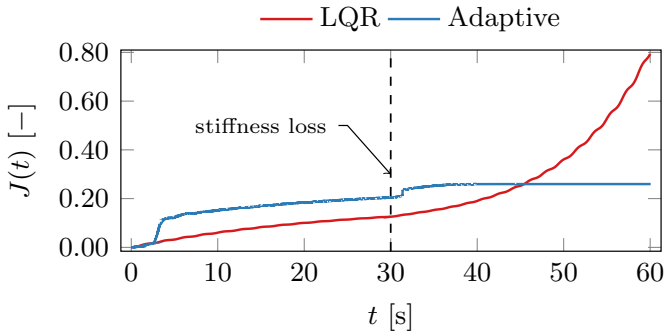

Figure 5.52: The objective functions achieved by the adaptive control and the LQR regulator. Dashed line represents the change of the stiffness of the system.

this transition phase, the adaptive controller achieve the same effectiveness as the LQR algorithm. The main advantage of this adaptive control method is then the ability to converge to the optimal performance algorithm, without the full knowledge of the system's dynamics.

After $T_s = 30\,\mathrm{s}$, when dynamical properties of the system suddenly change and the simulation starts over from the initial state, the LQR control destabilizes the mechanical system. All system variables diverge exponentially and energy is added to the system In addition, the envelope of the control increases.

Response of the adaptive controller is dramatically different. As presented in Figure 5.51, the change of the system's properties is detected almost immediately. The control law is set to initial, stabilizing form. The system is taken to the equilibrium state in about 15 seconds. These observations are validated by the measure of the performance presented in Figure 5.52. During the transition time, the objective functional for the adaptive control quickly increases, but when the control policy converges, the difference between both controllers became steady. When the stiffness is reduced, the adaptive control quickly converges and steers the system to its equilibrium state. In contrast, the objective of the LQR simulation starts to grow exponentially. Considering only the second part of the simulation, the final objective functionals achieved by both algorithms are equal to 0.6679 for the LQR algorithm and 0.0555 for the adaptive method, the improvement of the performance is equal to 91.690%.

Chapter 6

Conclusions

In Chapter 2, the general control problem of stabilization of the system affected by unpredictable uncertainties has been stated. The necessary and sufficient conditions of optimality of the control have been formulated via calculus of variations, Maximum Principle, and Principle of Optimality. It has been shown that computation of the optimal control requires full knowledge about the future value of the disturbance that affects the system. This condition cannot be satisfied in the real-life application scenario. As a solution, the general framework of the adaptive control has been proposed that makes simplifying assumptions that allow for computation of the optimal or near-optimal control and updates frequently enough to provide a satisfying approximation of the actual, time-varying control problem. This framework is based on the Model Predictive Control scheme. The adaptive control methods for particular variants of the general problem have been formulated in Chapters 3 and 4.

In Chapter 3, the focus is on the stabilization of systems affected by an external disturbance. The proposed control method is based on the subsequent identification of the dynamical model of the disturbance. This approximate model transforms the original, time-variant dynamical system into the autonomous one. Independence of time significantly reduces the complexity of the solution to the optimal control problem.

In the case of the active control, the resulting optimal control has analytical form and is known as the Linear Quadratic Regulator. The first control method proposed in Chapter 3 relies on the finite horizon LQR. The second approach reduces the computational burden by the employment of the infinite horizon LQR. In this case, the alpha-shift modification of the performance criterion has been introduced to guarantee, that the modified optimal control problem is well-posed.

The third control method is designed to stabilize mechanical systems via semi-active devices. In this case, the near-optimal control method is proposed that is based on the Lyapunov control theory. It has been proven that the method stabilizes the control system and provides better performance than the constant control.

Chapter 4 focuses on the stabilization of the actively-controlled system subjected to a sudden change of its internal parameters. A novel adaptive control method has been designed for this control problem. The approach relies on the online identification of the

special Lyapunov function and computation of the series of control laws. This series has been proven to be stabilizing and converging to the optimal control law.

Chapter 5 presents the results of the numerical verification of the designed control methods. The method described in Section 3.2 is tested against LQG control in the problem of stabilization of the drilling machine. The proposed controller has outperformed the classical LQG regulator in every considered type of excitation. In addition, the dependence of the performance of the controller on its parameters has been also analysed numerically.

The control method formulated in Section 3.3 is employed in the stabilization of the building subjected to the earthquake. Its performance is compared to the LQG and H_∞ controls. Four different excitation signals have been used, two of them are the historical earthquake signals and the next two are the polyharmonic signals with frequencies corresponding to the natural frequencies of the building. In each scenario, the proposed adaptive scheme provided better control results than the comparative controllers.

The problem of stabilisation of the beam under a moving load has been chosen as a verification scenario for the method designed in Section 3.4. The results have been compared to the passive control and the optimal control computed via the direct multiple shooting method. The beam has been subjected to the load moving with varying velocity. For each considered trajectory of the load, the proposed adaptive strategy outperformed the passive case. In addition, the comparison to the optimal control has proved that the adaptive method provides near-optimal performance.

The adaptive controller defined in Chapter 4 has been tested numerically via simulation of the conjugate oscillators subjected to the sudden change of the internal stiffness. The method has been compared to the classical LQR controller. It has been verified, that the proposed control method quickly converges to the optimal control law after the change of the system's dynamics. The LQR controller in the same simulation destabilized the system.

The adaptive control methods designed in Thesis have been proved to be of low computational complexity and are characterized by such beneficial properties as stability and near-optimality. The numerical simulations have proven that the methods outperform the classical, non-adaptive schemes.

Future works

The results of the present work are planned to be extended in future works. These include:

- design of the semi-active adaptive controller for the systems affected by the change of parameters,
- theoretical and numerical analysis of the performance of the switching control law defined in Section 3.4 in comparison to other switching control laws, such as clipped-LQR or Prestress-Accumulation-Release strategy,
- adaptation of the control methods to the distributed control approach while maintaining the stability and near-optimality of the controllers.

Appendix A

Identification of simplified model of structure

In this appendix, the numerical identification procedure of the SM model (5.33) based on the response of the RM model is presented. Stiffness parameters k_i are determined by a static testing of the reference model. Constant forces were applied to subsequent levels and the static deflections of all floors were then measured. Let the force applied to each floor be equal to f_{static} and let the vector $\mathbf{X}_i^{meas.} \in \mathbb{R}^{20}$ represent the measured static deflections of the on-ground levels under the force f_{static} applied to i-th floor. The dependence between the deformation of the simplified model and this set of static forces can be written as:

$$\begin{bmatrix} \mathbf{X}_1^{model} & \mathbf{X}_2^{model} & \cdots & \mathbf{X}_{20}^{model} \end{bmatrix} = \left(\mathbf{K}\left(\boldsymbol{\xi}\right)\right)^{-1} f_{static}. \tag{A.1}$$

Obviously, the goal of the identification scheme is to find the parameters $\boldsymbol{\xi}$ such that the static response of the simplified model $\begin{bmatrix} \mathbf{X}_1^{model} & \cdots & \mathbf{X}_{20}^{model} \end{bmatrix}$ fits the static response of the reference model $\begin{bmatrix} \mathbf{X}_1^{meas.} & \cdots & \mathbf{X}_{20}^{meas.} \end{bmatrix}$. The stiffness parameters that we seek are the solution of the optimization problem:

$$\boldsymbol{\xi} = \arg\min_{\boldsymbol{\xi}} \left\| \begin{bmatrix} \mathbf{X}_1^{meas.} & \cdots & \mathbf{X}_{20}^{meas.} \end{bmatrix} - \left(\mathbf{K}(\boldsymbol{\xi})\right)^{-1} f_{static} \right\|_2^2. \tag{A.2}$$

For the rest of the appendix we assume $\mathbf{K} = \mathbf{K}(\boldsymbol{\xi})$ with $\boldsymbol{\xi}$ obtained in optimization problem (A.2).

The remaining mass and damping parameters were determined by the harmonic characteristics of the RM model. Analogously to the stiffness determining, the RM model was excited by a sinusoidal force with constant amplitude that was applied subsequently to every on-ground floor of the structure. In addition to these 20 excitations, the harmonic excitation by the acceleration of the base was also carried out. The system was tested for uniformly distributed frequencies in the range $(0; 1.02]$ Hz. This frequency spectrum was chosen to cover the first three modes of the RM model. The amplitudes $\mathrm{Amp}_{ik}(\omega)$ of the steady-state oscillations of the i-th floor deflection excited by k-th excitation source were then measured.

The analogous amplitude characteristic for the simplified model was obtained by the Laplace transform. Let us rewrite (5.33) in the state-space form:

$$\begin{bmatrix}\dot{\mathbf{q}}\\ \ddot{\mathbf{q}}\end{bmatrix}(t)=\begin{bmatrix}\mathbf{0} & \mathbb{I}\\ -\mathbf{M}^{-1}(\boldsymbol{\kappa})\,\mathbf{K} & -\mathbf{M}^{-1}(\boldsymbol{\kappa})\,\mathbf{C}(\boldsymbol{\lambda})\end{bmatrix}\begin{bmatrix}\mathbf{q}\\ \dot{\mathbf{q}}\end{bmatrix}+\begin{bmatrix}\mathbf{0} & \mathbf{0}\\ \mathbf{M}^{-1}(\boldsymbol{\kappa}) & \mathbf{1}\end{bmatrix}\begin{bmatrix}\mathbf{F}(\mathbf{u})\\ \ddot{x}_e\end{bmatrix}, \tag{A.3}$$

where $\mathbf{q}$ and $\dot{\mathbf{q}}$ are vectors of the floor's displacements and the floor's velocities, respectively. The frequency spectrum of the linear dynamical system (A.3) is closely related to the transfer function

$$\mathbf{G}(s,\boldsymbol{\kappa},\boldsymbol{\lambda})=\\ \begin{bmatrix}\mathbb{I} & \mathbf{0}\end{bmatrix}\left(s\mathbb{I}_{40}-\begin{bmatrix}\mathbf{0} & \mathbb{I}_{20}\\ -\mathbf{M}^{-1}(\boldsymbol{\kappa})\,\mathbf{K} & -\mathbf{M}^{-1}(\boldsymbol{\kappa})\,\mathbf{C}(\boldsymbol{\lambda})\end{bmatrix}\right)^{-1}\begin{bmatrix}\mathbf{0} & \mathbf{0}\\ \mathbf{M}^{-1}(\boldsymbol{\kappa}) & \mathbf{1}\end{bmatrix}. \tag{A.4}$$

This transfer function calculated for $s=j\omega$, $\mathbf{G}(j\omega,\boldsymbol{\kappa},\boldsymbol{\lambda})=(g_{ik}(j\omega,\boldsymbol{\kappa},\boldsymbol{\lambda}))\in\mathbb{C}^{20\times 21}$ can be interpreted as a complex steady-state response of the i-th floor displacement excited by sinusoidal excitation of the k-th input (20 forces and base acceleration) with an angular frequency ω. The steady-state amplitude is provided by $|g_{ik}(j\omega)|$.

The optimization procedure is used to determine the parameters that fit measured amplitude of a harmonic response:

$$(\boldsymbol{\kappa},\boldsymbol{\lambda})=\arg\min_{(\boldsymbol{\kappa},\boldsymbol{\lambda})}\sum_{i=1}^{20}\sum_{k=1}^{21}\sum_{w}\left[|g_{ik}(j\omega,\boldsymbol{\kappa},\boldsymbol{\lambda})|-\mathrm{Amp}_{ik}(\omega)\right]^2. \tag{A.5}$$

The established parameters are presented in Table A.1. It can be emphasized that the

Table A.1: The values of the simplified model parameters.

Index	mass $\left[10^5\cdot\mathrm{kg}\right]$	stiffness $\left[10^7\cdot\frac{\mathrm{N}}{\mathrm{m}}\right]$	damp. coeff. $\left[\frac{\mathrm{Ns}}{\mathrm{m}}\right]$
1	3.3642	5.8212	$9.4115\cdot10^6$
2	3.3988	10.865	$2.9099\cdot10^2$
3	3.3894	9.0599	$8.5249\cdot10^6$
4	3.4034	8.527	$9.5108\cdot10^6$
5	2.305	8.1943	$1.1999\cdot10^7$
6	2.3035	10.470	$1.4528\cdot10^7$
7	3.1852	7.7363	$9.8897\cdot10^6$
8	2.3181	7.3938	$1.2645\cdot10^7$
9	2.2823	9.9801	$2.064\cdot10^7$
10	2.2767	6.4702	$4.9535\cdot10^6$
11	2.2893	7.9895	$2.8286\cdot10^2$
12	3.3379	6.2556	$1.4224\cdot10^7$
13	3.3844	7.2358	$1.0301\cdot10^7$
14	3.367	6.5338	$1.1744\cdot10^7$
15	2.7544	5.5089	$1.1078\cdot10^7$
16	2.2899	6.0224	$9.6148\cdot10^6$
17	2.2762	6.8858	$6.8505\cdot10^6$
18	2.3288	5.0551	$1.7492\cdot10^2$
19	3.4071	4.5663	$7.3097\cdot10^6$
20	3.4095	3.399	$1.008\cdot10^7$

sum of estimated masses equals $5.7071 \cdot 10^6$ kg, which differs from the actual mass of the structure (neglecting the mass of the basement and first levels) equal to $5.543 \cdot 10^6$ kg by only 3%.

To verify the accuracy of the identification procedure, the time responses of the simplified and reference models subjected to the same acceleration excitation were compared. The signal that we used is the recorded earthquake in El Centro, 1940 (Figure A.1). Figure

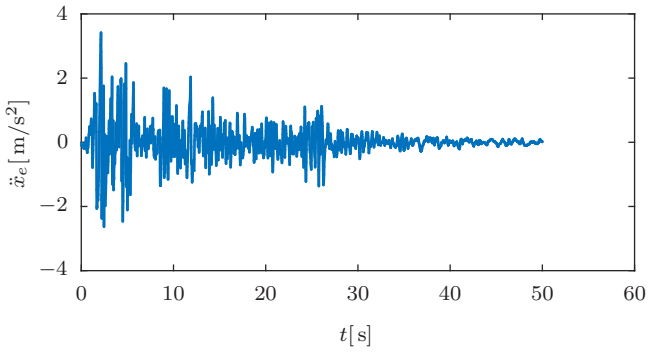

Figure A.1: Ground acceleration measured at El Centro 1940 earthquake.

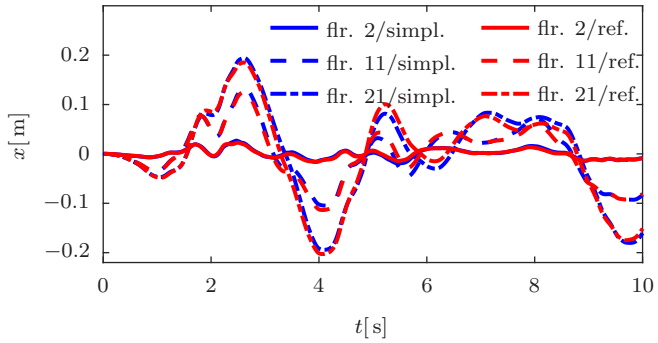

Figure A.2: Comparison of 2., 11., 21. floors deflection of the reference and simplified models excited by the El Centro earthquake signal.

A.2 shows the course of deformation of the 1st, 2nd and 20th (roof) floors of SM model and the corresponding 2nd, 11th and 21st floors of RM model. As can be seen, the simplified model accurately reproduces the time characteristics of the reference model.

Bibliography

[1] Othmar H. Amman, Theodore von Karman, and Glenn B. Woodruff. *The failure of the Tacoma Narrows bridge*. Tech. rep. Washington, D. C.: Federal Works Agency, 1941. URL: https://authors.library.caltech.edu/45680/.

[2] Steven H. Strogatz et al. "Crowd synchrony on the Millennium Bridge". In: *Nature* 438.7064 (Nov. 2005), pp. 43–44. ISSN: 0028-0836. DOI: 10.1038/43843a. URL: https://doi.org/10.1038/43843a.

[3] James T. P. Yao. "Concept of Structural Control". In: *Journal of the Structural Division* 98.7 (1972), pp. 1567–1574. URL: https://trid.trb.org/view/109407.

[4] Takuji Kobori et al. "Seismic-response-controlled structure with active mass driver system. Part 1: Design". In: *Earthquake Engineering & Structural Dynamics* 20.2 (1991), pp. 133–149. ISSN: 00988847. DOI: 10.1002/eqe.4290200204. URL: https://doi.org/10.1002/eqe.4290200204.

[5] Rudolf Emil Kalman. "Contributions to the Theory of Optimal Control". In: *Bolentin de la Sociedad Matematica Mexicana* 5 (1960), pp. 102–119. ISSN: 00160032.

[6] A. Laub. "A Schur method for solving algebraic Riccati equations". In: *IEEE Transactions on Automatic Control* 24.6 (Dec. 1979), pp. 913–921. ISSN: 0018-9286. DOI: 10.1109/TAC.1979.1102178. URL: https://doi.org/10.1109/TAC.1979.1102178.

[7] M. Seto, Y. Toba, and Y. Matsumoto. "Reduced order modeling and vibration control methods for flexible structures arranged in parallel". In: *Proceedings of 1995 American Control Conference - ACC'95*. Vol. 3. American Autom Control Council, 1995, pp. 2344–2348. ISBN: 0-7803-2445-5. DOI: 10.1109/ACC.1995.531391. URL: https://doi.org/10.1109/ACC.1995.531391.

[8] U. Aldemir, M. Bakioglu, and S. S. Akhiev. "Optimal control of linear buildings under seismic excitations". In: *Earthquake Engineering & Structural Dynamics* 30.6 (June 2001), pp. 835–851. ISSN: 0098-8847. DOI: 10.1002/eqe.41. URL: https://doi.org/10.1002/eqe.41.

[9] Kazuhiko Yamada and Takuji Kobori. "Linear quadratic regulator for structure under on-line predicted future seismic excitation". In: *Earthquake Engineering and Structural Dynamics* 25.6 (June 1996), pp. 631–644. ISSN: 00988847. DOI: 10.1002/(SICI)1096-9845(199606)25:6<631::AID-EQE574>3.0.CO;2-K. URL: https://doi.

org/10.1002/(SICI)1096-9845(199606)25:6%3C631::AID-EQE574%3E3.0.CO;2-K.

[10] Jong-Cheng Wu and Jann N. Yang. "LQG control of lateral-torsional motion of Nanjing TV transmission tower". In: *Earthquake Engineering & Structural Dynamics* 29.8 (Aug. 2000), pp. 1111–1130. ISSN: 0098-8847. DOI: 10.1002/1096-9845(20000 8)29:8<1111::AID-EQE957>3.0.CO;2-R. URL: https://doi.org/10.1002/1096-9845(200008)29:8%3C1111::AID-EQE957%3E3.0.CO;2-R.

[11] Sheng-Guo Wang. "LQG-α control and its simulations for structural benchmark problems against winds and earthquakes". In: *42nd IEEE International Conference on Decision and Control*. Vol. 6. IEEE, 2003, pp. 6572–6577. ISBN: 0-7803-7924-1. DOI: 10.1109/CDC.2003.1272428. URL: https://doi.org/10.1109/CDC.2003.1272428.

[12] B.D.O. Anderson and J.B. Moore. "Linear system optimisation with prescribed degree of stability". In: *Proceedings of the Institution of Electrical Engineers* 116.12 (1969), p. 2083. ISSN: 00203270. DOI: 10.1049/piee.1969.0383. URL: https://doi.org/10.1049/piee.1969.0383.

[13] Gang Mei, Ahsan Kareem, and Jeffrey C. Kantor. "Model Predictive Control of Structures under Earthquakes using Acceleration Feedback". In: *Journal of Engineering Mechanics* 128.5 (May 2002), pp. 574–585. ISSN: 0733-9399. DOI: 10.1061/(ASCE)07 33-9399(2002)128:5(574). arXiv: Ok. URL: https://doi.org/10.1061/(ASCE)0733-9399(2002)128:5(574).

[14] Gang Mei, Ahsan Kareem, and Jeffrey C. Kantor. "Model Predictive Control of Wind-Excited Building: Benchmark Study". In: *Journal of Engineering Mechanics* 130.4 (Apr. 2004), pp. 459–465. ISSN: 0733-9399. DOI: 10.1061/(ASCE)0733-9399(2004)130 :4(459). URL: {https://doi.org/10.1061/(ASCE)0733-9399(2004)130:4(459)}.

[15] Johanes Suhardjo. "Frequency domain techniques for control of civil engineering structures with some robustness considerations". PhD Dissertation. University of Notre Dame, 1990.

[16] J. Geoffrey Chase and H. Allison Smith. "Robust H_∞ Control Considering Actuator Saturation. I: Theory". In: *Journal of Engineering Mechanics* 122.10 (Oct. 1996), pp. 976–983. ISSN: 0733-9399. DOI: 10.1061/(ASCE)0733-9399(1996)122:10(976). URL: https://doi.org/10.1061/(ASCE)0733-9399(1996)122:10(976).

[17] Yang Chen, Wenlong Zhang, and Huijun Gao. "Finite frequency control for building under earthquake excitation". In: *Mechatronics* 20.1 (Feb. 2010), pp. 128–142. ISSN: 09574158. DOI: 10.1016/j.mechatronics.2009.11.001. URL: http://dx.doi.org/10.1016/j.mechatronics.2009.11.001.

[18] Weichao Sun, Huijun Gao, and Bin Yao. "Adaptive Robust Vibration Control of Full-Car Active Suspensions With Electrohydraulic Actuators". In: *IEEE Transactions on Control Systems Technology* 21.6 (Nov. 2013), pp. 2417–2422. ISSN: 1063-6536. DOI: 10 .1109/TCST.2012.2237174. URL: https://doi.org/10.1109/TCST.2012.2237174.

[19] Oguz Yakut and Hasan Alli. "Neural based sliding-mode control with moving sliding surface for the seismic isolation of structures". In: *Journal of Vibration and Control* 17.14 (Dec. 2011), pp. 2103–2116. ISSN: 1077-5463. DOI: 10.1177/1077546310395964. URL: https://doi.org/10.1177/1077546310395964.

[20] Teresa Orlowska-Kowalska, Marcin Kaminski, and Krzysztof Szabat. "Implementation of a Sliding-Mode Controller With an Integral Function and Fuzzy Gain Value for the Electrical Drive With an Elastic Joint". In: *IEEE Transactions on Industrial Electronics* 57.4 (Apr. 2010), pp. 1309–1317. ISSN: 0278-0046. DOI: 10.1109/TIE.2009.2030823. URL: https://doi.org/10.1109/TIE.2009.2030823.

[21] Shubo Wang, Xuemei Ren, and Jing Na. "Adaptive dynamic surface control based on fuzzy disturbance observer for drive system with elastic coupling". In: *Journal of the Franklin Institute* 353.8 (May 2016), pp. 1899–1919. ISSN: 00160032. DOI: 10.1016/j.jfranklin.2016.03.006. URL: https://doi.org/10.1016/j.jfranklin.2016.03.006.

[22] D. Karnopp, M. J. Crosby, and R. A. Harwood. "Vibration Control Using Semi-Active Force Generators". In: *Journal of Engineering for Industry* 96.2 (1974), p. 619. ISSN: 00220817. DOI: 10.1115/1.3438373. URL: https://doi.org/10.1115/1.3438373.

[23] George Leitmann. "Semiactive Control for Vibration Attenuation". In: *Journal of Intelligent Material Systems and Structures* 5.6 (Nov. 1994), pp. 841–846. ISSN: 1045-389X. DOI: 10.1177/1045389X9400500616. URL: https://doi.org/10.1177/1045389X9400500616.

[24] N.H. McClamroch and H.P. Gavin. "Closed loop structural control using electrorheological dampers". In: *Proceedings of 1995 American Control Conference - ACC'95*. Vol. 6. American Autom Control Council, 1995, pp. 4173–4177. ISBN: 0-7803-2445-5. DOI: 10.1109/ACC.1995.532717. URL: https://doi.org/10.1109/ACC.1995.532717.

[25] Xiaojie Wang and Faramarz Gordaninejad. "Lyapunov-Based Control of a Bridge Using Magneto-Rheological Fluid Dampers". In: *Journal of Intelligent Material Systems and Structures* 13.7-8 (July 2002), pp. 415–419. ISSN: 1045-389X. DOI: 10.1106/104538902025939. URL: https://doi.org/10.1106/104538902025939.

[26] Dominik Pisarski et al. "Vibration control in smart coupled beams subjected to pulse excitations". In: *Journal of Sound and Vibration* 380 (Oct. 2016), pp. 37–50. ISSN: 0022460X. DOI: 10.1016/j.jsv.2016.05.050. URL: https://doi.org/10.1016/j.jsv.2016.05.050.

[27] Dominik Pisarski. "Decentralized stabilization of semi-active vibrating structures". In: *Mechanical Systems and Signal Processing* 100 (Feb. 2018), pp. 694–705. ISSN: 08883270. DOI: 10.1016/j.ymssp.2017.08.003. URL: https://doi.org/10.1016/j.ymssp.2017.08.003.

[28] S.J. Dyke et al. "Seismic Response Reduction Using Magnetorheological Dampers". In: *IFAC Proceedings Volumes* 29.1 (1996), pp. 5530–5535. ISSN: 14746670. DOI: 10.1016/S1474-6670(17)58562-6. URL: https://doi.org/10.1016/S1474-6670(17)58562-6.

[29] J. S. Lane, A. A. Ferri, and B. S. Heck. "Vibration control using semi-active friction damping". In: *ASME* 49 (1992), pp. 165–171.

[30] Dominik Pisarski and Czesław I. Bajer. "Smart Suspension System for Linear Guideways". In: *Journal of Intelligent & Robotic Systems* 62.3-4 (June 2011), pp. 451–466. ISSN: 0921-0296. DOI: 10.1007/s10846-010-9450-7. URL: https://doi.org/10.1007/s10846-010-9450-7.

[31] Dominik Pisarski. "Optimal control of structures subjected to traveling load". In: *Journal of Vibration and Control* 24.7 (Apr. 2018), pp. 1283–1299. ISSN: 1077-5463. DOI: 10.1177/1077546316657244. URL: https://doi.org/10.1177/1077546316657244.

[32] Michael D. Symans and Steven W. Kelly. "Fuzzy logic control of bridge structures using intelligent semi-active seismic isolation systems". In: *Earthquake Engineering & Structural Dynamics* 28.1 (Jan. 1999), pp. 37–60. ISSN: 0098-8847. DOI: 10.1002/(SICI)1096-9845(199901)28:1<37::AID-EQE803>3.0.CO;2-Z. URL: https://doi.org/10.1002/(SICI)1096-9845(199901)28:1%3C37::AID-EQE803%3E3.0.CO;2-Z.

[33] Kang-Min Choi et al. "Semi-active fuzzy control for seismic response reduction using magnetorheological dampers". In: *Earthquake Engineering & Structural Dynamics* 33.6 (May 2004), pp. 723–736. ISSN: 0098-8847. DOI: 10.1002/eqe.372. URL: https://doi.org/10.1002/eqe.372.

[34] D. L. Guo, H. Y. Hu, and J. Q. Yi. "Neural Network Control for a Semi-Active Vehicle Suspension with a Magnetorheological Damper". In: *Journal of Vibration and Control* 10.3 (Mar. 2004), pp. 461–471. ISSN: 1066-0763. DOI: {10.1177/1077546304038968}. URL: https://doi.org/10.1177/1077546304038968.

[35] Alexander G. Parlos, Moises A. Abraham, and James R. Morgan. "Gain-Scheduled Adaptive Control for Seismically Excited Hybrid Structures". In: *Journal of Structural Engineering* 127.11 (Nov. 2001), pp. 1286–1294. ISSN: 0733-9445. DOI: 10.1061/(ASCE)0733-9445(2001)127:11(1286). URL: https://doi.org/10.1061/(ASCE)0733-9445(2001)127:11(1286).

[36] Amin Hosseini, Touraj Taghikhany, and Arash Yeganeh Fallah. "Direct adaptive algorithm for seismic control of damaged structures with faulty sensors". In: *Journal of Vibration and Control* (Jan. 2017), p. 107754631668795. ISSN: 1077-5463. DOI: 10.1177/1077546316687958. URL: https://doi.org/10.1177/1077546316687958.

[37] Dominik Pisarski and Andrzej Myśliński. "Online adaptive algorithm for optimal control of structures subjected to travelling loads". In: *Optimal Control Applications and Methods* 38.6 (Nov. 2017), pp. 1168–1186. ISSN: 01432087. DOI: 10.1002/oca.2321. URL: https://doi.org/10.1002/oca.2321.

[38] Daguna Vrabie et al. "Adaptive optimal control for continuous-time linear systems based on policy iteration". In: *Automatica* 45.2 (Feb. 2009), pp. 477–484. ISSN: 00051098. DOI: 10.1016/j.automatica.2008.08.017. URL: https://doi.org/10.1016/j.automatica.2008.08.017.

[39] V. Adetola and M. Guay. "Robust Adaptive MPC for Systems with Exogeneous Disturbances". In: *IFAC Proceedings Volumes* 42.11 (2009), pp. 249–254. ISSN: 14746670. DOI: 10.3182/20090712-4-TR-2008.00038. URL: https://doi.org/10.3182/20090712-4-TR-2008.00038.

[40] Bing Zhu and Xiaohua Xia. "Adaptive Model Predictive Control for Unconstrained Discrete-Time Linear Systems With Parametric Uncertainties". In: *IEEE Transactions on Automatic Control* 61.10 (Oct. 2016), pp. 3171–3176. ISSN: 0018-9286. DOI: 10.1109/TAC.2015.2505783. URL: https://doi.org/10.1109/TAC.2015.2505783.

[41] Long Cheng, Zeng-Guang Hou, and Min Tan. "Adaptive neural network tracking control for manipulators with uncertain kinematics, dynamics and actuator model". In: *Automatica* 45.10 (Oct. 2009), pp. 2312–2318. ISSN: 00051098. DOI: 10.1016/j.automatica.2009.06.007. URL: https://doi.org/10.1016/j.automatica.2009.06.007.

[42] Wei He, Yuhao Chen, and Zhao Yin. "Adaptive Neural Network Control of an Uncertain Robot With Full-State Constraints". In: *IEEE Transactions on Cybernetics* 46.3 (Mar. 2016), pp. 620–629. ISSN: 2168-2267. DOI: 10.1109/TCYB.2015.2411285. URL: https://doi.org/10.1109/TCYB.2015.2411285.

[43] Mou Chen and Shuzhi Sam Ge. "Adaptive Neural Output Feedback Control of Uncertain Nonlinear Systems With Unknown Hysteresis Using Disturbance Observer". In: *IEEE Transactions on Industrial Electronics* 62.12 (2015), pp. 7706–7716. ISSN: 02780046. DOI: 10.1109/TIE.2015.2455053. URL: https://doi.org/10.1109/TIE.2015.2455053.

[44] Wei He et al. "Adaptive Neural Network Control for Robotic Manipulators With Unknown Deadzone". In: *IEEE Transactions on Cybernetics* 48.9 (2018), pp. 2670–2682. ISSN: 2168-2267. DOI: 10.1109/TCYB.2017.2748418. URL: https://doi.org/10.1109/TCYB.2017.2748418.

[45] V. Nekoukar and A. Erfanian. "Adaptive fuzzy terminal sliding mode control for a class of MIMO uncertain nonlinear systems". In: *Fuzzy Sets and Systems* 179.1 (Sept. 2011), pp. 34–49. ISSN: 01650114. DOI: 10.1016/j.fss.2011.05.009. URL: https://doi.org/10.1016/j.fss.2011.05.009.

[46] Maciej Wasilewski, Dominik Pisarski, and Czesław I. Bajer. "Adaptive stabilization of partially damaged vibrating structures". In: *Machine Dynamics Research* 40.1 (2016), pp. 65–82.

[47] Maciej Wasilewski et al. "A new efficient adaptive control of torsional vibrations induced by switched nonlinear disturbances". In: *International Journal of Applied Mathematics and Computer Science* 29.2 (2019).

[48] Maciej Wasilewski and Dominik Pisarski. "Adaptive optimal control algorithm for vibrational systems under nonlinear friction". In: *2017 22nd International Conference on Methods and Models in Automation and Robotics (MMAR)*. IEEE, 2017, pp. 107–112. ISBN: 978-1-5386-2402-9.

[49] Maciej Wasilewski et al. "New efficient adaptive control of torsional vibrations induced by sudden nonlinear disturbances". In: *22nd International Conference on Computer Methods in Mechanics*. 2. 2017, pp. 1–2.

[50] Maciej Wasilewski and Dominik Pisarski. "On Suboptimal Switched State-Feedback Control of Semi-Active Vibrating Structures". In: *2019 American Control Conference*. Philadelphia, 2019.

[51] Maciej Wasilewski, Dominik Pisarski, and Czesław I. Bajer. "Adaptive optimal control for seismically excited structures". In: *Automation in Construction* (2019).

[52] Daniel Liberzon. *Calculus of Variations and Optimal Control Theory: A Concise Introduction*. 1st ed. Princeton, New Jersey: Princeton University Press, 2012.

[53] Lev Semyonovich Pontryagin. *Mathematical Theory of Optimal Processes*. New York: Interscience, May 1962. ISBN: 9780203749319. DOI: 10.1201/9780203749319. URL: https://doi.org/10.1201/9780203749319.

[54] Alberto Bressan and Benedetto Piccoli. *Introduction to the Mathematical Theory of Control*. 1st ed. Springfield: American Institute of Mathematical Sciences, 2007. ISBN: 978-1601330024.

[55] C. L. Hwang and L. T. Fan. "A Discrete Version of Pontryagin's Maximum Principle". In: *Operations Research* 15.1 (Feb. 1967), pp. 139–146. ISSN: 0030-364X. DOI: 10.1287/opre.15.1.139. URL: https://doi.org/10.1287/opre.15.1.139.

[56] Richard Bellman. *Dynamic Programming*. Princeton: Princeton University Press, 1957.

[57] Lennart Ljung. "System Identification". In: *Wiley Encyclopedia of Electrical and Electronics Engineering*. Hoboken, NJ, USA: John Wiley & Sons, Inc., Dec. 1999. DOI: 10.1002/047134608X.W1046. URL: https://doi.org/10.1002/047134608X.W1046.

[58] Hirotugu Akaike. "Fitting autoregressive models for prediction". In: *Annals of the Institute of Statistical Mathematics* 21.1 (1969), pp. 243–247. DOI: 10.1007/BF02532251. URL: https://doi.org/10.1007/BF02532251.

[59] Volker Strassen. "Gaussian elimination is not optimal". In: *Numerische Mathematik* 13.4 (Aug. 1969), pp. 354–356. ISSN: 0029-599X. DOI: 10.1007/BF02165411. URL: https://doi.org/10.1007/BF02165411.

[60] M. Alamir and G. Bornard. "Stability of a truncated infinite constrained receding horizon scheme: the general discrete nonlinear case". In: *Automatica* 31.9 (Sept. 1995), pp. 1353–1356. ISSN: 00051098. DOI: 10.1016/0005-1098(95)00042-U. URL: http://linkinghub.elsevier.com/retrieve/pii/000510989500042U.

[61] W. Murray Wonham. "On a Matrix Riccati Equation of Stochastic Control". In: *SIAM Journal on Control* 6.4 (Nov. 1968), pp. 681–697. ISSN: 0036-1402. DOI: 10.1137/0306044. URL: https://doi.org/10.1137/0306044.

[62] B.D.O. Anderson and J.B. Moore. *Optimal Control: Linear Quadratic Methods*. 1st ed. New York: Prentice-Hall, 1989.

[63] Huibert Kwakernaak and Raphael Sivan. *Linear Optimal Control Systems*. John Wiley & Sons, Inc., 1972.

[64] D. S. Bernstein and S. P. Bhat. "Lyapunov Stability, Semistability, and Asymptotic Stability of Matrix Second-Order Systems". In: *Journal of Vibration and Acoustics* 117.B (1995), p. 145. ISSN: 07393717. DOI: 10.1115/1.2838656. URL: http://vibrationacoustics.asmedigitalcollection.asme.org/article.aspx?articleid=1469678.

[65] Michael A. Budin. "Minimal realization of discrete linear systems from input-output observations". In: *IEEE Transactions on Automatic Control* 16.5 (Oct. 1971), pp. 395–401. ISSN: 0018-9286. DOI: 10.1109/TAC.1971.1099789. URL: https://doi.org/10.1109/TAC.1971.1099789.

[66] R. E. Kalman. "Canonical Structure of Linear Dynamical Systems". In: *Proceedings of the National Academy of Sciences* 48.4 (Apr. 1962), pp. 596–600. ISSN: 0027-8424. DOI: 10.1073/pnas.48.4.596. URL: https://doi.org/10.1073/pnas.48.4.596.

[67] I. Gelfand. "Normierte Ringe". In: *Recueil Mathematique* 9.1 (1941), pp. 3–24.

[68] Aleksei Fedorovich Filippov. *Differential Equations with Discontinuous Righthand Sides*. Ed. by F. M. Arscott. Kluwer Academic Publishers, 1988, p. 304. ISBN: 90-277-2699-X.

[69] Joaquin Alvarez, Iouri Orlov, and Leonardo Acho. "An Invariance Principle for Discontinuous Dynamic Systems With Application to a Coulomb Friction Oscillator". In: *Journal of Dynamic Systems, Measurement, and Control* 122.4 (2000), p. 687. ISSN: 00220434. DOI: 10.1115/1.1317229. URL: https://doi.org/10.1115/1.1317229.

[70] Ole A. Nielsen. *An Introduction to Integration and Measure Theory*. 1st ed. John Wiley & Sons, Inc., 1997.

[71] R. H. Bartels and G. W. Stewart. "Solution of the matrix equation AX + XB = C". In: *Communications of the ACM* 15.9 (Sept. 1972), pp. 820–826. ISSN: 00010782. DOI: 10.1145/361573.361582. URL: https://doi.org/10.1145/361573.361582.

[72] Murad Abu-Khalaf and Frank L. Lewis. "Nearly optimal control laws for nonlinear systems with saturating actuators using a neural network HJB approach". In: *Automatica* 41.5 (May 2005), pp. 779–791. ISSN: 00051098. DOI: 10.1016/j.automatica.2004.11.034. URL: http://linkinghub.elsevier.com/retrieve/pii/S0005109805000105.

[73] Asma Al-Tamimi and Frank Lewis. "Discrete-time nonlinear HJB solution using Approximate dynamic programming: Convergence Proof". In: *2007 IEEE International Symposium on Approximate Dynamic Programming and Reinforcement Learning*. Vol. 38. Adprl. IEEE, Apr. 2007, pp. 38–43. ISBN: 1-4244-0706-0. DOI: 10.1109/ADPRL.2007.368167. URL: http://ieeexplore.ieee.org/lpdocs/epic03/wrapper.htm?arnumber=4220812.

[74] Draguna Vrabie and Frank Lewis. "Neural network approach to continuous-time direct adaptive optimal control for partially unknown nonlinear systems". In: *Neural Networks* 22.3 (Apr. 2009), pp. 237–246. ISSN: 08936080. DOI: 10.1016/j.neunet.2009.03.008. URL: http://linkinghub.elsevier.com/retrieve/pii/S0893608009000446http://dx.doi.org/10.1016/j.neunet.2009.03.008.

[75] Randal W. Beard, George N. Saridis, and John T. Wen. "Galerkin approximations of the generalized Hamilton-Jacobi-Bellman equation". In: *Automatica* 33.12 (Dec. 1997), pp. 2159–2177. ISSN: 00051098. DOI: 10.1016/S0005-1098(97)00128-3. URL: http://linkinghub.elsevier.com/retrieve/pii/S0005109897001283.

[76] Kemin Zhou and John C. Doyle. *Essentials of Robust Control*. 1st ed. Pearson, 1997. ISBN: 978-0135258330.

[77] Jürgen Jost. *Postmodern Analysis*. 3rd ed. Springer-Verlag Berlin Heidelberg, 2005.

[78] Joshua E. Davis et al. "Eliminating Stick-Slip by Managing Bit Depth of Cut and Minimizing Variable Torque in the Drillstring". In: *IADC/SPE Drilling Conference and Exhibition, 6-8 March 2012, San Diego, California, USA*. San Diego, CA, 2012, pp. 402–410. ISBN: 9781618397928. DOI: 10.2118/151133-MS. URL: https://doi.org/10.2118/151133-MS.

[79] Jeffrey R. Bailey and Stephen M. Remmert. "Managing Drilling Vibrations Through BHA Design Optimization". In: *SPE Drilling & Completion* 25.4 (2010), pp. 458–471. ISSN: 1064-6671. DOI: 10.2118/139426-PA. URL: https://doi.org/10.2118/139426-PA.

[80] M J Fear and Fereidoun Abbassian. "Experience in the Detection and Suppression of Torsional Vibration From Mud Logging Data". In: *European Petroleum Conference*. London, 1994, pp. 433–448. DOI: 10.2118/28908-MS. URL: https://doi.org/10.2118/28908-MS.

[81] R. Hernandez-Suarez et al. "An Integral High-Order Sliding Mode Control Approach for Stick-Slip Suppression in Oil Drillstrings". In: *Petroleum Science and Technology* 27.8 (June 2009), pp. 788–800. ISSN: 1091-6466. DOI: 10.1080/10916460802455483. URL: https://doi.org/10.1080/10916460802455483.

[82] Johan Dirk Jansen and Leon van den Steen. "Active damping of self-excited torsional vibrations in oil well drillstrings". In: *Journal of Sound and Vibration* 179.4 (1995), pp. 647–668. ISSN: 0022460X. DOI: 10.1006/jsvi.1995.0042. URL: https://doi.org/10.1006/jsvi.1995.0042.

[83] A.P. P Christoforou and A.S. S Yigit. "Fully coupled vibrations of actively controlled drillstrings". In: *Journal of Sound and Vibration* 267.5 (2003), pp. 1029–1045. ISSN: 0022460X. DOI: 10.1016/S0022-460X(03)00359-6. URL: https://doi.org/10.1016/S0022-460X(03)00359-6.

[84] A. F A Serrarens et al. "H_∞ control for suppressing stick-slip in oil well drillstrings". In: *IEEE Control Systems Magazine* 18.2 (1998), pp. 19–30. ISSN: 02721708. DOI: 10.1109/37.664652. URL: https://doi.org/10.1109/37.664652.

[85] Hugo L.S. S Monteiro and Marcelo A. Trindade. "Performance analysis of proportional-integral feedback control for the reduction of stick-slip-induced torsional vibrations in oil well drillstrings". In: *Journal of Sound and Vibration* 398 (2017), pp. 28–38. ISSN: 0022460X. DOI: 10.1016/j.jsv.2017.03.013. URL: https://doi.org/10.1016/j.jsv.2017.03.013.

[86] Xiaohua Zhu, Liping Tang, and Qiming Yang. "A Literature Review of Approaches for Stick-Slip Vibration Suppression in Oilwell Drillstring". In: *Advances in Mechanical Engineering* 6 (2015), pp. 1–17. ISSN: 1687-8132. DOI: 10.1155/2014/967952. URL: https://doi.org/10.1155/2014/967952.

[87] Krzysztof Szabat, Than Tran-Van, and Marcin Kaminski. "A Modified Fuzzy Luenberger Observer for a Two-Mass Drive System". In: *IEEE Transactions on Industrial Informatics* 11.2 (2015), pp. 531–539. ISSN: 1551-3203. DOI: 10.1109/TII.2014.2327912. URL: https://doi.org/10.1109/TII.2014.2327912.

[88] E. Kreuzer and M. Steidl. "Controlling torsional vibrations of drill strings via decomposition of traveling waves". In: *Archive of Applied Mechanics* 82.4 (Apr. 2012), pp. 515–531. ISSN: 0939-1533. DOI: 10.1007/s00419-011-0570-8. URL: https://doi.org/10.1007/s00419-011-0570-8.

[89] B. L. van de Vrande, D. H. van Campen, and A. de Kraker. "An Approximate Analysis of Dry-Friction-Induced Stick-Slip Vibrations by a Smoothing Procedure". In: *Nonlinear Dynamics* 19.2 (1999), pp. 159–171. ISSN: 0924090X. DOI: 10.1023/A:1008306327781. URL: https://doi.org/10.1023/A:1008306327781.

[90] N. Mihajlović et al. "Analysis of Friction-Induced Limit Cycling in an Experimental Drill-String System". In: *Journal of Dynamic Systems, Measurement, and Control* 126.4 (2004), pp. 709–720. ISSN: 00220434. DOI: 10.1115/1.1850535. URL: https://doi.org/10.1115/1.1850535.

[91] Frank L. Lewis, Lihua Xie, and Dan Popa. *Optimal and Robust Estimation With an Introduction to Stochastic Control Theory*. Ed. by Frank L. Lewis and Shuzi Sam Ge. 2nd ed. Boca Raton: Taylor & Francis Group, LLC, 2008.

[92] Ali Alavinasab, Hamid Moharrami, and Amir Khajepour. "Active Control of Structures Using Energy-Based LQR Method". In: *Computer-Aided Civil and Infrastructure Engineering* 21.8 (Nov. 2006), pp. 605–611. ISSN: 1093-9687. DOI: 10.1111/j

.1467-8667.2006.00460.x. arXiv: 0k. URL: https://doi.org/10.1111/j.1467-8667.2006.00460.x.

[93] Biswajit Basu and Satish Nagarajaiah. "A wavelet-based time-varying adaptive LQR algorithm for structural control". In: *Engineering Structures* 30.9 (Sept. 2008), pp. 2470–2477. ISSN: 01410296. DOI: 10.1016/j.engstruct.2008.01.011. URL: https://doi.org/10.1016/j.engstruct.2008.01.011.

[94] Chih-Chergn Ho and Chih-Kao Ma. "Active vibration control of structural systems by a combination of the linear quadratic Gaussian and input estimation approaches". In: *Journal of Sound and Vibration* 301.3-5 (Apr. 2007), pp. 429–449. ISSN: 0022460X. DOI: 10.1016/j.jsv.2005.12.061. URL: https://doi.org/10.1016/j.jsv.2005.12.061.

[95] W. E. Schmitendorf, Faryar Jabbari, and J. N. Yang. "Robust control techniques for buildings under earthquake excitation". In: *Earthquake Engineering & Structural Dynamics* 23.5 (May 1994), pp. 539–552. ISSN: 00988847. DOI: 10.1002/eqe.4290230506. URL: https://doi.org/10.1002/eqe.4290230506.

[96] J. N. Yang et al. "Experimental Verifications of H_∞ and Sliding Mode Control for Seismically Excited Buildings". In: *Journal of Structural Engineering* 122.1 (Jan. 1996), pp. 69–75. ISSN: 0733-9445. DOI: 10.1061/(ASCE)0733-9445(1996)122:1(69). URL: https://doi.org/10.1061/(ASCE)0733-9445(1996)122:1(69).

[97] Jong-Cheng Wu, Hsin-Hsien Chih, and Chern-Hwa Chen. "A robust control method for seismic protection of civil frame building". In: *Journal of Sound and Vibration* 294.1-2 (June 2006), pp. 314–328. ISSN: 0022460X. DOI: 10.1016/j.jsv.2005.11.019. URL: https://doi.org/10.1016/j.jsv.2005.11.019.

[98] Ali Kazemy, Xian-Ming Zhang, and Qing-Long Han. "Dynamic output feedback control for seismic-excited buildings". In: *Journal of Sound and Vibration* 411 (Dec. 2017), pp. 88–107. ISSN: 0022460X. DOI: 10.1016/j.jsv.2017.08.017. URL: https://doi.org/10.1016/j.jsv.2017.08.017.

[99] An-Pei Wang and Yung-hing Lin. "Vibration control of a tall building subjected to earthquake excitation". In: *Journal of Sound and Vibration* 299.4-5 (Feb. 2007), pp. 757–773. ISSN: 0022460X. DOI: 10.1016/j.jsv.2006.07.016. URL: https://doi.org/10.1016/j.jsv.2006.07.016.

[100] Rahmi Guclu and Hakan Yazici. "Vibration control of a structure with ATMD against earthquake using fuzzy logic controllers". In: *Journal of Sound and Vibration* 318.1-2 (Nov. 2008), pp. 36–49. ISSN: 0022460X. DOI: 10.1016/j.jsv.2008.03.058. URL: https://doi.org/10.1016/j.jsv.2008.03.058.

[101] Rajiv Kumar, S.P. Singh, and H.N. Chandrawat. "MIMO adaptive vibration control of smart structures with quickly varying parameters: Neural networks vs classical control approach". In: *Journal of Sound and Vibration* 307.3-5 (Nov. 2007), pp. 639–

661. ISSN: 0022460X. DOI: 10.1016/j.jsv.2007.06.028. URL: https://doi.org/10.1016/j.jsv.2007.06.028.

[102] G. W. Housner et al. "Structural Control: Past, Present, and Future". In: *Journal of Engineering Mechanics* 123.9 (Sept. 1997), pp. 897–971. ISSN: 0733-9399. DOI: 10.1061/(ASCE)0733-9399(1997)123:9(897). URL: https://doi.org/10.1061/(ASCE)0733-9399(1997)123:9(897).

[103] R. J. Guyan. "Reduction of stiffness and mass matrices". In: *AIAA Journal* 3.2 (Feb. 1965), pp. 380–380. ISSN: 0001-1452. DOI: 10.2514/3.2874. URL: https://doi.org/10.2514/3.2874.

[104] Robert D. Cook et al. *Concepts and Applications of Finite Element Analysis*. 4th. Wiley, 2001. ISBN: 978-0-471-35605-9. URL: https://www.wiley.com/en-us/Concepts+and+Applications+of+Finite+Element+Analysis%2C+4th+Edition-p-9780471356059.

[105] Billie F. Spencer Jr., R. E. Christenson, and Shirley J Dyke. "Next Generation Benchmark Control Problem for Seismically Excited Buildings". In: *Proceeding of the second world conference on structural control*. Ed. by Takuji Kobori et al. Vol. 2. John Wiley & Sons, June 1998, pp. 1135–1360. DOI: 10.1002/stc.4300060115. URL: https://doi.org/10.1002/stc.4300060115.

[106] S. J. Dyke et al. "Role of Control-Structure Interaction in Protective System Design". In: *Journal of Engineering Mechanics* 121.2 (Feb. 1995), pp. 322–338. ISSN: 0733-9399. DOI: 10.1061/(ASCE)0733-9399(1995)121:2(322). URL: https://doi.org/10.1061/(ASCE)0733-9399(1995)121:2(322).

[107] R. E. Kalman. "A New Approach to Linear Filtering and Prediction Problems". In: *Journal of Basic Engineering* 82.1 (1960), p. 35. ISSN: 00219223. DOI: 10.1115/1.3662552. arXiv: NIHMS150003. URL: https://doi.org/10.1115/1.3662552.

[108] Michael Athans. "The role and use of the stochastic linear-quadratic-Gaussian problem in control system design". In: *IEEE Transactions on Automatic Control* 16.6 (Dec. 1971), pp. 529–552. ISSN: 0018-9286. DOI: 10.1109/TAC.1971.1099818. URL: https://doi.org/10.1109/TAC.1971.1099818.

[109] Keith Glover and John C. Doyle. "State-space formulae for all stabilizing controllers that satisfy an H_∞-norm bound and relations to relations to risk sensitivity". In: *Systems & Control Letters* 11.3 (Sept. 1988), pp. 167–172. ISSN: 01676911. DOI: 10.1016/0167-6911(88)90055-2. URL: https://doi.org/10.1016/0167-6911(88)90055-2.

[110] J.C. Doyle et al. "State-space solutions to standard H_2 and H_∞ control problems". In: *IEEE Transactions on Automatic Control* 34.8 (1989), pp. 831–847. ISSN: 00189286. DOI: 10.1109/9.29425. URL: https://doi.org/10.1109/9.29425.

[111] Czesław I. Bajer and R. Bogacz. "Active control of beams under moving load". In: *Journal of Theoretical and Applied Mechanics* 38 (2000), pp. 523–530.

[112] P. Flont and J. Holnicki-Szulc. "Bridges with adaptive railway track". In: *Journal of Theoretical and Applied Mechanics* 3.40 (2002), pp. 533–547.

[113] Dominik Pisarski and Czesław I. Bajer. "Semi-active control of 1D continuum vibrations under a travelling load". In: *Journal of Sound and Vibration* 329.2 (Jan. 2010), pp. 140–149. ISSN: 0022460X. DOI: 10.1016/j.jsv.2009.09.006. arXiv: 1707.04192. URL: https://doi.org/10.1016/j.jsv.2009.09.006.

[114] Dominik Pisarski. "Distributed Control Design for Structures Subjected to Traveling Loads". In: *Mathematical Problems in Engineering* 2015 (2015), pp. 1–12. ISSN: 1024-123X. DOI: 10.1155/2015/206870. URL: http://www.hindawi.com/journals/mpe/2015/206870/.

[115] Czesław I. Bajer et al. "Intelligent damping layer under a plate subjected to a pair of masses moving in opposite directions". In: *Journal of Sound and Vibration* 394 (2017), pp. 333–347. ISSN: 0022460X. DOI: 10.1016/j.jsv.2017.01.046. URL: https://doi.org/10.1016/j.jsv.2017.01.046.

[116] Ismail Kucuk et al. "Active control of forced vibrations in a beam via Maximum principle". In: *2013 5th International Conference on Modeling, Simulation and Applied Optimization (ICMSAO)*. Hammamet: IEEE, Apr. 2013, pp. 1–4. ISBN: 978-1-4673-5814-9. DOI: 10.1109/ICMSAO.2013.6552558. URL: https://doi.org/10.1109/ICMSAO.2013.6552558.

[117] T. Söderström and M Mossberg. "Performance evaluation of methods for identifying continuous-time autoregressive processes". In: *Automatica* 36.1 (Jan. 2000), pp. 53–59. ISSN: 00051098. DOI: 10.1016/S0005-1098(99)00104-1. URL: https://doi.org/10.1016/S0005-1098(99)00104-1.

[118] Joel Andersson, Johan Åkesson, and Moritz Diehl. "CasADi: A Symbolic Package for Automatic Differentiation and Optimal Control". In: *Recent Advances in Algorithmic Differentiation. Lecture Notes in Computational Science and Engineering*. Ed. by S. Forth et al. Vol. 87. January. Berlin: Springer, 2012, pp. 297–307. ISBN: 978-3-642-30022-6. DOI: 10.1007/978-3-642-30023-3_27. arXiv: arXiv:1011.1669v3. URL: https://doi.org/10.1007/978-3-642-30023-3_27.